

**Cardioprotective Effects of Soluble Epoxide Hydrolase Inhibition
Following Myocardial Infarction**

by

Kristi Lockhart Jamieson

A thesis submitted in partial fulfillment of the requirements for the degree of

Doctor of Philosophy
in
Pharmaceutical Sciences

Faculty of Pharmacy and Pharmaceutical Sciences
University of Alberta

© Kristi Lockhart Jamieson, 2020

ABSTRACT

Ischemic heart disease (IHD) is a significant cause of morbidity and mortality for Canadians. While mortality rates from myocardial infarction (MI) and heart failure (HF) have decreased, IHD remains the number one cause of premature mortality. Both age and sex are important contributors for IHD risk. Aging promotes pathophysiological changes over time that reduce the ability of the heart to adequately respond to stress. Importantly, there are differences in cardiac aging between the sexes. CYP450 metabolism of N-3 and N-6 polyunsaturated fatty acids (PUFAs) generates numerous metabolites, oxylipids, that exhibit a wide range of cellular effects. Previous studies demonstrate oxylipids can regulate and protect mitochondria resulting in preserved cardiac function following ischemic injury. Oxylipids are further metabolised by soluble epoxide hydrolase (sEH) into corresponding diol products with numerous activities. The work presented in this dissertation investigated the effects of inhibiting sEH in aged mice. Moreover, we analyse human myocardial samples from male and female explanted hearts to characterize oxylipid metabolism and mitochondrial function in non-failing control (NFC) and ischemic cardiomyopathy (ICM) patients.

MI was induced in young and aged mice using permanent occlusion of the left anterior descending coronary artery (LAD). Human tissues were obtained from male and female patients with MI (ICM) as part of the Human Explanted Heart Program (HELP) and NFC cardiac tissues were obtained from the Human Organ Procurement and Exchange (HOPE) program at the University of Alberta. Key results suggest mice with genetic deletion or oral treatment with sEH inhibitor *t*AUCB exhibit significantly preserved cardiac function and increased survivability following MI. These results were associated with conserved

mitochondrial function. Importantly, these cardioprotective effects were blunted over age and were more robust in females. In human myocardial samples, individuals with a previous MI had significantly elevated levels of sEH expression correlating with changes to the PUFA metabolite profile and decreases in mitochondrial function.

In summary, the data presented in this thesis suggest targeting sEH in aged mice effectively reduces ischemic injury through preserving mitochondrial function. Unexpectedly, data from our aged mouse model indicate an age-dependent sex-difference, suggesting targeting sEH may be more effective in improving post-ischemic heart function in aged females. Moreover, data from human explanted hearts suggest sEH may be a potential pharmacological target for humans with ischemic cardiomyopathy.

PREFACE

This thesis is an original work by K. Lockhart Jamieson. The human research conducted for part this thesis forms part of an internal research collaboration led by Dr. Gavin Oudit from the Faculty of Medicine, with Dr. John Seubert the senior collaborator from the Faculty of Pharmacy and Pharmaceutical Sciences. Dr. Oudit is the coordinator for the Human Explanted Heart Program (HELP) and Human Organ Procurement and Exchange Program (HOPE) at the University of Alberta.

Parts of the introduction have been previously published as KL Jamieson, T Endo, AM Darwesh, V Samokhvalov, JM Seubert. “Cytochrome P450-derived eicosanoids and heart function.” *Pharm Ther*, 2017:179(47-83). T Endo was responsible for the writing of Chapter 1.7 “Cytochrome P450 polymorphisms and modulated PUFA cardiovascular effects,” and the design of Figure 2 and Table 1.2. AM Darwesh was responsible for the writing of Chapter 1.10 “Pharmacological approaches to regulate CYP-derived eicosanoids” and as the design of Table 1.3. V. Samokhvalov was responsible for writing and editing portions of the manuscript, as well as Table 1.1 and Figure 1.2. JM Seubert was the primary investigator.

Parts of Chapters 2-4 of this thesis have been previously published under KL Jamieson, V Samokhvalov, MK Akhnokh, K Lee, WJ Cho, A Takawale, X Wang, Z Kassiri, JM Seubert. “Genetic deletion of soluble epoxide hydrolase provides cardioprotective responses following myocardial infarction in aged mice.” *Prostaglandins and Other Lipid Mediators*. 2017:132(47-58). V. Samokhvalov performed the caspase-3, aconitase, proteasome, assisted with cardiac fibre respiration and aided in writing. MK Akhnokh collected the young animal data. K. Lee performed immunoblotting. WJ Cho completed the TEM as part of the

University of Alberta Cell Imaging Centre. A. Takawale under the supervision of Z. Kassiri aided assessment of infarct size. X Wang was the surgeon who performed the LAD surgeries, under the supervision of Z. Kassiri. Donna Beker, noted in the acknowledgements, ran and analysed all the echocardiography for this study as part of the Cardiovascular Research Centre (CVRC) at the University of Alberta. These data are presented in Chapter 3.1.

Parts of Chapters 2-4 of this thesis have been submitted for publication to Cardiovascular Research as of March 20, 2020, as: Jamieson KL, Darwesh AM, Sosnowski DK, Zhang H, Shah S, Wang W, Zhabyeyev P, Yang J, Hammock B, Edin ML, Zeldin DC, Oudit GY, Kassiri Z, Seubert JM. “Sexual Dimorphic Responses to Myocardial Infarction Following Inhibition of Soluble Epoxide Hydrolase in Aged Mice and Human Explanted Hearts”. Submitted to *Cardiovascular Research*, March 20, 2020. These data are presented in Chapters 3.2 and 3.3. For Chapter 3.2, AM Darwesh ran respiration and immunoblotting experiments. DK Sosnowski aided with immunoblotting, animal maintenance and revisions. P Zhabyeyev, a member of GY Oudit’s research group, carried out telemetry and helped with analysis. J Yang from B. Hammock’s research group assessed *tAUCB* plasma levels. W Wang, a member of Z Kassiri’s group, performed all the LAD surgeries for this project. ML Edin, a member of DC Zeldin’s research group, performed the LC-MS/MS used to generate oxylipid metabolites described in Chapters 3.2 and 3.3. H Zhang and S Shah, from GY Oudit’s group, provided the human tissue samples and helped analyse the human clinical data outlined in Table 3.3.1. Donna Beker from the CVRC performed echocardiography (2016-2017). Following acquisition of a Vevo 3100, she trained and assisted me in running and analysing the remainder of the ECHO presented in Chapter 3.2 (2017-2019).

DEDICATION

I dedicate this thesis with love and gratitude to my family and friends

“Isn't it splendid to think of all the things there are to find out about? It just makes me feel glad to be alive – it's such an interesting world. It wouldn't be half so interesting if we know all about everything, would it?”

L.M. Montgomery, *Anne of Green Gables*

ACKNOWLEDGEMENTS

I would like to profusely thank my supervisor, Dr. John Seubert, for his guidance and support over the years. I truly could not have asked for a more patient supervisor or a better mentor. I feel exceedingly lucky to have had the chance to learn in his lab and I am incredibly grateful for all the opportunities he so generously provided for me.

I would also like to thank my supervisory committee, Dr. Peter Light and Dr. Paul Jurasz for their insight and encouragement throughout my graduate studies. Moreover, I would like to thank Dr. Zam Kassiri for her advice, collaboration and mentorship over the years. I would also like to acknowledge Dr. Gavin Oudit whose collaboration was an absolutely invaluable addition to my research project. I must also recognize Dr. Bruce Hammock, who so generously provided the drug used in my research, as well as Drs. Matthew Edin and Darryl Zeldin, whose contributions were invaluable.

I owe so much to my previous lab “sisters”, Maria Akhnokh, Kyra Lee and Dr. Tomoko Endo for their friendship and solidarity while “in the trenches” with me. I would also like to thank our previous research associate, Dr. Victor Samokhvalov, who taught me much and who always helped me so generously. I am incredibly grateful for all my current lab members, especially Ahmed Darwesh, who I am so proud to call my only lab “brother”.

Also thank you to my actual brothers, Jason, Nick and Andy for their years of constant mockery that gave me the thick skin required for graduate school. And thank you to my sister Jen and my hand-picked sister, Deanna, for their unconditional support.

I would like to thank my friends Natalie DC, Maddie B, Sarah R-I-mean-C, Sheldon B, Nathan Z, Dustin B, Craig Y, Chloe C and Danica E whose unwavering encouragement helped me through all the long days and weekends, even if they still don’t know exactly what

it is I do. I also need to profusely thank Natasha G, for her friendship, patience and steadfast encouragement through the hardest times of this degree, and for never being more than a text away. I also would like to recognize my trainer Jenn and everyone at Pinnacle Equestrian that has supported and encouraged me throughout my life at uni.

I could not have achieved anything without the lifetime of love and support provided by my parents, Debra and Dennis Jamieson, who fed, housed and generally put up with me long after their legal obligation to do so ended. I would also like to thank my grandmother, Elaine Klemmensen and indeed all of my extended family for their encouragement throughout my studies.

I extend my gratitude to everyone in the Faculty of Graduate Studies and the Faculty of Pharmacy and Pharmaceutical Sciences. Thanks to all my fellow students, especially Takeshi, Ben, Daniela and Deanna, for being such great colleagues, friends and peers, and for making my time in this faculty so incredibly bright. Thanks to the past and present Dean and to all of the administrative staff for their constant willingness to assist in all my issues, no matter how small.

Finally, I would like to recognize the funding agencies that backed this research, the Heart and Stroke Foundation and Canadian Institutes of Health Research, as well as my funding source, Alberta Innovates-Health Solutions and all the University donors that allowed for institutional scholarships.

TABLE OF CONTENTS

	Page Numbers
CHAPTER 1: INTRODUCTION	1
1.1 SUMMARY	2
1.1.1 <i>Overview of cardiovascular pathophysiology</i>	3
1.1.2 <i>Overview of N-6 polyunsaturated fatty acids</i>	6
1.1.3 <i>Overview of N-3 polyunsaturated fatty acids</i>	7
1.2 CYTOCHROME P450S AND GENERATION OF PUFA METABOLITES	9
1.2.1 <i>CYP-derived metabolites of N-6 PUFAs</i>	13
1.2.2 <i>CYP-derived metabolites of N-3 PUFAs</i>	15
1.3 N-6 PUFAS AND CARDIOVASCULAR DISEASES	17
1.3.1 <i>HETEs in cardiovascular disease progression</i>	17
1.3.1.1 <i>20-HETE and pathogenesis of CVD</i>	19
1.3.1.2 <i>19-HETE: an emerging cardioprotective N-6 PUFA</i>	27
1.3.2 <i>EETs in cardiovascular health and disease</i>	28
1.3.2.1 <i>EETs and mitochondrial protection</i>	31
1.3.2.2 <i>Role of EETs n myocardial ischemia and ischemia-reperfusion injury</i>	32
1.3.2.3 <i>EET-mediated regulation of cell death</i>	37
1.3.2.4 <i>Biological actions of EETs in inflammatory cells and fibroblasts</i>	39
1.3.2.5 <i>Role of endothelial-derived EETs in cardiovascular diseases</i>	40
1.3.2.6 <i>EET-mediated cardioprotection</i>	42
1.3.3 <i>EETs in non-ischemic cardiomyopathy</i>	44

1.3.3.1 EETs have multiple protective effects against non-ischemic cardiomyopathy	44
1.3.3.2 EETs have protective effects against diabetic cardiomyopathy	47
1.4 N-3 PUFAS AND CARDIOVASCULAR DISEASES	49
1.4.1 <i>Effect N-3 PUFAs on heart rate and blood pressure</i>	51
1.4.2 <i>Anti-arrhythmic properties of N-3 PUFAs</i>	52
1.4.3 <i>N-3 PUFAs and mitochondrial protection</i>	53
1.4.4 <i>Cardioprotective responses of N-3 PUFAs against MI</i>	53
1.4.5 <i>N-3 PUFAs against cardiac failure and fibrosis</i>	54
1.5 PHYSIOLOGICAL AND PATHOPHYSIOLOGICAL PROPERTIES OF LINOLEIC ACID	
METABOLISM	56
1.6 EICOSANOID RECEPTORS	58
1.7 CYTOCHROME P450 POLYMORPHISMS AND MODULATED PUFA CARDIOVASCULAR	
EFFECTS	63
1.8 EFFECTS OF BIOLOGICAL SEX ON EICOSANOID-MEDIATED CVD	71
1.8.1 <i>Sex and gender in cardiovascular research</i>	71
1.8.2 <i>Sexual dimorphism in eicosanoid-mediated cardioprotection</i>	72
1.9 AGING AND EICOSANOID-MEDIATED PROGRESSION OF CVD	74
1.9.1 <i>HETEs over aging: CVD effects</i>	75
1.9.2 <i>EETs and age-related CVD</i>	76
1.10 PHARMACOLOGICAL APPROACHES TO REGULATE CYP-DERIVED EICOSANOIDS	78
1.11 THESIS OVERVIEW	91

1.11.1 <i>Rationale</i>	91
1.11.2 <i>Hypothesis</i>	92
1.11.3 <i>Aims</i>	92
CHAPTER 2: EXPANDED MATERIALS AND METHODS	94
2.1 PROCUREMENT OF HUMAN HEART TISSUE	95
2.2 ANIMAL MODEL	95
2.2.1 <i>Colony maintenance and breeding</i>	95
2.2.2 <i>Myocardial infarction</i>	96
2.2.3 <i>Pharmacologic administration and water intake</i>	96
2.2.4 <i>Tissue collection and processing</i>	97
2.2.5 <i>Infarct size assessment</i>	98
2.2.6 <i>Cardiac function</i>	98
2.2.6.1 <i>Echocardiography</i>	98
2.2.6.2 <i>Electrocardiogram</i>	99
2.3 ASSESSMENT OF MITOCHONDRIAL FORM AND FUNCTION	99
2.3.1 <i>Mitochondrial catalytic enzymatic activity</i>	99
2.3.2 <i>Mitochondrial respiration</i>	100
2.3.3 <i>Mitochondrial ultrastructure</i>	101
2.4 IMMUNOBLOTTING	102
2.4.1 <i>Tissue homogenization</i>	102
2.4.2 <i>SDS-PAGE and western blotting</i>	103

2.5 ELISA ASSAYS	103
2.5.1 <i>Caspase-3</i>	103
2.5.2 <i>Proteasome</i>	103
2.5.3 <i>Aconitase</i>	104
2.5.4 <i>14,15-DHET measurements</i>	104
2.5.5 <i>ATP assessment</i>	104
2.6 LC-MS/MS	105
2.7 STATISTICS	106
2.7.1 <i>Acute animal model</i>	106
2.7.2 <i>Chronic animal model</i>	106
2.7.3 <i>Human clinical and tissue data</i>	106
CHAPTER 3: RESULTS	108
3.1 sEH DELETION PROTECTS AGAINST MYOCARDIAL INFARCTION IN AGED MICE ...	109
3.1.1 <i>sEH deletion limits cardiac functional decline following MI</i>	109
3.1.2 <i>sEH deletion limits post-MI injury in aged animals</i>	113
3.1.3 <i>Mitochondrial enzyme activities significantly decreased with age</i>	122
3.1.4 <i>Aging affects epoxide hydrolase activity</i>	126
3.1.5 <i>sEH deletion preserved mitochondrial bioenergetics post-MI</i>	130
3.1.6 <i>Conclusion</i>	133
3.2 sEH GENETIC DELETION OR PHARMACOLOGICAL INHIBITION IN CHRONIC ISCHEMIA	134

3.2.1 <i>sEH</i> deletion and pharmacologic inhibition exhibits sexual dimorphic effects on survival post-MI	135
3.2.2 <i>sEH</i> genetic deletion and <i>tAUCB</i> pre-treatment protects cardiac function in female mice post-MI.....	148
3.2.3 Murine left ventricle demonstrates marked changes in oxylipid metabolism ...	156
3.2.4 Female mice with genetic deletion of <i>sEH</i> demonstrated improved protein expression and mitochondrial function post-MI	162
3.2.5 Conclusion	178
3.3 OXYLIPID METABOLISM CHARACTERIZED IN HUMAN LEFT VENTRICULAR TISSUE	179
3.3.1 Clinical parameters from human explanted hearts.....	179
3.3.2 Epoxide hydrolases are upregulated in myocardium from ICM patients	181
3.3.3 Decreased mitochondrial function in LV myocardium from ICM hearts	185
3.3.4 Human LV from ICM patients demonstrates marked changes in oxylipid metabolism	189
3.3.5 Human LV demonstrates loss of mitochondrial ultrastructure and organization	195
3.3.6 Conclusions	199
CHAPTER 4: DISCUSSION AND CONCLUSIONS	200
4.1 Age-related changes in cardioprotective effects arising from <i>sEH</i> genetic deletion	203

4.2 <i>Sexual dimorphism in cardiac responses to sEH genetic deletion or pharmacologic inhibition in a chronic LAD model</i>	210
4.3 <i>Characterization of human explanted myocardium</i>	215
4.4 <i>Final Conclusions</i>	217
CHAPTER 5: FUTURE DIRECTIONS	220
5.1 <i>Mechanisms of sexual dimorphism following myocardial infarction in mice with genetic deletion or pharmacologic inhibition of sEH</i>	221
5.2 <i>Alternative transgenic lines to assess oxylipid metabolism in ischemia</i>	224
5.3 <i>In vivo ischemia/reperfusion injury in aged mice with deletion or inhibition of sEH and effects of inflammation</i>	225
5.4 <i>Assessing earlier endpoints is essential in myocardial response to ischemia</i>	226
REFERENCES	228
APPENDIX	268

LIST OF TABLES

TABLE 1.1	CYP enzymes expressed in the heart	11
TABLE 1.2	Known CYP polymorphisms associated with CVD	66
TABLE 1.3	Summary of CYP and sEH inhibitors affecting cardiovascular function	80
TABLE 3.1.1	Cardiac function determined by echocardiography in young and aged WT and sEH null mice at baseline and 7 days post-MI	111
TABLE 3.1.2	Percent change in baseline cardiac function in aged hearts	112
TABLE 3.1.3	Respirometry and ATP analysis of young and aged WT and sEH null mice pre- and post-MI	132
TABLE 3.2.1	Cardiac functional parameters in sham mice treated with <i>tAUCB ad libitum</i> for 28 days	149
TABLE 3.2.2	Cardiac functional parameters assessed by echocardiography in aged female WT and CYP2J2-Tr mice at baseline and 28-days post-MI	150
TABLE 3.2.3	Cardiac functional parameters assessed by echocardiography in aged female mice at baseline, 7 and 28-days post-MI	152
TABLE 3.2.4	Cardiac functional parameters assessed by echocardiography in aged male mice at baseline, 7 and 28-days post-MI	153

TABLE 3.2.5	Cardiac functional parameters assessed by electrocardiogram in aged female mice at baseline, 7 and 28-days post-MI	155
TABLE 3.2.6	Cardiac functional parameters assessed by electrocardiogram in aged male mice at baseline, 7 and 28-days post-MI	155
TABLE 3.2.7	Oxylipid metabolite profile in female mouse left ventricle myocardium measured by LC-MS/MS	157
TABLE 3.3.1	Clinical parameters for NFC and ICM patients	180
TABLE 3.3.2	Oxylipid metabolite profile in human left ventricle myocardium measured by LC-MS/MS	191

LIST OF FIGURES

FIGURE 1.1	Overview of the development of cardiovascular pathophysiology	5
FIGURE 1.2	CYP-dependent pathways involved in biological transformation of N-3 and N-6 PUFA	14
FIGURE 1.3	Schematic representation of the key CYP-derived metabolites of arachidonic acid and their primary known function within the heart	18
FIGURE 1.4	A schematic representation of the main signaling mechanisms of 20-HETE found in vascular endothelial and smooth muscle cells	26
FIGURE 1.5	A schematic representation of the main signaling mechanisms for EETs found within the heart and their primary biological activities	30
FIGURE 1.6	An outline of primary effects of EPA and DHA metabolites within the heart.	50
FIGURE 3.1.1	Infarct size quantified by TTC from transverse heart slices from young and aged WT and sEH null mice	114
FIGURE 3.1.2	Caspase-3 activity in young and aged WT and sEH null sham and 7-day post-MI hearts	115
FIGURE 3.1.3	20S proteasome activation in young and aged WT and sEH null sham and 7-day post-MI hearts	117

FIGURE 3.1.4	Aconitase activation in young and aged WT and sEH null sham and 7-day post-MI hearts	119
FIGURE 3.1.5	Electron microscopy in young hearts at 7 days post-MI	121
FIGURE 3.1.6	Electron microscopy in aged hearts at 7 days post-MI	121
FIGURE 3.1.7	Protein expression of key mitochondrial enzymatic subunits in WT and sEH null sham and non-infarcted left ventricle	123
FIGURE 3.1.8	Activities of key mitochondrial enzymes in non-infarct regions of young and age WT and sEH null left ventricle	125
FIGURE 3.1.9	Soluble epoxide hydrolase expression in young and aged sham and post-MI WT and sEH null hearts	126
FIGURE 3.1.10	Microsomal epoxide hydrolase expression in young and aged sham and post-MI WT and sEH null hearts	127
FIGURE 3.1.11	14,15-DHET levels in young and aged sham and post-MI WT and sEH null hearts	129
FIGURE 3.2.1	Infarct size (%) as measured by TTC in WT, sEH null and <i>tAUCB:0d</i> (same-day) treated mice	135
FIGURE 3.2.2	Percent survival over 28 days in aged female WT, sEH null, CYP2J2-Tr and <i>tAUCB</i> -treated mice with permanent LAD occlusion	137

FIGURE 3.2.3	Body weights in aged female and male WT, sEH null and <i>tAUCB</i> -treated mice at baseline, 7 days and 28 days following permanent LAD occlusion	138
FIGURE 3.2.4	Wet lung and heart weight at necropsy compared to tibial length in female control and 28 days post-MI	140
FIGURE 3.2.5	Percent survival over 28 days in aged male WT, sEH null, and <i>tAUCB</i> same-day treated mice with permanent LAD occlusion	141
FIGURE 3.2.6	Wet lung and heart weight at necropsy compared to tibial length in male control and 28 days post-MI	142
FIGURE 3.2.7	sEH expression in aged female WT, sEH null and <i>tAUCB</i> treated control and post-MI mice	144
FIGURE 3.2.8	sEH expression in aged female and male WT, sEH null and <i>tAUCB</i> treated control and post-MI mice	145
FIGURE 3.2.9	Water intake over 28 days for control and post-MO vehicle and <i>tAUCB</i> -treated females and males	146
FIGURE 3.2.10	<i>tAUCB</i> levels in plasma for WT vehicle control and <i>tAUCB</i> treated male and female mice	147
FIGURE 3.2.11	Linoleic acid epoxygenase metabolites in female mouse LV myocardial tissue measure by LC-MS/MS	158

FIGURE 3.2.12	Arachidonic acid epoxygenase metabolites in female mouse LV myocardial tissue measure by LC-MS/MS	160
FIGURE 3.2.13	DHA and EPA epoxy lipid metabolites in female mouse LV myocardium	161
FIGURE 3.2.14	Mitochondrial ETC protein expression in female WT, sEH null and <i>tAUCB</i> -treated myocardium	163
FIGURE 3.2.15	Mitochondrial ETC protein expression in female WT, sEH null and <i>tAUCB</i> -treated myocardium	164
FIGURE 3.2.16	ETC enzymatic activities in female control, non-infarct and peri-infarct myocardium from WT, sEH null and <i>tAUCB</i> treated mice	166
FIGURE 3.2.17	ETC enzymatic activities in male control, non-infarct and peri-infarct myocardium from WT, sEH null and <i>tAUCB</i> treated mice	167
FIGURE 3.2.18	Protein expression in mitochondrial fractions from female control, non-infarct and peri-infarct myocardium in WT, sEH null and <i>tAUCB</i> treated mice	169
FIGURE 3.2.19	Protein expression in microsomal and cytosolic fractions from female control, non-infarct and peri-infarct myocardium in WT, sEH null and <i>tAUCB</i> treated mice	171

FIGURE 3.2.20	Protein expression in mitochondrial, microsomal and cytosolic fractions from male control, non-infarct and peri-infarct myocardium in WT and sEH null mice	172
FIGURE 3.2.21	Respiratory parameters in whole cardiac fibres from WT and sEH null female mice	175
FIGURE 3.2.22	Respiratory parameters in whole cardiac fibres from WT and sEH null mice	176
FIGURE 3.2.23	Proposed schematic of cardioprotection in female sEH null and <i>t</i> AUCB treated mice at 28 days post-MI	177
FIGURE 3.3.1	CYP epoxygenase expression NFC and ICM human male and female myocardium	182
FIGURE 3.3.2	Epoxide hydrolase expression NFC and ICM human male and female myocardium	184
FIGURE 3.3.3	ETC enzymatic activity in NFC and ICM female hearts	186
FIGURE 3.3.4	ETC enzymatic activity in NFC and ICM male hearts	187
FIGURE 3.3.5	Expression of mitochondrial ETC proteins in human female and male NFC and ICM patient myocardium	188
FIGURE 3.3.6	Linoleic acid epoxygenase metabolites in human female and male NFC and ICM patient myocardium	192

FIGURE 3.3.7	Arachidonic acid epoxygenase metabolites in human female and male NFC and ICM patient myocardium	193
FIGURE 3.3.8	DHA metabolite 19,20-EpDPE in human female and male NFC and ICM patient myocardium	194
FIGURE 3.3.9	Protein expression in mitochondrial, microsomal and cytosolic fractions in human female NFC and ICM patient myocardium	196
FIGURE 3.3.10	Protein expression in mitochondrial, microsomal and cytosolic fractions in human female NFC and ICM patient myocardium	197
FIGURE 3.3.11	Transmission electron microscopy from female and male NFC and ICM hearts	198

LIST OF ABBREVIATIONS AND SYMBOLS

AA	arachidonic acid
ACS	acute coronary syndrome
ALA	alpha-linolenic acid
AMPK	5' adenosine monophosphate-activated protein kinase
Ang II	angiotensin II
ANP	atrial natriuretic peptide;
BaP	benzo(α)pyrene
BK _{Ca}	large Ca ²⁺ sensitive potassium channels
CAD	coronary artery disease
CHD	coronary heart disease
COX	cyclooxygenase
CVD	cardiovascular disease
CYP-450	cytochrome p-450
DCM	diabetic cardiomyopathy
DDMS	N-methylsulfonyl-12,12-dibromododec-11-enamide
DHA	docosahexaenoic acid
DHET	dihydroxyeicosatrienoic acid
DiHOME	dihydroxyoctadecenoic acid
DM	diabetes mellitus
EDP, EpDPE	epoxydocosapentaenoic acids
EEQ, EpETE	epoxyeicosatetraenoic acids
EET	epoxyeicosatrienoic acids

EET-B	(N-(5-((2-acetamidobenzo[d]thiazol-4-yl)oxy)pentyl)-N isopropylheptanamide)
EEZE	epoxyeicosa-5(Z)-enoic acids
EPA	ecosapentaenoic acids
EPHX2	gene encoding soluble epoxide hydrolase enzyme
EpOME	epoxyoctadecamonoenic acid
ER	endoplasmic reticulum
GPCR	G-protein coupled receptor;
GSK2256294	(1R,3S)-N-(4-cyano-2-(trifluoromethyl)benzyl)-3-((4- methyl-6-(methylamino)-1,3,5-triazin-2- yl)amino)cyclohexane-1 carboxamide
HET0016	N-hydroxy-N'-(4-butyl-2-methylphenyl)-formamidine
HETE	hydroxyeicosatetraenoic acid
HF	heart failure;
HO-1	heme oxygenase-1
HR	hypoxia/reoxygenation
ICM	ischemic cardiomyopathy
IHD	ischemic heart disease
INH	isoniazid
IR	ischemia reperfusion
IRI	ischemia reperfusion injury
ISO	isoproterenol
LA	linoleic acid

LAD	left anterior descending coronary artery
LOX	lipoxygenase
LPS	lipopolysaccharide
LV	left ventricle
LVDP	left ventricular developed pressure
MAG	monoacylglyceride
MAPK	mitogen-activated protein kinase
MI	myocardial infarction
MPTP	mitochondrial permeability transition pore
NCM	non-failing control
NF- κ B	nuclear factor kappa B
NICM	non-ischemic cardiomyopathy
PI3K	phosphatidylinositol-3 kinase
PIP	phosphatidylinositol
PKB	(AKT) Protein kinase B
PLA2	phospholipases A2
PPAR	proliferative peroxisome activated receptor
PUFA	polyunsaturated fatty acid
ROS	reactive oxygen species
sEH	soluble epoxide hydrolase
sEHi	soluble epoxide hydrolase inhibitor
SHR	spontaneously hypertensive rat
SIRT	sirtuin

SNP	single nucleotide polymorphisms
SOD2	superoxide dismutase 2
STZ	streptozotocin
TAC	transverse aortic constriction
<i>t</i> AUCB	4-[[trans-4-[[[(tricyclo[3.3.1.1 ^{3,7}]dec-1-ylamino) carbonyl]amino] cyclohexyl]oxy] benzoic acid
TGFβ1	transforming growth factor beta 1
TNF-α	tumor necrosis factor alpha; TP, thromboxane;
TUPS	1-(1-methanesulfonyl-piperidin-4-yl)-3-(4-trifluoro-methoxy-phenyl)-urea
UA-8	13-(3-propylureido)tridec-8-enoic acid;
VDAC	voltage dependent anion channel
VSMC	vascular smooth muscle cells
WT	wild-type

Chapter 1

INTRODUCTION

¹This chapter has been adapted from a previously published manuscript: Jamieson KL, Endo T, Darwesh AM, Samokhvalov V, Seubert JM. Cytochrome P450-derived eicosanoids and heart function. *Pharm Ther*, 2017.

1.1 SUMMARY

Cardiovascular disease (CVD) remains a major cause of illness, disability and death in both Western societies and developing nations. As populations' age and co-morbidities such as obesity and diabetes become more prevalent both the human health cost and economic burden of these conditions will increase. The ability to manage risk factors such as dietary fat intake has an important role in reducing the development of CVD. The long-chain n-3 and n-6 polyunsaturated fatty acids (PUFA) are important fatty acids obtained from dietary sources. These fatty acids are required components of phospholipid membranes and serve as precursors to large family of eicosanoids. The metabolism of n-3 and n-6 PUFAs into a plethora of bioactive eicosanoids occurs through three primary enzymatic systems such as cyclooxygenases (COX), lipoxygenases (LOX) and cytochrome P450 (CYP) enzymes. There is a growing understanding of the relative contribution of CYP-derived eicosanoids toward cardiac function and dysfunction suggesting the importance of these metabolites. Further elucidation of their role in both physiological and pathophysiological states of an individual's heart will provide novel therapeutic strategies to improve cardiovascular health.

The importance of dietary fatty acids in the reduction of CVD has been recognized for many years [1, 2]. Early studies investigating the association of serum cholesterol with coronary heart disease (CHD) suggested that unsaturated fatty acids lowered serum cholesterol levels compared to saturated fatty acids (SFA) [3-5]. Evidence demonstrates the adverse effects of both *trans* fatty acids (TFA) and SFA, whereas PUFAs are associated with a lower incidence of CVD [6-8]. These latter studies showed a lower incidence of cardiac death, as well as decreases in blood pressure, blood viscosity, plasma triglycerides, ventricular fibrillation, arrhythmia, and myocardial infarction (heart attack, MI) [6, 7, 9, 10].

While the exact molecular mechanisms by which fatty acids regulate cardiac function or trigger dysfunction are not fully defined, it is recognized they are pleiotropic. Beneficial and detrimental outcomes ultimately depend on the levels and type of fatty acids predominating within the body or cell. The challenge for researchers is to determine the extent fatty acids influence physical properties and biochemical processes, which provide protection toward contractile dysfunction, energetics and CVD. Targeting the metabolism of fatty acids in the context of CVD is the primary focus of this thesis.

1.1.1. Overview of Cardiovascular Pathophysiology

Cardiovascular disease is an all-encompassing term reflecting many pathophysiological problems impacting both vascular and cardiac function, which may lead to MI, heart failure (HF) and stroke [11]. Influencing the development of CVD are both controllable and uncontrollable risk factors, such as age, hypertension, dyslipidemia, obesity, diabetes mellitus and smoking, all of which comprise multiple organ systems that convalesce to drive significant changes in cardiovascular structure, function, metabolism and bioenergetics (Figure 1.1). The end point for many CVD patients is HF, which is characterized by decreased cardiac output. HF is not a single disease entity but a defined pathogenesis cumulating in failed systolic and/or diastolic function resulting an inability of the heart to meet the energetic demands of the body [12]. The stiffening of the vasculature resulting from prolonged endothelial dysfunction and oxidizing lipid particles, as found in atherosclerosis, is one of the greatest contributors to coronary artery disease (CAD) and CHD [11]. Rupture of unstable atherosclerotic plaques can cause the formation of thrombi and/or emboli, leading to myocardial ischemia, angina and acute myocardial infarction (AMI) [13]. AMI is a common outcome of persistent CHD with death usually arising from arrhythmias or left

ventricular rupture (sudden cardiac death) [13]. Damage immediately following AMI is typified by apoptotic and necrotic cell death, activation of inflammatory cascades, severe mitochondrial alterations in bioenergetic and cell death regulation, and ionic and metabolic disturbances [14]. While success with early reperfusion strategies and adjuvant therapies has decreased acute mortality rates, there has been a paradoxical increase in the incidence of chronic heart failure. Deterioration of cardiac function post-AMI includes extensive ventricular remodelling involving formation of fibrotic scar tissue as damaged cardiomyocytes are replaced with myofibroblasts [14]. This shifts the injury from an acute index event to a chronic disease where individuals live with damaged hearts, in which patients often progress to HF. HF can also arise from hypertension, where the heart attempts to contract more forcefully to account for the extra workload, resulting in compensatory hypertrophy and extensive ventricular remodelling [12, 15]. Eventually the ventricular wall thins, and coupled with a dilated chamber progresses to dilated cardiomyopathy [12]. In response to decreased output, the body activates many neuronal and hormonal compensatory symptoms such as the renin-angiotensin system (RAS), and the sympathetic nervous system, which feedback to increase cardiac contractility, at the detriment of the heart [12]. HF is an increasingly observed clinical end point as pharmacological and surgical interventions increase life expectancy following acute ischemic events, and prolong lives of hypertensive patients [15, 16].

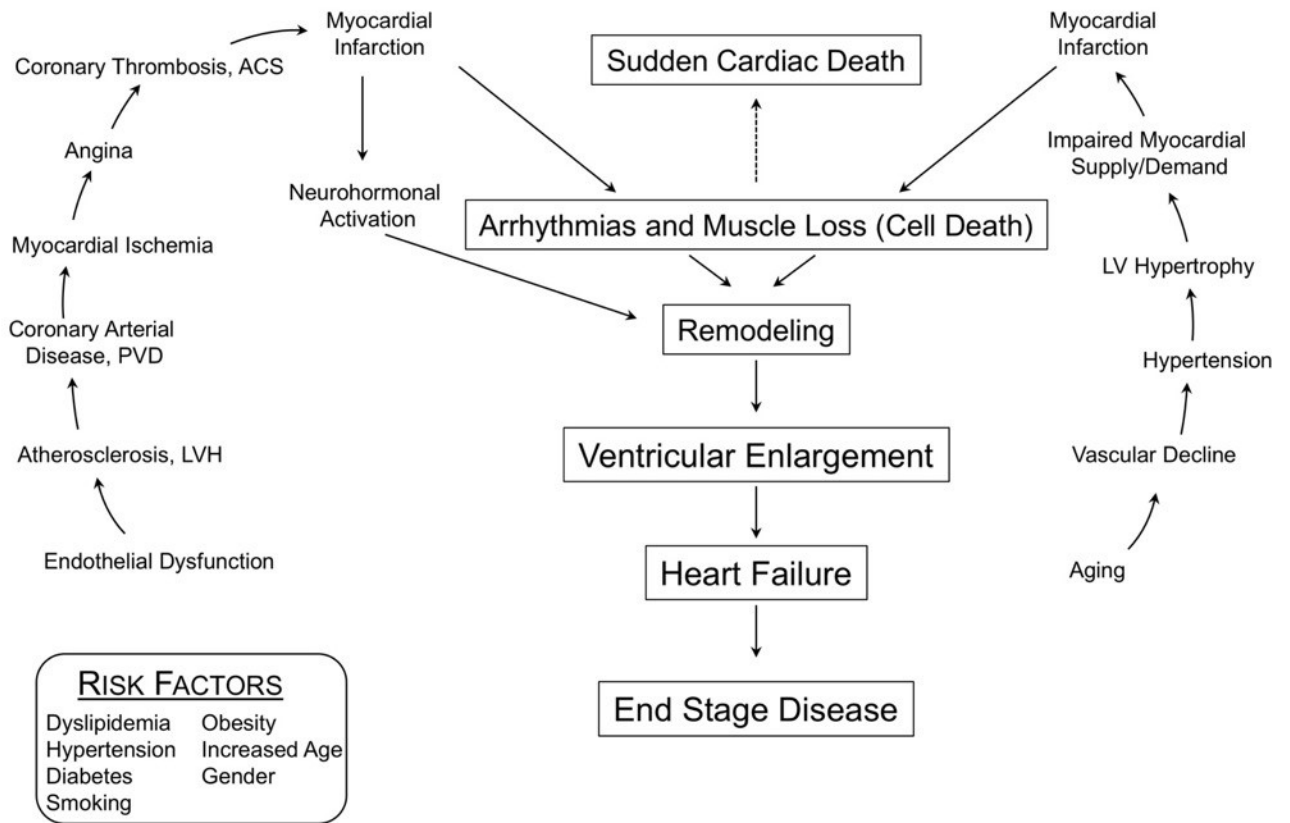


FIGURE 1.1. Overview of the development of cardiovascular pathophysiology. Adapted from Kim, Park and O'Rourke[17].

1.1.2. *Overview of n-6 polyunsaturated fatty acids*

Dietary sources of n-6 fatty acids may be obtained from liquid vegetable oils, including soybean, corn, sunflower, safflower and cottonseed oils. Linoleic acid (18:2n6, LA) is the primary source of the essential n-6 PUFA, which is converted to arachidonic acid (20:4n6, AA) by desaturation and elongation via enzyme systems within the body. Importantly, both n-6 and n-3 PUFA compete for the rate-limiting desaturase for conversion to longer chain PUFA [18]. Therefore, an overabundance of LA will limit the conversion of alpha-linolenic acid (ALA) to eicosapentaenoic acid (EPA) or docosahexaenoic acid (DHA) thereby influencing physiological events.

There are discrepancies in the literature over the beneficial or adverse effects of n-6 PUFA toward cardiovascular health and disease. Some studies indicate a high intake of LA is associated with an increased risk of heart disease [19]. The metabolism of n-6 PUFA by COX and LOX enzymes produces pro-inflammatory, pro-thrombotic and pro-constrictive eicosanoids [19]. These biologically active products contribute to effects such as increased blood viscosity, thrombosis, vasospasm, vasoconstriction and decreased bleeding time, which increase risk of CVD [10]. Conversely early epidemiological studies demonstrated that a higher intake of LA reduced the risk of coronary heart diseases, whereas a lower dietary intake of LA was associated with higher incidences of MI [20]. In the 1960s and again in the 1980s, Western countries recommended replacing saturated fatty acids with unsaturated fatty acids, which resulted in an increased intake of LA and a significant reduction in the mortality rates [21]. Beneficial aspects of CYP-derived metabolites of n-6 PUFA have been reported to be cardioprotective in animal models [22-25]. CYP epoxygenase metabolites of AA, epoxyeicosatrienoic acids (EETs), are important components of many intracellular signaling

pathways in both cardiac and extracardiac tissues [26]. For example, EETs activate large Ca^{2+} -sensitive K^+ channels (BK_{Ca}) in vascular smooth muscle cells (VSMCs) resulting in hyperpolarization of the resting membrane potential and vasodilation of the coronary circulation [26-29]. EETs have been shown to have anti-inflammatory and angiogenic properties within the vasculature. Notably, EETs inhibit platelet aggregation and adhesion to endothelial cells and enhance activity of plasminogen activator, suggesting a potential thrombolytic role for these metabolites [30]. Moreover, drugs that prevent degradation of EETs have been demonstrated to reverse pathological alterations in cardiac hypertrophy in animal models [31]. Alternatively, AA can be metabolized by CYPs to 20-HETE, which evidence demonstrates has primarily cardiotoxic effects due to its actions in the vasculature [32]. It is important to note that the effects mediated by oxylipids depend on the physiological context. For instance, increased 20-HETE-mediated vasoconstriction as a response to hypotension from sEH ablation can be viewed as protective, as severe hypotension is itself an adverse effect that can result in improper organ perfusion and death [33]. Alternatively, increased EETs may have beneficial effects on the heart but adverse effects in other organ systems. The direct effects of 20-HETE on the heart remain to be fully elucidated. Overall, the beneficial or adverse effects of n-6 PUFA in CVD depends not just on the individual metabolites created, but in what physiological or pathophysiological context they are being produced.

1.1.3. *Overview of n-3 polyunsaturated fatty acids*

Dietary consumption of green leaves, canola oil, soybean oil, flaxseed, nuts and oily fish or food products enriched with n-3 PUFA, such as eggs and bread, are the main sources of ALA (18:3n3), EPA (20:5n3) and DHA (22:6n3). ALA may be converted to EPA or DHA

in endoplasmic reticulum (ER) by the action of desaturase and elongase enzymes; however, the conversion is very limited in humans [34]. The cardioprotective role of n-3 PUFA was first suggested in studies reporting lower mortality rates caused by CVD in Greenland Inuit, who had higher dietary fish oil intake compared to Americans and Danes [35]. Further evidence demonstrated that individuals from Japan and Nunavik had lower incidences of thrombotic events and mortality caused by CVD, which was attributed to the effects of n-3 PUFA in the lipid profile [36]. Data from a randomized, double-blind, placebo-controlled trial, the “GISSI-HF Trial,” demonstrated that n-3 PUFA supplementation was associated with reduced mortality and admission to hospital for cardiovascular reasons in patients receiving standard treatment for HF [37]. Fish oil consumption in the diet was therefore inversely related to CHD mortality.

However, not all the studies have shown beneficial effects of n-3 PUFA in terms of preventing the overall risk of cardiac events. For instance, no significance was observed in any CHD including non-fatal MI, sudden cardiac death, coronary artery bypass grafting, or angioplasty in the Health Professionals’ Follow-up Study [38]. Similarly, a randomized double-blind trial by the “Alpha-Omega Trial Group” showed no significant benefit for n-3 PUFA toward cardiovascular events post-MI [39]. Other studies have also shown that there is only minor correlation between fish intake and reduced risk of fatal MI, non-sudden cardiac death and total cardiovascular mortality [40]. Genetic profiling of Greenland Inuit demonstrated a genetic and physiological adaptation to a diet rich in PUFAs, suggesting the extrapolation of results from Inuit populations to other populations is problematic [41]. For example, these individuals demonstrate increased frequency of fatty acid desaturases (FADS) responsible for converting LA and ALA into their respective PUFAs, and thus may

have enhanced ability to produce bioactive circulating PUFAs [41]. Recently, Hu et al. demonstrated the Inuit may in fact have higher risk for stroke and MI than the general Canadian population, an observation they suggest may be linked to changing dietary patterns and accumulation of environmental toxins such as methyl mercury[42]. Other differences may be partially attributed to study design as some studies were performed in populations with a high baseline intake of n-3 PUFA while others utilized lower doses of EPA and DHA. Additional confounding factors include alcohol consumption, exercise habits and misclassification of dietary saturated fatty acids or n-6 PUFA.

Whether or not n-3 PUFAs are beneficial in preventing CVDs remains controversial; however, the majority of the literature strongly indicates that n-3 PUFA are cardioprotective. Experimental studies have demonstrated a broad range of overlapping cardiovascular effects attributed to increased intake of n-3 PUFA. These include effects on resting heart rate, signaling and gene expression, anti-arrhythmic properties, anti-atherogenic effects, reduced blood pressure, reduced blood clotting factor (fibrin), decreased plasma triacylglycerol, altered membrane microdomains and arterial cholesterol levels [43, 44].

1.2. CYTOCHROME P450S AND GENERATION OF PUFA METABOLITES

Cytochrome (CYP) P450 genes encode a super-family of mixed function monooxygenases which contain more than 6000 individual enzymes (<http://drnelson.uthsc.edu/CytochromeP450.html>) [45]. CYP enzymes play a major role in the metabolism of lipophilic xenobiotics, including drugs and chemical carcinogens, as well as endogenous compounds such as steroids, fat-soluble vitamins, fatty acids and biogenic amines [45]. Multiple CYP enzymes have overlapping substrate selectivity; many individual

isoforms demonstrate unique regio- or stereoselectivity toward particular substrates, for example AA, EPA and DHA. CYP expression and activity is under the control of hormones, growth factors, and transcription factors. Indeed, different CYP subfamilies can display complex sex-, tissue-, and development-specific expression patterns [46, 47]. In mammalian cells, CYP enzymes are found localized to the endoplasmic reticulum with limited expression occurring in mitochondria [48]. While CYPs are predominantly expressed in the liver, there are significant levels of CYP isozymes found in extrahepatic tissues including brain, lung, kidney, gastrointestinal tract and heart [46, 47, 49, 50]. Cardiac expression of CYP subfamilies identified in mammalian species include, CYP1A, CYP1B, CYP2A, CYP2B, CYP2D, CYP2E, CYP2J, CYP2R, CYP2S, CYP2U, CYP4A, CYP4B, CYP4F and CYP11B (Table 1). Many genetic and environmental factors alter CYP expression resulting in significant changes in the production or removal of bioactive products. Importantly, the impact on the heart remains largely unknown. Our current level of knowledge regarding the role of cardiac specific CYPs in heart physiology and pathophysiology is limited. However, emerging evidence suggests CYPs located within the heart can influence both drug metabolism and endogenous cellular function.

TABLE 1.1. CYP enzymes expressed in the heart

Isozyme	Level	Expression in Heart	Species	Known Function	References
CYP1A1	mRNA	Right & left ventricle	Human Rat	Drug metabolism PUFA metabolism	[51-55]
CYP1A2	mRNA	Endothelium, endocardium, coronary vessels	Human Rat	PUFA metabolism	[51, 56]
CYP1B1	mRNA	Heart	Human Rat	AA epoxygenase & hydroxylase	[53, 57, 58]
CYP2A6/7	mRNA	Heart	Human	Low epoxygenase activity	[54]
CYP2B1	mRNA	Heart	Rat	AA epoxygenase	[53, 59]
CYP2B2	mRNA	Heart	Rat		[53]
CYP2B6/7	mRNA	Right & left ventricle	Human	Drug metabolism	[54, 55]
CYP2C8- 19	mRNA	Right ventricle	Human	Drug metabolism	[55]
CYP2C8	mRNA Protein	Heart, left ventricle	Human	AA epoxygenase Drug metabolism	[52, 54, 60]
CYP2C9	mRNA Protein	coronary endothelial cells aorta and coronary artery	Human	PUFA metabolism	[57, 60, 61]
CYP2C11	mRNA Protein	Heart	Rat	Main AA epoxygenase	[53, 62]
CYP2D6	mRNA	Right ventricle	Human	Drug metabolism	[55, 63]
CYP2E1	mRNA Protein	Human heart, great vessels, left ventricle endothelium of endocardium and coronary vessels	Human Rat	Epoxyde hydrolase	[52-56, 64]
CYP2J2	mRNA Protein	Heart, aorta and coronary artery, left ventricle	Human	Drug metabolism (doxorubicin), Major AA epoxygenase Higher expression in ischemic heart	[52, 54, 60, 65]
CYP2J3	Protein	Heart	Rat	Major AA epoxygenase	[49, 53, 62]
CYP2J4		Heart	Rat	Contribute to EET & HETE formation	[66]

CYP2U1	mRNA	Heart	Mice		[67]
CYP3A4	Protein	Endothelium of endocardium and coronary vessels	Human		[56]
CYP4A1	mRNA	Heart membrane fraction	Dog	Major AA hydroxylase	[53, 62, 68]
	Protein	Heart	Rat		
CYP4A2	Protein	Heart membrane fraction	Dog	Major AA hydroxylase	[69]
CYP4A3	mRNA	Heart	Rat		[53]
CYP4A11	mRNA	Left ventricle	Human	AA hydroxylase	[52, 54]
CYP4B1	mRNA	Right ventricle	Human	Drug metabolism	[55]
CYP4F	Protein	Heart membrane fraction	Dog		[69]
CYP4F4	mRNA	Heart	Rat		[53]
CYP4F5	mRNA	Heart	Rat		[53]

1.2.1. *CYP-derived metabolites of n-6 PUFAs*

AA is normally esterified in glycerophospholipids and requires a cellular stimulus wherein phospholipases A2 (PLA2) are activated to release free AA [70]. In the myocardium, calcium-independent phospholipase 2 beta (iPLA2 β) is a central PLA2 responsible for the release of free AA [71]. Regulated by Ca²⁺ and cellular bioenergetic status, iPLA2 β is activated during ischemia contributing to the availability of AA [72]. The CYP450 monooxygenases are the third major pathway for AA metabolism, the first two being the COX and LOX pathways [73]. CYP enzymes convert AA into bioactive EETs through an olefin epoxidation (epoxygenase reaction), hydroxyeicosatetraenoic acids (HETEs) through hydroxylation at or near the terminal methyl group (ω -/ ω -1 hydroxylase reaction) and cis,trans-conjugated 'mid-chain' HETEs by allylic oxidation [26, 74] (Figure 1.2).

In humans, the predominant CYP epoxygenases are the CYP 2J, 2B and 2C sub-families while the CYP ω -hydroxylases primarily comprise the CYP 4A and 4F subfamilies [32, 75]. CYP2J2, CYP2C8 and CYP2C9 are the most constitutively expressed CYP epoxygenases in non-diseased human cardiovascular tissue, responsible for converting AA into four regiosomeric cis-epoxyeicosatrienoic acids (5,6-, 8,9-, 11,12-, and 14,15-EET), which exist as either R,S- or the S,R-enantiomer [60, 65, 75]. EETs are further metabolised to the less active dihydroxyeicosatrienoic acids (DHETs) by soluble (sEH) or microsomal (mEH) epoxide hydrolase [76] (Figure 1.2).

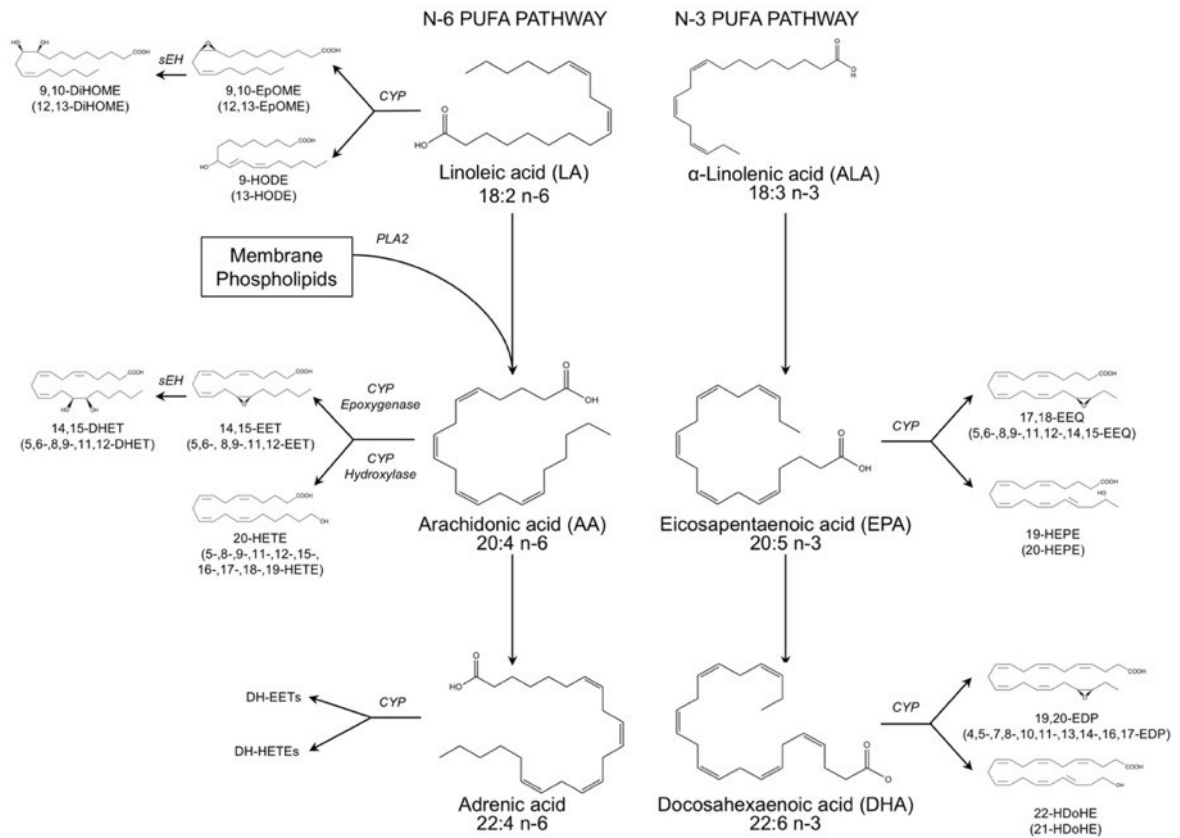


FIGURE 1.2. CYP-dependent pathways involved in biological transformation of N-3 and N-6 PUFA. CYP2J2 and CYP2C8 are the most relevant CYP enzymes for the myocardium. sEH and mEH metabolise the CYP metabolites to their respective diol forms. Different CYP isoforms produce a spectrum of epoxy- and hydroxy-derivatives that demonstrate biological activity in the heart.

CYP ω -hydroxylase isozymes from the CYP4A and 4F subfamilies hydroxylate AA on the terminal methyl group producing 20-HETE and minor amounts of 19-HETE [74], which exist as R- or S- enantiomers. CYP1A1, CYP1A2 and CYP2E1 also function as hydroxylases, producing mainly terminal HETEs (16-,17-,18-, and 19-HETE) [77, 78]. While the ‘mid-chain’ HETEs, such as 5-,8-,9-,11-,12- and 15-HETE, contain cis-trans-conjugated dienol groups and are produced mainly by the LOX system but also via CYP-mediated allylic oxidation [79]. HETEs can be further metabolised by COX-2, UDP glucuronosyltransferases (UGT), alcohol dehydrogenase (ADH) or beta-oxidation for increased excretion [32, 80, 81]. EETs, DHETs and HETEs undergo rapid cellular uptake and are subsequently incorporated into cellular phospholipids, though the metabolites are generally less active than their parent compounds [82]. EETs and HETEs have strikingly different effects on the heart. For example, 20-HETE is a potent vasoconstrictor and pro-inflammatory mediator that regulates vascular tone, blood pressure and renal function [32]. However, emerging evidence has suggested that other HETEs, particularly 19-HETE, may not produce these same cardiotoxic effects [32]. EETs are generally cardioprotective compounds, limiting injury and protecting mitochondrial function [27, 75, 83]. The recent research of the n-6 PUFA eicosanoids and their influence on cardiovascular function in health and disease is the focus of Chapter 1.3.

1.2.2. *CYP-derived metabolites of n-3 PUFAs*

The characterization and understanding of the CYP-mediated metabolism of EPA and DHA is rapidly expanding. The n-3 PUFAs, EPA and DHA, can replace AA for binding at sn-2 positions on glycerophospholipids increasing their availability for metabolism by CYP isozymes, where they may compete with AA as alternate substrates [74, 84]. CYP ω -

hydroxylase isozymes metabolize EPA into ω / $(\omega-1)$ - hydroxyeicosapentaenoic acids (19- and 20-HEPE) and DHA into ω / $(\omega-1)$ -hydroxydocosahexaenoic acids (21- and 22-HDoHE) [85, 86]. CYP epoxygenases metabolize EPA into 5 regioisomeric epoxyeicosatetraenoic acids (5,6-, 8,9-, 11,12-, 14,15-, 17,18-EEQ) and DHA into 6 regioisomeric epoxydocosapentaenoic acids (4,5-, 7,8-, 10,11-, 13,14-, 16,17-, 19,20-EDP). The epoxy metabolites EEQ and EDP may then undergo further metabolism by epoxide hydrolase enzymes to corresponding diols.

To date, experimental data indicate the major CYP enzymes involved in metabolizing AA, including subfamilies CYP1A, 2C, 2E, 2J, 2U, 4A and 4F, accept EPA and DHA as substrates [84]. The CYP isozymes demonstrate differences in substrate preference as well regio- and stereoselectivities when metabolizing AA, EPA and DHA. Important cardiac CYP epoxygenase isoforms, CYP2C and CYP2J, primarily produce R,S-enantiomers of 17,18-EEQ and 19,20-EDP, except the specific isozymes CYP2C8 and CYP2D6 that favour producing S,R-enantiomers [87, 88]. Interestingly, CYP1A almost exclusively metabolizes EPA to 17(R),18(S)-EEQ and DHA to 19(R),20(S)-EDP metabolites. CYP4A and CYP4F isozymes metabolize EPA to 20-HEPE and DHA to 22-HDoHE, as well demonstrate epoxygenase activities toward EPA and DHA. The role of CYP isozymes in the metabolism of n-3 PUFA has been observed in dietary studies in which animals were supplemented with EPA and DHA. This resulted in elevating EPA/DHA levels and replacing AA in membrane phospholipids. Moreover, the endogenous epoxide metabolite ratio shifted from a predominance of EETs to increased EEQ and EDP [89]. Interestingly, 17,18-EEQ and 19,20-EDP were the predominant epoxy metabolites identified in the kidney, heart and lung. Nonetheless, specific alterations in metabolites follow the endogenous CYP profile, which

can occur in a tissue-specific manner. N-3 PUFA eicosanoids and their influence on cardiovascular function in health and disease is the focus of Chapter 1.4 of this thesis.

1.3. N-6 PUFAS AND CARDIOVASCULAR DISEASES

1.3.1. HETEs in cardiovascular disease progression

CYP-derived products of AA exhibit a diverse range of biological responses in the cardiovascular system. The “mid-chain” HETEs (5-, 8-, 9-, 11-, 12- and 15-HETE) are not well characterized but demonstrate inflammatory, angiogenic and hypertrophic properties, with 12- and 15-HETE shown to be involved in cardiac fibrosis and HF respectively [90, 91].

For the remainder of this section, I will focus on 20-HETE, the most well characterized endogenous HETE produced and 19-HETE, which is emerging as a potential cardioprotective treatment strategy (Figure 1.3).

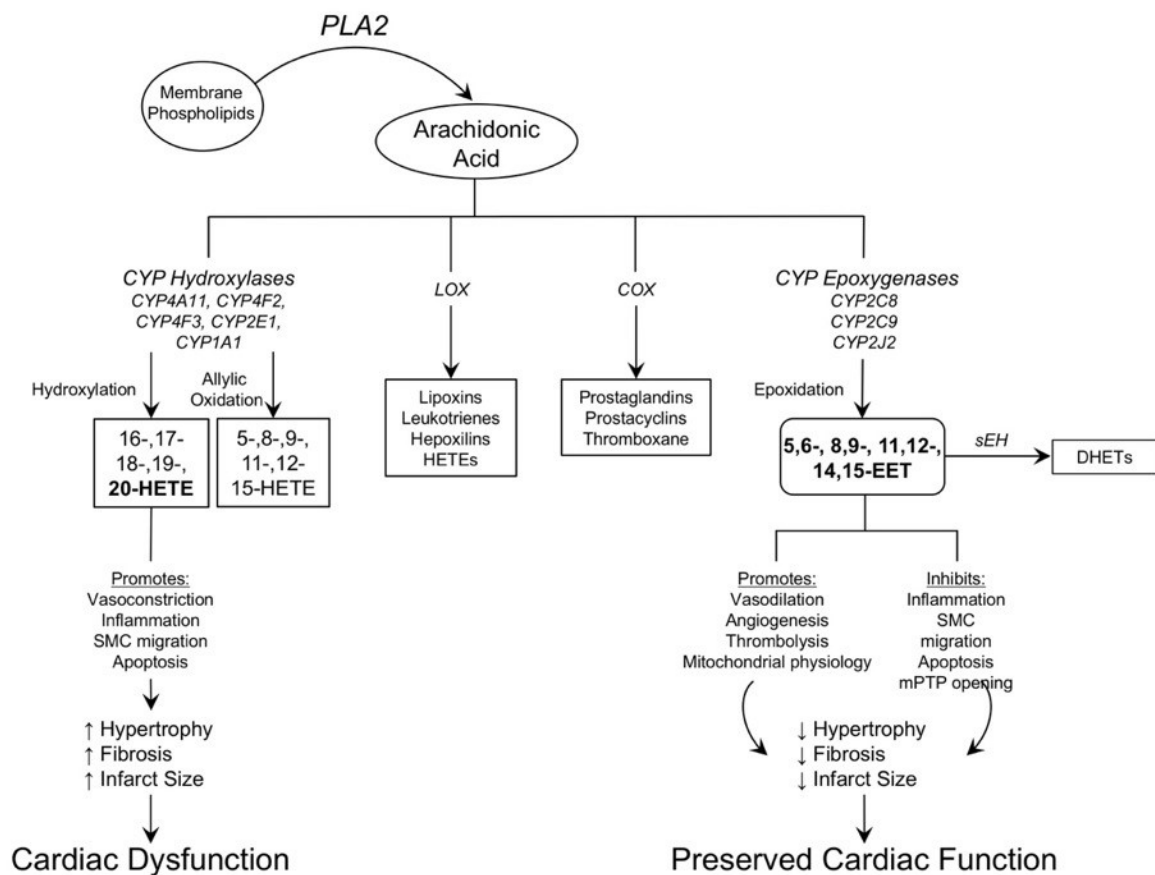


FIGURE 1.3. Schematic representation of the key CYP-derived metabolites of arachidonic acid and their primary known function within the heart.

1.3.1.1. 20-HETE and pathogenesis of CVD

The heart is significantly affected by vascular dysfunction, where a sustained increase in blood pressure may result in the development of left ventricular hypertrophy, myocardial ischemia and heart failure. The direct influence of 20-HETE towards blood pressure and hypertension indirectly impacts cardiac function [92]. During normal physiological states 20-HETE is a crucial mediator of the myogenic response that elevates transmural pressure and of the autoregulation of blood flow in the renal and cerebral circulation [93, 94]. In pathogenic states including hypertension, CHD and following ischemia reperfusion (IR) injury production of 20-HETE is elevated due to increased CYP ω -hydroxylases [94]. Increased 20-HETE triggers vasoconstriction of the cardiac vasculature in an endothelium-dependent manner directly impacting the cardiovascular system [94]. Studies designed to limit 20-HETE-induced hypertension in the renal system have demonstrated beneficial effects, which lead to reductions secondary cardiac injury [80, 95, 96]. Thus, understanding the direct role 20-HETE has in vascular dysfunction will provide insight into the cardiac injury.

The mechanistic actions of 20-HETE have been extensively reviewed [92, 97-99]. A brief summary of their actions is given Figure 1.4. 20-HETE is produced primarily in vascular smooth muscle cells (VSMCs), including the cardiac microvasculature [100, 101]. It may also be released from myeloid cells [102], neutrophils and platelets [103]. While endothelial progenitor cells (EPCs) can also produce 20-HETE, endothelial cells of the vasculature in most circulatory beds do not produce biologically relevant levels of 20-HETE [104]. Release of 20-HETE stimulates smooth muscle cell migration, proliferation, angiogenesis, inflammation and leads to endothelial dysfunction [94, 104-107]. 20-HETE

also mediates Na⁺ reabsorption in the renal tubules and thick ascending limb of Henle through its inhibition of Na⁺/K⁺-ATPase activity, and is thus a mediator of salt retention and intake [108, 109]. However, 20-HETE is most well-characterized as a potent vasoconstrictor, working through downstream effectors including protein kinase C (PKC), mitogen-activated protein kinase (MAPK) and c-src-type tyrosine kinase that inhibit BK_{Ca} conductance causing depolarization [110, 111]. Upon the inhibition of BK_{Ca} channels, Ca²⁺ movement through L-type Ca²⁺ channels escalates resulting in an elevated cellular [Ca²⁺] and enhancing vasoconstriction [112]. In small coronaries 20-HETE activates Rho kinase, further sensitizing the contractile apparatus to Ca²⁺ [113]. The complete regulation, metabolism and mechanism of action of 20-HETE is complex, with many other factors such as endothelin-1 (ET-1), Ang II, atrial natriuretic peptide (ANP), serotonin and nitric oxide (NO) mediating its release and downstream effects in the vasculature of the heart, brain, and kidney [114]. For instance ET-1, itself a potent vasoconstrictor, stimulates release of 20-HETE from the rat kidney [97, 115]. ET-1 stimulation of receptors ET_A and ET_B is coupled to CYP ω-hydroxylase production of 20-HETE in rat preglomerular arterioles, resulting in vasoconstriction and increases in blood pressure [115]. In rat neonatal cardiomyocytes, inhibiting 20-HETE synthesis hindered ET-1-driven secretion of ANP, indicating a clear interactive role for these endogenous autocooids in the heart [116].

There is a well-established relationship between 20-HETE production and NO, the major endothelial derived relaxation factor [117]. Many studies have validated the importance of NO-mediated vasodilation in the maintenance of normal vascular tone and blood pressure [118-120]. NO has both direct and indirect actions on VSMCs. Direct response to NO occurs secondarily to activation of guanylate cyclase and formation of cyclic

GMP (cGMP), ultimately cumulating in phosphorylation of myosin light-chain kinase and dilation of the vessel [121]. This mechanism has been demonstrated in many arteries including the aorta and coronaries [122-126]. Later studies demonstrated NO also works independently from its effects on cGMP; notably, NO inhibits vascular 20-HETE synthesis [122, 127, 128]. NO binds the heme group of the CYP1B, 2C and 4A families of CYP ω -hydroxylases, consequently inhibiting renal synthesis of 20-HETE [129]. This effectively removes the inhibition and depolarization of BK_{Ca} channels, the key mechanism of action of 20-HETE-mediated vasoconstriction [112, 128, 130]. Later studies have shown prostaglandin E₂ as a possible key mediator in this dichotomy of NO and 20-HETE vasoactivity [131]. Removing NO-mediated vasodilation with NO inhibitors actively up-regulates vasoconstrictive stimuli including 20-HETE in the renal and peripheral vasculature [120]. Inversely, 20-HETE also impedes NO regulation by uncoupling endothelial nitric oxide synthase (eNOS) and increasing ROS that scavenge NO and reduce its bioavailability [107, 132]. 20-HETE uncoupling of eNOS has been shown to be mediated through MAPK/IKK/NF- κ B pathways, ultimately encouraging endothelial activation and subsequent endothelial dysfunction that contributes to CVD [104, 106]. 20-HETE and NO act inversely to regulate vasoactivity, where NO is a crucial mediator of 20-HETE function in both the vascular endothelia and smooth muscle cells.

Considering this physiological role as a potent vasoconstrictor, research into 20-HETE has focused primarily on significant pathological effects in hypertension and blood pressure regulation. Indeed, the initial discovery of 20-HETE activity was as a key participant in the pathogenesis of hypertension in the spontaneously hypertensive rat (SHR) [133, 134]. 20-HETE has complex interactions with the renin-angiotensin system (RAS), a fundamental

regulator of blood pressure and a key target in hypertension. Experimental models of hypertension, including SHR and androgen-induced models have demonstrated 20-HETE can drive microvascular dysfunction and remodelling in an angiotensin converting enzyme (ACE)-independent manner [132, 135]. Yet, both 20-HETE-mediated induction of endothelial ACE or direct interaction with Ang II and its receptors activates RAS [136]. Furthermore, 20-HETE can concurrently increase Ang II levels and induce ACE and angiotensin II type 1 receptor expression in the kidneys [137]. Conversely, Ang II induces synthesis and release of 20-HETE in preglomerular vessels ultimately heightening its own pressor effects [138, 139]. 20-HETE mediates the effects of Ang II in the small coronary arteries through its interaction with Ras/MAP kinase pathways, and ultimately arbitrates the renal response to Ang II and development of subsequent hypertrophy [97, 99, 113]. Inhibiting either 20-HETE production or angiotensin II receptors significantly ameliorates 20-HETE promotion of hypertension [137]. These data suggest a complex network between 20-HETE, ACE, Ang II and the RAS system which, when dysregulated, can work in a synergistic manner to disrupt regulation of the cardiovascular-renal axis, promoting hypertension and CVD.

While most research has investigated the effects of 20-HETE in the vasculature, growing evidence suggests 20-HETE can directly target the heart. 20-HETE can specifically affect the heart through direct actions enhancing pathophysiological responses, such as the progression of HF, by influencing the development of cardiac hypertrophy and fibrosis. Experimental rat models of cardiac hypertrophy using isoproterenol (ISO) or doxorubicin (DOX)-induced cardiotoxicity have been correlated with increased 20-HETE formation in cardiac tissue [53, 140]. Cardiac fibrosis is the process by which increased collagen and other

extracellular matrices replaces the smooth muscle of the left ventricle (LV), reducing left ventricular compliance until eventually HF ensues [141]. While no studies have demonstrated a direct effect of 20-HETE on cardiac fibroblasts, it is proposed that the potent pro-inflammatory properties of 20-HETE, increasing local inflammatory cytokine and chemokine production, plays a role in the response [106, 142, 143].

Pharmacological inhibition of CYP ω -hydroxylase activity has provided insight into the adverse effects of 20-HETE toward cardiac function and injury. A major factor involved in the development of cardiac dysfunction following IR injury and associated with HF is the increased activation of myocardial apoptosis [144]. Early studies have demonstrated administration of CYP4A inhibitors 17-octadecynoic acid (17-ODYA) or *N*-methylsulfonyl-12, 12-dibromododec-11-enamide (DDMS) reduced the development infarct size in rat and canine models of IR injury [69, 145]. Recent support for these findings demonstrated the cardioprotective CYP ω -hydroxylase inhibitor dihydrotanshinone I reduced 20-HETE production and myocardial apoptosis following IR injury in rats [146]. Evidence suggests 20-HETE promotes apoptosis by activating the intrinsic mitochondrial pathway and increasing reactive oxygen species (ROS) production [147]. *In vitro* models in neonatal ventricular cardiomyocytes demonstrate that treatment with CYP ω -hydroxylase inhibitor *N*-hydroxy-*N'*-(4-butyl-2-methylphenyl)-formamidine (HET0016) has potent anti-apoptotic effects following culture with Ang II [148]. Interestingly, Ang II and 20-HETE interact to induce apoptosis in primary rat cardiomyocytes; inhibiting 20-HETE production negates the pro-apoptotic effect of Ang II [148]. CYP ω -hydroxylase inhibitor studies provide evidence for specific effects of 20-HETE in cardiomyocytes. Importantly, HETEs are incorporated into membrane lipids and released upon stimulation in a tissue-specific manner [139]. In

coronary endothelial cells, incorporation of 20-HETE into phospholipids had significant regulatory effects on vasomotor function in response to endothelial agonists [149]. Since most studies use CYP ω -hydroxylase inhibitors in order to assess 20-HETE function, the timing of inhibition to prevent release of stored 20-HETE becomes critical.

The adverse effects of 20-HETE in the myocardium may be also influenced by the specific disease state and comorbidity. 20-HETE production was increased in the hearts of streptozotocin (STZ)-induced diabetic rats, correlating with impaired functional recovery following IR [150]. No change in EET or dihydroxy-5Z,8Z,11Z,17Z-eicosatetraenoic acid (DiHETE) production was noted. Interestingly, both perfusion of the sEH inhibitor (sEHi) 1-cyclohexyl-3-dodecyl urea (CDU) or pre-treatment with the selective 20-HETE synthesis inhibitor HET0016 resulted in improved recovery in diabetic hearts; when both agents were given together, recovery was substantially greater than with the single drug [150]. Importantly, inhibiting ATP-sensitive K^+ channels with glibenclamide prevented these protective effects [150]. These data indicate that 20-HETE formation and increased EET metabolism may be crucial mediators of ischemic damage in diabetic cardiomyopathy. Intriguingly, in a rat model of metabolic syndrome elevated 20-HETE unexpectedly impaired collateral growth contrary to its known pro-angiogenic properties [151]. In this study, a series of repetitive ischemic events coupled with metabolic syndrome resulted in increased 20-HETE levels triggering excessive neutrophil activation eventually encouraging endothelial dysfunction and apoptosis. Antagonism of 20-HETE in these rats restored collateral formation [151]. These data suggest targeting the formation of 20-HETE as a viable cardioprotective strategy in diabetic patients also at risk for MI, but that care needs to be taken when faced with comorbidities such as metabolic syndrome where the underlying

disease state crucially influences protective strategies. Thus, understanding the unique mechanism of 20-HETE in specific disease states is crucial for the use of ω -hydroxylase inhibitors as therapeutics.

Targeting 20-HETE synthesis and function remains a primary method by which researchers seek to ameliorate its vasoconstrictive and hypertensive effects, and thereby reduce CVD. Reducing 20-HETE production confers significant whole-body protection against CVD, primarily by reducing cardiotoxic pro-inflammatory and hypertensive effects. The evidence demonstrates that local production of 20-HETE in the heart indeed produces direct cardiac effects outside of its renal function. While many of these new studies are *in vitro*, the development of cardiac-specific inhibitors of 20-HETE or targets of specific receptors in the future may allow for treatment options for patients with extensive comorbidities, such as renal disease.

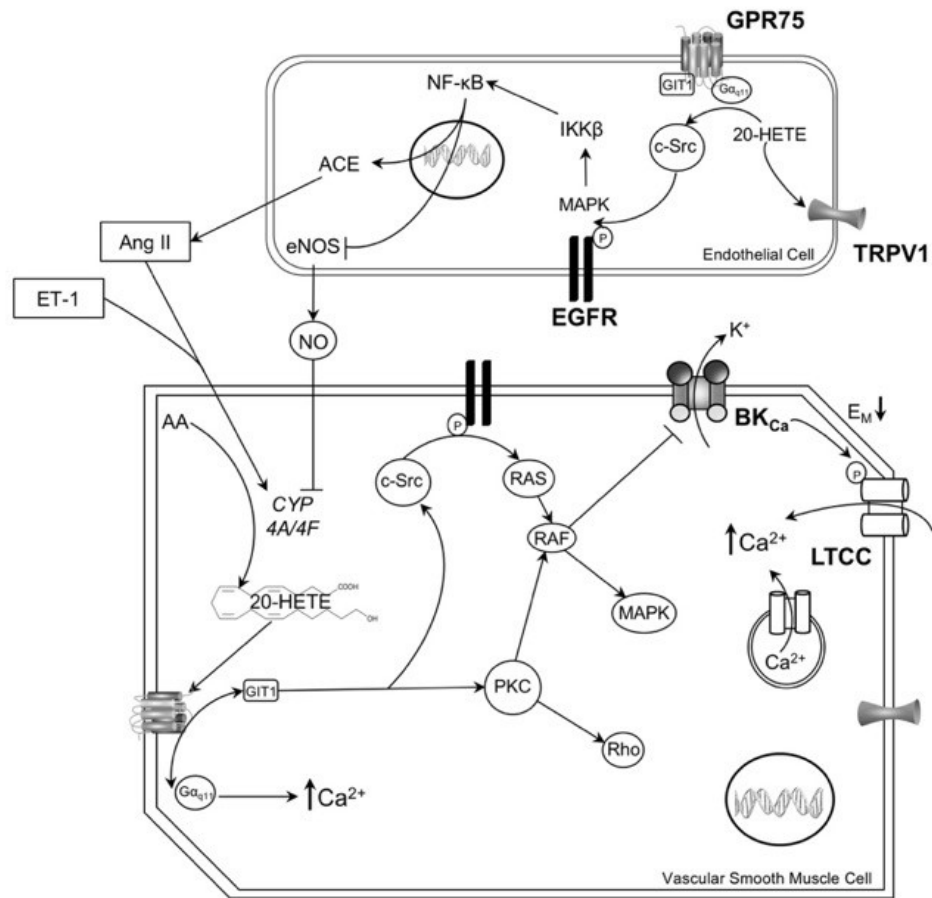


FIGURE 1.4. A schematic representation of the main signalling mechanisms of 20-HETE found in vascular endothelial and smooth muscle cells. EGFR (endothelial growth factor receptor); BKCa (large Ca²⁺-sensitive K⁺ channel); LTCC (L-type calcium channel); eNOS (endothelial nitric oxide synthase); EM (membrane potential); Rho (rho kinase); ET-1 (endothelin-1); Ang II (angiotensin II); ACE (angiotensin converting enzyme).

1.3.1.2. 19-HETE: an emerging cardioprotective n-6 PUFA

The formation of 19-HETE in the rat liver and heart has been attributed to CYP2E1 [77] and CYP4A [152] isoforms. In mice, CYP2C and CYP2J subfamilies are primarily responsible for the formation of 19-HETE [153, 154]. Induction of CYP2E1 with isoniazid results in increased production of 19-HETE in the rat liver [77, 152, 155]. In the kidney, 19-HETE contributes to the regulation of renal function by stimulating renal cortical Na⁺/K⁺-ATPase activity, which is essential for transtubular transport processes and vasodilating renal arcuate arteries [156-158]. Interestingly, early evidence suggested that 19-HETE counteracted the effects of 20-HETE in the kidney, where 19-HETE inhibited 20-HETE mediated vasoconstriction in renal interlobular arteries [90]. Furthermore, increased arterial sensitivity to phenylephrine, a vasoconstrictor, in SHR was attributed to a vasoregulatory imbalance produced by a deficit in vascular CYP2E1-derived products, including 19(R)-HETE and 18(R)-HETE [159]. This deficit in vascular production of 19-HETE in SHR facilitated the sensitizing action of 20-HETE on agonist-induced vasoconstriction and thus increased vascular reactivity [159]. The addition of 19(R)-HETE *ex vivo* to bovine aortic endothelial cells reversed 20-HETE impaired relaxation [105]. Interestingly, 19(R)-HETE antagonised 20-HETE-mediated endothelial dysfunction without itself affecting NO or superoxide production [105].

More recent studies have begun to analyse the effect of 19-HETE in cardiac disease progression, such as hypertrophy and HF. In a model of pressure-induced cardiac hypertrophy, formation of 20-HETE increased while 19-HETE formation decreased, indicating a possible role for these HETEs in hypertrophic progression [51]. In a follow-up study using human ventricular cardiomyocytes 19-HETE was able to effectively reverse the

hypertrophic effect resulting from Ang II treatment [160]. Interestingly, isoniazid was shown to downregulate CYP2E1 expression in the heart in contrast to its role in the liver, as well as shift metabolism to 19-HETE over the more favoured CYP metabolites, the EETs and 20-HETE [160]. This study suggested 19-HETE is a cardioprotective agent in Ang II mediated cardiac hypertrophy in part through its role as a 20-HETE antagonist.

A recent retrospective case-control study found patients with acute coronary syndrome (ACS) had higher levels of 19-HETE compared to patient controls without coronary heart disease (CHD) [161]. Blood plasma samples from the ACS patients demonstrated levels above 0.13ng/ml of 19-HETE correlated with improved prognosis, including decreased risk of major adverse cardiovascular events following treatment with coronary artery bypass and stenting [161]. 19-HETE was also found in hypertrophic myocardial tissue, suggesting it may play a role in cardiac hypertrophy related to ACS [161]. While 19-HETE may be a useful biomarker, it is too unstable to chronically administer. Targeting the upregulation of 19-HETE is complicated by the fact that CYP4A also metabolizes AA to 20-HETE, effectively negating any cardioprotective effect. More research needs to be done on the specifics of the HETEs in cardiac disease progression, however these emerging data indicate they have the potential to be useful in targeted cardioprotective strategies and in predicting disease progression.

1.3.2. *EETs in cardiovascular health and disease*

It is well established that CYP epoxygenase metabolites of AA, EETs, act as lipid mediators eliciting numerous biological responses in both cardiac and extra-cardiac tissues. Within the cardiovascular system the EETs demonstrate potent anti-inflammatory, vasodilatory, anti-apoptotic, pro-angiogenic, SMC anti-migratory and mitochondrial effects

[31]. EETs display both acute and chronic effects in multiple models of CVD, but the underlying mechanisms have not been fully elucidated [162, 163]. Human studies demonstrating associations between genetic polymorphisms in CYP epoxygenase and sEH enzymes with the risk of developing CVD provide insight into the role EETs have in the heart [162]. This section will discuss the effects of CYP-derived EETs within the heart (Figure 1.5).

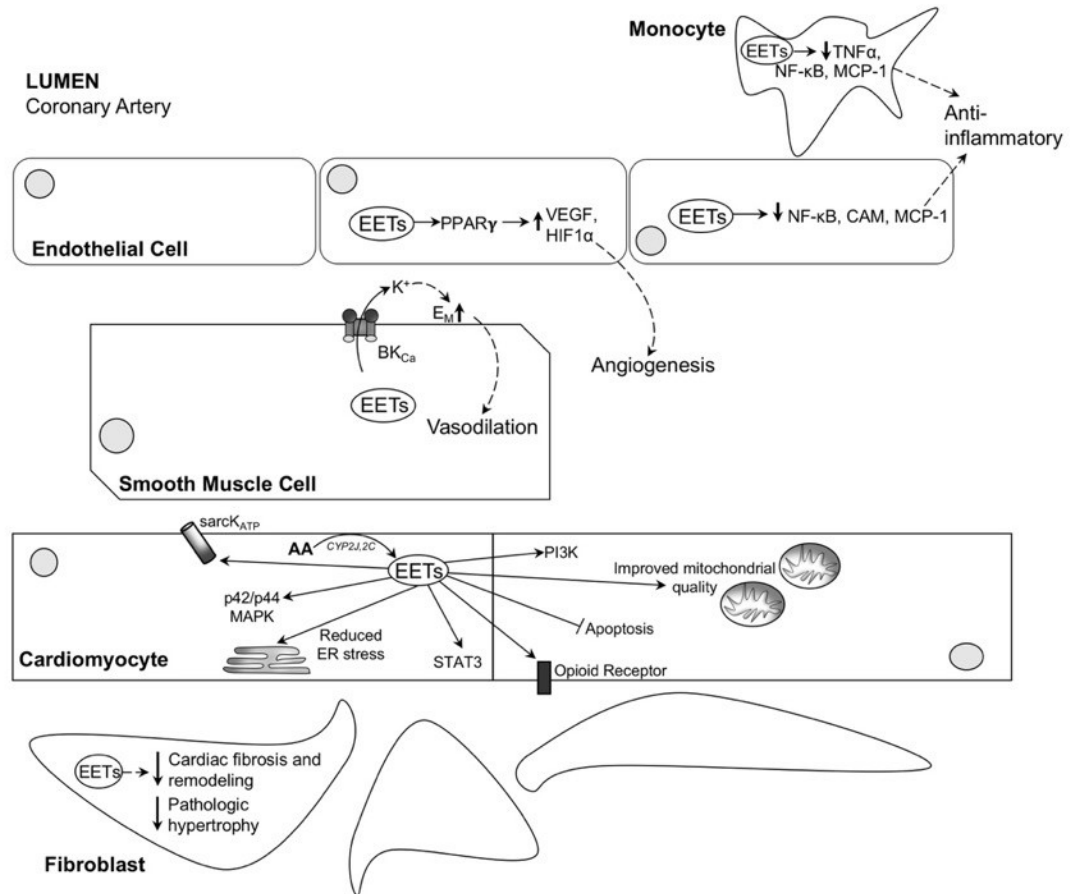


FIGURE 1.5. A schematic representation of the main signalling mechanisms for EETs found within the heart and their primary biological activities. BKCa (large Ca²⁺-sensitive K⁺ channel); EM (membrane potential); VEGF (vascular endothelial growth factor); HIF1 α (hypoxia inducible factor-1-alpha); TNF- α (tissue necrosis factor-alpha); MCP-1 (monocyte chemoattractant protein-1); sarcKATP (sarcolemmal ATP-dependent K⁺ channel); CAM (cellular adhesion molecule). Adapted from Oni-Orisan, A., Alsaleh, N., Lee, C.R., Seubert, J.M., 2014.

1.3.2.1. EETs and mitochondrial protection

Mitochondria are the primary cellular fuel source for the cardiac contractile apparatus regulating calcium homeostasis, cell death and cell survival [164]. Ischemic injury causes irrevocable mitochondrial damage leading to increased necrotic and apoptotic cell death and subsequent cardiac dysfunction [165]. Prolonged ischemic insult causes calcium overload, high inorganic phosphate [Pi] and decreased adenosine nucleotides in the cell; following reperfusion, the mitochondria experience Ca^{2+} overload and severe oxidative stress [166]. These effects cumulate in the opening of the mitochondrial permeability transition pore (mPTP), allowing molecules $<1.5\text{kDa}$ to freely enter the mitochondria [165, 166]. The accumulation of these molecules and the onslaught of oxidative stress ultimately results in mitochondrial swelling and dysfunction, permanent ATP loss, significant cell death and infarct formation [165]. Maintenance of an electrochemical gradient is critical to ATP production and collapse of the mitochondrial membrane potential ($\Delta\psi_m$) is correlated with mPTP opening, where reduced $\Delta\psi_m$ can trigger mPTP opening upon reperfusion [167]. Targeting mPTP opening with various agents is an approach employed to prevent ischemic injury and reduce infarct size expansion [168].

Initial studies suggested the cardioprotective response observed in mice overexpressing CYP2J2 or deletion of sEH was associated with reduced mitochondrial damage and preserved function [25, 169, 170]. These *in vitro* experiments demonstrated exogenous EETs slow the dissipation of $\Delta\psi_m$ and opening of the mPTP in rat cardiomyocytes and H9c2 cells, an effect that was abolished upon co-treatment with EET antagonist 14, 15-epoxyeicosa-5(Z)-enoic acid (14,15-EEZE) [23, 170, 171]. Evidence from non-cardiac cells provides supportive data demonstrating mitochondrial protective effects of EETs. In rat neonatal

hippocampal astrocytes, 11,12- and 14,15-EET attenuated mitochondrial fragmentation, preserved $\Delta\psi_m$ and improved respiration following treatment with amyloid- β protein [172]. Cytotoxic effects from photodynamically activated chemotherapeutic agent, SLO17, that caused the collapse of $\Delta\psi_m$ in human lung fibroblasts was attenuated by 11,12-EET [173]. However, it remains unknown how EET-mediated events preserve the $\Delta\psi_m$ and/or whether the preservation is through a direct or indirect effect on the mitochondria. These data provide a role for EETs in minimizing the loss of $\Delta\psi_m$ and limit mPTP opening, thus contributing to overall cardiac protection under stress. Recent data propose a general hypothesis that EET-mediated events are involved in regulating mitochondrial quality. In a starvation model using cardiac HL-1 cells, the mitochondrial pool found in EET-treated cells were significantly healthier compared to controls. While the quantity of mitochondria was similar between EET-treated and control cells, the treated cells had preserved mitochondrial ultrastructure, respiration and evidence of mitochondrial biogenesis, suggesting a cascade of reactions directed to maintaining a healthy pool of mitochondria promoting cell survival [174]. Recent *in vivo* data demonstrated mitochondrial preservation in *Ephx2*^{-/-} mice is associated with physiological recovery following cardiac ischemic injury [175]. In a murine model using permanent ligation of the left anterior descending coronary artery model (LAD), genetic or pharmacological inhibition of sEH maintained mitochondrial form, function and bioenergetics, preserved cardiac insulin sensitivity, and attenuated LV dysfunction post-MI [175]. Together, these data suggest EET-mediated mitochondrial protection occurring *in vitro* may translate into improved cardiac function in ischemic animal models.

1.3.2.2. Role of EETs in myocardial ischemia and ischemia reperfusion injury

Myocardial ischemic injury occurs when coronary flow is obstructed, resulting in widespread damage and remodelling of the heart. MI is characterized by extensive fibrosis, remodeling, inflammation and myocardial apoptosis that eventually progresses to HF and mortality. One common method of inducing MI *in vivo* is through LAD occlusion [176]. This results in a clear and defined infarct region and mimics much of the injury and functional deficits seen post-MI in humans. *Ex vivo* models include isolated Langendorff or working heart models to induce IR injury. *In vitro*, hypoxia/reoxygenation (HR) models are typical, although not exactly equivalent to ischemic injury since lack of blood flow *in vivo* comes with other consequences. Evidence from multiple laboratories and species has demonstrated that EETs provide protection to hearts subjected IR injury [25, 169, 175, 177-181] As potent lipid mediators, EETs have been shown to elicit numerous cardioprotective mechanisms. Acutely, EETs attenuate apoptosis, promote pro-survival signalling and preserve mitochondrial structure and function. Chronically, EETs can prevent adverse remodelling and help sustain systolic function.

Different approaches to regulate EETs have demonstrated the cardioprotective role they play toward IR injury. For example, Langendorff isolated heart experiments using cardiomyocyte overexpression of CYP2J2 demonstrated a robust cardioprotective response, which was abrogated with CYP epoxygenase inhibitor *N*-methylsulphonyl-6-(2-propargyloxyphenyl)hexamide (MSPPOH) suggesting a role for EETs [169]. Further studies using the EET antagonist 15-EEZE in *Ephx2*^{-/-} mice supported the role of EETs in providing cardioprotection against IR injury [25]. Moreover, isolated mouse hearts treated with directly with EETs or a dual-acting compound possessing EET mimetic and sEH inhibitory properties had reduced infarct size and preserved left ventricular developed

pressure (LVDP) compared to controls [182]. While the underlying protective mechanism of EETs is unknown, results from rat, mouse and canine models have provided consistent evidence suggesting activation of the K_{ATP} channels and phosphatidylinositol-3 kinase (PI3K) signalling are involved in EET-mediated cardioprotection [25, 178, 183]. Cardiac sarcolemmal K_{ATP} channels regulate ionic homeostasis under conditions of metabolic stress and have been shown to provide cardioprotective effects towards IR injury [184, 185]. Sarcolemmal K_{ATP} channels can be activated during cardiac ischemia when cytoplasmic ATP is depleted affecting membrane excitability. Activation of K_{ATP} channels during ischemia leads to shortening of the cardiac action potential and opposes membrane depolarization [186] consequently reducing intracellular calcium overload thus limiting the activation of phosphatase enzymes and reducing contractile dysfunction [187]. PI3Ks are members of a family of lipid kinases that phosphorylate the 3'-hydroxyl group of phosphatidylinositol (PIP) and PIP_2 at the third position, to form PIP_2 and PIP_3 , which activate downstream kinases such as AKT and glycogen synthase kinase 3 ($GSK-3\beta$), which during IR injury results in reduced cell death and infarct size [188].

The Kir6.2 subunit found in K_{ATP} channels is critical for channel-gating behaviour, regulating K^+ conduction and ATP-dependent inhibition [185, 189]. The C-terminal region of the Kir6.2 subunit contains overlapping binding sites for both PIP's and EETs, which reduces channel sensitivity to ATP resulting in activation of K_{ATP} channels [189-191]. Thus, this suggests EETs might activate K_{ATP} channels by either direct binding to the C-terminal or through activation of PI3K. Perfusion of 11,12-EET to Kir6.2 deficient mice failed to improve post-ischemic recovery, however increased levels of p-Akt were still observed suggesting activation of PI3K, and an important role for sarcolemmal K_{ATP} channels. Patch-

clamp experiments demonstrated that 11,12-EET could not activate *pmK_{ATP}* currents in myocytes pre-treated with class-I PI3K inhibitor PI-103, indicating PI3K α as the pertinent isoform involved in activating *K_{ATP}* channels [23, 192].

There have been numerous reports demonstrating the role of other channels and signalling pathways in EET-mediated cardioprotection. For instance, EETs administered during pre-conditioning suggested eNOS signalling pathways and *mitoK_{ATP}* activation were important components of the cardioprotective response [193]. Furthermore, inhibition of the signal transducer and activator of transcription 3 (STAT3) pathway abolished EET-mediated cardioprotection [194]. Co-treatment of 14,15-EET or sEHi 12-(3-adamantan-1-yl-ureido) dodecanoic acid (AUDA) with the STAT3 inhibitor attenuated the EET-mediated protective effect toward cardiomyocyte viability and reduced infarct size [194]. An initial study from Terashvili et al. demonstrated that 14,15-EET produces dose-dependent analgesia in rats, mediated through the stimulation of μ - and δ - opioid receptors and the activation of β -endorphin and δ -active peptide Met-enkephalin [195]. Gross et al. demonstrated *in vivo* that both 11,12-EET and 14,15-EET attenuated cardiac infarct size following LAD ligation in a mechanism dependent on the release of Met-enkephalin and subsequent activation of the δ -opioid receptor [196]. This was supported in Langendorff experiments where treatment with naloxone, a nonselective opioid antagonist, attenuated the protective effect of 11,12-EET toward LVDP and infarct size [196]. EET-mediated cardioprotective responses occur through a multitude of pathways, many of which remain to be fully elucidated.

Intriguingly, a recent study has suggested direct cardiac action of EETs with heme oxygenase-1 (HO-1) and subsequent angiogenic upregulation is involved in EET-mediated cardioprotection. Administering an EET agonist after the onset of post-MI cardiac

remodelling effectively attenuated cardiac dysfunction post-MI [197]. The EET agonist, (S)-2-(11-(nonyloxy)undec-8(Z)-enamido)succinic acid (NUDSA), stimulated myocardial angiogenesis by interacting with HO-1 and subsequently stimulating the canonical (β -catenin dependent) Wnt pathway, crucial to angiogenesis through its stimulation of vascular endothelial growth factor (VEGF) and other pro-angiogenic mediators [197]. EETs have long been understood to interact with HO-1 [198]. EETs increase HO-1 production in the aortic endothelium, mediating systemic arterial vasodilation and endothelial function [199, 200]. HO-1 and EETs target nuclear factor kappa B (NF- κ B) signalling and have been implicated in cardioprotection following ischemic injury [197]. Induction of HO-1 in infarcted hearts resulted in reduced apoptosis, increased cardiomyocyte proliferation and repair and decreased perivascular fibrosis contributing to an overall decrease in adverse ventricular remodeling [201]. Evidence suggests EET-mediated protective responses involve HO-1, as the HO-1 inhibitor stannic mesoporphyrin abolished post-MI EET-mediated cardioprotection [197]. The novel study from Cao et al. demonstrates the protective synergy between EETs and HO-1 in mediating cardioprotective myocardial angiogenesis post-MI is mediated through increased Wnt signaling [197]. However, there is conflicting evidence as to whether targeting the stimulation of the Wnt1 pathway is an appropriate strategy post-MI. A recent study showed that inhibiting Wnt1 signalling directly after MI actually resulted in improved cardiac function, as well as reduced remodeling and infarct size [202]. Moreover, increased activation of β -catenin and the Wnt pathway in endothelial cells was demonstrated to induce HF [203]. The regulation of Wnt signaling post-MI is complex and often contradictory, with both antagonism of Wnt and up-regulation of the upstream β -catenin demonstrating cardioprotective effects [204]. Understanding the connection between EETs

and the Wnt signaling pathway warrants more investigation before definitive conclusions can be made.

1.3.2.3. EET-mediated regulation of cell death

Early evidence demonstrated that 14,15-EET inhibited apoptosis via PI3K-dependent pathway in LLCPKc14 cells [205]. Since these initial studies, there has been a significant amount of data demonstrating the role of EETs in reducing cellular injury and damage through regulation of cell death pathways [206, 207]. For example, human endothelial cells treated with 8,9- or 14,15-EET followed by serum deprivation exhibited decreased binding of annexin V and reduced caspase-3 activity compared to controls [208]. Similar reductions in apoptosis following treatment with 11,12- and 14,15-EET have been revealed in human pulmonary artery endothelial cells and astrocytes using HR models [209, 210]. CYP2J2 overexpression in bovine aortic endothelial cells decreased caspase-3 activity following treatment with tumor necrosis factor alpha (TNF- α) [211], while TUNEL staining of renal samples from cisplatin-treated *Ephx*^{-/-} mice and mice co-treated with sEHi AR9273 showed reduced necrosis and apoptosis compared to controls [212]. These protective effects were mediated by decreased caspase-3 activation, decreased ROS formation and overall decreased activation of the intrinsic apoptotic pathway [213]. Moreover, several studies indicate these effects are mediated through MAPK and PI3K [177, 207, 211, 212]. The anti-apoptotic effects of EETs are particularly crucial in CVDs, where cardiomyocyte loss cannot be replenished by normal cell division resulting in extensive fibrosis.

In the heart, cardiomyocyte apoptosis occurs rapidly following IR injury and is a defining factor of infarct size and ultimately heart function post-injury [214]. In an *in vitro* study using HL-1 cells and ventricular neonatal cardiomyocytes, pre-treatment with 8,9-,

11,12- and 14,15-EET demonstrated increased cell viability with decreased annexin V binding, nuclear fragmentation and caspase-3 activity compared to controls following HR [177]. Importantly, 11,12-EET improved cell viability and mitochondrial membrane stability, and decreased caspase-3 activity and apoptotic indices following HR in human tissues with CVD, indicating a preservation of these effects across species [23]. These effects were mediated through activation of PI3K and K_{ATP} channels [23]. Together these data indicate a primary mechanism of EET-mediated cardioprotection is through the attenuation of cell death pathways, particularly apoptotic extrinsic and intrinsic pathways.

The extent of cellular insult and the specific survival mechanism(s) activated are fundamental determinants of the fate of the cell. Involvement of EETs in regulating cell death pathways has historically been limited to their anti-apoptotic effect, however, emerging research has suggested a role in autophagy. Cell experiments in HL-1 cardiac cells and neonatal cardiomyocytes demonstrated EET-mediated events increase viability by enhancing an autophagic response and shifting the cell death pathway toward survival [215]. In terminally differentiated cells such as cardiomyocytes autophagy is particularly crucial in preserving mitochondrial integrity and cell survival under stress conditions [216]. EET-mediated autophagic response involved sarcolemmal K_{ATP} channels and increased phosphorylation (activation) of 5' adenosine monophosphate-activated protein kinase (AMPK); moreover, EETs protected mitochondrial function [215]. It was speculated that the EET-mediated events preserved the mitochondrial pool by promoting autophagy to removed damaged mitochondria. Conversely, in a mouse model of obesity inhibition of sEH with trans-4-(4-[3-(4 trifluoromethoxyphenyl)ureido]cyclohexyloxy) benzoic acid (*t*-TUCB) attenuated the increase in autophagy proteins LC3-II, Atg12 and Atg5 in the liver and adipose

tissue [217]. The limited EET data suggest enhancing the autophagic machinery may be important for proper function of terminally differentiated cardiomyocytes; however, there is a need for a better understanding of this area of research.

1.3.2.4. Biological actions of EETs in inflammatory cells and cardiac fibroblasts

Inflammation is potent driver of cardiac remodelling and fibrosis that contribute to overall LV dysfunction [218, 219]. In acute myocardial infarction (AMI), bone-marrow derived neutrophils and monocytes can infiltrate the damaged myocardium and ultimately encourage proliferation of fibroblasts and development of fibrosis [220]. Cardiac fibroblasts also release growth factors and cytokines that contribute to maladaptive remodelling in CVD [221]. EETs oppose monocyte and neutrophil infiltration in the vasculature and can inhibit NF- κ B, ultimately abrogating endothelial and monocyte inflammation, although these effects have not been demonstrated in the coronary vasculature post-MI [222-224]. *In vivo*, sEH inhibition obstructs macrophage infiltration in peri-infarct regions, although not the infarct region of the myocardium in an LAD model of MI [225]. sEH inhibition was also found to prevent the proliferation, differentiation, migration and secretion of cardiac fibroblasts [225, 226]. In neonatal cardiomyocytes, EETs improved cell viability and mitochondrial function following treatment with potent inflammatory molecule, lipopolysaccharide (LPS) [227]. Interestingly, these protective effects were abolished with inhibitors of proliferative peroxisome activated receptor γ (PPAR γ), suggesting the vital role of this receptor in EET-mediated anti-inflammation [227]. Models using CYP2J2 overexpression have demonstrated preserved cardiac function following treatment with TNF- α when co-treated with EETs [83]. Moreover, CYP2J2 expression in rAAV-CYP2J2 mice protected against cardiac dysfunction following LPS injection [228]. EETs contribute

to this process by acting through PPAR γ and HO-1 pathways reducing M1 macrophage polarization and infiltration, and inhibiting NF- κ B ultimately reducing inflammatory cytokine production [228]. In a model of non-ischemic HF, α MHC-CYP2J2-Tr mice exhibited significantly decreased cardiac fibrosis and cardiac inflammation following treatment with Ang II or ISO [229]. In this model 14,15-EET treatment of rat cardiomyocytes suppressed NF- κ B nuclear translocation, confirming *in vitro* a direct role for EETs inhibition of Ang II- or ISO-stimulated inflammation [229]. Inflammation and fibrosis are important to the overall pathogenesis of CVD. Taken together, these data suggest EETs act in a myriad of ways to protect the heart of ischemic and non-ischemic cardiomyopathies.

1.3.2.5. Role of endothelial-derived EETs in cardiovascular diseases

Endothelial cells that form the endocardium, the interior lining of blood vessels and cardiac valves, have been shown to express both CYP epoxygenases and sEH enzymes [230-232]. The role of CYP-derived eicosanoids originating from blood vessels in regulating vascular function has been studied for many years and is the subject of many excellent reviews [28, 233-235]. Early research revealed that EETs may regulate VSMC tone by activating BK $_{Ca}$, causing a hyperpolarization of VSMCs and subsequent vasodilation in the coronary vessels, considered an endothelium-derived hyperpolarizing factor (EDHF) response independent of NO or prostaglandins [236-243]. The vasodilation of endothelial-derived EETs seems to be more potent in the resistance coronary arterioles than in the larger conduit coronary arteries [244]. The current understanding suggests the involvement of other channels and ions, such as Ca $^{2+}$, K $^{+}$ channels, Na $^{+}$ /K $^{+}$ -ATPase and gap junctions [234]. Indeed, EETs have been investigated in co-morbidities such as hypertension, diabetes and atherosclerosis, yet further *in vivo* and clinical studies are needed to fully elucidate the extent

to which their effects on VSMCs are involved in heart disease [236].

Recently the role of endothelial-derived EETs has been investigated in coronary reactive hyperemia (CRH), a protective cardiac reaction to ischemia that results in temporarily increased blood flow to the heart to improve nutrient and oxygen delivery as well as waste removal [245]. Isolated hearts of Tie2-sEH-Tr mice displaying endothelial over-expression of sEH demonstrated decreased CRH following ischemia and shifts in the CYP ω -hydroxylases as measured by the oxylipin profiles [246]. Treatment with an sEHi and inhibiting CYP ω -hydroxylases restored CRH in these hearts, although not to control levels [246]. Taken together these data suggest that simultaneously inhibiting sEH and CYP ω -hydroxylase metabolism may synergistically enhance CRH following acute ischemia [246]. Interestingly, similar results were seen in an isolated heart model using a whole-body knockout of sEH, wherein these results were partially mediated by PPAR γ [247]. Although much further research is needed, these data suggest a novel role for endothelial-derived EETs in CVDs.

Angiogenesis is particularly important to ischemic heart disease, where it is associated with protective revascularization in the chronic period following acute MI [248]. Endothelial-derived EETs are documented pro-angiogenic mediators however the effects and mechanisms are not fully understood [249-252]. Evidence from *in vitro* experiments has demonstrated different signalling pathways may be involved in EET-mediated cell proliferation and angiogenesis including epidermal growth factor receptor (EGFR), Akt, MAPK, FOXO1/FOXO3a and cyclin-dependent kinase (CDK) inhibitor p27^{kip1} [251-255]. In a rat model of hind-limb ischemia overexpression of CYP2C11 or CYP2J2 increased muscle capillary density promoting an angiogenic phenotype [254]. In addition, increased

capillary tube formation was observed when isolated endothelial progenitor cells (EPCs) from acute MI patients treated with a sEHi [256].

Investigation into CYP-derived EETs originating from endothelial cells was accomplished in mice with Tie2-promoter-driven endothelial expression of CYP2J2, CYP2C8 and sEH [257]. Interestingly, endothelial-derived EETs did not offer protection against IR injury, differing significantly from cardiomyocyte-derived EETs. Overexpression of transgenic CYP2J2 or sEH did not change LVDP or infarct size following IR injury suggesting endothelial-derived EETs do not exert a significant impact on acute myocardial recovery. Moreover, endothelial overexpression of CYP2C8 resulted in a worsening of the LVDP and increased infarct size compared to controls, which was attributed to increases in ROS levels and cardiotoxic LA-derived metabolites [257].

An optimally functioning heart requires numerous different cell types to contribute to structural, biochemical, mechanical and electrical properties. This includes cardiomyocytes, endothelial cells, epicardial cells, pacemaker cells, Purkinje fibres, fibroblasts (that make up >50% of cell population) and smooth muscle cells [232]. The majority of research investigating the effects of EETs on overall cardiac function has focused primarily on cardiomyocytes. As such, there is limited knowledge regarding the importance of EETs in other cardiac cells.

1.3.2.6. EET-mediated cardioprotection

Following the acute phase of recovery, the post-ischemic heart undergoes extensive remodelling, which is marked by inflammation and cardiomyocyte apoptosis. Since the heart has limited regenerative capacity, these cells are replaced by a fibrotic scar that while maintaining cardiac structural integrity in turn contributes to extensive cardiac hypertrophy,

stiffening, and LV dysfunction, ultimately severely affecting cardiac function [258]. Fibrotic scar formation predisposes patients to electrical conductance abnormalities, arrhythmias, LV rupture and a higher risk for sudden cardiac death. Maladaptive remodelling is associated with worse prognosis following MI, and many patients progress to HF even after surviving MI. Chronic studies analysing the effects of EETs on long-term endpoints post-MI have demonstrated beneficial effects. An initial mouse study administered an sEHi 3 days before undergoing LAD ligation for 45 minutes, followed by 3-week reperfusion and demonstrated these mice had reduced fibrosis, were less prone to arrhythmias and had improved overall systolic function [259]. A limitation in the study was the administration of the sEHi before the onset of ischemic injury, making it unable to determine whether the protective effects were a result of the prevention of chronic maladaptive remodelling or from beneficial acute effects, such as a reduction of infarct size. To address this issue, one study administered sEHi, AUDA, at distinct time points after LAD ligation in which one group received therapy 8 days post-MI for 42 days and second group received therapy 47 days post-MI for 3 days [260]. Both regimens improved LV ejection fraction but only chronic treatment demonstrated marked preservation of diastolic function [260]. These effects were attributed to augmentation of EET bioavailability arising from sEH inhibition [260]. A study using male rats treated with an sEHi, (N-((4-bromo-2-[(trifluoromethyl)oxy]phenyl)methyl)-1-[4-methyl-6-(methylamino)-1,3,5-triazin-2-yl]-4-piperidinecarboxamide) GSK2188931B immediately following permanent LAD occlusion exhibited beneficial anti-remodeling effects such as reduced inflammation, reduced hypertrophy, reduced ventricular fibrosis and maintained systolic function 5 weeks post-MI [225]. These effects were independent of collagen deposition and the reduction in fibrosis was not associated with increased risk of

LV rupture [225]. The beneficial effects of sEH inhibition toward adverse cardiac remodelling was demonstrated in two different animal models, ischemic cardiomyopathy and pressure-overload hypertrophy. In these studies, the sEHi, 1-Trifluoromethoxyphenyl-3-(1-Propionylpiperidine-4-yl)Urea (TPPU), significantly reduced the proliferative capacity, percentages and activation of cardiac fibroblasts three weeks following MI, significantly attenuating cardiac fibrosis [226]. While these studies do not directly address all the potential epoxy lipids involved, they importantly highlight the beneficial effects obtained by inhibiting sEH towards long-term adverse cardiac effects.

1.3.3. *EETs in non-ischemic cardiomyopathy*

In broad terms, non-ischemic cardiomyopathy (NICM) is myocardial injury leading to arrhythmia, ventricular dysfunction, HFHF and mortality that is not directly associated with acute MI [261]. Causes of NICM are complex and varied including drug toxicity, genetic predisposition, infection, haemodynamic pathology and immunologic abnormalities [261]. Several models are often employed to induce NICM in *in vivo*, such as transverse aortic constriction (TAC), a surgical model used to stimulate pressure-induced HF, or infusion of Ang II or ISO to induce cardiac hypertrophy and HF. EETs have demonstrated significant cardioprotective effects in models of NICM unrelated to their use of anti-hypertensives. In this section, we discuss the effects of EETs toward the development of NICM, including the attenuation of cardiac hypertrophy, arrhythmia, cardiac fibrosis and myocardial apoptosis.

1.3.3.1. EETs have multiple protective effects against non-ischemic cardiomyopathy

A range of experimental approaches investigating the importance of the CYP/sEH pathway in non-ischemic cardiomyopathies suggests a beneficial role toward cardiac

hypertrophy and arrhythmias. For example, infusion of Ang II into mice increased the expression of sEH and resulted in cardiac hypertrophy, which was attenuated by inhibition of sEH [262]. In a TAC mouse model sEH inhibition abrogated the development of cardiac hypertrophy and decreased cardiac susceptibility to ventricular arrhythmias [179]. Similarly, *Ephx*^{-/-} mice that underwent either TAC-induced or Ang II-induced hypertrophy demonstrated preserved cardiac function compared to controls [180]. In addition, the *Ephx2*^{-/-} mice displayed stable sinus rhythm with prolonged cardiac repolarization, indicating a protective effect of gene ablation on cardiac arrhythmias [180]. Comparable studies in mice with cardiomyocyte over-expression of CYP2J2 subjected to TAC or ISO infusion revealed that enhanced cardiac EET biosynthesis is protective against electrical remodeling, ventricular tacharrhythmia and atrial fibrillation associated with cardiac hypertrophy [263]. CYP2J2 overexpression protected gap junction integrity in the TAC model and attenuated the development of fibrosis in the ISO model. The increased survival rate observed in CYP2J2 transgenic mice is attributed to better cardiac electrical stability as only moderate improvements were observed in pump function or hypertrophy [263]. Recently, results from these mice with cardiomyocyte-specific CYP2J2 overexpression demonstrate that EETs attenuate Ang II-induced cardiac hypertrophy and remodelling in a mechanism dependent on AMPK α 2 and a subsequent increase of ANP [264]. In the cardiovascular system ANP acts as a vasodilator on vessel volume and vascular tone, as well as an inhibitor of fibrosis and renin/aldosterone secretion [265]. This study furthermore demonstrated that 11,12-EET stimulated the γ 1 domain of AMPK α 2 β 2 γ 1 to bind directly with protein kinase domain of AKT1, accelerating the translocation of p-AKT1 to the nucleus resulting in increased expression of ANP and abrogation of cardiac hypertrophy [264].

The pathogenesis of HF is a complex process involving many factors including cytokines like $\text{TNF}\alpha$, which, similar to events following acute myocardial ischemia, can activate inflammatory responses and myocardial apoptosis. Numerous *in vitro* and *in vivo* studies provide strong evidence that EETs have anti-inflammatory properties [223, 224], which involve inhibiting the IKK-NF- κ B cascade activated by $\text{TNF}\alpha$ [266]. In an experimental approach to increase the biosynthesis of endogenous EETs, overexpression of CYP2J2 in both cell culture and mouse models, attenuated cardiac dysfunction arising from systemic inflammation caused by $\text{TNF}\alpha$ administration [83]. The protective effect of overexpression of CYP2J2 or EETs was likely mediated via EGFR and PPAR γ activation. Importantly, these studies used models of NICM, i.e. HF induced without an acute ischemic event. Consistent with these data, studies using ISO or Ang II to induce cardiac fibrosis, hypertrophy and dysfunction in mice with overexpression of CYP2J2 demonstrated an abrogated inflammatory response through limited activation of NF- κ B [229]. Interesting data investigating the protective response of EETs toward LPS-induced cardiac dysfunction suggested that EET-mediated inhibition of NF- κ B activation and up-regulation on PPAR α/γ and HO-1 results in inhibiting M1 macrophage polarization while retaining M2 polarization [228] as a potential mechanism. An additional mechanism proposed for ISO and Ang II induced HF has suggested overexpression of CYP2J2 and EETs reduce endoplasmic reticulum (ER) stress and apoptosis culminating in improved systolic and diastolic function [267]. Other studies using sEHi's as an approach to increase the bioavailability of EETs and increase EET-mediated cardioprotective effects have demonstrated similar benefits in models of cardiac hypertrophy and HF [179, 268]. Animal models investigating EET-mediated cardioprotection in models of NICM are becoming more common, although

ischemic models remain general preferred, particularly for cases of HF. Thus, as with many of the CYP-derived eicosanoids, clinical data remains scarce and represents a potential area for future research.

1.3.3.2. EETs protective effects against diabetic cardiomyopathy

Diabetes is a significant risk factor in the development of heart disease. Individuals with either Type 1 (T1DM) or Type 2 (T2DM) diabetes mellitus are at greater risk for cardiovascular complications and resultant mortality than their age-matched controls [269-271]. While diabetes alone carries a risk for heart disease, T2DM is often further coupled with other comorbidities such as obesity and metabolic syndrome that additionally complicate the prevention, treatment and prognosis of patients with diabetic cardiomyopathy (DCM) [271]. DCM describes diabetes-related changes in the heart that are separate from CAD and hypertension associated forms of CVD, although patients with DCM also frequently progress to HF [272]. Hallmarks of DCM include LV hypertrophy, myocardial lipotoxicity, increased oxidative stress, myocardial cell death, interstitial and perivascular fibrosis and mitochondrial abnormalities that ultimately cumulate with decreased diastolic and systolic function, progression to HF and mortality [272]. As lipid mediators involved in inflammation, hypertension and glucose homeostasis, EETs are viable method to protect against DCM. Mouse models using streptozotocin (STZ) to induce T1DM have demonstrated that inhibiting or genetically ablating sEH prevents hyperglycaemia and apoptosis and improves glucose-stimulated insulin secretion and glucose tolerance in islet beta cells [273, 274]. Rodent models of T2DM and obesity show that over-expression of CYP epoxygenase or genetic ablation of sEH improves insulin signalling and sensitivity, abrogates decreased AMPK signalling in the heart and enhances insulin receptor signalling

[275, 276]. The extensive role of EETs and sEH in diabetic whole-body pathogenesis was recently extensively reviewed [277]. Yet, emerging evidence suggests that EETs provide cardiac-specific protection against the development of DCM.

STZ and high-fat diet (HFD) are common models used to mimic T1DM and T2DM, respectively, although there are some genetic models available. Akita mice are a strain developed particularly for study of T1DM; male Akita mice demonstrated an increase of up to 145% in sEH cardiac expression over the development of DCM, with no accompanying change of expression in the liver [278]. Moreover, sEH inhibition resulted in improved glucose tolerance and decreased cardiac fibrosis, hypertrophy and inflammation cumulating in maintained diastolic function in a mouse obesity-driven model of T2DM with leptin receptor deletion (db/db mice) [279]. Importantly, in their novel study Ma et al. used transgenic mice overexpressing cardiac CYP2J2 treated with STZ or HFD to demonstrate overall cardiac function in these mice was greatly preserved compared to controls [280]. In particular, the cardiac overexpression of CYP2J2 maintained contractile ability, improved heart-specific glucose uptake and insulin sensitivity, and attenuated cardiac hypertrophy associated with diabetes through increased ANP production [280]. Accompanying mechanisms involved included beneficial actions on insulin-like growth factor 1 (IGF-1), insulin receptor substrate 1 (IRS-1), PI3K, p-AKT, AMPK and PPAR γ signalling pathways; CYP2J2 over-expression also attenuated increased PDK4 expression, which has been suggested to contribute to DCM by decreasing the pyruvate dehydrogenase complex [280]. This study is fundamental as it suggests EETs mediate cardioprotection against DCM in different models of diabetes. Ultimately these studies suggest EETs retain their cardioprotective effects in DCM and may be a useful therapy for patients with co-morbidities

of diabetes and CVD. Finally, in their cross-sectional study using human plasma Theken et al. noted an association between diabetes and decreased activity CYP epoxygenase coupled with increased sEH activity, indicating expression of the mediators of EETs are involved with diabetes [281]. However, since the data is correlative it is not possible to determine whether the shifts in expression influence the onset of diabetes or are a result of the disease itself. Unfortunately, there is a lack of clinical data on EETs with diabetic patients, particularly T1DM patients. Further research in this area is needed to determine whether EETs can be utilized in humans as a cardioprotective strategy against DCM.

1.4. N-3 PUFAS AND CARDIOVASCULAR DISEASES

The evidence obtained from cell studies, animal experiments, observational studies and clinical trials, support the cardiovascular benefits of long-chain (n-3) PUFAs and considers them as important regulators of cardiovascular health [282-285]. While there remain conflicting data supporting these beneficial effects of EPA and DHA toward CVD, the limited but growing understanding of the mechanisms of how CYP-derived metabolites of n-3 PUFA impact cardiac function and protection will provide better insight into their potential role within the heart and vascular system (Figure 1.6).

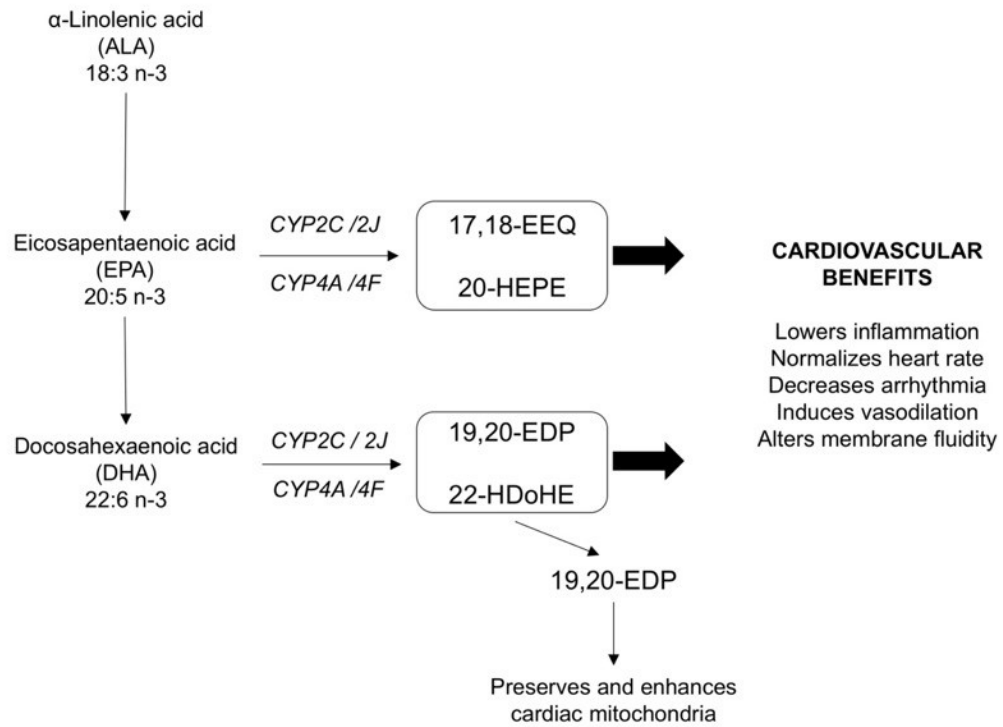


FIGURE 1.6. An outline of primary effects of EPA and DHA metabolites within the heart.

1.4.1. *Effect n-3 PUFAs on heart rate and blood pressure*

Administration of n-3 PUFAs in animal or clinical studies have shown mixed results demonstrating beneficial effects, where the combined consumption of EPA and DHA can lower resting heart rate and blood pressure [284]. In the prospective Cardiovascular Health Study 2735 U.S. adults without CVD were assessed for plasma phospholipid concentrations of long-chain ω -3 fatty acids. The results demonstrated changes in plasma phospholipid EPA levels were not significantly associated with reductions in resting heart rate or blood pressure, whereas increased DHA levels were correlated with lower blood pressure [286]. Evidence from several controlled clinical trials are consistent with these observations, suggesting increased DHA levels could effectively lower heart rate and/or blood pressure [287-291]. Conversely, in a trial involving 59 patients with T2DM associated with hypertension, neither EPA nor DHA (4 g/d each) significantly affected heart rate [292]. Furthermore, data from a larger study demonstrated that 224 healthy men supplemented with either DHA or EPA (4 g/d each) failed to reduce heart rate or result in improved cardiac diastolic filling [287]. However, when the authors of the study normalized the data to circulating levels of either DHA or EPA individually, DHA was directly associated with changes in heart rate [287]. In a study where 38 overweight adults were given both EPA and DHA (3 g/day each for 7 weeks) assessment of aortic flow and peripheral pressures demonstrated improved systemic arterial compliance [293]. A small randomized double-blind trial where DHA was given to 38 healthy men (0.7g/day) resulted in lowered diastolic blood pressure, but increased DHA did not affect endothelial function or arterial stiffness [291]. Together, these limited data with mixed results suggest n-3 PUFA, notably DHA, can

lower both blood pressure and heart rate. However, at present it is unclear what complete role CYP-derived epoxy metabolites have in regulating heart rate and blood pressure.

1.4.2. *Anti-arrhythmic properties of n-3 PUFAs*

The antiarrhythmic properties of n-3 PUFAs have been attributed to their ability to alter the function of membrane ion channels, including Na⁺, L-type Ca²⁺, and Na⁺-Ca²⁺ exchangers as evidenced in both cell culture and animal experiments [294-296]. Early studies demonstrated that EPA was able to reduce the spontaneous beating rate of the cultured heart cells in isolated, neonatal rat cardiac myocytes [297]. In addition, EPA attenuated the response to β-adrenergic stimulation and increase in extracellular calcium concentrations while terminating the induced arrhythmia [297-299]. Several studies proposed that the CYP-derived metabolites of EPA and DHA, 17,18-EEQ and 19,20-EDP, are responsible for mediating the antiarrhythmic effects, for example, 17,18-EEQ was able to inhibit the calcium-induced arrhythmias in cardiomyocytes. However, the effect of 17,18-EEQ was highly stereoselective in which both the racemate and 17(R),18(S)-EEQ enantiomer reduced the spontaneous beating rate of neonatal cardiomyocytes, whereas 17(S),18(R)-EEQ was inactive [89, 300, 301]. Furthermore, the effect of 17(R),18(S)-EEQ was dose-dependent with an EC50 value of 1-2 nM, indicating that this CYP-dependent metabolite was 1000-fold more potent compared to its parental n-3 PUFA [300]. 19,20-EDP also displayed the same enantioselectivity as observed with 17,18-EEQ [89]. The same antagonist, 11,12-EET, blocked the negative chronotropic effect of both EEQ and EDP, suggesting that they act via the same mechanism [89]. The 17(R),18(S)-EEQ metabolite responsible for mediating the anti-arrhythmic effects of EPA exerted a negative chronotropic effect, protecting neonatal rat cardiomyocytes against Ca²⁺-overload [89, 300].

1.4.3. *N-3 PUFAs and mitochondrial protection*

An *in vivo* study investigating the role of DHA intake on cardiac mitochondrial function in diabetic rat models involved supplementing the diet for 3 months. Interestingly, increased DHA resulted in partial protection of cardiac mitochondrial dysfunction caused by insulin deficiency and resistance, which was attributed to modification of fatty acid composition of cardiac and mitochondrial membranes by DHA [302]. Data from cell culture experiments, demonstrated pre-treatment of rat H9c2 cardiac myoblast cells with the n-3 PUFAs, EPA or DHA, provided protection against DOX-induced decrease in mitochondrial uncoupling protein 2 (UCP2) expression and attenuated the increase in ROS production and apoptosis [303]. Furthermore, a following study showed that EPA attenuated oxidative stress-induced cardiomyocyte apoptosis and increased cell viability by activating an adaptive autophagic response in H9C2 cardiac cells [304]. Recently, the CYP-derived epoxy metabolite of DHA, 19,20-EDP, was shown able to protect mouse atrial HL-1 cardiac cells against LPS-induced cytotoxicity and apoptosis via activation of sirtuin 1 (SIRT1). Activation of SIRT1 pathway preserved a healthy pool of mitochondria, enhanced mitochondrial function and promoted mitobiogenesis, resulting in increased cell survival [305].

1.4.4. *Cardioprotective responses of n-3 PUFAs against MI*

There is growing experimental evidence indicating EPA and DHA produce a cardioprotective response against IR injury. For example, neonatal cardiomyocytes treated with EPA were protected against HR-induced apoptosis through activation of ERK and inactivation of the pro-apoptotic kinase, p38 MAPK [306]. Similarly, hearts isolated from animals fed a diet enriched in n-3 PUFAs for 8 weeks demonstrated increased cardiac antioxidant defense system, reduced infarct size and improved post-ischemic functional

recovery [307, 308]. In an *ex vivo* model, perfusion of hearts isolated from Sprague-Dawley rats with DHA before IR injury resulted in a cardioprotective response that increased the antioxidant abilities and significantly diminished cardiac damage [309]. In support of these studies, an intravenous bolus administration of n-3 PUFA (EPA:DHA 6:1) 30min after ischemia and 10min before reperfusion decreased vascular failure and shock in a LAD model of myocardial ischemia in male Wistar rats [310]. More recent studies have begun to investigate the protective effects of CYP-derived metabolites of DHA toward HR injury. In an *in vitro* model of HR, mouse atrial HL-1 cardiac cells treated with 19,20-EDP were protected from damage via a mechanism that preserved mitochondrial quality and enhanced mitochondrial respiration in SIRT1-dependent fashion [311]. While these studies highlight novel intracellular biological activity of EDPs, the understanding of their mechanism(s) of action remains very limited and needs to be further investigated.

1.4.5. *N-3 PUFAs against cardiac failure and fibrosis*

N-3 PUFAs have demonstrated promising modulatory effects against HF in different studies. For example, oral administration of (1 g/kg) EPA-ethyl ester or DHA-ethyl ester for 21d, starting 3d prior to induction of HF using subcutaneous injection of monocrotaline, modified heart fatty acid composition and consequently enhanced cardiac function and ameliorated congestive HF in male rats [312]. Additionally, these data illustrated the ability of EPA to ameliorate palmitate-induced lipotoxicity in H9c2 cells via AMPK activation, which subsequently suppressed mitochondrial fragmentation. These findings provided some evidence to the molecular mechanisms of EPA-mediated protection against HF [313]. These studies are supported by clinical trials that demonstrate a correlation with n-3 PUFAs and

improved outcomes in HF patients [314-317]. Despite the limited evidence and potential benefits, the use of n-3 PUFAs in HF remains controversial.

Mice fed a diet enriched with n-3-PUFA were protected against cardiac dysfunction and interstitial fibrosis in a TAC model [318]. The anti-fibrotic properties of n-3 PUFA were attributed to their ability to prevent a pro-fibrotic response including collagen I and III expression, fibroblast proliferation, and myofibroblast transformation [318]. Both EPA and DHA inhibited the transforming growth factor beta 1 (TGF β 1) pro-fibrotic signalling pathway in primary cultures of cardiac fibroblasts [318]. In another mouse model of pressure overload-induced HFHF only EPA, but not DHA, prevented fibrosis via activation of free fatty acid receptor 4 (FFAR4), which blocked TGF β 1 fibrotic pathway [319]. Similarly, long-term administration of EPA ethyl ester (1 g/kg/d) in C57BL/6J mice for 28 days before and 28 days after experimental MI induction, using LAD ligation, attenuated the post-MI fibrotic cascade via inhibition of the TGF- β /Smad signaling pathway, demonstrating a direct effect of EPA on cardiac fibroblasts [320]. Moreover, oral administration of either low dose (300 mg/kg/day) or high dose (1,000 mg/kg/day) EPA from age 9 to 13 weeks in DahlS.Z-*Lepr^{fa}/Lepr^{fa}* (DS/obese) rats increased adiponectin secretion which activated AMPK and inactivated NF- κ B signaling in the hearts leading to a reduction in cardiac fibrosis and attenuation of diastolic dysfunction [321]. Intriguingly, EPA also attenuated the post-MI cardiac remodeling process by modulating the proinflammatory M1 macrophages activity and consequently reduced the mortality rate after MI [320]. These studies established evidence for the n-3 PUFA EPA as a promising therapeutic agent for improving the prognosis of post-MI cardiac remodeling and fibrosis, however the role of CYP-derived N-3 metabolites as a whole remains unknown.

1.5. PHYSIOLOGICAL AND PATHOPHYSIOLOGICAL PROPERTIES OF LINOLEIC ACID METABOLITES

LA is an N-6 essential fatty acid, the precursor of AA acid and present at high levels in the Western diet [74, 322]. Biological transformation of LA may occur through CYP-mediated hydroxylation, epoxidation and allylic oxidation. The primary CYP-derived epoxy metabolites are two regioisomeric epoxides, 9,10- epoxyoctadecamonoenic acid (EpOME) and 12,13-EpOME. Both of these metabolites are rapidly hydrolyzed by sEH to the corresponding vicinal diols, 9,10-dihydroxyoctadecenoic acid (9,10-DiHOME) and 12,13-DiHOME [74, 323].

Early studies suggested high levels of EpOMEs were linked with acute respiratory distress syndrome thus adversely impacting the cardiovascular system [324]. However, as the specific roles EpOMEs have in inflammation and cellular homeostasis remain relatively poorly understood, evidence indicates many of the cytotoxic effects attributed EpOMEs are in fact caused by their secondary metabolites DiHOMEs, formed in the reaction catalyzed by sEH [28]. DiHOMEs are thus may very well be the crucial metabolites mediating the toxicity of LA epoxides [325].

Currently, there is limited information regarding the biological activity of the CYP-derived metabolites of LA in the heart. Overexpression of CYP2C8 in mice has been demonstrated to reduce postischemic functional recovery in isolated hearts [257]. The decreased recovery was partially attributed to increased generation of ROS presumably by CYP2C8, but the cardiotoxicity was associated with accumulation of LA catabolism, particularly 9,10-DiHOME [257]. Consistent with these data, the cardioprotective effect of

CYP2J2 overexpression towards ischemic injury observed in young (3 months) mice was lost in older (12 months) animals [326]. Both young and aged sEH null mice demonstrated improved post-ischemic functional recovery compared to WT and aged CYP2J2 mice. Interestingly, the aged CYP2J2 overexpressing mice had increased levels of 9,10-DiHOME found in the heart perfusate. Perfusing the aged CYP2J2 hearts with a sEHi decreased the production of 9,10-DiHOME and resulted in the same cardioprotective response observed in young CYP2J2 hearts [326].

Conversely, there is evidence DiHOMEs have an endogenous physiological role depending on the cell and tissue. For example, protective properties of 12,13-DiHOME have been shown to suppress the oxidative burst and inflammatory response in neutrophils [327]. One mouse model used spleens from irradiated mice to assess the influence of sEH on the formation of short-term repopulating hematopoietic progenitor cell colonies [328]. Solvent-treated bone marrow cells from *Ephx*^{-/-} mice formed significantly fewer colonies than cells from WT mice, whereas incubation of cells from *Ephx*^{-/-} mice with 11,12-DHET or 12,13-DiHOME effectively restored the colony-forming ability of the cells [328]. Data indicated 12,13-DiHOME and 11,12-DHET, but not 11,12-EET or 12,13-EpOME, induced the nuclear translocation of β -catenin, a protein involved in cell-cell adhesion, in bone marrow cells, restored spleen colony-forming ability of cells isolated from sEH deficient mice and, following transplantation, increased murine stem cell and short term repopulating progenitor populations [328]. These data suggest the vicinal diol metabolites, DiHOMEs and DHETs, have roles in progenitor cell mobilization and subsequent physiological repair processes. This study revealed previously uncharacterized interactions between the CYP/sEH pathway and hematopoietic progenitor cell proliferation, mobilization and subsequent role in

vascularization [328]. Based on the current data, we predict DiHOMEs at low concentrations may potentially stimulate cardiac stem cells and have an active role in cardiac healing.

Our current understanding of the pathophysiological and physiological effects of EpOMEs and DiHOMEs promoting deleterious, protective or combined responses in the heart and vasculature remains limited. Indeed, more work is required to elucidate the function of CYP-derived products of LA.

1.6. EICOSANOID RECEPTORS

A multitude of preclinical data has contributed to the characterization and understanding of how CYP-derived metabolites function within the cardiovascular system. However, the identity of the specific receptor(s) involved in epoxy lipid responses remains unknown. Data from structure-activity relationships demonstrating variance in potency among endogenously produced regioisomers and synthetic analogs that act to agonize or antagonize their effects at varying degrees suggest the existence of specific receptors. The identification of the receptor(s) and their characterization will provide critical insight into the diverse biology and drive future research.

Multiple lines of evidence suggest the actions of EETs are in part mediated via G-protein coupled receptor (GPCR) signalling. Earlier studies indicated the existence of a specific high affinity receptor for EETs on the cell surfaces and recent data identified several low-affinity GPCR receptors located in the vasculature [329-334]. Moreover, several studies report the significance of Gs proteins in mediating 11,12-EET signaling [335-337]. The existence of a Gs-coupled EET receptor supported the dependence of EET-induced signaling on cAMP/PKA mediators [338]. However, data investigating EET-induced changes in cAMP

signalling as a response to classical GPCR cellular responses remain inconclusive [28, 233]. It has been reported EETs can induce vasodilation via antagonizing thromboxane (TP) receptors in the vascular system [339]. This was supported by the observation that binding of the selective TP receptor antagonist, SQ-29548, to TP receptor was largely prevented by 14,15-EET without having significant effects on other prostanoid or leukotriene receptors [339]. However, physiological actions of the EETs could not be ascribed to TP antagonism because the effect was only observed using supraphysiological concentrations of EETs [340].

GPR120, known as FFA4 or ω -3 fatty acid receptor 1, functions as a receptor for unsaturated long-chain free fatty acids and mediates a wide range of cellular functions [341-344]. GPR120 was shown to bind both n-3 (EPA and DHA) and n-6 (AA) PUFAs initiating similar signaling pathways [345]. Numerous reports show GPR120 mediates many PUFA-induced actions including, anti-inflammatory effects [346, 347], adipogenesis [348], as well as lipid and glucose metabolism [344, 349]. Further evidence demonstrated unsaturated long-chain free fatty acids could mediate tumor promotion in human colorectal carcinoma via GPR120 [350]. Interestingly, GPR120 has been proposed to act as a lipid sensor detecting changes in dietary fat and playing a role in the development of obesity, whereas dysfunction of GPR120 was associated with energy imbalance and obesity in both humans and rodents [347, 351]. A similar receptor dependency for the anti-inflammatory effects of n-3 PUFA was observed in hypothalamus and Kupffer cells [352, 353]. PUFAs can also activate other groups of orphan receptors, such as GPR40 (FFA1), GPR41 (FFA3), GPR43 (FFA2), and GPR84 [342]. ALA, EPA, and DHA are all ligands for GPR40 which is highly expressed in human brain, pancreas and different immune cells [354-358]. A plethora of studies reported that n-3 PUFA modulates insulin secretion from pancreatic β -cells through GPR40 [356,

359-362]. Recently, Ma et al. showed that GPR40 mediated the mitogenic responses of EETs in HEK293 cells [363].

CYP-derived PUFA epoxides are generated intracellularly implying their cellular actions are mediated by interacting with intracellular targets such as the PPAR family. A plethora of studies showed that PUFAs and their metabolic derivatives have the ability to activate PPARs [364-367]. Numerous reports illustrate the effects of PPAR α and PPAR γ activation with EETs. PPARs are involved in regulating lipid metabolism, inflammation, immune function, cell proliferation and insulin secretion [368-372]. The overexpression of human CYP2J2 in HEK293 cells induced a synergistic activation of PPAR α , - β/δ , and - γ reporter gene activity [373]. Epoxy metabolites of AA, 8,9-, 11,12- and 14,15-EET as well as 14,15-DHET were reported to bind with a high affinity to PPAR α [373-375]. However, EETs generated in both endothelial cells and 3T3-L1 preadipocytes targeted and activated PPAR γ inhibiting inflammatory signalling, which was blocked by PPAR- γ antagonists [376, 377]. Moreover, 8,9-EET and 11,12-EET were shown to activate PPAR α in the heart responsible for the switching of glucose to fatty acid metabolism during fasting [373, 378]. Recent data in immortalized rat H9c2 cardiac cells demonstrated cytotoxic effects of CYP-derived metabolites of DHA, EDPs, were mediated via PPAR δ signaling [379]. Although, PPARs represent workable receptor targets through which epoxy-PUFA products could regulate cellular metabolism and function, the significance of PPAR activation in mediating effects of epoxy-PUFAs needs further investigation to draw a clear mechanistic pathway.

Several reports demonstrate n-3 PUFAs have a role in membrane structure and function, tissue metabolism, and genetic regulation [284, 379-381]. With long hydrocarbon chains and multiple double bonds, both EPA and DHA alter lipid membrane properties [382, 383]. In

rat aortic endothelial cells, DHA incorporation increased membrane fluidity more than EPA [384]. DHA may also alter membrane protein function via close range interactions, potentially related to the property of DHA to efficiently pack adjacent to membrane proteins. In molecular simulation studies, DHA formed tight associations with rhodopsin (a prototypical G-protein-coupled membrane receptor, the primary visual light receptor) in a limited number of specific locations, which may facilitate the transition of the protein into its active form [385].

Investigation into identifying a 20-HETE receptor demonstrated the non-selective cation channel transient receptor potential vanilloid 1 channel (TRPV1) as potential target. Using whole cell voltage clamping, 20-HETE activated human TRPV1 in kidney and ganglionic cell lines; these effects were mitigated with co-treatment of known TRPV1 inhibitor capsazapine, suggesting this receptor is at least one specific target of 20-HETE [386]. TRPV1 is a capsaicin-sensitive nociceptive receptor located in sensory neurons as well as in vascular and cardiac smooth muscle and endothelial cells [387-389]. Long-term activation of arterial TRPV1 with capsaicin was beneficial in hypertension, at least partly through increased endothelial-derived NO and enhanced endothelial-dependent vasodilation [390]. While the role of TRPV1 in the heart is complex, epicardial surface TRPV1 are involved in regulating cardiac sympathetic responses [391]. In the myocardium, early studies using Langendorff perfused mouse hearts showed that gene deletion or acute inhibition of *Trpv1* impaired post-ischemic recovery, as well as reduced protection arising from pre-conditioning of isolated hearts, indicating a protective effect of the *Trpv1* channel in cardiac ischemia-reperfusion injury [392, 393]. Inversely, other studies have shown that TRPV1 gene deletion or pharmacological inhibition actually confers protection in models of cardiac hypertrophy

and HF [394, 395]. The effects of TRPV1 activation or blockade thus appear to depend on the pathological state [395]. While 20-HETE can activate TRPV1 this is clearly not its only receptor, particularly since it is established that inhibiting 20-HETE synthesis offers protection in cardiac IR injury, yet inhibiting or ablating *Trpv1* impairs recovery following IR injury [145, 396]. Due to the diverse range of signalling in which TRPV1 is implicated, it may be a sensor for cardiac ischemic injury involved in highly complex immunological and neuronal regulatory pathways, simultaneously mediating some cardiotoxic effects of 20-HETE while other cardiotoxic effects of 20-HETE, particularly in IR injury, are mediated through other unknown or uncharacterized receptors. Intriguingly, one such receptor recently identified as a potential 20-HETE binder is G-protein coupled receptor GPR75 (G_q) [397].

GPR75 is one of many orphan receptors of the rhodopsin type A family expressed in the central nervous system, retina and pancreatic islets [398, 399]. In their novel study, Garcia et al. report that GPR75 is widely distributed in C57BL/6 mouse tissues, including brain, heart, kidney and lung, which have a high degree of vascularization [397]. Using human microvascular endothelial cells (HMVEC) and rat aortic VSMCs, Garcia et al. present compelling data confirming 20-HETE both specifically binds to and functionally activates GPR75 (Kd value of 3.75 nmol/L) [397]. GPR75 expression is associated with $G\alpha_{q/11}$ and G Protein-Coupled Receptor Kinase Interactor 1 (GIT1); 20-HETE application significantly changed the interactions of these associated proteins [397]. After 20-HETE binds GPR75, GIT1 and c-Src work downstream to increase the phosphorylation and activation of epidermal growth factor receptor (EGFR) which links 20-HETE to activation of known MAPK-IKK β -NF κ B signaling pathways [397, 400]. These changes are functionally relevant. Deletion of GPR75 receptor effectively removed the induction of ACE mRNA

caused by application of 20-HETE; furthermore, Cyp4a12 transgenic mice treated with control shRNA demonstrated increases in systolic blood pressure, vascular ACE expression, endothelial dysfunction and cardiac remodeling compared to mice treated with shRNA against GPR75 [397]. The pairing of 20-HETE-GPR75-GIT1 was confirmed in rat aortic VSMCs, indicating a likely role of these proteins in 20-HETE mediated vasoconstriction and hypertension outside of the endothelial dysregulation [397]. These data provide convincing evidence that GPR75 is a 20-HETE receptor that may be a novel target in combatting CVD [397]. Potential interactions with other protein pathways, including the TRPV1, might improve understanding of the biological actions of 20-HETE and remove some discrepancies between 20-HETE levels, receptor activation and biological effects in the heart. It is important to note that GPR75 and TRPV1 have not been definitively proven to be the only 20-HETE receptors and others might exist. Regardless, these data demonstrate the complex cellular roles for 20-HETE beyond its role as a regulator of vasoactivity.

1.7. CYTOCHROME P450 POLYMORPHISMS AND MODULATED PUFA CARDIOVASCULAR EFFECTS

Interindividual variability in the pharmacodynamic and pharmacokinetic response to certain medications and toxic insults, or pharmacogenomics, is quickly emerging as an important field that offers enormous potential to improve clinical outcome. Multiple functional polymorphisms in genes responsible for EET biosynthesis (CYP2C8/9, CYP2J2) or EET hydrolysis (*EPHX2*) have been associated with the development of CVD [401-407] (Table 2). Differential CYP epoxygenase expression has been shown to correlate with increased risk of endothelial dysfunction and acute cardiovascular events. For instance, separate German and Taiwanese studies reported a polymorphism of the CYP2J2 gene

(rs890293) with decreased enzymatic activity independently correlated with increased risk of CAD and premature MI, respectively [408, 409]. Similarly, in Bulgarian men the *CYP2J2*–50G>T polymorphism with decreased enzymatic activity was associated with increased risk of CAD, while *CYP2C8**3 polymorphism with decreased enzymatic activity significantly increased risk for essential hypertension but not CAD or MI [405]. Complicating matters however, is the fact that studies have also shown different profiles between ethnicities, often with different outcomes depending on the ethnicity and variant under question. For instance, *EPHX2* gene variation was associated with coronary artery calcification in African-Americans, but not in non-Hispanic white subjects [410]. Furthermore, while *EPHX2* polymorphism increased risk of CHD in Caucasians, variants of *CYP2J2**7 polymorphism in African-Americans unexpectedly correlated with a significantly lower risk of CAD in a cohort study [411, 412]. A study conducted in three ethnicities (Uygur, Kazakh, and Han) in Xinjiang, China suggested an association between the *EPHX2* (rs751141) G/A allele and the development of essential hypertension in Han but not Kazakh or Uygur subjects [407]. Finally, different polymorphisms of *EPHX2* appear to increase risk for either African-American or white subjects, but such effects were strongly influenced by smoking [413]. Indeed, lifestyle factors and comorbidities concomitant with CVD, such as smoking and diabetes mellitus, likely also contribute to at least some of these data inconsistencies within and between ethnic populations [401, 402, 408, 409, 411-413]. Further investigation is required to determine the mechanisms by which these polymorphisms alter susceptibility to CVD in the context of lifestyle and comorbidities, and to what degree these effects can be separately targeted in clinical medicine. Furthermore

beyond population genetics, lifestyle and comorbidities, the effects of CYP epoxygenous polymorphisms are significantly altered by biological sex.

TABLE 1.2. Known CYP polymorphisms associated with CVD

Genotype (rs: reference SNP ID No.)	Population/ Country (Sex-specific)	Associated Disease	Reference
CYP2C8			
CYP2C8*3	Sweden (female)	Myocardial infarction (MI)	[414]
CYP2C8*3 (rs1050968)	Bulgaria (male)	Essential hypertension	[405]
No association (or lower risk: LR)			
N/A CYP2C8*2,CYP2C8*3	South India	MI	[402]
N/A CYP2C8*2/*3/*4	USA	Coronary artery disease (CAD)	[412]
N/A CYP2C8*3 (rs1050968)	Bulgaria (male)	CAD	[405]
CYP2C9			
CYP2C9*2,CYP2C9*3	Sweden (female)	MI	[414]
CYP2C9 (rs2475376) CC genotype (rs4086116, rs2475376, rs1057810, rs1934967) C-C-A-T	Chinese Han (female)	CAD	[403]
No association (or lower risk: LR)			
N/A CYP2C9*2,CYP2C9*3	South India	MI	[402]
N/A CYP2C9 (rs1057810)	Chinese Han (female)	CAD	[403]
CYP2J2			
CYP2J2-50T (rs890293)	Germany	CAD	[408]
CYP2J2*7 (rs890293)	Taiwanese	MI	[409]
CYP2J2*7 (rs890293)	Chinese (male)	Hypertension	[404]
CYP2J2-50T (rs890293)	Russia	Hypertension	[415]
CYP2J2 (rs2280275)	Chinese Uygur (male)	CAD	[401]
CYP2J2*7 (rs890293)	Bulgaria	CAD	[405]
CYP2J2*7 (rs890293)	South India	MI	[402]
No association (or lower risk: LR)			
LR CYP2J2-50T	USA	CAD	[412]
CYP4A11			
CYP4A11 (rs1126742) CC	African American	Blood pressure	[80]

	CYP4A11 (rs1126742)	Germany	Hypertension	[416, 417]
	CYP4A11 (rs1126742)	Chinese Han (male)	Hypertension	[418]
	CYP4A11 (rs1126742) TC+TT CYP4A11 (rs2269231, rs1126742, and 9333025) A-T-G	Japanese (male)	Hypertension	[419, 420]
	CYP4A11 (-845A/G, -366C/T, 7119C/T, and 8590T/C) G-C-T-T	Japanese	Hypertension	[421]
	CYP4A11 (rs9332978, rs3890011, and rs1126742) G-G-T	Chinese Han	CAD	[422]
	CYP4A11 (rs4660980)	China (male)	Blood pressure	[423]
	CYP4A11 (rs389011) GG	Chinese Han (male)	CAD	[422, 424]
	CYP4A11 (rs9333025) GG	Chinese Mongolian (male)	Hypertension	[425]
	CYP4A11 (rs9333025) GG	Chinese	Ischemic stroke	[426]
No association (or lower risk: LR)				
N/A	CYP4A11 (rs1126742)	Japanese	Hypertension	[421]
N/A	CYP4A11 (rs2269231, rs1126742 and rs9333025)	Japanese	MI	[427]
LR	CYP4A11 (rs2269231, rs1126742 and rs9333025) T-T-A	Japanese (male)	MI	[427]
N/A	CYP4A11 (rs9332982 and rs3890011)	China	Blood pressure	[423]
N/A	CYP4A11 (rs389011)	Chinese Uygur (male)	CAD	[424]
N/A	CYP4A11 (rs9333025)	Chinese Han (male)	Hypertension	[425]
N/A	CYP4A11 (rs2269231, rs2108622 and rs3093135)	Chinese	Ischemic stroke	[426]
N/A	CYP4A11 (rs1126742) TC/CC	Australia	Blood pressure	[428]
CYP4F2				
	CYP4F2 (rs1558139) CC	Japanese (male)	Hypertension	[419]

	CYP4F2 (rs3093105, rs1558139, rs2108622) T-T-G			
	CYP4F2 (rs2108622, V433M) M	Sweden	Blood pressure	[429]
	CYP4F2 (rs2108622) G	Japanese (male)	MI	[430]
	CYP4F2 (rs3093135, rs1558139, rs2108622) T-C-G			
	CYP4F2 (rs2108622)	Meta-analysis	Ischemic stroke	[431]
	CYP4F2 (rs2108622) GA/AA	Australia	Blood pressure	[428]
No association (or lower risk: LR)				
LR	CYP4F2 (rs3093135, rs1558139, rs2108622) T-C-A	Japanese (male)	MI	[430]
N/A	CYP4F2 (rs2108622)	Meta-analysis	Hypertension	[432]
N/A	CYP4F2 (rs2108622, rs3093135)	Chinese	Ischemic stroke	[426]

Endogenous estrogens have numerous whole-body effects, cumulating in a decreased risk of CVD in pre-menopausal women. The relationships between CYP-epoxygenase single nucleotide polymorphisms (SNPs), CVD and sex have thus been studied. Associations between *CYP2J2* polymorphisms and CAD and hypertension have been found in males [401, 404]. Often expression of these alleles in females is non-existent or inversely correlated with disease progression. However, a Swedish study suggests that female carriers of rare allelic variants with decreased enzymatic activity, *CYP2C8**3, *CYP2C9**2 and *CYP2C9**3, have an increased risk of acute MI [414]. Moreover, a study in Chinese Han population suggest that certain *CYP2C9* variants correlate with a female-only risk for CAD, although not all variants share the same degree of risk in females [403]. Finally, a study conducted in a South Indian population suggested that while individuals carrying the *CYP2J2**7 (rs890293) T allele with decreased enzymatic activity have a 2.0-fold higher risk for MI, polymorphisms in *CYP2C9* and *CYP2C8* were not associated with MI in either sex, although the lack of sex differences may be a result of significantly lower numbers of female MI cases in this study [402]. Female hormones such as estrogen may act as antagonists of *CYP2C8*-mediated pro-inflammatory pathways, increasing the expression of enzymes from *CYP2C* family and resulting in overall protective cardiovascular effects [405]. The presence of sex hormones coupled with genetic CYP polymorphisms undoubtedly has crucial effects on the development of CVD. However, the relationship between sex and eicosanoid metabolism remains to be determined, and it is not known whether these two factors – genetic polymorphism and biological sex – can truly be separated to be targeted independently.

Genetic variability exists in the CYP ω -hydroxylases enzymes, notably *CYP4A* and *CYP4F* sub-families, with the majority of studies investigating their associations with

hypertension. Two common functional polymorphisms *CYP4A11* T8590C and the *CYP4F2* G1347A have been associated with increased blood pressure in population studies and have been postulated to act by altering 20-HETE levels. A study investigating 5 different SNPs associated with *CYP4F2* resulting in altered AA metabolism, revealed that rs1558139 might be a genetic marker for essential hypertension in Japanese men [419]. A Swedish study reported that *CYP4F2* variants were associated with significantly higher blood pressures as well as increased risk of hypertension and ischemic stroke; a large meta-analysis demonstrated carriers of *CYP4F2* (rs2108622) polymorphism, with increased enzymatic activity, had a significantly higher risk of ischemic stroke [429, 431]. There are conflicting reports in the literature where some have reported no association between *CYP4F2* SNPs and hypertension [432], as well no significant associations of *CYP4A11* and *CYP4F2* polymorphisms in ischemic stroke ([426]). However, in a parallel controlled trial of overweight volunteers from an Australian population the *CYP4A11* T8590C and *CYP4F2* G1347A polymorphisms were associated with altered urinary 20-HETE excretion and blood pressure; *CYP4A11* (rs1126742) TC/CC genotype had significantly lower 20-HETE excretion not correlating with either systolic (SBP) or diastolic blood pressure (DBP), while *CYP4F2* (rs2108622) GA/AA genotype significantly increased 20-HETE excretion, correlated with elevated SBP [428]. Further evidence has demonstrated *CYP4A11* polymorphisms in the development of hypertension in male Chinese, Japanese, African American and Caucasian European populations [416-418, 420, 433]. Some newer variants and haplotypes of *CYP4A11* correlate with a dysregulation of blood pressure associated with hypertension, ischemic stroke and CAD [422-426]. These effects appear to be sex-related, with males typically showing increased expression of *CYP4A11* polymorphism having

increased enzymatic activities correlating with increased risk of associated CVD [420, 422, 425]. Indeed, a sex-specific association related to the androgen-mediated activity of the *CYP4A11* enzyme has been suggested to account for the sex differences, although this theory has been challenged [420, 421]. Further investigation into the effects of the variants in cardiac tissue is warranted. Ultimately, the impact of CYP genetic variability toward CVD is complex and dependent on multiple factors and co-morbidities, such as lifestyle choices, sex and ethnicity.

1.8. SEXUAL DIMORPHISM IN OXYLIPID-MEDIATED CARDIOPROTECTION

1.8.1. SEX AND GENDER IN IHD

While inextricably linked, sex and gender are fundamentally different. “Sex” is the biological attributes associated with both sex chromosomes and sex hormones, generally related to the reproductive anatomy. Conversely, human “gender” is a product of roles, norms and expectations in a given social context and over a particular period of time [434, 435]. Both sex and gender influence pathophysiology, presentation, treatment and prognosis of IHD. For example, male sex is an independent risk factor for the development of IHD [436] while females may experience other unique risk factors, e.g. preeclampsia [437]. The largest covariable influencing the development of IHD between the sexes is undoubtedly age. It is well-appreciated pre-menopausal women are at a lower risk of heart disease and stroke than men [438]. This is attributed to the influence of estrogen, which acts as a vasodilator and reduces vascular tone [439]. Once women go through menopause, which occurs on average at 52 years old in western countries, estrogen levels drop dramatically and IHD becomes a predominant form of morbidity and mortality [440].

The focus on menopause has left many peri-menopausal women under-estimating their risk of IHD [437]. It is inarguable that MI in young women is less common compared to men, yet this cohort has repeatedly demonstrated significantly higher mortality rates post-MI compared to age-matched males [441-445]. This is true in Canada, wherein women 45-65 years of age experience higher all-cause mortality compared to men in the first year post-MI [446]. Women may not experience the same symptoms as men, leading to late diagnosis and prolonged time to treatment, subsequently increasing mortality [437]. Younger women are also less likely to be managed effectively with guideline-based therapy [447]. Moreover, these effects are at least partially due to a higher burden of comorbidities, such as diabetes mellitus and hypertension, which can accelerate disease progression in women [448]. Ultimately, MI in women remains relatively under-studied.

1.8.2. *Sexual dimorphism in N-6 eicosanoid cardioprotective effects*

Emerging evidence has pointed to sexual dimorphisms in the n-6 eicosanoids. sEH gene expression has been shown to differ between men and women in the kidneys, liver, brain and vasculature, although apparently without effect on function [449-451]. Later studies have demonstrated significant effects of this gender divide in models of cerebral ischemia [452, 453]. Although sEH is also widely expressed in the heart, sex differences in sEH expression/EET axis and the influence in CVD have only recently been addressed, and then only in young animal models that are not fully representative of the aged, anestrus state of human women. Young male *Ephx2*^{-/-} mice exhibited decreased blood pressure while no such change was seen in age-matched females, due to sex-specific regulation of sEH [454]. In a follow-up study, vascular sEH protein expression was four times lower in female controls than males [455]. Subsequently, *Ephx2*^{-/-} female mice exhibited similar vascular effects as

female controls, indicating a sex-specific difference that effectively removed the response to sEH gene deletion in females, i.e. while sEH ablation was protective in males, it had no significant effect in females [455]. Yet, recent evidence shows this female-specific sEH downregulation is also associated with the promotion of vasodilation and reduced coronary myogenic vasoconstriction [456]. This study suggested a mechanism in which EETs and nitric oxide work sequentially in the female coronary vasculature to attenuate coronary resistance, thus helping the heart, and contributing to female cardioprotection [456].

Characterization of mouse hearts revealed young female mice had reduced myocardial sEH protein expression compared to males [451]. This may be linked to epigenetic silencing; Yang et al. demonstrated that working through estrogen receptors, estrogen can trigger CG methylation on the *Ephx2* promoter region effectively silencing sEH gene expression [457]. Female WT and *Ephx2*^{-/-} mice moreover demonstrated greater cardiac contractility upon challenge with the same preload compared to WT male mice [451]. This study demonstrated sex-specific and genotype-dependent cardioprotective outcomes; importantly, all these protective effects were removed when EET bioavailability was attenuated with 14,15-EEZE [451]. Thus, estrogenic down-regulation of sEH may act to stabilize and enhance EET availability [458]. These data suggest altered EET levels in the cardiovascular system may have potent effects in the pathogenesis of CVD in pre-menopausal women. However, we have demonstrated no sex differences in cardiac responses in young male and female sEH null or *t*AUCB-treated mice in our ischemic models [175, 459].

Difficulties arise when comparing female rodent models of reproductive senescence to human models, notably as CVD risk in women increases drastically post-menopause. It has been suggested as little as 25% of female rodents demonstrate a similar menopausal

transition (anestrus) compared to humans [460]. Although all rodents eventually enter an anestrus state, most female rodents demonstrate a transition into brief state of constant estrus that includes increased plasma levels of 17β -estradiol, a primary estrogen that has significant effects on the cardiovascular system and development of heart disease [460]. Species differences require consideration and further elucidation in order to better understand the effect sex has toward EETs and their relevance to CVD. The differences between the sexes in response to sEH inhibition or deletion is ultimately a key consideration of this thesis.

1.9. AGEING AND EICOSANOID-MEDIATED PROGRESSION OF CVD

CVD remains the leading cause of morbidity and mortality worldwide, where approximately half of the individuals afflicted with CVD are advanced in age (>55 years) [461]. Importantly, more than 75% of the cases reported for CAD or HF are observed in aged individuals [461]. Acute MI is responsible for a large portion of the illness, disability and death linked to CVD in the elderly. While mortality rates have decreased over the last 30 years, myocardial ischemic injury remains a critical problem. Survival after the index episode often leads to individuals living with significantly damaged hearts; over 30-40% of heart attack survivors progress to HF [462-464]. Determining the pathophysiological progression is made more difficult by the multiple changes to cardiovascular structure and function that occur during normal ageing. Evidence from animal models and humans indicate a decreased ability of the aged heart to tolerate stress compared to young counterparts [465-467]. For instance, an aged heart is more susceptible to adverse events, such as IR injury, and often unable to adequately overcome an event [468]. Elderly patients often present at a clinic in an atypical manner, indicative of other diseases and complicating factors, which not

only impedes diagnosis and treatment but increases susceptibility of the aged heart to more injury [465].

Mitochondria are fundamental facilitators of myocardial energy production through the ETC and cell life/death pathways. Mitochondria exhibit age-related dysfunction, even in otherwise healthy myocardium, and these differences become more apparent following ischemic injury. Mitochondria from aged hearts demonstrate decreases in oxidative phosphorylation, increased ROS production coupled with reduced ROS scavenging, and cristae breakdown and matrix derangement [469, 470]. Adding to the complexity of mitochondrial age research is sex effects. Animal studies in female hearts demonstrate better outcomes following ischemic injury and oxygen deprivation than males [471, 472] and while female hearts demonstrate lower mitochondrial content, these mitochondria are more efficient, further differentiated, produce less ROS and exhibit higher antioxidant capacity than mitochondria from male hearts [473-475]. The intersection of age, sex and mitochondrial function in the context of cardiac ischemic injury and oxylipid metabolism is a major theme of this dissertation.

1.9.1. *HETEs over aging: CVD effects*

Similar to EETs, there is limited information regarding changes to 20-HETE with age or their role in age-related diseases. Aged female rats demonstrated increased expression of CYP ω -hydroxylase activity and 20-HETE levels in the cerebral microvasculature compared to young females; in contrast, the renal microvasculature demonstrated decreased 20-HETE levels [476]. This study suggests renal tubules may compensate by downregulating CYP ω -hydroxylase activity to combat increased blood pressure arising from other systemic changes from menopause [476]. Data taken from male Sprague-Dawley rat mesenteric arteries

suggested an increased contribution of CYP4A ω -hydroxylase activity to α 1-receptor adrenergic vasoconstriction with age [477]. A follow-up study in aged female ovariectomized Sprague-Dawley rats found a similar increase in CYP4A ω -hydroxylase activity in mesenteric arteries [478]. In a MI model, mice fed high PUFA diet over aging had increased LV pro-inflammatory lipid mediators post-MI, including increased 12-HETE, which were associated with worse prognosis than the control-diet mice [479]. 20-HETE inhibitors have been investigated for their protective effects in aged murine models of postmenopausal hypertension, hypertension and diabetes [476, 480-483]. In some of these studies, the protective vascular adaptive responses seen in young animals can be completely attenuated in aged animals [480]. Some clinical studies have been utilized to obtain plasma levels of the HETEs in human CVD. Interestingly, no difference in the serum levels of 20-HETE were observed in aged individuals with CAD compared when compared to healthy controls [281]. In aged patients with pulmonary arterial hypertension, plasma 12- and 15-HETE were both indicators of poor long-term survival, suggesting some HETEs do influence vascular pathogenesis [484]. It would be interesting to know how HETE levels differ in aged and young humans, especially those with CVD. Taken together, the limited data suggest changes in CYP4A ω -hydroxylase enzymes and HETE levels occur with age but the impact remains unknown.

1.9.2. *EETs and Age-related CVD*

Currently, there remains limited information regarding the changes in expression patterns of CYP/sEH pathway, which occurs during the process of aging or in age-related disease states. In the mesenteric arteries of aged ovariectomized Sprague-Dawley rats sEH expression was significantly reduced compared to their sham-operated controls, while

castration of male littermates increased sEH expression compared to their sham controls [485]. Interestingly, the ovariectomized aged females and the male sham rats showed no difference in sEH expression in the mesenteric arteries [485]. A study in female Norway-Brown rats aged 22 months showed that neither age nor estrogen had effects on circulating EETs, sEH and CYP2J2 expression in the LV, although CYP2C6 and 2C2 expression declined [486]. Interestingly, it was recently demonstrated EET levels decreased in male fawn-hooded spontaneous hypertensive (FHH) rats with age, contributing to local endothelial dysfunction and the development of kidney disease [487]. In an *ex vivo* study of cardiac IR injury no change in sEH expression in the aged mouse heart was observed compared to young controls [326]. Investigation into genetic variants associated with HF identified *Ephx2* as a susceptibility gene, where persistently high cardiac expression levels together with hypertension and LV hypertrophy present a high-risk for disease progression to HF [180]. Human biopsies from ischemic HF patients indicated a significant decrease in sEH expression compared to age-matched controls; however, comparison to young cohorts would benefit understanding age-related changes [180]. Analysis of changes to the CYP/sEH metabolite profile in a population of patients with stable CAD was compared to healthy volunteers [281]. The study utilized middle-aged (<65 year old) patients with various comorbidities such as diabetes and hypertension as well as lifestyle risks including obesity and smoking. The results demonstrated a marked dysregulation in eicosanoid metabolism and suggested decreased sEH expression maybe an adaptive mechanism for CAD but advanced age and obesity were associated with lower EET levels [180, 281]. Ultimately, the cardioprotective effect of EETs in aged individuals remains unknown.

Ageing studies in cerebral and renal ischemic injury models have noted significant protection using sEH inhibition, but data from post-ischemic aged cardiovascular studies are limited [452]. An *ex vivo* study investigating the effects of aging on IR injury in mice overexpressing cardiomyocyte CYP2J2 and sEH null mice demonstrated improved functional recovery in young and aged sEH null mice [326]. However, the protective effect observed in young overexpressing CYP2J2 mice was lost in the aged mice. Interestingly, inhibition of sEH in the aged CYP2J2 mice resulted in improved post-ischemic functional recovery. The data suggested an accumulation of cardiotoxic LA metabolites, notably 12,13-DiHOME, occurred in the aged CYP2J2 transgenic mice linked with increased oxidative stress and activation of PP2A [326]. A recent *in vivo* MI study investigated the effects of aging in sEH null (16-month-old) mice compared to young mice (3-month-old) [488]. Results confirmed a decline in basal cardiac function occurs with age, which significantly blunted the cardioprotective effects of sEH deletion observed in young mice [488]. Post-MI hearts from aged sEH null mice had moderately better mitochondrial ultrastructure, mitochondrial enzymatic activity and overall cardiac function, but these effects were not as robust compared to young animal studies [175, 488]. These limited results suggest the normal age-related decline in heart function has significant effects on cardioprotective strategies involving EETs, although further studies are required.

1.10. PHARMACOLOGICAL APPROACHES TO REGULATE CYP-DERIVED EICOSANOIDS

Numerous different methods have been utilized to modulate CYP-mediated PUFA metabolism as a potential therapeutic target to prevent and/or treat different CVDs. Investigators have worked to development compounds using 3 main approaches: (i) to

regulate CYP enzymatic activity, either increasing or decreasing production of epoxy metabolites; (ii) compounds that act as either mimetics or antagonists; or (iii) compounds to inhibit sEH activity preventing the degradation of epoxy metabolites (Table 1.3).

TABLE 1.3: Summary of CYP and sEH inhibitors affecting cardiovascular function

Compound	Full name	Category	Animal or cell line model	Effect	References
CYP inhibitors					
ABT	1-aminobenzotriazole.	Mechanism-based CYP ω -hydroxylase inhibitor	Male heterozygous Ren-2 transgenic rats	Reduced the development of HTN	[489]
			Rats fed a low-salt diet	Reduced blood pressure	[490]
			Rats fed a high-salt diet	Promoted the development of HTN	[490]
			Ang II-induced HTN in rats	Attenuated arterial blood pressure	[99]
			SHR	Reduced mean arterial pressure	[491]
DDMS	N-methylsulfonyl-12,12-dibromododec-11 enamide.	Competitive CYP ω -hydroxylase inhibitor	Ren-2 transgenic rats	Reduced cardiac hypertrophy	[492]
			<i>In vivo</i> induced I/R injury via surgical occlusion of LAD in canines	Potentiated the cardioprotective effects of IPC and reduced the infarct size	[396]
			<i>In vivo</i> induced I/R injury via surgical occlusion of LAD in canines	Reduced myocardial infarct size	[69]
HET0016	N-hydroxy-N ₂ -(4-n-butyl-2-methylphenyl) formamidine.	Competitive CYP ω -hydroxylase inhibitor	Ang II and 20-HETE induced injury in neonatal rat ventricular cardiomyocytes	Showed potent anti-apoptotic effects and negated the pro-apoptotic effect of Ang II and 20-HETE	[148]
			BaP-induced cardiac hypertrophy in rats	Protected against cardiac hypertrophy	[493]
			<i>Ex vivo</i> induced I/R injury in hearts isolated from diabetic rats	Improved the recovery of cardiac functions	[150]
			<i>In vivo</i> induced I/R injury via surgical occlusion of LAD in rats	Demonstrated potent antiapoptotic effect	[144]
MSPPOH	N-methylsulphonyl-6-(2-propargyloxyphenyl) hexamide.	CYP epoxygenase inhibitor	RPCT induced by abdominal incision through the skin in rats subjected to <i>In vivo</i> induced I/R injury via surgical occlusion of LAD	Completely blocked the cardioprotective effect of RPCT induced by EETs	[494]
			CHF rats	Abolished the beneficial effects of EETs on LV function and perfusion	[260]

			RPCT induced by abdominal incision through the skin in adult mongrel dogs subjected to <i>in vivo</i> induced I/R injury via surgical occlusion of LAD	Completely blocked the cardioprotective effect of RPCT induced by EETs	[495]
			<i>Ex vivo</i> induced I/R injury in transgenic mice with cardiomyocyte-specific overexpression of CYP2J2	Abrogated the cardioprotective effect of EETs	[169]
17-ODYA	17-Octadecynoic Acid.	Mechanism-based CYP ω -hydroxylase inhibitor	<i>In vivo</i> induced I/R injury via surgical occlusion of LAD in canines	Reduced myocardial infarct size	[69]
SPZ (SUL)	4-amino-N-(1-phenyl-1Hpyrazol-5-yl) benzene sulfonamide (Sulfaphenazole).	CYP epoxygenase inhibitor	<i>In vivo</i> induced I/R injury via surgical occlusion of LAD in rats	Attenuated the myocardial cell apoptosis by inhibiting the mitochondrial dysfunction	[496]
			<i>In vivo</i> induced I/R injury via surgical occlusion of LAD in rats	Demonstrated cardioprotective effect by suppressing myocardial cell apoptosis	[497]
			<i>In vivo</i> induced I/R injury via surgical occlusion of LAD in rats	Suppressed the development of MI and improved the declined cardiac function	[498]
			<i>In vivo</i> hypertensive patients	Blunted vasodilation to ACh and BDK	[499]
			<i>Ex vivo</i> induced I/R injury in hearts isolated from rats	Conferred a protective effect in post-ischemic vascular dysfunction through a reduction of superoxide production	[500]
			<i>In vivo</i> human subjects	Altered the blood flow increase induced by exercise	[501]
10-SUYS	sodium 10-undecynyl sulfate.	Mechanism-based CYP ω -hydroxylase inhibitor	SHR	Reduced mean arterial blood pressure and attenuated the vasoconstrictor response of renal interlobar arteries to Ang II <i>in vitro</i>	[502, 503]
TS-011	[N-(3-chloro-4-morpholin-4-yl) phenyl-N0-hydroxyimido formamide].	Mechanism-based CYP ω -hydroxylase inhibitor	SHR	Reversed the vasospasm resulting from subarachnoid hemorrhage and reduced the infarct size in stroke ischemic models	[504]
sEH inhibitors					
AEPU	1-adamantan-3-(5-(2-(2-ethylethoxy)ethoxy) pentyl) urea.	Selective sEHi	ApoE knockout (-/-) mice	Reduced atherosclerotic lesions in the descending aortae	[505]
AR9281	[1-(1-acetyl-piperidin-4-yl)-3-adamantan-1-yl-urea.	Selective sEHi	Ang II-induced HTN in rats	Attenuated HTN	[506]
			Mouse model of diet-induced obesity	Attenuated the enhanced glucose excursion following GTT	[506]

AUDA	12-(3-adamantane-1-yl-ureido) dodecanoic acid.	sEHi and weak activator of PPAR α	<i>In vivo</i> induced I/R injury via surgical occlusion of LAD in dogs	Reduced the cardiac infarct size	[178]
			Obese rats	Reduced HTN and renal damage	[374, 507, 508].
BI00611953	N-(2-chloro-4-methanesulfonyl-benzyl)-6-(2,2,2-trifluoro-ethoxy)-nicotinamide.	Selective sEHi	<i>Ex vivo</i> induced I/R injury in mice	Improved postischemic LVDP and reduced infarct size	[171]
CDU	1-cyclohexyl-3-dodecyl-urea.	Selective sEHi	HTN induced by Ang II infusion in rats	Lowered blood pressure	[509]
DCU	N,N'-dicyclohexylurea.	Selective sEHi	SHR	Lowered blood pressure	[510]
GSK218893 1B	[N-([4-bromo-2-[(trifluoromethyl)oxy]phenyl)methyl]-1-[4-methyl-6-(methylamino-1,3,5-triazin-2-yl)]-4-piperidinecarboxamide].	Selective sEHi	<i>In vivo</i> induced I/R injury via surgical occlusion of LAD in male rats	Exerted beneficial effects on cardiac function and ventricular remodeling post-MI	[225]
GSK225629 4	((1R,3S)-N-(4-cyano-2-(trifluoromethyl)benzyl)-3-((4-methyl-6-(methylamino)-1,3,5-triazin-2-yl)amino)cyclohexane-1-carboxamide).	Selective sEHi in Phase 1 clinical trial	<i>In vivo</i> and <i>in vitro</i> models using COPD patients and human resistance arteries	Attenuated smoking related EET-mediated endothelial dysfunction both <i>in vivo</i> and <i>in vitro</i>	[511]
8-HUDE	12-(3-hexylureido) dodec-8-enoic acid.	EET-mimetic and sEHi	Rat PA and PSMCs	Increased PA vascular tone	[301]
KM55	1-(3-(5-(hydroxyureido)methyl-2-methoxyphenoxy)propyl)-3-[4-(trifluoromethoxy)phenyl] urea.	sEH/5-LO inhibitor	Human leucocytes (monocytic THP-1 cells) and HUVECs	Inhibited the LPS-induced adhesion of leukocytes to endothelial cells	[512]
NCND	N-cyclohexyl- N-dodecyl urea.	Selective sEHi	Ren-2 transgenic rats	Reduced cardiac hypertrophy	[492]
PTUPB	[4-(5-phenyl-3-{3-[3-(4-trifluoromethylphenyl)-ureido]-propyl)-pyrazol-1-yl)-benzenesulfonamide].	COX-2/sEH inhibitor	Type 2 diabetic ZDF rat model	Prevented the development of metabolic abnormalities and diabetic kidney injury	[513]
tAUCB	4-[[trans-4[[[(tricyclo[3.3.1.1 ^{3,7}]dec-1-ylamino)carbonyl] amino]cyclohexyl]oxy]-benzoic acid.	Selective sEHi	<i>In vivo</i> induced I/R injury via surgical occlusion of LAD in mice	Protected against ischemic injury by preserving cardiac function and maintaining mitochondrial efficiency	[175]
			Obese insulin-resistant mice	Improved coronary endothelial function and prevented cardiac remodeling and diastolic dysfunction	[279]

			EPCs from patients with acute MI	Positively modulated the function of EPCs	[256]
			<i>Ex vivo</i> induced I/R injury in hearts isolated from both young and aged mice	Improved postischemic functional recovery	[326]
<i>t</i> -CUPM	[trans-5-[4-[3-(4-chloro-3-trifluoromethylphenyl)-ureido]-cyclohexyloxy]-pyridine-2-carboxylic acid methylamide.	c-RAF/sEH inhibitor	LSL-Kras(G12D)/Pdx1-Cre mice	Prevented chronic pancreatitis and carcinogenesis	[514]
TPAU	1-trifluoromethoxyphenyl-3-(1-acetylpiperidin-4-yl) urea.	Selective sEHi	C57BL/6 mice	Reduced niacin-induced flushing	[515]
TUPS	1-(1-methanesulfonylpiperidin-4-yl)-3-(4-trifluoromethoxyphenyl)-urea.	Selective sEHi	Cultured rat and human VSMCs and carotid-artery balloon injury model in Sprague-Dawley rats	Ameliorated the vascular occlusive disease and attenuated VSMC dedifferentiation and migration under pathological conditions	[516]
			ISO-induced cardiac hypertrophy in male rats	Partially protected against ISO-induced cardiac hypertrophy	[517]
			BaP-induced cardiac hypertrophy in male rats	Protected against cardiac hypertrophy and corrected the BaP-induced deviations in CYP-mediated AA metabolism	[518]
UA-8	13-(3-propylureido)tridec-8-enoic acid.	EET-mimetic and sEHi	HL-1 and neonatal cardiomyocytes following starvation-induced cell death	Preserved the mitochondria pool in both HL-1 and neonatal cardiomyocytes following starvation-induced cell death	[174, 215]
			Rat neonatal cardiomyocytes exposed to the bacterial wall endotoxin LPS	Improved cell viability and mitochondrial function	[227]
			<i>Ex vivo</i> induced I/R injury in mice	Improved post-ischemic functional recovery, limited infarct size and prevented cell death	[182]

Early animal studies inhibiting CYP epoxygenases had different effects on cardiovascular function and recovery from injury. Inhibition of CYP2C isozymes with sulfaphenazole (SPZ) was found to reduce myocardial infarction accompanied with global IR in isolated perfused rat hearts [519]. Moreover, intravenous administration of SPZ at the time of reperfusion reduced the myocardial infarct size and improved the cardiac function in an *in vivo* rat IR model [498]. The same group revealed that the suppressive effects of SPZ on myocardial infarction were achieved by the attenuation of the cardiac ROS levels derived from CYP450s [520]. Interestingly, SPZ-induced cardioprotection was mediated by the enhancement of NO bioavailability due to the increased expression of inducible nitric oxide synthase (iNOS) in a rat Langendorff preparation [521]. PKC activation and subsequent autophagy were involved in the cardioprotection induced by SPZ, also using Langendorff preparations [497]. More recently, it was concluded that treatment with SPZ could attenuate the myocardial cell apoptosis accompanied with IR by inhibiting the mitochondrial dysfunction due to decreases in the expression of BimEL and Noxa using an *in vivo* rat model of cardiac IR [522]. While the exact mechanisms remain unknown, the data suggested increased ROS formation from CYP2C isozymes, most likely from endothelial cells, are a major factor in worse post-ischemic recovery.

Utilization of the specific inhibitor of CYP epoxygenase, MSPPOH, abrogated the cardioprotective effect of EETs in *ex vivo* IR injury model in transgenic mice with cardiomyocyte-specific overexpression of CYP2J2 [169]. These data suggest the importance of CYP-derived EETs in the cardiomyocytes toward cardioprotection. This was supported by data demonstrating MSPPOH abolished the beneficial effects of EETs toward LV function and perfusion in a CHF rat model [260]. Intriguingly, Gross et al. reported that

MSPPOH completely blocked the cardioprotective effect of remote preconditioning of trauma induced by EETs in both adult mongrel dogs [495] and rats [495] subjected to *in vivo* induced IR injury via surgical occlusion of LAD.

CYP ω -hydroxylase inhibitors have been extensively studied to counteract the effects of 20-HETE on cardiovascular system [94, 96, 523]. Several studies showed that inhibition of synthesis or blockade of action of 20-HETE protected the heart and attenuated cardiac dysfunction [68, 69, 145]. For instance, the CYP ω -hydroxylase inhibitors, 17-Octadecynoic Acid (17-ODYA) and (N-methylsulfonyl-12,12-dibromododec-11-enamide (DDMS), markedly reduced myocardial infarct size in the canine heart after ischemia reperfusion IR injury [69]. A follow-up study also showed that inhibiting the synthesis of 20-HETE with DDMS potentiated the cardioprotective effects of ischemia preconditioning (IPC) and reduced the infarct size following cardiac IR in a canine heart model [396]. Furthermore, a more recent study demonstrated that simultaneous inhibition of 20-HETE formation, using DDMS, and metabolism of EETs, using the sEHi N-cyclohexyl-N-dodecyl urea (NCND), reduced cardiac hypertrophy in Ren-2 transgenic rats, the hypertensive rat transgenic for the mouse Ren-2 renin gene that represents a unique Ang II-dependent hypertensive animal model [492]. HET0016, a selective inhibitor of CYP4A and 4F isozymes, limits the formation of 20-HETE [524, 525]. Experiments using HET0016 have demonstrated cardioprotective effects including reduced apoptosis from IR injury, attenuated benzo(α)pyrene (BaP)-induced cardiac hypertrophy and a beneficially effected recovery of cardiac function following IR injury in diabetic rats [144, 150]. Recent evidence showed HET0016 resulted in anti-apoptotic effects toward Ang II and 20-HETE induced injury in neonatal rat ventricular cardiomyocytes [148]. Despite the promising pharmacological

properties, the preparation of an injectable formulation of HET0016 is limited by its poor solubility under neutral conditions and instability under acidic conditions [526]. Compounds that can act as 20-HETE antagonists have been developed as potential therapeutic agents. One of these compounds is a putative 20-HETE receptor antagonist 20-hydroxyeicosa-6(Z),15(Z)-dienoic acid (20-HEDE) [90]. For example, in a canine heart model of IR injury, it was demonstrated the adverse effects of 20-HETE were antagonized by 20-HEDE, limiting myocardial infarct size [396]. Interestingly, co-treatment with 19-HETE has been shown to block the vasoconstrictor response to 20-HETE in renal arterioles, antagonize 20-HETE-mediated endothelial dysfunction in bovine aortic cells and increased 19-HETE levels correlated with improved prognosis in patients with ACS [90, 105, 161]. Experiments have attempted to increase the formation of 19-HETE with isoniazid to induce CYP2E1, Ang II-induced cardiac hypertrophy in rats [160].

Regarding the regulation of CYP2J2 expression, several studies have reported the ability of PPAR α agonists, such as fenofibrate, to induce the cardiac P450 epoxygenase enzymes and their associated EET metabolites, while decreasing the cardiac ω -hydroxylase and their associated 20-HETE metabolites ultimately protecting against cardiac hypertrophy [527, 528]. There has been limited evidence of specific inducers of CYP2J isozymes; an *in vitro* study using adult human primary cardiomyocytes indicated rosiglitazone increased mRNA levels [529]. However, a very recent study showed that PPAR γ activation in mouse hearts using rosiglitazone increased the production of EETs, maintaining protective CRH, a physiological response to ischemic insult that prevents the potential harm associated with an interruption of blood supply [247].

To date, different formulations of n-3 PUFA supplements have been developed and investigated include free fatty acid, ethyl ester, triacylglyceride or phospholipids forms [530, 531]. Recently, EPA, DHA and DPA monoacylglyceride (MAG-EPA, MAG-DHA and MAG-DPA) have been synthesized [532]. These fatty acid monoacylglyceride forms show increased absorption and higher bioavailability compared to free, triacylglyceride or ethyl ester forms [532-534]. Interestingly, several research studies demonstrated the beneficial effects of MAG- ω 3 precursors in various models of established diseases [535-537]. For instance, Morin et al. demonstrated that oral administration of MAG-DHA prevented high fat/high carbohydrate-diet induced systemic hypertension in rodents [538]. The properties of these new formulations encourage their use in future investigation for their possible role in prevention and/or treatment of CVDs.

EETs are rapidly taken up into the cells when applied exogenously and can be readily metabolized via sEH, undergo β -oxidation, followed by esterification to phospholipids or conjugation to glutathione. The use of EETs is also complicated by difficulties with synthesizing regioisomeric pure compounds, limited solubility, and storage issues [325, 539, 540]. Several generations of EET analogs/agonists have been synthesized and proved to have improved solubility as well as to resist auto-oxidation and metabolism by sEH [541-544]. More recently, newer generations of orally active EET analogues have been developed, which demonstrate cardiovascular therapeutic potential when administered *in vivo* either acutely or chronically [545]. One such compound is disodium (S)-2-(13-(3-pentyl)ureido)-tridec-8(Z)-enamido)succinate (EET-A), which had a direct vasodilatory effect and attenuated the development of hypertension in Ang II-infused rats [546, 547]. Furthermore, EET-A attenuated the development of experimental Ang II-dependent malignant

hypertension, and hypertension-induced end-organ damage [548]. Another novel orally active EET analogue with promising cardiovascular effects is N-(5-((2-acetamidobenzo[d]thiazol-4-yl)oxy) pentyl)-N-isopropylheptanamide) (EET-B). EET-B provided protection against kidney injury in salt-sensitive hypertensive rats by reducing oxidative stress, inflammation and endoplasmic reticulum stress [549]. A more recent study showed that EET-B administration decreased the elevated blood pressure, protected the kidney and markedly lowered renal inflammation in Ang II hypertension [550]. These findings encourage the use of these novel EET analogues in future investigations to assess their therapeutic role in different CVDs.

Inhibitors of sEH have proven to be valuable tools in exploring the biological activities of CYP-derived metabolites as well serve as potential therapeutic targets (see reviews [29, 406, 551, 552]. Initial compounds were based on using dicyclohexyl urea as the central pharmacophore, which was found to act as a reversible inhibitor of sEH [552, 553]. The further development of more potent sEHi with better oral bioavailability and pharmacokinetics involved approaches to modify a secondary site positioned near the carbonyl of the primary pharmacophore with an ether, heterocycle or amide (Morisseau & Hammock, 2013). Several sEHi have been extensively tested for their cardiovascular therapeutic potential and shown to have effects against several CVDs including hypertension [507, 554], VSMC proliferation and inflammation [376, 555-557] atherosclerosis [558], IR injury [225], cardiac hypertrophy [559] and HF [260].

Characterization of earlier sEHi (4-[[*trans*-4-[[tricyclo[3.3.1.1^{3,7}]dec-1-ylamino) carbonyl]amino]cyclohexyl]oxy]-benzoic acid (*t*AUCB) and 1-trifluoromethoxyphenyl-3-(1-acetylpiperidin-4-yl) urea (TPAU) demonstrated good oral bioavailability and metabolic

stability than their predecessors [560]. These inhibitors have been used as model compounds to investigate cardioprotective properties. For example, *ex vivo* heart perfusions with *t*AUCB resulted improved post-ischemic functional recovery and cardioprotection in both young and aged mice [326]. Additionally, *t*AUCB positively modulated the function of EPCs in patients with acute MI suggesting the potential utility of sEHi's in the therapy of ischemic heart disease [256]. Recently, *in vivo* studies demonstrated *t*AUCB protected against ischemic injury by preserving cardiac function and maintaining mitochondrial efficiency [175]. The inhibition of sEH using *t*AUCB improved coronary endothelial function and prevented cardiac remodeling and diastolic dysfunction in obese insulin-resistant mice [279]. Nicotinamide-based approaches to develop sEHi by Boehringer Ingelheim resulted in compounds with favourable properties and inhibitory activity [561, 562]. *Ex vivo* heart perfusions with N-(2-chloro-4-methanesulfonyl-benzyl)-6-(2,2,2-trifluoro-ethoxy)-nicotinamide (BI00611953), significantly improved post-ischemic LVDP and reduced infarct size following IR injury similar to hearts perfused with 11,12-EETs in Langendorff models [171].

A piperidine-based derivative sEHi 1-(1-methanesulfonyl-piperidin-4-yl)-3-(4-trifluoro-methoxy-phenyl)-urea (TUPS), was shown to protect against BaP-induced cardiac hypertrophy and corrected the BaP-induced deviations in CYP-mediated AA metabolism [518]. Furthermore, data demonstrated that TUPS partially protected against ISO-induced cardiac hypertrophy [517]. A recent study showed that TUPS largely ameliorated the vascular occlusive disease and attenuated VSMC dedifferentiation and migration under pathological conditions [516]. Another study demonstrated that inhibition of sEH with (GSK2188931B) exerted beneficial effects on cardiac function and ventricular remodeling

post-MI [225]. GSK2256294 ((1R,3S)-N-(4-cyano-2-(trifluoromethyl)benzyl)-3-((4-methyl-6-(methylamino)-1,3,5-triazin-2-yl)amino)cyclohexane-1-carboxamide) is a novel potent sEHi in Phase 1 clinical development, with the potential to impact systemic and pulmonary endothelial function [563]. Several clinical trials (NCT02262689, NCT02006537, NCT01762774) were conducted to evaluate GSK2256294 safety, tolerability, pharmacokinetics, and pharmacodynamics and the effect of GSK2256294 exposure on pulmonary artery systolic pressure (PASP) under hypoxic conditions in healthy, obese, smokers, young or elderly volunteers. A very recent report indicated GSK2256294 attenuated smoking-related EET-mediated endothelial dysfunction in human resistance vessels both in vitro and in vivo. This suggested the potential therapeutic benefits of GSK2256294 in patients with chronic obstructive pulmonary disease (COPD) [511]. Since, smoking and COPD are risk factors for endothelial dysfunction and CVD [564-566], using sEHi for preventing and/or treating several CVDs remains a promising approach.

New approaches in drug discovery include designing compounds, which exhibit improved safety and efficacy but possess multi-target or dual function properties [567-569]. Dual functioning compounds have been developed that possess sEH properties together with EET analogues, 5-LOX inhibitors, COX-2 inhibitors or inhibitors of RAS-activated RAF1 proto-oncogene serine/threonine kinase (c-RAF) [570]. An example of a novel synthetic compound that possesses both EET-mimetic and sEH inhibitory properties is 13-(3-propylureido)tridec-8-enoic acid (UA-8) [571]. *Ex vivo* heart perfusions with UA-8 significantly improved post-ischemic functional recovery, limited infarct size and prevented cell death [182]. Further cardiac cellular properties of the dual functioning compound demonstrated UA-8 preserved the mitochondria pool in both HL-1 and neonatal

cardiomyocytes following starvation-induced cell death by promoting an autophagic response shifting the cell response from apoptosis to cell survival [174, 215]. Another *in vitro* study demonstrated that UA-8 improved cell viability and mitochondrial function of rat neonatal cardiomyocytes exposed to the bacterial wall endotoxin LPS [227] which is known to induce myocardial inflammation and significant cardiotoxicity [572]. Together, these studies provide insight into the benefits of developing novel compounds that possess dual function such as sEH inhibition and epoxy lipid properties.

1.11. THESIS OVERVIEW

1.11.1. Rationale

IHD accounts for a significant proportion of death and morbidity in aged individuals. Importantly, age and sex influence the progression, pathophysiology and prognosis of IHD. Aged hearts demonstrate decreased capability to respond to stress even in the absence of comorbidities. Moreover, it is well-characterized that risk for MI varies by sex. The risk for females is low until menopause, at which point it reaches or even exceeds that of males. Interestingly, peri-menopausal women, generally 45-65 years of age, exhibit higher mortality post-MI compared to age-matched males and elderly females (>65 years). Despite these clinical data, in animal studies female mice typically demonstrate greater cardioprotection from ischemic injury than males. The CYP-derived oxylipids derived from N-3 and N-6 PUFAs have multitudinous effects in the cardiovascular system. These oxylipids are further metabolised by sEH, reducing their activity. Data from our group and others demonstrate reducing sEH activity through genetic whole-body knockout or pharmacologic inhibition in ischemia is cardioprotective in both males and females, but data regarding effects *in vivo*

using aged animals remains limited. Moreover, though the mechanisms are unknown, cardioprotective effects from sEH inhibition or deletion in ischemia are mediated at least partially through improvements in mitochondrial form and function. The overall aim of this dissertation is to assess inhibition of sEH following ischemic injury in males and females in the context of natural aging, with focus on the contribution of the mitochondria. Moreover, we seek to characterize epoxide hydrolase oxylipid metabolism and mitochondrial function in human explanted hearts from male and female patients with ischemic cardiomyopathy, a clinically-relevant cohort.

1.11.2. *Hypothesis*

Global hypothesis: Cardiac function following MI is preserved by genetic or pharmacologic inhibition of sEH.

1. Cardiac function declines over normal aging in mice, exemplified by decreased systolic function and impaired mitochondrial efficiency.
2. Cardiac function post-MI is preserved in aged mice with sEH deletion or inhibition, associated with conserved mitochondrial efficiency.
3. Aged male and female mice with deletion or inhibition of sEH do not demonstrate sexually dimorphic differences in cardioprotective responses post-MI.
4. Ischemic cardiomyopathy in humans is associated with significantly altered oxylipid metabolism and reduced mitochondrial function in LV myocardia.

1.11.3. *Aims*

1. To investigate differential effects of sEH genetic deletion or pharmacologic inhibition in aged vs young myocardial tissue (described in Chapter 3.1)

2. To investigate the effects of sEH genetic deletion or pharmacologic inhibition in protecting the aged murine myocardium from chronic ischemic injury, focusing on potential sex differences (described in Chapter 3.2)
3. To characterize oxylipid metabolism in human left ventricular tissue, separated by sex (described in Chapter 3.3)

Chapter 2

EXPANDED MATERIALS AND METHODS

²The methods outlined below are expanded versions adapted from:

Jamieson KL, Samokhvalov V, Akhnokh M, Lee K, Cho WJ, Takawale A, et al. Genetic Deletion of Soluble Epoxide Hydrolase Provides Cardioprotective Responses Following Myocardial Infarction in Aged Mice. *Prostaglandins Other Lipid Mediat.* 2017;132(47-58)

Jamieson KL, Darwesh AM, Sosnowski DK, Zhang H, Shah S, Wang W, Zhabyeyev P, Yang J, Hammock B, Edin ML, et al. Sexual Dimorphic Responses to Myocardial Infarction Following Inhibition of Soluble Epoxide Hydrolase in Aged Mice and Human Explanted Hearts. Submitted to JMCC, April 2020.

2.1 PROCUREMENT OF HUMAN EXPLANTED HEART TISSUE

Human heart tissues were obtained under protocols approved by the Health Research Ethics Board of the University of Alberta. Adult non-failing control (NFC; N=5 female, N=5 male) heart tissues (LVEF \geq 60%) were collected from donors with no cardiovascular history and transplants were unsuitable due to medical or technical issues, such as ABO blood type incompatibility. Adult failing heart samples were procured from patients with end-stage heart failure secondary to ischemic cardiomyopathy (ICM; N=5 female, N=12 male). Collections were conducted during cardiac transplantations at the Mazankowski Alberta Heart Institute (MAHI) as part of the Human Explanted Heart Program (HELP) and Human Organ Procurement and Exchange Program (HOPE) at the University of Alberta. All myocardium samples were excised from the left ventricular free wall avoiding epicardial adipose tissue within 5-10 minutes of its excision following cold cardioplegia. Three samples from each ICM heart were obtained from the non-infarct (remote region, viable tissue), peri-infarct (border region containing viable and non-viable tissue) and infarct (direct injury, fibrotic) regions. The samples were immediately flash-frozen in liquid nitrogen and stored in ultra-low (-80°C) freezers.

2.2 ANIMAL MODEL

All animal experimental protocols were approved by the University of Alberta Health Sciences Welfare Committee and were performed in strict adherence to the guidelines set by the Canadian Council of Animal Care.

2.2.1 Colony Maintenance and Breeding

Colonies of mice with targeted deletion of *Ephx2* (sEH null) or mice over-expressing cardiomyocyte-specific human cardiac epoxygenase CYP2J2 (CYP2J2-Tr) were maintained at the University of Alberta. Colonies were preserved on C57BL/6 background by back-crossing with mice from Charles River every 3 years. Wild-type (WT) littermates from each colony served as controls. Unless noted, males and females were used for all experiments. For acute MI (Chapter 3.1) WT and sEH null mice were aged to 16 months old while young mice were on average 3 months old. For chronic MI (Chapter 3.2) mice were aged to 13-15 months old at which point they underwent LAD ligation, ultimately sacrificed at 14-16 months old. This age range was chosen to be roughly equivalent to mouse “middle-age” [574]. Senescent mice (18-24 months old) are representative of elderly individuals; however, the middle-age range used here is more representative of the age at which CVD manifests for many individuals, particularly males. Moreover, elderly mice may exhibit other confounding age-related pathophysiology, e.g. frailty[575].

2.2.2 Myocardial Infarction

Myocardial infarction was achieved through permanent occlusion of the left anterior descending (LAD) coronary artery [576]. Mice were anaesthetized with 1-2% isoflurane and intubated before undergoing left thoracotomy in the fifth intercostal space. Once the pericardium was opened, the LAD was encircled under the left atrial appendage and permanently ligated. The chest was closed using 6-0 silk suture. The same procedures were used for sham mice, excepting the ligation. The surgeon was blinded to the genotype and sex of all mice. Mice were intraperitoneally administered 3 mg/kg of meloxicam for three days post-MI and inspected twice daily for the duration of the experiment.

2.2.3 Pharmacologic Administration and Water Intake

For sEH inhibitor studies, WT mice were given sEH inhibitor trans-4-[4-(3-adamantan-1-yl-ureido)-cyclohexyloxy]-benzoic acid (*t*AUCB; 10mg/L) or vehicle (0.1% DMSO) in drinking water either immediately following ligation (*t*AUCB:0d or same-day treatment) or 4 days prior to ligation (*t*AUCB:4d or pre-treatment). Both groups received continued administration *ad libitum* in the drinking water for the duration of the experiment. Water intake was measured weekly when bottles were changed and fresh water administered. *t*AUCB was a kind gift from Dr. Bruce Hammock from UC Davis.

2.2.4 Animal Tissue Collection and Processing

For acute MI, surgical and sham mice were euthanized with an intraperitoneal injection of 100mg/kg dose of pentobarbital 7 days after surgery. For chronic MI, euthanasia was performed 28 days post-MI. Blood draw was taken from the right femoral artery, added to K₂EDTA-coated microcentrifuge tubes, centrifuged at 2500 x rpm for 10 min at 4°C and supernatant was taken as plasma. Hearts were quickly excised, rinsed with ice-cold phosphate-buffered saline and quickly weighed (heart weight, HW). For wet lung weight, all lung tissue was excised and weighed. Both HW and WL weights were compared to tibia length (TL) measured with digital calipers. Animals that reached humane endpoint before 28 days were euthanized using the same method; tissues were collected but not analysed. MI hearts were separated into infarct, peri-infarct and non-infarct regions with a razor blade under a dissecting microscope. Peri-infarct region was taken as the region ~1mm above the infarct region, visible under the dissecting microscope. Unless otherwise stated, regions consisting of both the septum and free wall segments of the left ventricle were used for experiments. All other tissue excepting lung was stored in separate Eppendorff tubes, flash frozen in liquid nitrogen and stored at -80°C awaiting analysis.

2.2.5 Infarct Size Assessment

Following excision, hearts were frozen in liquid nitrogen and sliced transversely from the apex to the point of ligation in 0.5-mm slices. These slices were incubated at 37°C in a 1% solution of triphenyltetrazolium chloride (TTC) for 10 minutes. TTC stains viable tissues a brick red colour due to the action of reductive dehydrogenases. In necrotic tissues that lack these reducing enzymes, myocardial colouring remains white. ImageJ software was used to analyse the percent infarct area [577].

2.2.6 Cardiac Functional Assessment

2.2.6.1 Echocardiography (ECHO) measurements

Cardiac structure and function were assessed noninvasively in males and females by transthoracic 2D echocardiography following animal anesthesia with 1-2% isoflurane. For acute study, ECHO was performed one day prior to LAD surgery (baseline) and 7 days post-MI. Recordings were taken using a Vevo 2100 high-resolution imaging system, 30 MHz transducer (RMV-707B; VisualSonics). For chronic study, baseline readings were taken 1 week prior to surgery and then at 7 and 28 days post-MI. The Vevo 3100 high-resolution imaging system with 40MHz transducer (MX550S; Visual Sonics) was used for recording for the chronic study. For both models, analysis on acquired images was done with Visual Sonics VevoLab software. Left ventricular internal diameters, as well as the diameters of the intraventricular septum (IVS) and posterior walls (LVPW) were taken from m-mode images acquired at mid-papillary level. Simpson's modified method was used to determine systolic parameters, ejection fraction (%EF, $\%EF = [(LVEDV - LVESV)/LVEDV] \times 100$), fractional area change (%FAC), left ventricular end diastolic (LVEDV) and end systolic (LVESV) volumes. Simpson's method is assessed using LV endocardial border tracing in

multiple slices. This allows for a better overall assessment of systolic changes arising from the infarction. For these studies, systolic function was assessed through multiple parameters due to the fact %EF changes based on afterload and preload. Pulsed-wave Doppler imaging of the transmitral filling pattern was used to assess diastolic function with the early transmitral wave (E-wave) followed by the late filling wave due to atrial contraction (A-wave), when applicable. A limitation of this method is the fact the a-wave is often lost from extensive remodelling, thus diastolic function can be hard to accurately estimate in this model. Tissue doppler imaging was used to acquire isovolumetric relaxation (IVRT) and contraction (IVCT) times and with aortic ejection time (ET) used to calculate myocardial performance or Tei index (IVCT + IVRT/ET). Tissue doppler taken at the mitral annulus was used to describe LV filling pressure described by E', E'/A' and E/E'.

2.2.6.2 Electrocardiogram (ECG) Measurements

For chronic study, electrocardiogram (ECG) was obtained using telemetry in mice at baseline, 7 days and 28 days post-MI [578]. Mice were anesthetized using 1-2% isoflurane and maintained on heating pad. Three electrodes were subcutaneously inserted into the right axilla, left axilla and left inguinal areas (Lead I orientation) [579]. Signal was acquired using ACQ-7700 (Data Science International, USA) with P3 Plus software (ver. 5.0, Data Science International, USA) used to compute the data.

2.3 ASSESSMENT OF MITOCHONDRIAL FORM AND FUNCTION

2.3.1 *Mitochondrial catalytic enzymatic activity*

Enzymatic activity of key electron transport enzymes was assessed in human and mouse LV tissues. LV tissue was ground on dry ice with mortar and pestle cooled with liquid

nitrogen. 25-300mg of sample was homogenized in ice-cold muscle homogenization buffer (20mM Tris, 40mM KCl, 2mM EGTA, pH=7.4, with 50mM sucrose added the day of homogenization) and spun at 600 x g for 10 min at 4°C to remove cellular debris. Supernatant was collected and used to assess the activity of NADH:ubiquinone oxidoreductase (complex I), succinate dehydrogenase (SDH, complex II), cytochrome C oxidase (COX IV, complex IV) and citrate synthase (CS) [580]. Complex activity in each case was based on the utilization of particular substrate, stimulating a colour change measured. Activities for all assessed were normalized to volume and protein concentration following measurement using standard Bradford assay [581].

2.3.2 *Mitochondrial respiration*

The rates of oxygen consumption were measured using a Clark electrode to assess mitochondrial respiration in permeabilized whole cardiac fibres. Cardiac fibres from human and experimental mouse hearts were separated from the mid-wall of the left ventricle [582]. A small section of left ventricular free wall (~3mm³) was isolated into ice-cold isolation buffer (2.77 mM CaKEGTA, 7.23 mM K₂ EGTA, 20 mM imidazole, 20 mM taurine, 49 mM K-MES, 3 mM K₂ HPO₄, 9.5 mM MgCl₂, 5.7 mM ATP, 1 M leupeptin, 15 mM phosphocreatine). All fat and remaining vasculature were removed and myocardium was dissected into fibre bundles containing 6-8 fibres each, 1-2 mm wide and 3-4mm long. Fibres were permeabilized on ice for 20 minutes in 2ml isolation buffer containing 100µg/ml saponin; following permeabilization fibres were rinsed thrice in ice-cold respiration buffer (0.5mM EGTA, 3mM MgCl₂.6H₂O, 20mM taurine, 10 mM KH₂P₀₄, 20 mM HEPES, 1g/L BSA, 60mM potassium-lactobionate, 110mM mannitol, 0.3mM dithiothreitol, adjusted to pH 7.1 with 5 N KOH) and immediately added to a respiratory chamber with conditions of

2ml respiration buffer at 30°C connected to an OXYGRAPH-PLUS system (Hansatech Instruments Ltd, Norfolk, England). Basal respiration was taken as the oxygen consumption rate following addition of the substrates glutamate (10mM) and malate (5mM). ADP-stimulated respiration was taken following the addition of 0.5mM ADP. The contribution of complex II respiration was assessed by determining the rate following addition of succinate (10mM). All rates were taken over a period of at least 3.5 minutes. Before the addition of each substrate, a 35µl sample of chamber buffer was taken and flash frozen in liquid nitrogen. All rates used for analysis were measured before the relevant chamber sample was removed. At the end of the run, fibres were removed from the chamber and dried on pre-weighed tin foil in a tissue oven at 60°C for at least 24 hours. Dry fibre weights were then used to normalize oxygen consumption rates over time for each sample run.

2.3.3 Mitochondrial ultrastructure

Mitochondrial ultrastructure was assessed in left ventricular tissue from infarct and non-infarct regions from both WT and sEH null animals. A 1-2 mm³ sample of tissue was pre-fixed in a mixture of 3% glutaraldehyde and 3% paraformaldehyde in 0.1M sodium cacodylate buffer (pH 7.4) overnight at 4°C, followed by post-fixing in a mixture of 1.5% potassium ferrocyanide [K₄Fe(CN)₆] and 2% osmium tetroxide (OsO₄) in 0.15M sodium cacodylate buffer for 1 hour on ice. These tissues were additionally fixed in 2% OsO₄ in milli-Q water for 30 minutes at room temperature, followed by en bloc staining in 1% uranyl acetate solution (pH 5.0) overnight at 4°C, then additional staining in Walton's lead aspartate solution (pH 5.5) for 30 minutes at 60°C [583]. The tissues were continuously dehydrated in a series of ethyl alcohol (30, 50, 70, 80, 90, 95, 100%) followed by propylene oxide, embedded with a mixture of araldite 502 and embed 812 resin, and thermally polymerized

for 48 hours at 60°C. Serial ultra-thin sections (70 nm in thickness) were cut by an ultramicrotome (Leica UC7, Leica Microsystems Inc., Vienna, Austria) and coated by a carbon coater (Leica EM ACE600, Leica Microscystems Inc., Vienna, Austria). The carbon-coated sections were examined by a transmission electron microscope (Hitachi H-7650 TEM, Hitachi High-Technologies Canada, Inc.) at 60 kV equipped with a 16 megapixel EMCCD camera (XR111, Advanced Microscopy Technique, MA, USA).

2.4 IMMUNOBLOTTING

2.4.1 Tissue Homogenization

Frozen LV tissues were ground and homogenized on dry ice in a ceramic homogenizer cooled with liquid nitrogen. Samples were homogenized in ice-cold homogenization buffer (20mM Tris-HCl, 50mM NaCl, 50mM NaF, 5mM sodium pyrophosphate, 0.25M sucrose). Samples were spun at 700 x g for 10 minutes (4°C) to remove debris and the resultant supernatant was used as whole tissue lysate.

For subcellular fractionates, differential centrifugation was used to obtain mitochondrial, microsomal and cytosolic fractions of LV tissue[326]. Microsomal fractions contain both sarcoplasmic and endoplasmic reticula membranes. Tissues were homogenized in ice-cold fractionation buffer (sucrose 250 mM, TrisHCL 10 mM, EDTA 1 mM, sodium orthovanadate 1 mM, sodium fluoride 1 mM, aproptinin 10 µg/L, leupeptin 2 µg/L, pepstatin 100 µg/L). The homogenate was centrifuged for 10min at 700 x g and debris was removed. The supernatant was again centrifuged for 20 min at 10 000 x g (4°C) and the resulting pellet was taken as the mitochondrial fraction. The resultant supernatant was centrifuged for 1h at 100 000 x g (4°C), after which the resultant pellet was taken as the microsomal fraction. The

resultant supernatant was used as the cytosolic fraction. Both the mitochondrial and microsomal pellets were then resuspended in 35-50µl fractionation buffer and with the cytosolic fraction used for analysis. The protein concentrations of all three fractions were determined colourimetrically by Bradford assay.

2.4.2 SDS-PAGE and Western Blotting

Following Bradford assay 25-30µg of protein was loaded onto 4-15% TGX® gels (BioRad, Canada). Gels were run at 90V with 1X running buffer (25mM Tris base, 190mM glycine, 0.1% SDS) and transferred onto 0.2µM PVDF membranes in 1X transfer buffer (23mM, 190mM, with 20% methanol). Probing was done with antibodies against sEH (ELabscience, EAB-10489 or sc-22344), mEH (sc135984) (Santa Cruz Biotechnology Inc), CYP2J2 (ABS1605, SDHa (ab5839s), MFN1 (ab104274), Citrate Synthase (ab129095), VDAC (ab14734), α -tubulin (ab4074), (Abcam, Toronto, ON, CAN), OPA1 (bd612606) (Becton Dickinson Canada Inc, Mississauga, ON, CAN), MFN2 (cs9482), COX IV (cs11967), GAPDH (cs5174), (Cell signaling Technology, Inc., New England Biolabs, Ltd., Whitby, ON, Canada). Quantitation of band strength using densitometry was done using Image J software (NIH, USA) to obtain relative protein expression. All treatment groups were normalized to the appropriate loading control lane.

2.5 ELISA ASSAYS

2.5.1 Caspase-3

Caspase-3 activity was determined in tissue lysates by a spectrophotometric assay, which quantitated the formation of the product p-nitroaniline (p-Na) after cleavage of the DEVD-pNa substrate (ab39401, Abcam Inc, Toronto, ON, Canada).

2.5.2 *Proteasome*

Protein proteolysis was measured in tissue lysates using a commercially available fluorometric assay (APT280, Chemicon®, EMD Millipore, Etobicoke, ON, Canada). The kit measures the formation of 7-Amino-4-methylcoumarin (AMC) from cleavage of substrate LLVY-AMC by the proteasome.

2.5.3 *Aconitase Activity*

Aconitase enzyme activity was measured in tissue lysates spectrophotometrically (ab109712, Abcam Inc, Toronto, ON, Canada). Aconitase converts aconitate to cis-aconitate, which can be detected by increases in absorbance (240 nm) in the tissue homogenates. The amount of cis-aconitate formed is proportional to aconitase activity.

2.5.4 *14,15 DHET measurement analysis*

Concentrations of 14,15-DHET were measured using a competitive ELISA kit (DH1/DH11/DH21/DH101, Detroit R&D, Detroit, MI, USA). Briefly, the 14,15-DHET epitope and a 14,15-DHET-HRP conjugate compete for binding sites on a 96-well plate coated with an anti-14,15-DHET antibody. The amount of conjugate bound in each cell is held as constant, thus inversely correlating with the amount of 14,15-DHET in the samples. A 14,15-DHET standard logarithmic curve is used to obtain sample concentrations. Plasma samples collected at the time of tissue collection were utilized to determine 14,15-DHET levels.

2.5.5 *ATP Assay*

ATP concentrations were measured using a fluorometric based assay kit (ab83355, Abcam Inc, Toronto, ON, Canada). For tissue concentrations, heart powders were homogenized in ice-cold assay buffer and centrifuged at 15,000xg for 2 min. The supernatant

was used to quantitate ATP at 535nm excitation and 587nm emission with a Biotek plate reader (Winooski, VT, USA). For ATP in respiration buffer, chamber samples following ADP addition were used in place of tissue samples and normalized to dry fibre weight. Results were expressed as pmol of ATP per mg of dry fibre weight.

2.6 LC-MS/MS

20-30mg of each LV sample was used for LC-MS/MS. LCMS methods and multiple reaction monitoring are adapted from previous reports [584]. Samples were homogenized in 5x volume of 0.1% acetic acid in 5% methanol containing 1 μ M trans-4-[4-(3-adamantan-1-yl-ureido)-cyclohexyloxy]-benzoic acid (tAUCB), spiked with 3 ng PGE2-d9, d11-11,12-DHET, d11-11,12-EET (Cayman) as internal standards, extracted by liquid:liquid extraction with 3 ml ethyl acetate and dried in vacuum centrifuge. Samples were analyzed in duplicate 10 μ L injections. Online liquid chromatography of extracted samples was performed with an Agilent 1200 Series capillary HPLC (Agilent Technologies, Santa Clara, CA, USA). Separations were achieved using a Halo C18 column (2.7 mm, 10062.1 mm; MAC-MOD Analytical, Chadds Ford, PA), which was held at 50°C. Mobile phase A was 85:15:0.1 water:acetonitrile:acetic acid. Mobile phase B was 70:30:0.1 acetonitrile:methanol:acetic acid. Flow rate was 400 ml/min. Gradient elution was used; mobile phase percentage B and flow rate were varied as follows: 20% B at 0 min, ramp from 0 to 5 min to 40% B, ramp from 5 to 7 min to 55% B, ramp from 7 to 13 min to 64% B. From 13 to 19 min the column was flushed with 100% B at a flow rate of 550 Turbo desolation gas was heated to 425°C at a flow rate of 6 L/min. Negative ion electrospray ionization tandem mass spectrometry with multiple reaction monitoring was used for detection. Quantification was done using Analyst

1.5.1 software comparing relative response ratios for each analyte/internal standard to standard curves for each analyte.

2.7 STATISTICAL ANALYSES

For the *in vivo* sections of this thesis, statistical power analysis was not performed but is an important consideration for future studies.

2.7.1 *Acute animal model*

For the 7-day post-LAD model, statistical significance was determined by one-way ANOVA with Bonferroni post hoc test to assess differences between groups. Statistics were assessed using Prism 6 software. Interactive effects between genotype and age are described in Table 3.1.2; these are descriptive values only and no statistical significance was assessed. Values are expressed as mean \pm standard error of mean (SEM). Values were considered significant when $p < 0.05$.

2.7.2 *Chronic animal model*

All statistics were done using Prism 8 software. For the 28-day LAD study, two-way ANOVA was carried out using Tukey's post-hoc testing with significance set at $p < 0.05$. Data was assessed either by comparing genotype (WT, sEH null) with days post-MI or myocardial area, or treatment (WT+vehicle, WT+tAUCB) with days post-MI or myocardial area. Males and females were analysed separately.

2.7.3 *Human clinical data*

For human clinical parameter assessment, the Mann Whitney was used for all quantitative parameters with qualitative counts assessed using standard chi squared testing.

For human tissue samples, analysis was done using one-way ANOVA with Tukey's post-hoc test. Significance was set at $p < 0.05$ for all cases.

Chapter 3

Results

³The results below are adapted from:

Chapter 3.1 has been previously published as: Jamieson KL, Samokhvalov V, Akhnokh M, Lee K, Cho WJ, Takawale A, et al. Genetic Deletion of Soluble Epoxide Hydrolase Provides Cardioprotective Responses Following Myocardial Infarction in Aged Mice. *Prostaglandins Other Lipid Mediat.* 2017;132(47-58)

Chapter 3.2 and 3.3 have been adapted from: Jamieson KL, Darwesh AM, Sosnowski DK, Zhang H, Shah S, Wang W, Zhabyeyev P, Yang J, Hammock B, Edin ML, et al. Sexual Dimorphic Responses to Myocardial Infarction Following Inhibition of Soluble Epoxide Hydrolase in Aged Mice and Human Explanted Hearts. Submitted to *Cardiovascular Research*, March 20, 2020.

3.1 sEH DELETION PROTECTS AGAINST ACUTE MYOCARDIAL INFARCTION IN AGED MICE

Previous evidence in young mice has demonstrated that pharmacological and genetic models of sEH suppression protect against IRI, preserving mitochondrial and cardiac function. The purpose of this study was to investigate whether the protective effects are observed in aged mice. To address this question, middle-aged 16-month-old and young 3-month-old mice underwent LAD ligation and were held for 7 days. The data discussed in this section demonstrate a decline in cardiac function associated with ageing in both WT and sEH null mice. Although less pronounced compared to those observed in young mice, deletion of sEH demonstrated protective responses toward ischemic injury in aged mice.

3.1.1 *sEH* deletion limits cardiac functional decline following MI

Baseline heart function was similar between WT and sEH null mice within each age group. However, there was an age-related decline in heart function in both WT and sEH null mice compared to their respective young baselines (Table 3.1.1 describes both basal and post-MI heart function assessed by one-way ANOVA with Bonferroni post-hoc test; Table 3.1.2 represents percent change between young and aged mice at baseline as a marker of the interaction effect between genotype and age, no statistics were assessed for this table). Table 3.1.1 shows the average heart rate of the young and aged animals before and after MI. There were no statistically significant changes between the groups indicating no changes to LV function can be attributed to changes in HR. Assessment of LV internal diameter during diastole and systole revealed age-dependent increases for WT and sEH null hearts. Consistently, LV volume and mass increased with ageing similarly in WT and sEH null mice (Table 3.1.1; Table 3.1.2). Pulsed wave Doppler of mitral filling revealed no significant changes in the E/A ratio with aged sham hearts in either WT or sEH null mice suggesting no

significant alterations in diastolic function (Table 3.1.1). The %EF calculated using the Simpson's method demonstrated a trend toward reduced systolic function in aged WT and sEH null hearts compared to baseline levels observed in young mice (Table 3.1.1; Table 3.1.2). Doppler-derived myocardial performance index (Tei index), defined as the sum of the isovolumic contraction and relaxation times divided by ejection time, can provide information about global left ventricular function. Results demonstrated a significantly higher value at baseline in aged WT and sEH null mice compared to their younger baseline controls, suggesting a decline general in myocardial performance with age (Table 3.1.1).

TABLE 3.1.1: Cardiac function pre- and post-MI determined by echocardiography in WT and sEH null young and aged mice. Values are represented mean \pm SEM, N=5-7, $p < 0.05$, *significantly different from its own baseline; #significantly different from WT equivalent at same age; ‡significantly different from corresponding young group.

	YOUNG				AGED			
	<i>WT</i>	<i>WT</i>	<i>sEH null</i>	<i>sEH null</i>	<i>WT</i>	<i>WT</i>	<i>sEH null</i>	<i>sEH null</i>
	Baseline (n=7)	Post-MI (n=7)	Baseline (n=5)	Post-MI (n=5)	Baseline (n=7)	Post-MI (n=6)	Baseline (n=7)	Post-MI (n=6)
Heart rate, beats/min	462 \pm 20	429 \pm 14	519 \pm 30	485 \pm 27	474 \pm 8	450 \pm 19	483 \pm 11	468 \pm 27
LVID-diastole, mm	3.80 \pm 0.17	4.95 \pm 0.14*	3.66 \pm 0.15	3.95 \pm 0.17#	4.34 \pm 0.17	4.81 \pm 0.07	4.53 \pm 0.09‡	4.72 \pm 0.16‡
LVID-systole, mm	2.41 \pm 0.21	4.28 \pm 0.19*	2.20 \pm 0.16	2.66 \pm 0.31#	3.10 \pm 0.19	3.88 \pm 0.15	3.12 \pm 0.12	3.64 \pm 0.20‡
LVEDV, μ l	58.66 \pm 4.61	116.14 \pm 7.43*	57.32 \pm 5.40	64.47 \pm 9.42#	66.94 \pm 2.75	112.04 \pm 17.26*	72.96 \pm 5.25	85.73 \pm 4.54
LVESV, μ l	18.90 \pm 3.36	83.67 \pm 8.96*	16.74 \pm 2.97	26.69 \pm 8.01#	29.19 \pm 2.16	73.58 \pm 11.17*	29.01 \pm 2.89	49.60 \pm 3.97
EF, %	69.37 \pm 3.52	28.20 \pm 5.31*	71.06 \pm 3.65	55.43 \pm 6.69#	56.39 \pm 2.56	34.25 \pm 2.68*	60.33 \pm 2.71	44.30 \pm 2.73
LV Mass, mg	72.15 \pm 5.23	84.80 \pm 8.11	75.15 \pm 3.04	74.48 \pm 10.52	128.9 \pm 12.8‡	163.4 \pm 9.40‡	126.1 \pm 8.94	150.2 \pm 18.95‡
Mitral E/A	1.63 \pm 0.07	3.16 \pm 0.70	1.72 \pm 0.09	1.96 \pm 0.13	1.54 \pm 0.14	4.64 \pm 1.06*	1.52 \pm 0.06	2.80 \pm 0.75
IVRT, ms	13.90 \pm 2.02	18.53 \pm 1.69	13.53 \pm 0.68	14.65 \pm 1.04	18.69 \pm 0.81	22.86 \pm 1.54	17.34 \pm 0.85	19.33 \pm 1.60
IVCT, ms	11.12 \pm 0.45	14.43 \pm 3.39	7.20 \pm 0.91	5.57 \pm 0.54#	16.23 \pm 1.34	18.84 \pm 1.39	15.16 \pm 1.22‡	18.67 \pm 2.03‡
ET, ms	53.21 \pm 2.63	50.13 \pm 0.78	41.12 \pm 2.11#	48.25 \pm 3.62	42.50 \pm 1.64‡	39.50 \pm 1.78‡	41.56 \pm 0.81	40.31 \pm 1.29
Tei Index	0.48 \pm 0.05	0.66 \pm 0.04	0.49 \pm 0.04	0.42 \pm 0.03#	0.83 \pm 0.04‡	1.11 \pm 0.06*‡	0.79 \pm 0.05‡	0.85 \pm 0.04#‡

TABLE 3.1.2. Percent change in baseline cardiac function in aged hearts. Cardiac function as assessed by echocardiography. Baseline values are expressed as the percent change in cardiac parameter in aged hearts from corresponding young animals. Positive and negative values represent an overall increase or decrease, respectively. N=5-7.

	<i>WT</i>	<i>sEH null</i>
Heart rate (beats/min)	+3	-7
LVID; d (mm)	+13	+19
LVID; s (mm)	+22	+30
LV Vol; d	+12	+22
LV Vol; s	+35	+42
% EF	-23	-18
LV Mass	+44	+41
Mitral E/A	-5	-13
IVRT (ms)	+26	+22
IVCT(ms)	+32	+53
ET (ms)	-25	+1
Tei Index	+42	+38

Post-MI cardiac dysfunction characterized by significant decreases in EF and increases in LV volumes and dimensions was primarily observed in WT mice (Table 3.1.1). Consistent with our previous observation, genetic deletion of sEH significantly attenuated the cardiac dysfunction observed in young WT mice 7 days following MI [215]. Post-MI hearts from aged WT mice showed greater LV dilation and increase in LV mass compared to age-matched sEH null mice. Post-MI hearts from aged sEH null mice only showed minor alterations in LV dimension and volume compared to aged baseline levels (Table 3.1.1). Alteration in the mitral E/A ratio was significantly higher in the aged WT post-MI group while no significance changes were observed in aged sEH null post-MI hearts. In post-MI aged WT animals, there was a significant decrease of systolic function as reflected by decreased EF, which was attenuated in sEH null post-MI hearts. In the ageing animals, post-MI WT mice demonstrated a significant increase in Tei index, which was significantly attenuated in sEH null mice suggesting preserved cardiac function.

3.1.2 *sEH deletion limits post-MI injury in aged animals*

Infarction was observed in both age groups following permanent LAD ligation in WT and sEH null mice (Figure 3.1.1). There was no difference in caspase-3 activity, a marker of apoptotic activation, in any of the sham groups, young or aged (Figure 3.1.2). However, post-MI young WT mice displayed a significant increase in caspase-3 activity compared to sham that was attenuated in the young sEH null mice post-MI (Figure 3.1.2). Aged WT mice post-MI displayed an increase in caspase-3 activity that was significant to the young WT post-MI group as well as to its aged sham (Figure 3.1.2). This increase in activity was significantly reduced in aged post-MI sEH null mice (Figure 3.1.2).

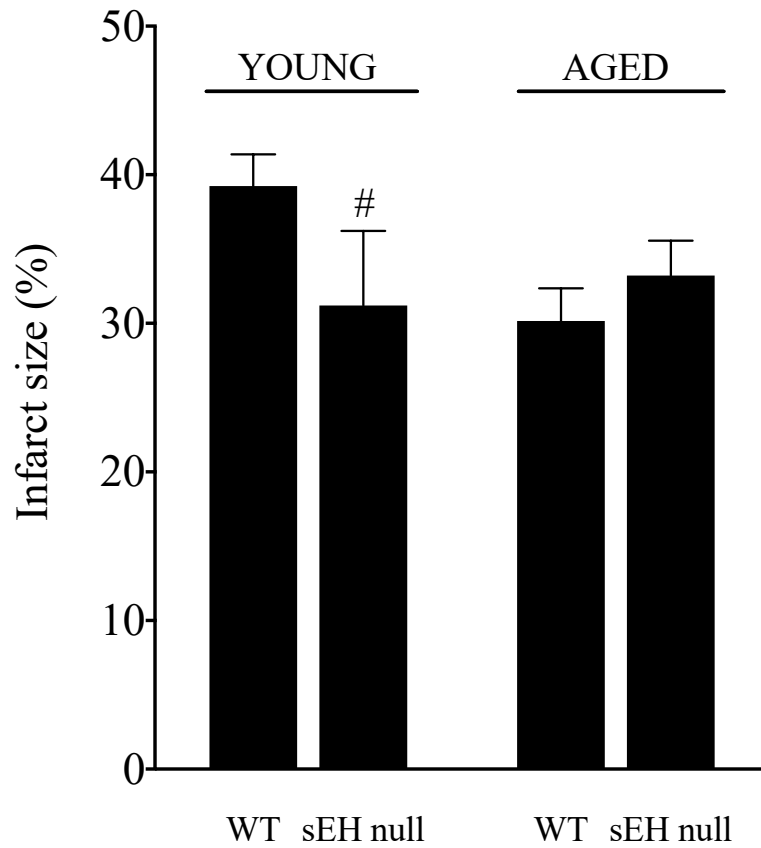


FIGURE. 3.1.1 Infarct size was quantified from transverse heart slices from young and aged mice stained with TTC. Background staining of shams was subtracted from post-MI groups, N=4. $p < 0.05$. # significantly different from WT equivalent at same age.

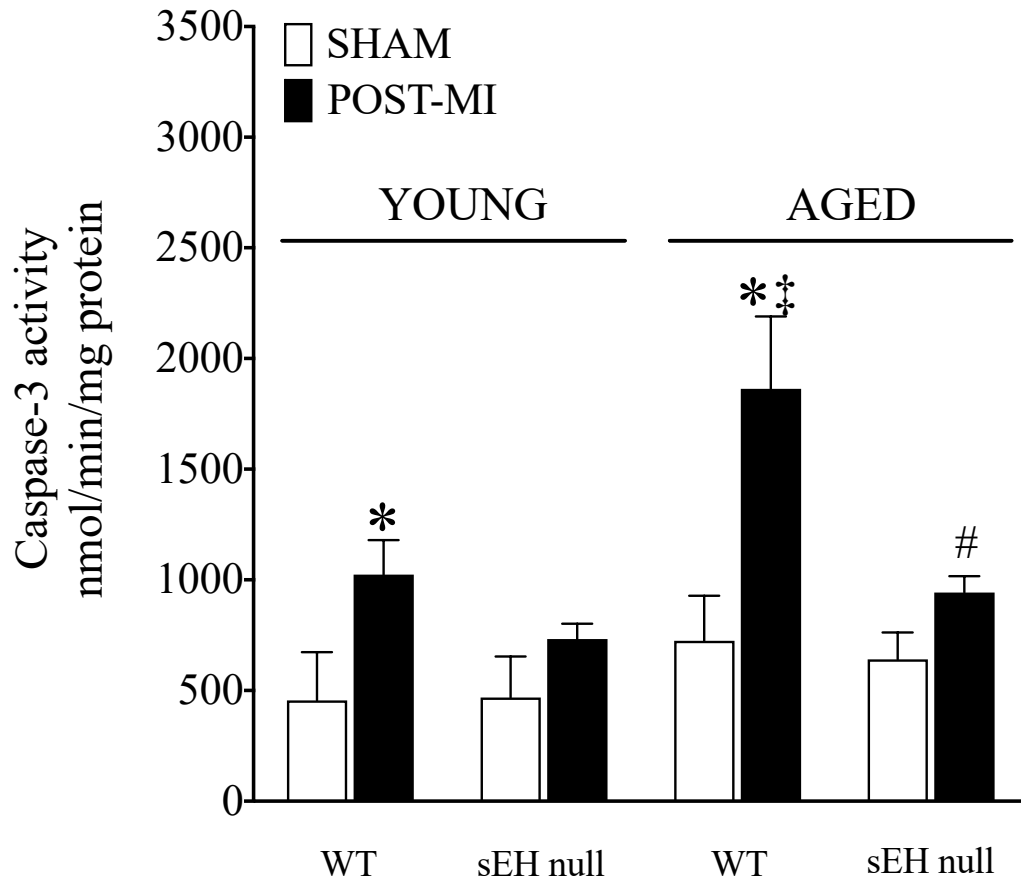


FIGURE. 3.1.2. Caspase-3 activity in young and aged hearts at sham and 7 days post-MI. Post-MI is tissue from non-infarct region. Values represent mean \pm SEM, N=5, $p < 0.05$. *significantly different from its baseline; #significantly different from WT equivalent at same age; ‡significantly different from corresponding young group.

Decline in quality control mechanisms regulating the cellular proteome has a critical role in the ageing process [585]. Notably, myocardial aging is accompanied by dysregulated proteasome expression and activity that can affect responses to ischemic injury, as such we used proteasome activity as a marker of cellular injury [586]. The 20S proteasome is the core unit of all proteasomal systems, which has a major role in protein degradation. There was a significant increase in 20S proteasome activity observed in aged WT compared to young WT hearts, both at sham and post-MI (Figure 3.1.3). Conversely, sham hearts from aged sEH null mice had similar proteasome activity as young mice (Figure 3.1.3). Moreover, 20S proteasome activity was significantly attenuated in aged sEH null mice compared to aged WT hearts. Both sham and post-MI hearts from aged WT mice demonstrated a significant increase in 20S proteasome, which was significantly attenuated in aged sEH null animals (Figure 3.1.3).

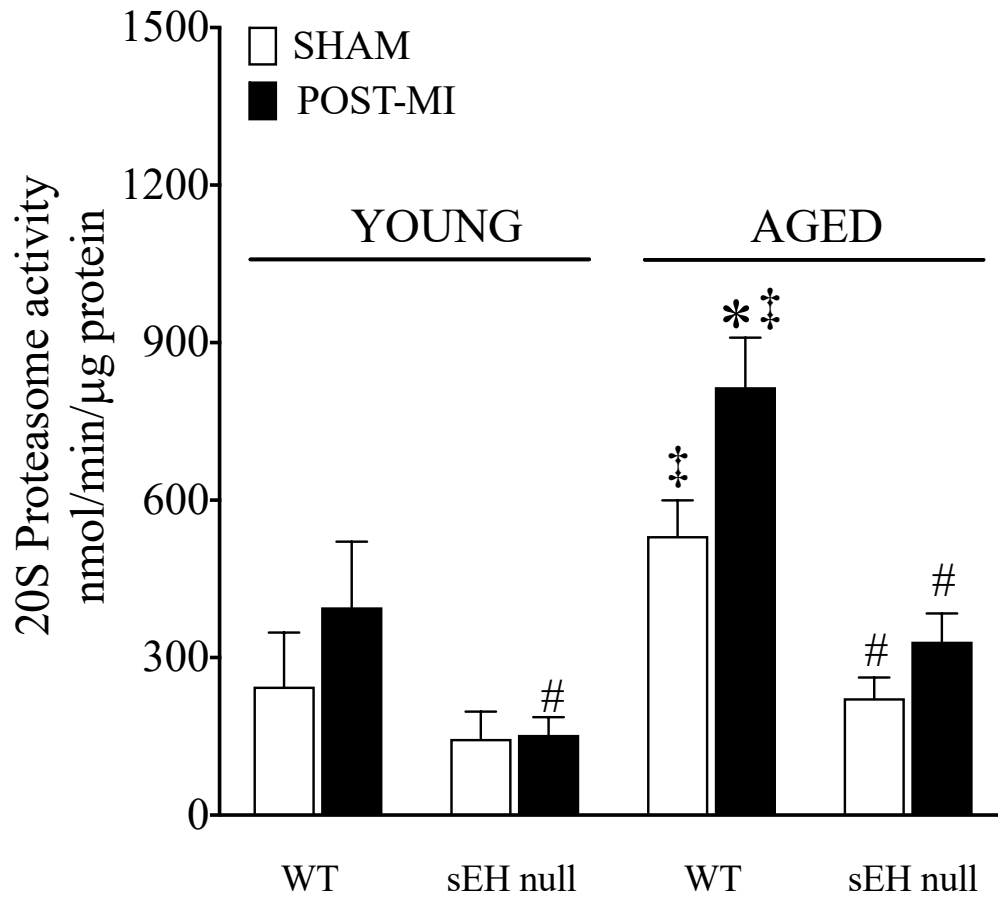


FIGURE 3.1.3. 20S proteasome activation in aged and young hearts at sham and 7-days post-MI. Post-MI is tissue from non-infarct region. Values represent mean \pm SEM, N=5, $p < 0.05$. *significantly different from its baseline; #significantly different from WT equivalent at same age; ‡significantly different from corresponding young group.

Aconitase, a key enzyme within the citric acid cycle that converts citrate to isocitrate, is known to be highly susceptible to oxidative damage associated with ageing [587]. A significant decrease in aconitase activity was observed in aged sham WT hearts compared to young WT hearts (Figure 3.1.4). However, the decline in activity was not observed in the sEH null hearts. Post-MI aged sEH null mice demonstrated a significant conservation in aconitase activity compared to the post-MI ageing WT mice (Figure 3.1.4).

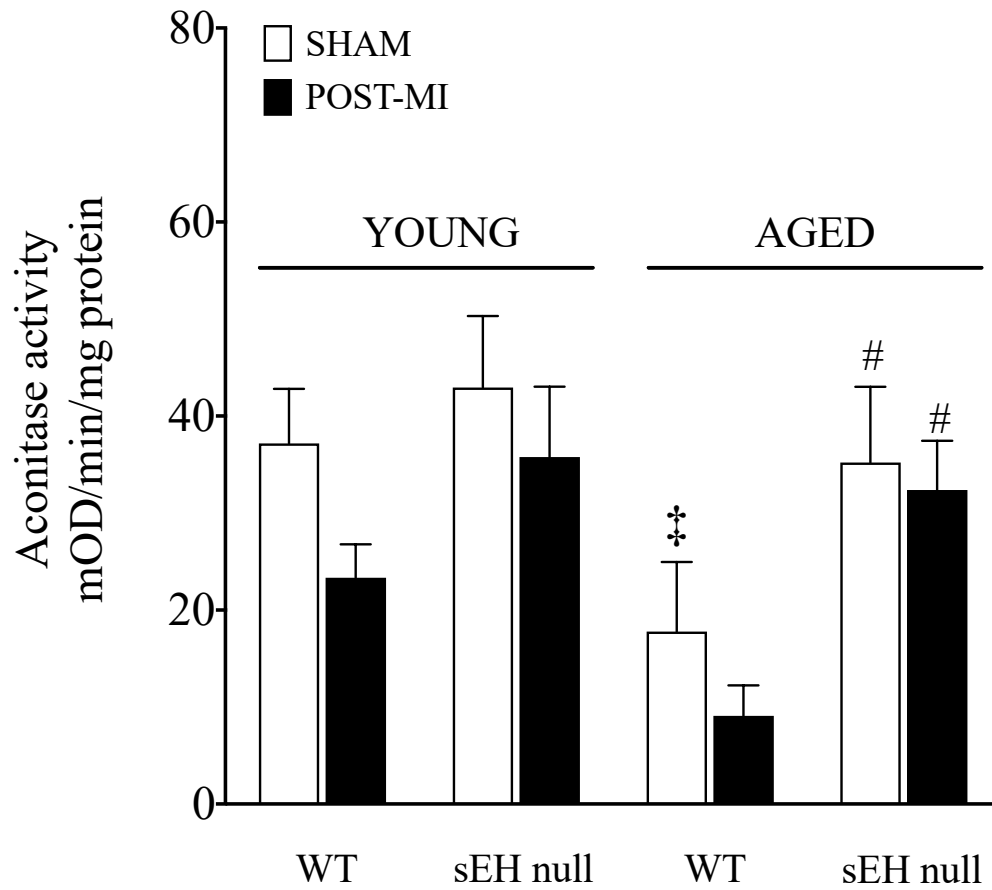


FIGURE 3.1.4. Aconitase activity in young and aged hearts, at sham and 7-days post-MI. Post-MI is tissue from non-infarct region. Values represent mean \pm SEM, N=5, $p < 0.05$. *significantly different from its baseline; #significantly different from WT equivalent at same age; ‡significantly different from corresponding young group.

Maintenance of ultrastructure is crucial to mitochondrial function and efficiency. EM images from both young WT and sEH null mice demonstrated similar ultrastructure and organization in the non-infarct region of the left ventricle post-MI hearts (Figure 3.1.5). The non-infarct regions in aged hearts indicated a loss of mitochondrial structural appearance, including decreased cristae density and general rounding, compared to their younger controls that was less pronounced in sEH null mice (Figure 3.1.6). In the infarct region, young WT mice displayed a complete loss of cellular organization, cristae and ultrastructure that was maintained in the young sEH null mice (Figure 3.1.5). Similarly, in aged hearts the mitochondrial ultrastructure in infarct regions was demonstrably damaged in both WT and sEH null hearts (Figure 3.1.6). Sections from sEH null mice demonstrated better structure within the infarct regions compared to WT young mice, however this difference was less obvious in aged mice.

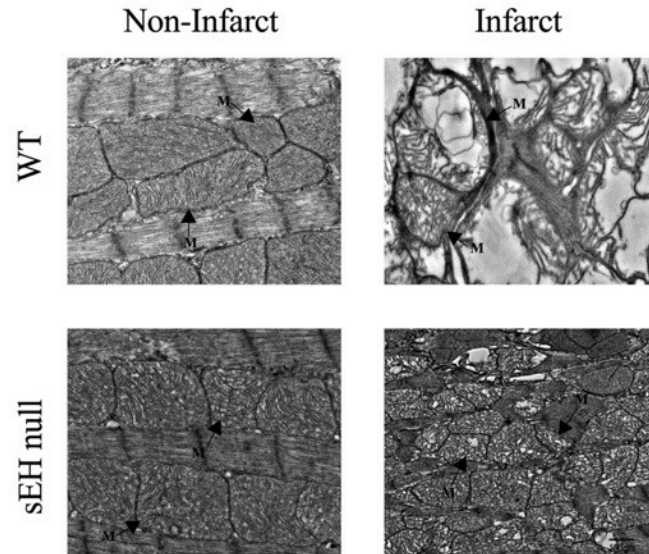


FIGURE 3.1.5. Representative electron micrograph images of non-infarct and infarct regions of left ventricles from post-MI young WT and sEH null mice. WT mice demonstrate damage throughout the infarcted heart, typified by loss of cristae structure and myofibrillar form. These effects were attenuated in sEH null mice. (Magnification = 6000 \times ; bar indicates 500 nm). Images were taken from the heart of one representative animal, each heart region sectioned into 5 sections.

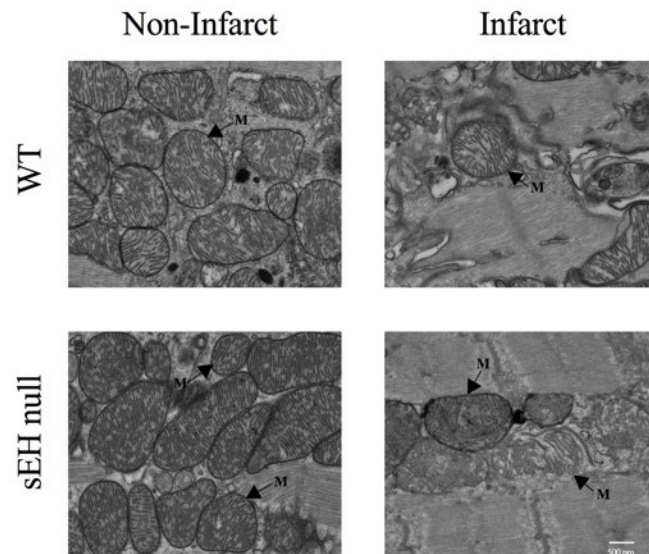


FIGURE 3.1.6. Representative electron micrograph images of non-infarct and infarct regions of left ventricles from post-MI aged WT and sEH null mice. Similar effects to young animals were observed in the infarct regions of both genotypes, however aged hearts demonstrated rounded mitochondria with diffuse cristae typical of aging. (Magnification = 6000×; bar indicates 500 nm). Images were taken from the heart of one representative animal, each heart region sectioned into 5 sections.

3.1.3 *Mitochondrial enzyme activities significantly decreased with age*

Immunoblots revealed no differences in the protein expression of citrate synthase (CS), succinate dehydrogenase A (SDH-A) or cytochrome C oxidase (COX IV) in WT and sEH null animals in either sham or post-MI groups (Figure 3.1.7A-D).

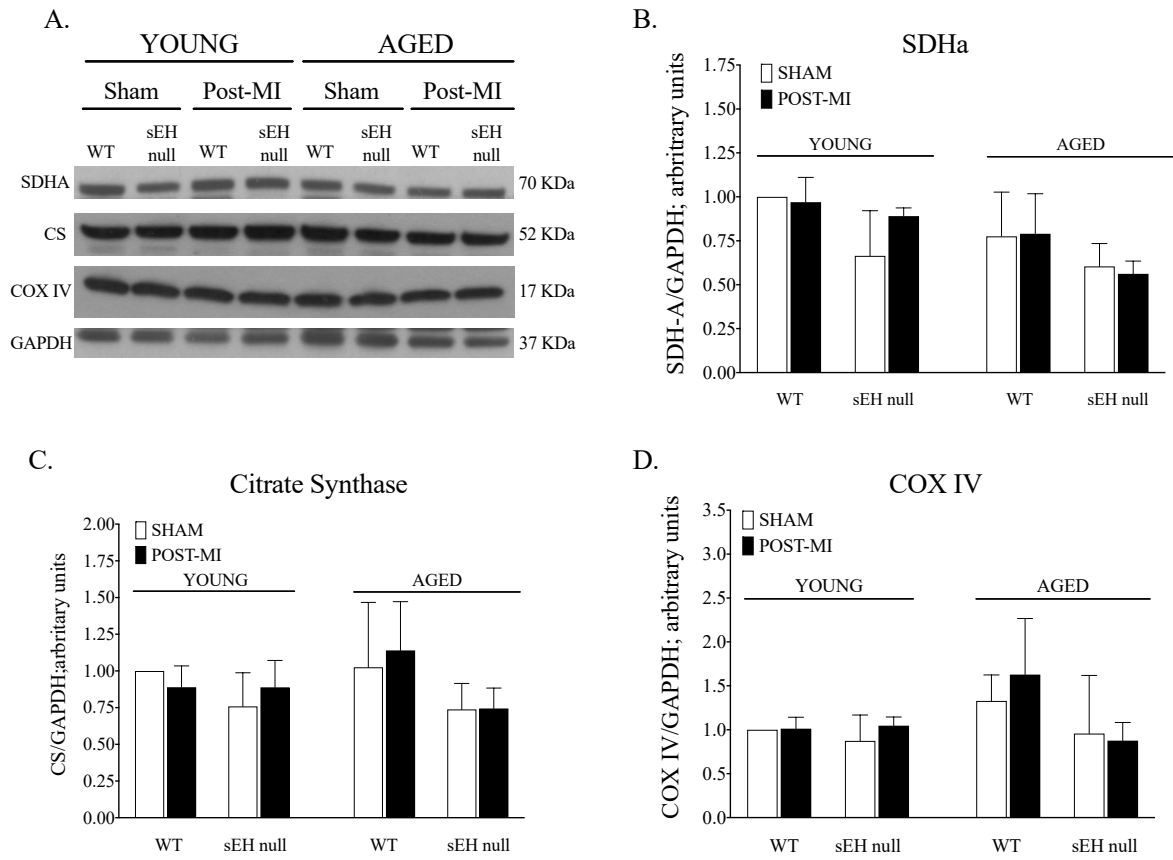


FIGURE 3.1.7. Protein expression of key mitochondrial enzymatic subunits in sham and non-infarct left ventricle. Representative western blots (A) and quantification of (B) succinate dehydrogenase subunit A (SDH-A), (C) citrate synthase (CS), and (D) COX-IV protein expression observed in LV non-infarct regions in aged sham operated and 7 day post-MI hearts. All expression was normalized to GAPDH. Values represent mean \pm SEM, N = 4, P < 0.05.

Next, the enzymatic activities of key ETC enzymes NADH:ubiquinone oxidoreductase, SDH and COX IV as well as CS activity were assessed (Figure 3.1.8A-D). Citrate synthase, localized in the mitochondrial matrix, is a key citric acid cycle enzyme and biomarker for intact mitochondria [580]. Post-MI CS activity was significantly decreased in young WT but not sEH null hearts; however, there was a large decrease in CS activity observed in all groups from aged mice (Fig 3.1.8A). Similarly, NADH:ubiquinone oxidoreductase activity significantly decreased in aged compared to in young animals (Fig 3.1.8B). While post-MI young WT mice exhibited decreased activity compared to sham hearts, activity was maintained post-MI in young sEH null animals (Fig 3.1.8B). There was a trend for decreased activity that was not statistically significant between aged WT and sEH null post-MI mice (Fig 3.1.8B). Both young WT and sEH null mice demonstrated a significant decline in SDH activity with time (Fig 3.1.8C). While there were no differences between aged WT and sEH null animals post-MI, young WT and sEH null both demonstrated significant decline of SDH activity following MI compared to their shams (Fig 3.1.8C). Comparably, COX IV activity significantly declined with age in both WT and sEH null animals (Fig 3.1.8D).

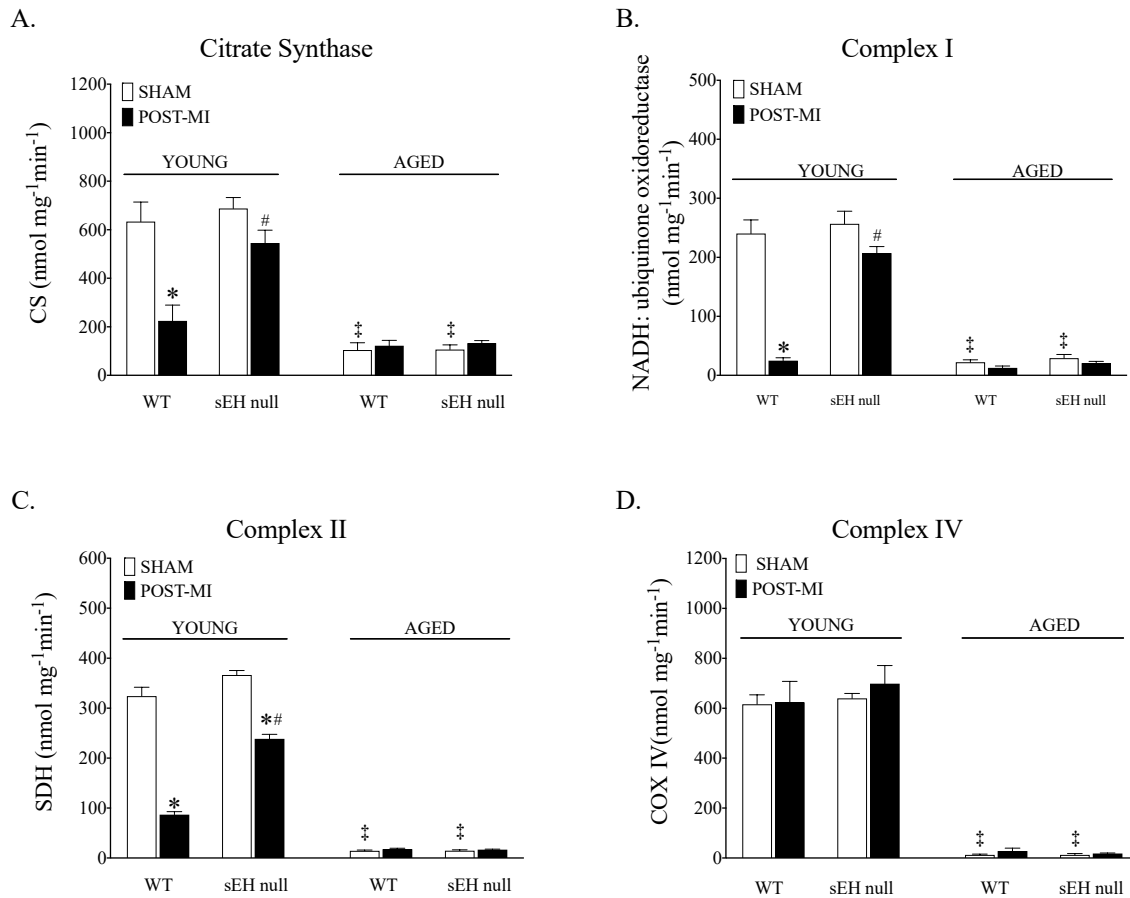


FIGURE 3.1.8. Activities of key mitochondrial enzymes were assessed spectrophotometrically in non-infarct regions of left ventricle. Activities of (A) CS, (B) NADH:ubiquinone oxidoreductase, (C) SDH, and (D) COX IV were determined. Values represent mean \pm SEM, N = 6, $p < 0.05$. *Significantly different from its sham group; # significantly different from WT equivalent at same age; ‡significantly different from corresponding young group.

3.1.4 Aging affects epoxide hydrolase activity

No sEH expression was detected by Western blot in sEH null animals confirming deletion (Figure 3.1.9 A, B). Furthermore, there was no significant change over ageing in sEH expression (Figure 3.1.9 B).

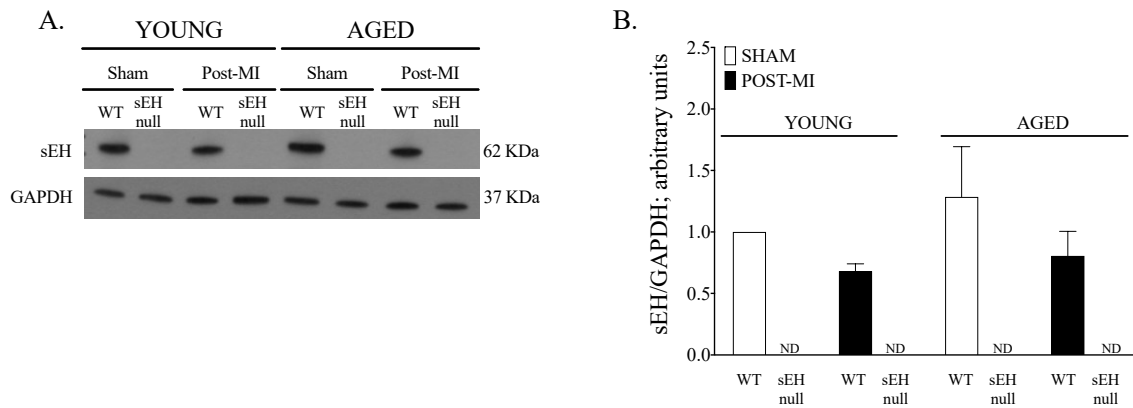


FIGURE 3.1.9. Soluble epoxide hydrolase expression. Representative western blots (A) and quantification of (B) sEH protein expression. Expression was normalized to GAPDH, N=4.

Microsomal epoxide hydrolase (mEH), a microsomal xenobiotic metabolising enzyme in the same family as sEH, has demonstrated diverse biological functions in humans [588]. While mEH is capable of metabolising arachidonic acid derivatives such as EETs, it has a reduced role in cardiac EET metabolism compared to sEH [588]. Interestingly, our results demonstrated a significant increase in mEH expression with age in both WT and sEH null sham hearts (Figure 3.1.10 A,B).

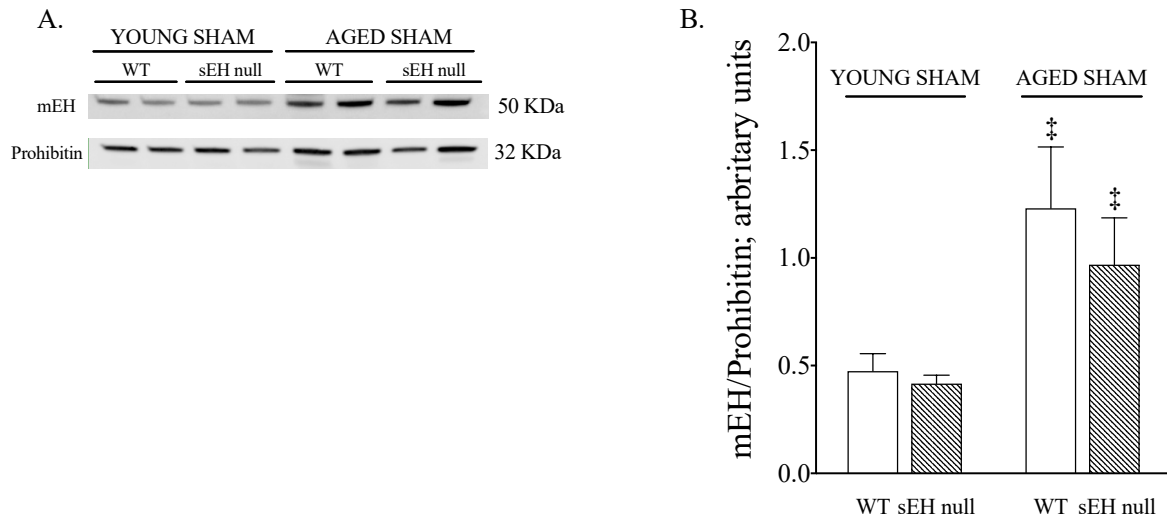


FIGURE 3.1.10. Microsomal epoxide hydrolase expression. Microsomal fractions were used for western blotting (A) to quantitate changes in microsomal epoxide hydrolase (mEH) during normal ageing (B), values are mean \pm SEM. N = 4, p < 0.05. Each band was normalized to microsomal protein, prohibitin. ‡significantly different from corresponding young group.

To obtain an indication of epoxide hydrolase enzymatic activity we assessed plasma levels of 14,15-dihydroxyeicosatrienoic acid (14,15-DHET), which is the primary metabolite produced from sEH-mediated metabolism of 14,15-EET [25]. Plasma from young post-MI WT mice demonstrated a significant increase in 14,15-DHET levels that was significantly attenuated in young sEH null mice (Figure 3.1.11). The 14,15-DHET levels observed in sEH null plasma might be attributed to mEH activity. Interestingly, baseline production of 14,15-DHET in WT mice did not differ between young and aged mice; however, in post-MI aged WT mice there was a significantly lower metabolite level compared to that observed in post-MI young mice (Figure 3.1.11).

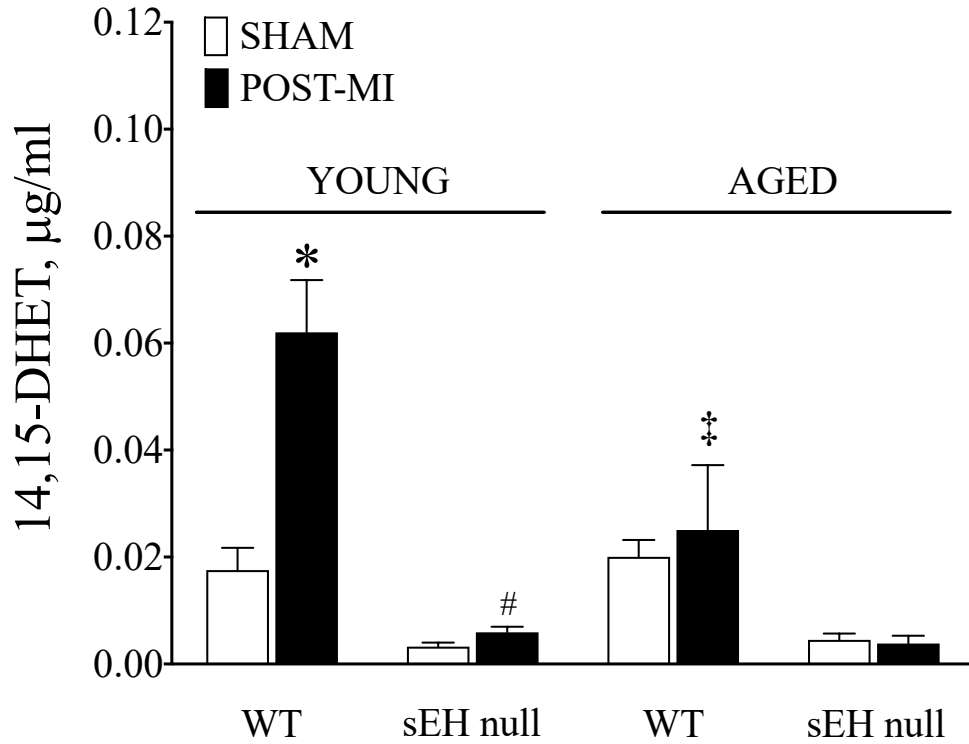


FIGURE 3.1.11. 14,15-DHET levels in sham and post-MI hearts. Plasma 14,15-DHET levels was measured using ELISA assay. N = 6, p < 0.05. *Significantly different from its sham group; # significantly different from WT equivalent at same age; ‡significantly different from corresponding young group.

3.1.5 *sEH deletion preserves mitochondrial bioenergetics post-MI*

In order to estimate cardiac mitochondria efficiency, we analyzed mitochondrial respiration in situ using cardiac fibres isolated from young and aged hearts. Basal respiration did not differ significantly between the experimental groups, although there was an apparent increased trend in aged WT and sEH post-MI groups (Table 3.1.3), which suggests a potentially compromised ability of the mitochondrial membrane to sustain the chemiosmotic gradient. Further analysis revealed a dramatic decline in the ADP-stimulated component of mitochondrial respiration post-MI in the young mice and in aged shams compare to younger equivalents, providing strong evidence that overall production of ATP was significantly lowered. Indeed, the respiratory control ratio (RCR), a marker of mitochondrial efficiency, significantly decreased in WT aged sham hearts compared to young WT animals (Table 3.1.3). However, the RCR values were maintained in aged sEH null hearts, suggesting more optimal mitochondrial oxidative respiration compared to WT mice. Aged post-MI mice had increased ADP-stimulated respiration, however overall decreased RCR values demonstrate that mitochondrial respiration was significantly reduced post-MI in both aged and young WT mice. This decrease in post-MI RCR values was attenuated in sEH null hearts (Table 3.1.3). Succinate is known to elicit a high respiratory activity associated with less efficient but more rapid production of ATP, which commonly occurs in injured tissues prior to cardiac failure [589]. Succinate was added at the middle of ADP-stimulated respiration to initiate the involvement of complex II. Our data demonstrate there were no differences in succinate oxidation between hearts from young WT and sEH null sham animals. However, there was a significant increase in post-MI aged WT hearts that was attenuated in aged sEH null hearts (Table 3.1.3). Thus, our data suggest activation of succinate oxidation was associated with

more severe cardiac dysfunction in aged WT post-MI group compared to the corresponding sEH null group. Next, we assessed ATP levels in the chamber respiration buffer comparing young and aged cardiac fibres. Consistent with decreased RCR, generation of ATP from fibers isolated from aged WT mice post-MI hearts was significantly lowered. This detrimental effect was attenuated in sEH null mice, suggesting protection of mitochondrial efficiency (Table 3.1.3).

TABLE 3.1.3. Respirometry and ATP analysis of young and aged WT and sEH null mice pre- and post-MI. Respiration in permeabilized muscle fibers from the non-infarct region of the left ventricle was measured using a Clark-electrode based chamber connected to oxygraph. Respiration rates are expressed as Respiratory Control Ratio (RCR). ATP content in the chamber buffer was determined 3.5 min following addition of ADP. Values are reported as mean \pm SEM, N = 5–6, $p < 0.05$, *significantly different from its own baseline; # significantly different from WT equivalent at same age; ‡significantly different from corresponding young group.

	YOUNG				AGED			
	<i>WT</i>	<i>WT</i>	<i>sEH null</i>	<i>sEH null</i>	<i>WT</i>	<i>WT</i>	<i>sEH null</i>	<i>sEH null</i>
	Sham	Post-MI	Sham	Post-MI	Sham	Post-MI	Sham	Post-MI
Basal Respiration (nmol O ₂ /min/mg)	2.67 \pm 0.60	2.51 \pm 0.54	2.81 \pm 0.32	1.96 \pm 0.32	2.24 \pm 0.34	5.01 \pm 1.24	1.74 \pm 0.22	4.20 \pm 0.77
ADP-stimulated (nmol O ₂ /min/mg)	12.26 \pm 2.37	6.20 \pm 0.99	11.27 \pm 1.32	5.01 \pm 1.00	5.89 \pm 0.93	9.24 \pm 1.72	7.01 \pm 0.62	11.93 \pm 2.17‡
RCR	5.1 \pm 0.96	2.1 \pm 0.39*	4.0 \pm 0.27	2.8 \pm 0.25	2.7 \pm 0.54‡	2.1 \pm 0.24	4.1 \pm 0.27	3.1 \pm 0.18
Succinate-stimulated (nmol O ₂ /min/mg)	12.06 \pm 2.18	10.19 \pm 1.24	11.98 \pm 1.41	8.47 \pm 1.77	8.48 \pm 0.73	25.00 \pm 6.87*‡	9.00 \pm 0.45	16.93 \pm 2.35
ATP (nmol/mg/min)	0.61 \pm 0.13	0.53 \pm 0.20	0.43 \pm 0.12	0.36 \pm 0.07	0.40 \pm 0.06	0.16 \pm 0.01*	0.36 \pm 0.05	0.27 \pm 0.07

3.1.6 *Conclusion*

In conclusion, we initially report that sEH deletion preserves cardiac function and mitochondrial bioenergetics in aged and young mice following MI. Post-MI aged sEH null mice demonstrated sustained systolic and diastolic function, maintained mitochondrial bioenergetics and attenuated markers of injury compared to age-matched WT animals. These results support our original hypotheses regarding the effects of sEH deletion on cardiac function post-MI, as well as the effects of aging on mitochondrial function in the absence of injury. However, in this initial study we did not assess sex differences, as previous reports in young animals reported no sexual dimorphism in this model of MI. As such, these results must be tempered by the clear sexual dimorphism we observed in our chronic model of MI described in the following chapter of this dissertation.

3.2 SEXUAL DIMORPHISM IN CARDIOPROTECTION FOLLOWING ISCHEMIC INJURY IN AGED MICE WITH GENETIC DELETION OR PHARMACOLOGIC INHIBITION OF sEH

In this section, we used a chronic model of permanent LAD ligation wherein mice were held to 28-days post-MI. WT, sEH null and CYP2J2-Tr mice were used, with WT and CYP2J2-Tr mice given sEHi *t*AUCB in the drinking water starting immediately after LAD ligation (*t*AUCB:0d, same-day). Another subset of WT mice were given *t*AUCB starting 4 days before surgery (*t*AUCB:4d, pre-treatment). Initial data collection revealed a key difference in animal survival that led to analysis of males and females separately. Unexpectedly, we demonstrate a sexual dimorphic response to sEH inhibition whereby cardioprotection was observed only in female mice. These data may have implications for drug development for women in middle-age.

3.2.1 sEH genetic deletion and pharmacologic inhibition exhibits sexually dimorphic effects on survival post-MI

Consistent with the 7-day injury model, tetrazolium chloride (TTC) staining was used to ensure infarct development in all groups (Figure 3.2.1).

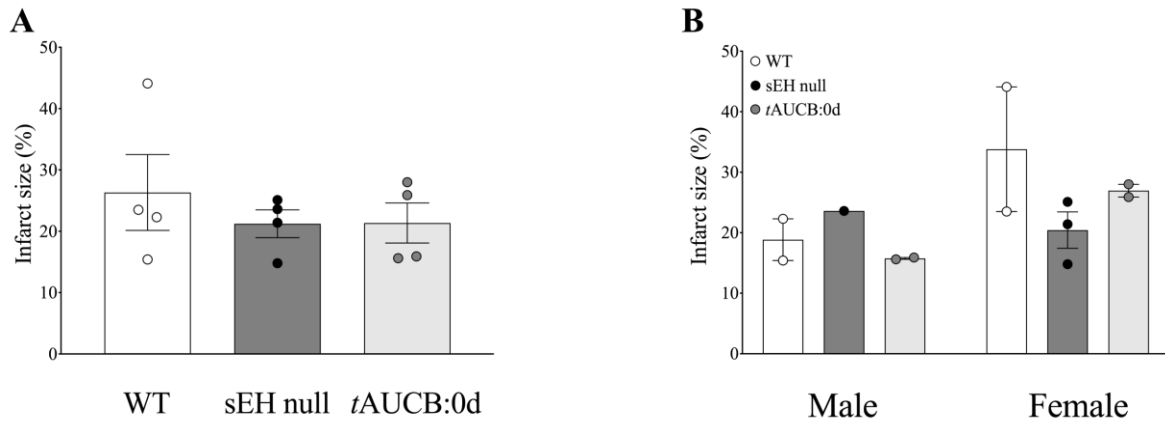


FIGURE 3.2.1. Infarct size measured by tetrazolium chloride (TTC) in WT, sEH null and tAUCB:0d with sexes combined (A) and separated by sex (B). N = 1-4. No differences in infarct size were present in combined data. Data are represented as mean \pm SEM. $p < 0.05$.

Survival in female mice is outlined in Figure 3.2.2. Female WT mice 28-days post-MI exhibited 58% survival while sEH null mice demonstrated better survival rates at 72%. Both *tAUCB* treatment groups demonstrated better survival at 80% for same-day treatment and 83% for 4-day pre-treatment females (Fig. 3.2.2). Female CYP2J2-Tr mice subjected to LAD had a 100% mortality rate prior to the 28-day endpoint, which was attenuated by same-day administration of the sEHi *tAUCB* (Fig. 3.2.2).

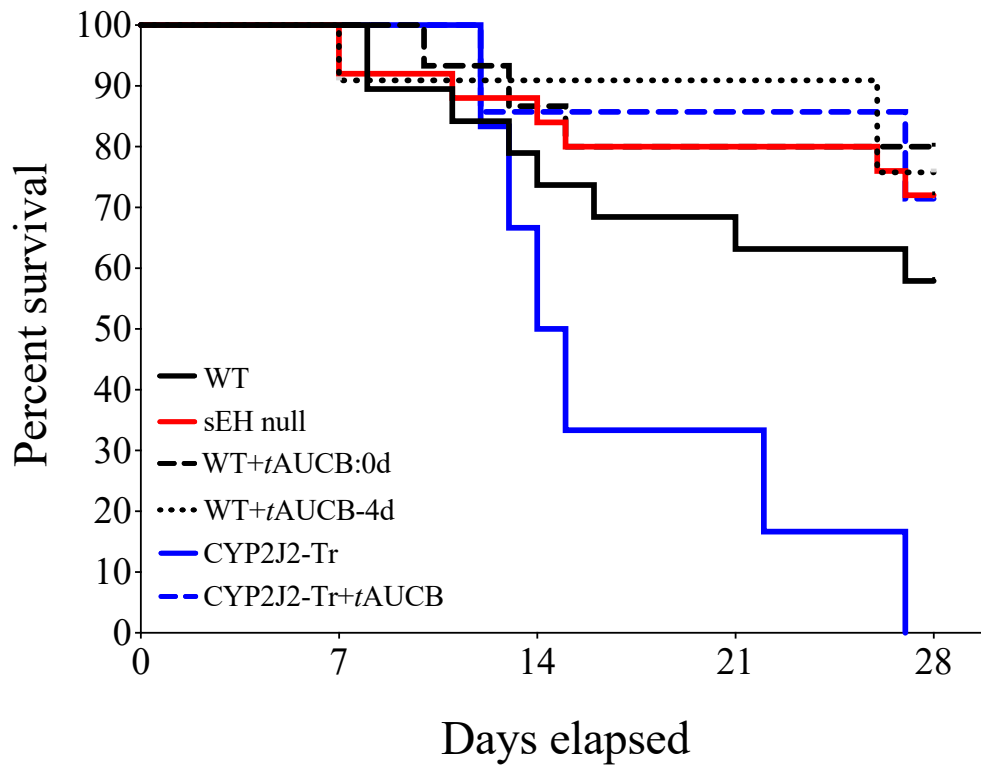


FIGURE 3.2.2. Percent survival for female mice over 28 days post-MI. WT (11/17, 58%) sEH null (18/23, 72%), WT+tAUCB:0d (12/15, 80%), WT+tAUCB:4d (5/6, 83%), CYP2J2-Tr (0/6, 0%), CYP2J2-Tr+tAUCB:0d (5/7, 71%).

Body weight was assessed in males and females at baseline, 7 days and 28 days post-MI. sEH null females and males demonstrated significantly reduced body weight at 28 days. All other changes were negligible (Fig. 3.2.3).

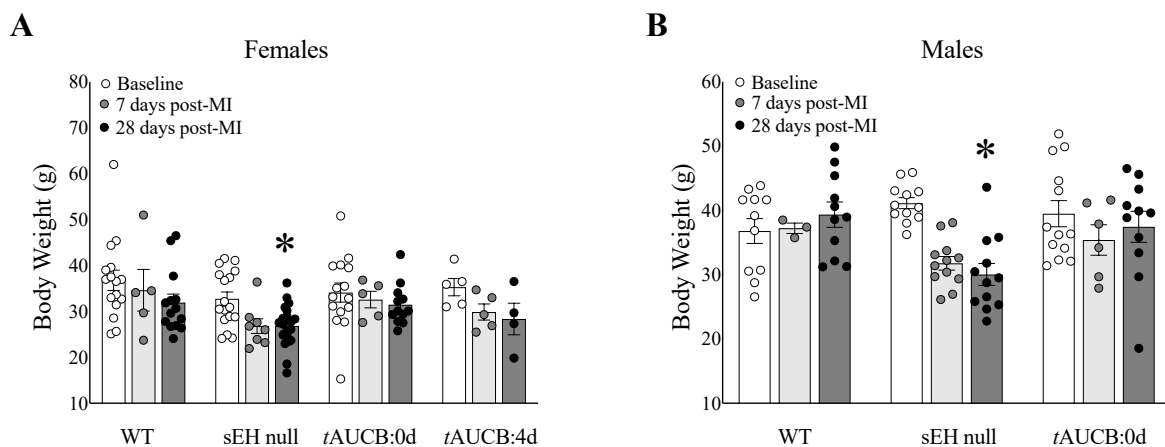


FIGURE 3.2.3. Body weight measured at baseline, 7d and 28 days post-MI in (A) female and (B) male WT, sEH null and tAUCB treated mice. Data are represented as mean \pm SEM. N = 5-22. $p < 0.05$; *vs baseline.

Tibial length was used as a standard comparator for tissue weights, due to the changes in the sEH null mice. Wet lung weight normalized to tibial length (LW:TL) is a marker of pulmonary congestion following myocardial infarction while heart weight normalized to tibial length (HW:TL) is a marker of hypertrophy. WT females demonstrated significantly increased LW:TL and HW:TL at 28-days compared to controls, an effect significantly attenuated in sEH null females (Fig. 3.2.4). Interestingly, female mice with same-day *t*AUCB treatment demonstrated significantly increased LW:TL and HW:TL, an effect not observed with *t*AUCB pre-treatment (Fig. 3.2.4). These data suggest that sEH genetic deletion protects the heart against maladaptive cardiac remodelling, correlating with improved survival. Similar effects were seen in pre-treatment, but not same-day, treatment with *t*AUCB suggesting treatment timing may play a critical role in mediating sEHⁱ response.

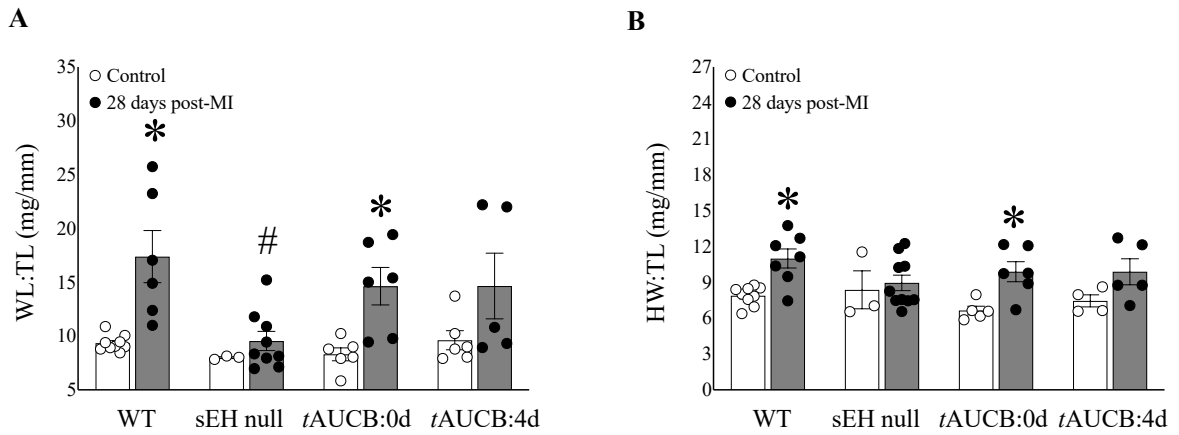


FIGURE 3.2.4. Physiological parameters upon necropsy for female mice. (A) Wet lung (WL) to tibia length (TL) (mg/mm) and (C) heart weight (HW) to TL (mg/mm) of WT, sEH null, *t*AUCB:0d- and *t*AUCB:4d-treated mice for control and at 28-days post-MI. Data are means \pm SEM, N = 3-10. $p < 0.05$; * vs Control; # vs WT group.

In contrast to their female counterparts, male CYP2J2-Tr mice and CYP2J2-Tr mice administered *t*AUCB had a 100% mortality by 14 days and experiments were required to be discontinued. There were no significant differences in survival rates between WT and sEH null null males; intriguingly, administration of *t*AUCB failed to provide any protective effect on survivability (Fig. 3.2.5).

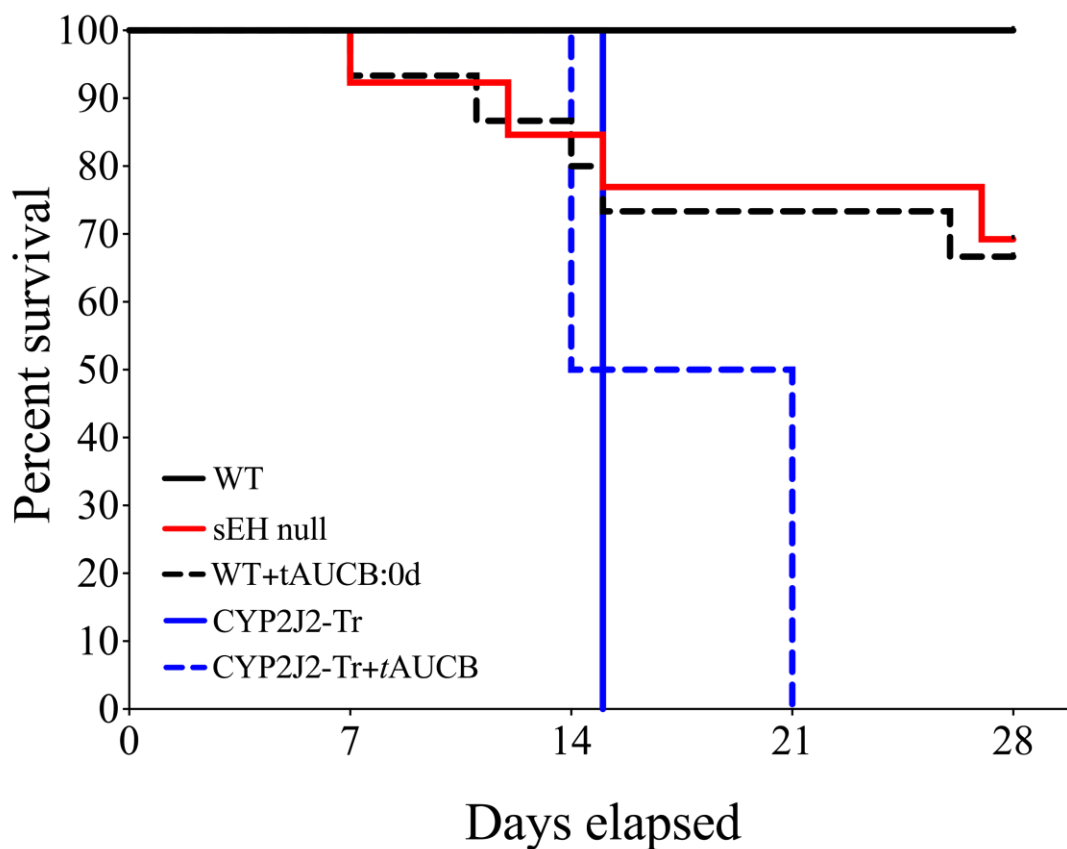


FIGURE 3.2.5. Percent survival of male mice over 28 days post-LAD ligation for WT (13/13, 100%), sEH null (9/13, 69%), WT+tAUCB:0d (9/14, 64%).

All male groups demonstrated a marked increase in WL:TL and HW:TL indicative of development in hypertrophy and pulmonary congestion (Fig. 3.2.6). These data suggest sEH inhibition does not provide protection in aged males.

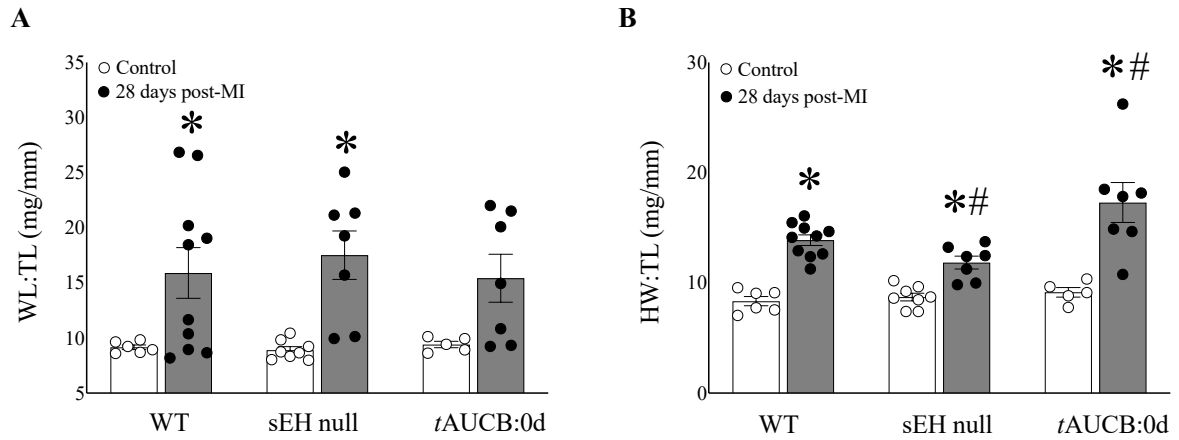
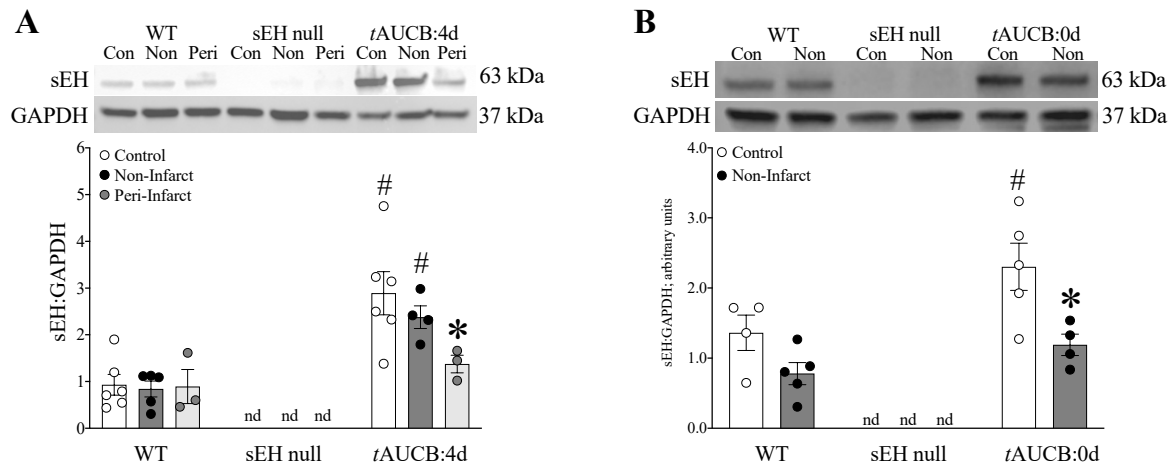


FIGURE 3.2.6. Physiological parameters upon necropsy for male mice (A) WL:TL (mg/mm) and (B) HW:TL (mg/mm) of male WT and sEH null mice at 28 days post-MI. Data are means \pm SEM, N = 5-10. $p < 0.05$; * vs Control; # vs WT group.

Cardiac sEH deletion was confirmed in both female and male null mice (Fig. 3.2.7). In contrast to human hearts, WT mice demonstrated little change in sEH expression post-MI while administration of *tAUCB* at either time point to females increased sEH expression in controls (Fig. 3.2.7A, B). Only the 4-day pre-treatment demonstrated increased sEH expression in the non-infarct region (Fig. 3.2.7A). Increased mEH expression was observed in the peri-infarct region of WT males but not females, suggesting a potential sex difference (Fig. 3.2.8). Female sEH null and *tAUCB* pre-treated mice had increased mEH expression in the peri-infarct regions (Fig. 3.2.8), suggesting a compensatory response to sEH inhibition in female mice.

Female



Male

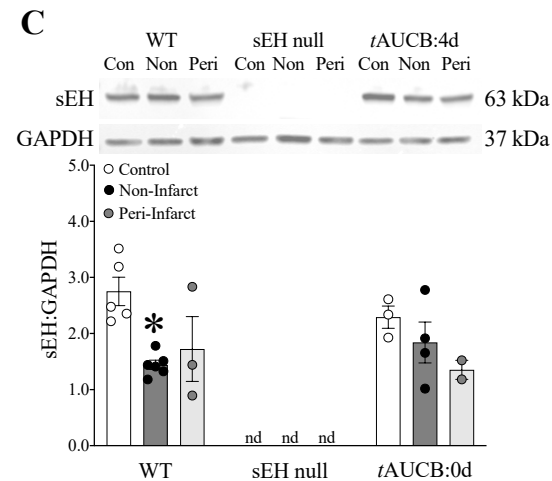


FIGURE 3.2.7. Soluble epoxide hydrolase protein expression normalized to GAPDH in LV tissue from female and male mice. A) Expression in female control, non-infarct and peri-infarct regions at 28-days post-MI for WT, sEH null and WT+tAUCB 4-day pre-treated mice. B) Expression in female control and non-infarct LV tissue at 28-days post-MI for WT, sEH null and WT+tAUCB same-day treated mice. Due to limited tissues, only non-infarct could be used. C) Expression in male control, non-infarct and peri-infarct LV tissue at 28-days post-MI for WT, sEH null and WT+tAUCB same-day pre-treated mice. Data are means \pm SEM, N = 3-6. $p < 0.05$; * vs Control; # vs WT group.

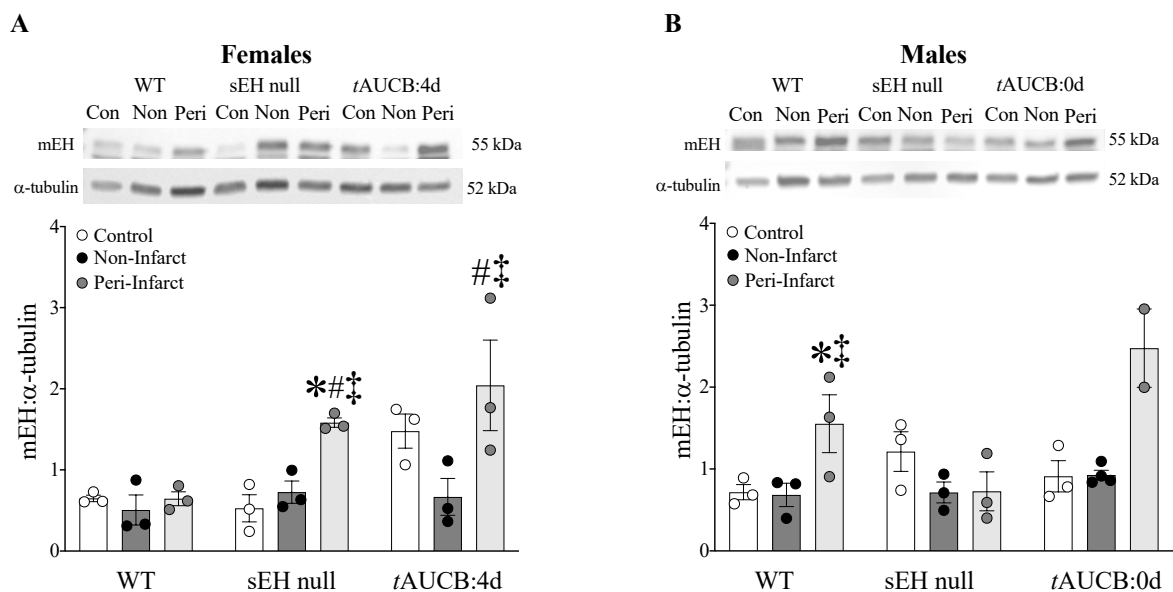


FIGURE 3.2.8. Microsomal epoxide hydrolase protein expression normalized to α -tubulin in LV tissue from female (A) and male (B) mice. A) Expression in female control, non-infarct and peri-infarct regions at 28-days post-MI for WT, sEH null and WT+tAUCB 4-day pre-treated mice. B) Expression in male control, non-infarct and peri-infarct LV tissue at 28-days post-MI for WT, sEH null and WT+tAUCB same-day pre-treated mice. Data are means \pm SEM, N = 2-6. $p < 0.05$; * vs Control; # vs WT group; ‡ vs non-infarct.

Total intake of *t*AUCB was similar between vehicle control and post-MI, and male and female mice over the 28 days (Fig. 3.2.9).

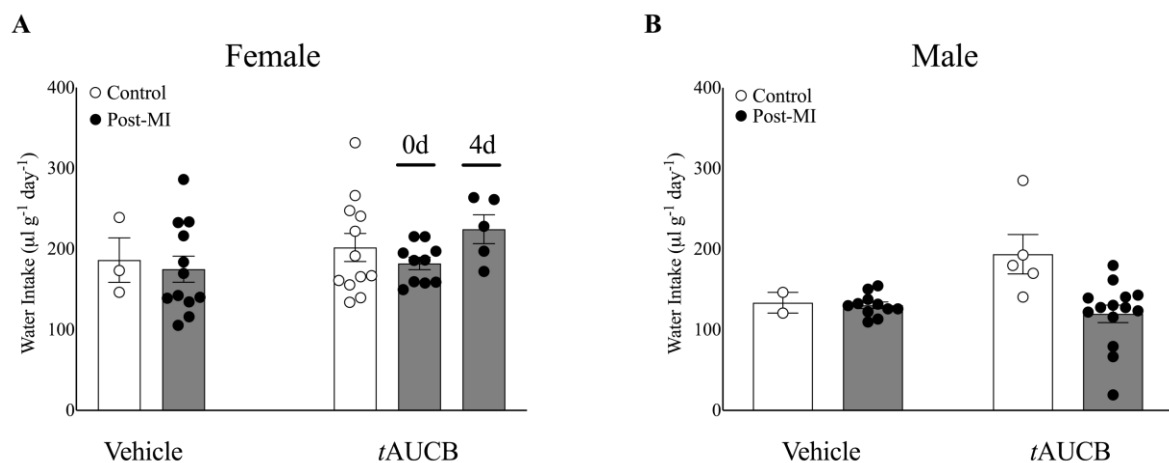


FIGURE 3.2.9. Water intake in (A) female and (B) male WT and *t*AUCB treated mice over the time span did not differ between groups. Only animals that survived are represented. Data are represented as mean \pm SEM. N = 5-22, $p < 0.05$.

Plasma *t*AUCB levels were significantly higher in both female control and post-MI mice at 28 days (Fig. 3.2.10). Interestingly, female mice trended to have higher plasma *t*AUCB levels compared to males. Both males and females had levels consistent with physiological inhibition as assessed by pharmacokinetics [590].

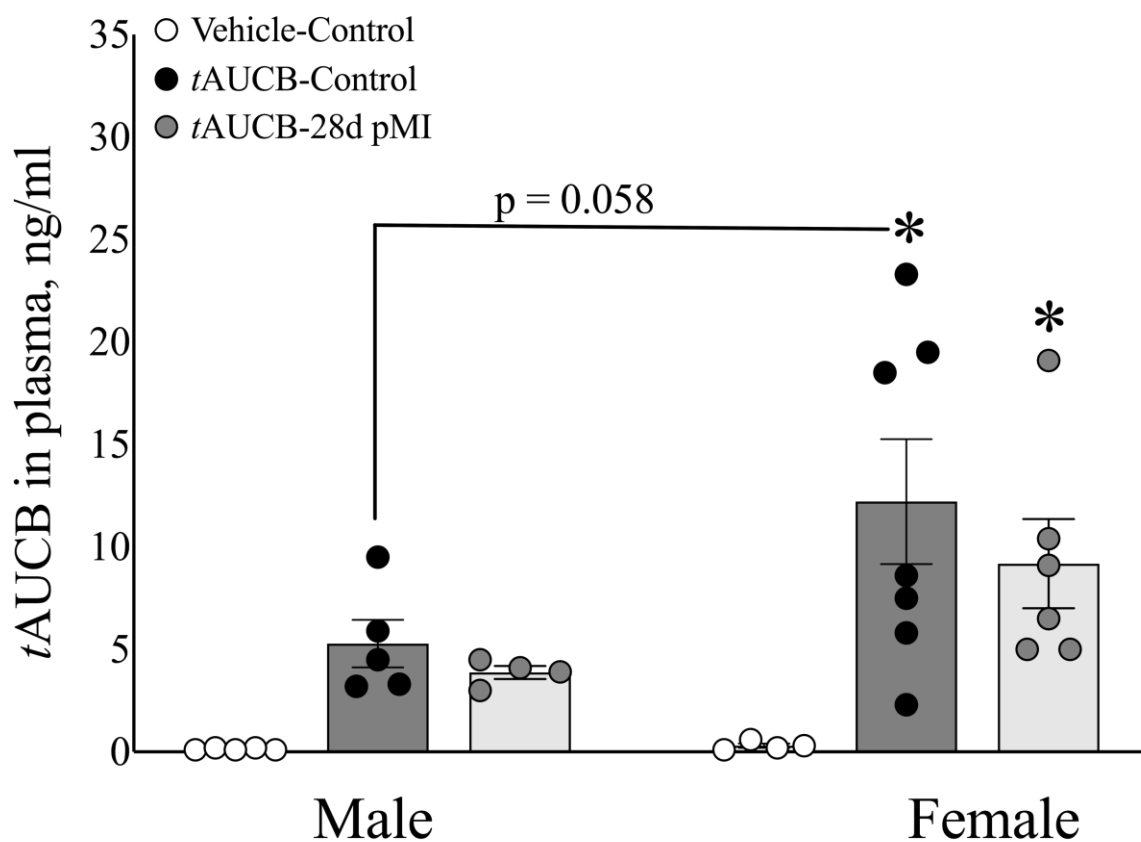


FIGURE 3.2.10. *t*AUCB levels in plasma for WT vehicle-treated sham control mice and *t*AUCB-treated sham and 28 days post-MI males and females Data are represented as mean \pm SEM. N = 4-7, $p < 0.05$; *vs vehicle control.

3.2.2 *sEH* genetic deletion and *tAUCB* pre-treatment protects cardiac function in female mice post-MI

Cardiac function was assessed in all groups by conventional 2D echocardiography (ECHO) and electrocardiogram (ECG) at baseline, 7 days and 28 days post-MI. *tAUCB* treatment in the absence of LAD occlusion did not have significant effects on heart function (Table 3.2.1). A comparison of all cardiac functional and structural parameters in female CYP2J2-Tr mice treated with *tAUCB* compared to WT at 28 days post-MI is provided in Table 3.2.2. Female CYP2J2-Tr mice treated with *tAUCB* demonstrated significantly reduced end-diastolic and end-systolic left ventricular chamber volumes (LVEDV;LVESV) at 28 days, suggesting modest protection. Ultimately, more studies at earlier endpoints are required to assess preservation of cardiac function in the CYP2J2-Tr cohort.

TABLE 3.2.1. Cardiac functional parameters in sham male and female mice treated with *t*AUCB at baseline and for 7 and 28 days measured by 2D echocardiography and electrocardiogram. Data are shown as mean \pm SEM, n=5-17 for ECHO, $p < 0.05$. N = 1-2 for ECG.

ECHOCARDIOGRAPHY	Male			Female		
	WT+ <i>t</i> AUCB-Sham			WT+ <i>t</i> AUCB-Sham		
	Baseline	7d	28d	Baseline	7d	28d
HR, beats/min	431 \pm 12	437 \pm 34	460 \pm 13	469 \pm 18	474 \pm 18	447 \pm 13
Wall measurements						
Corrected LV mass, mg	152.3 \pm 18.1	105.8 \pm 9.4	134.8 \pm 7.5	90.3 \pm 3.4	78.0 \pm 6.1	116.7 \pm 13.7
IVS-diastole, mm	0.98 \pm 0.12	0.87 \pm 0.16	1.02 \pm 0.03	0.78 \pm 0.05	0.76 \pm 0.04	0.89 \pm 0.05
IVS-systole, mm	1.33 \pm 0.09	1.20 \pm 0.18	1.44 \pm 0.05	1.16 \pm 0.07	1.07 \pm 0.01	1.31 \pm 0.09
LVPW-diastole, mm	1.15 \pm 0.11	0.93 \pm 0.11	1.00 \pm 0.07	0.84 \pm 0.03	0.79 \pm 0.04	0.91 \pm 0.02
LVPW-systole, mm	1.39 \pm 0.12	1.25 \pm 0.12	1.34 \pm 0.10	1.13 \pm 0.02	1.16 \pm 0.05	1.30 \pm 0.06
LVID-diastole, mm	4.21 \pm 0.17	3.99 \pm 0.39	4.10 \pm 0.19	3.88 \pm 0.16	3.66 \pm 0.21	4.11 \pm 0.22
LVID-systole, mm	2.95 \pm 0.11	2.79 \pm 0.34	2.79 \pm 0.25	2.61 \pm 0.13	2.37 \pm 0.17	2.67 \pm 0.18
Cardiac Function, Simpsons						
EF, %	58.05 \pm 2.89	54.33 \pm 4.25	61.13 \pm 4.00	61.39 \pm 1.06	62.11 \pm 1.81	61.48 \pm 0.35
FAC, %	49.09 \pm 2.36	44.44 \pm 4.67	52.46 \pm 4.72	52.76 \pm 3.02	54.46 \pm 1.08	53.58 \pm 1.71
LVEDV, μ l	97.70 \pm 6.92	97.15 \pm 16.25	92.48 \pm 12.92	67.98 \pm 5.88	77.93 \pm 6.64	71.42 \pm 7.80
LVESV, μ l	40.83 \pm 3.32	46.00 \pm 11.45	38.32 \pm 8.73	26.40 \pm 2.95	29.65 \pm 3.11	27.47 \pm 2.86
CO, ml/min	24.88 \pm 2.83	23.12 \pm 2.30	24.35 \pm 1.43	20.31 \pm 1.44	23.64 \pm 1.43	20.48 \pm 2.16
SV, μ l	56.87 \pm 5.38	51.15 \pm 6.04	54.17 \pm 4.68	41.58 \pm 3.0	48.28 \pm 4.05	43.96 \pm 4.95
Doppler Imaging						
IVRT, ms	19.43 \pm 2.79	20.20 \pm 2.61	17.17 \pm 1.61	14.68 \pm 1.00	12.63 \pm 0.39	15.91 \pm 1.24
IVCT, ms	13.80 \pm 2.37	20.03 \pm 2.84	17.22 \pm 1.68	14.48 \pm 1.66	12.70 \pm 1.67	14.03 \pm 0.79
ET, ms	43.15 \pm 1.54	45.35 \pm 2.49	43.87 \pm 3.16	43.65 \pm 2.99	46.73 \pm 2.15	43.00 \pm 1.62
Tei index	0.78 \pm 0.13	0.88 \pm 0.09	0.79 \pm 0.04	0.67 \pm 0.02	0.55 \pm 0.06	0.70 \pm 0.05
E'	19.10 \pm 5.65	18.20 \pm 3.99	20.72 \pm 4.01	23.35 \pm 1.92	24.90 \pm 1.15	25.24 \pm 2.75
E'/A'	0.90 \pm 0.18	0.91 \pm 0.11	0.99 \pm 0.12	1.00 \pm 0.13	1.06 \pm 0.07	1.28 \pm 0.06
E/E'	26.95 \pm 3.46	27.95 \pm 7.04	31.07 \pm 5.03	25.05 \pm 2.10	23.53 \pm 0.98	26.23 \pm 2.93
ELECTROCARDIOGRAM						
HR, beats/min	476 \pm 29	474 \pm 38	515 \pm 1	502	573	513
RR, ms	126.6 \pm 7.6	127.4 \pm 10.4	116.6 \pm 0.3	119.5	104.7	116.9
QRS, ms	11.0 \pm 0.1	11.9 \pm 1.4	11.7 \pm 1.3	10	9.5	10.3
PR, ms	40.5 \pm 0.6	38.7 \pm 0.6	39.4 \pm 1.4	44.4	41.3	40.7
QTcF, ms	54.0 \pm 1.6	49.6 \pm 0.7	51.1 \pm 0.4	46.9	48.0	51.5

TABLE 3.2.2. Cardiac functional parameters in female WT and CYP2J2-Tr mice at baseline and 28 days post-MI measured by 2D echocardiography. WT data are included for general comparison purposes only, as no CYP2J2-Tr mice with the vehicle survived. Data are shown as mean \pm SEM, n=5-17, p < 0.05, *vs baseline; # vs WT counterpart.

	Female WT		Female CYP2J2-Tr+tAUCB	
	Baseline	28d	Baseline	28d
HR, beats/min	483 \pm 10	488 \pm 11	488 \pm 11	481 \pm 19
Wall measurements				
Corrected LV mass, mg	114.6 \pm 10.0	149.4 \pm 9.9*	101.02 \pm 4.55	177.45 \pm 14.90*
IVS-diastole, mm	0.90 \pm 0.03	0.60 \pm 0.06*	0.84 \pm 0.02	0.91 \pm 0.05#
IVS-systole, mm	1.32 \pm 0.06	0.76 \pm 0.07*	1.21 \pm 0.05	1.13 \pm 0.08#
LVPW-diastole, mm	0.93 \pm 0.03	0.82 \pm 0.06	0.84 \pm 0.03	0.94 \pm 0.04
LVPW-systole, mm	1.32 \pm 0.04	0.99 \pm 0.10*	1.26 \pm 0.07	1.26 \pm 0.10
LVID-diastole, mm	3.98 \pm 0.13	5.69 \pm 0.16*	4.01 \pm 0.08	5.18 \pm 0.22*
LVID-systole, mm	2.67 \pm 0.14	5.04 \pm 0.21*	2.49 \pm 0.12	4.35 \pm 0.28*
Cardiac Function, Simpsons				
EF, %	59.17 \pm 1.58	23.13 \pm 3.76*	68.85 \pm 2.02	31.85 \pm 5.09*
FAC, %	48.86 \pm 2.38	16.63 \pm 3.04*	62.78 \pm 3.51	27.73 \pm 5.67*
LVEDV, μ l	75.76 \pm 4.20	179.78 \pm 19.63*	63.59 \pm 4.73	106.21 \pm 11.96#
LVESV, μ l	31.37 \pm 2.56	143.07 \pm 20.50*	19.95 \pm 2.21	73.96 \pm 12.55*#
CO, ml/min	21.31 \pm 1.00	16.86 \pm 1.64*	21.00 \pm 1.46	15.37 \pm 2.02
SV, μ l	44.39 \pm 2.09	35.97 \pm 3.41	43.64 \pm 3.01	32.35 \pm 4.77
Doppler Imaging				
IVRT, ms	16.52 \pm 0.81	19.95 \pm 1.94	18.42 \pm 0.89	21.47 \pm 0.97
IVCT, ms	14.95 \pm 1.21	31.28 \pm 7.58*	15.16 \pm 1.87	14.35 \pm 1.71#
ET, ms	41.02 \pm 1.58	39.22 \pm 2.37	43.32 \pm 1.36	41.28 \pm 2.54
Tei index	0.77 \pm 0.04	1.25 \pm 0.11*	0.77 \pm 0.06	1.01 \pm 0.16
E'	23.71 \pm 1.48	13.61 \pm 3.01*	26.92 \pm 1.98	25.27 \pm 8.91
E'/A'	1.14 \pm 0.06	1.22 \pm 0.32	1.10 \pm 0.09	0.81 \pm 0.10
E/E'	22.22 \pm 1.42	45.23 \pm 7.72	18.34 \pm 1.68	33.40 \pm 14.98

Echocardiography parameters for female WT, sEH null, *tAUCB* same-day and *tAUCB* 4-day pre-treated WT mice are summarized in Table 3.2.3. There were no differences in heart rate between groups that would account for the functional changes observed (Table 3.2.3). All groups of female mice demonstrated significantly reduced systolic function, %EF and %FAC (Table 3.2.3). Conversely, sEH null and *tAUCB* 4-day pre-treated females demonstrated significantly preserved systolic function compared to WT at 7 days post-MI, suggesting an early degree of systolic preservation (Table 3.2.3). sEH null females also demonstrated preserved LVEDV, LVESV at 28 days. Interestingly, both WT and sEH null females demonstrated prolonged E/E' at 28 days (Table 3.2.3). In humans, E/E' is a general marker of left ventricular diastolic pressure (LVDP)[591]. E/E' was preserved in both groups of *tAUCB* treated mice at 7 and 28 days, suggesting preservation of diastolic function may be an important contributor to survival effects observed with the sEHi treatment, however general cardiac function appears more robust with pre-treatment of *tAUCB* (Table 3.2.3). The protective changes observed in female mice were not observed in males (Table 3.2.4).

TABLE 3.2.3. Cardiac functional parameters in female mice at baseline, 7 and 28 days post-MI measured by 2D echocardiography. Data are shown as mean ± SEM, n=5-18, p < 0.05, *vs baseline; # vs WT counterpart; ‡ vs 7 days post-MI.

ECHOCARDIOGRAPHY	WT			sEH null			WT+/AUCB:0d Tx			WT+/AUCB:4d PreTx		
	Baseline	7d	28d	Baseline	7d	28d	Baseline	7d	28d	Baseline	7d	28d
HR, beats/min	483 ± 10	469 ± 20	488 ± 11	506 ± 9	486 ± 11	510 ± 13	435 ± 8	452 ± 8	502 ± 18	463 ± 13	476 ± 22	426 ± 7
Wall measurements												
Corrected LV mass, mg	114.6 ± 10.0	146.3 ± 12.3	149.4 ± 9.9*	93.9 ± 3.2	114.7 ± 7.2	134.3 ± 12.4*	93.8 ± 7.8	138.9 ± 11.4	149.6 ± 18.8*	94.80 ± 5.9	132.1 ± 13.5*	119.8 ± 14.0
IVS-diastole, mm	0.90 ± 0.03	0.69 ± 0.10	0.60 ± 0.06*	0.86 ± 0.02	0.71 ± 0.05	0.70 ± 0.07	0.81 ± 0.05	0.80 ± 0.05	0.72 ± 0.10	0.78 ± 0.04	0.74 ± 0.09	0.65 ± 0.17
IVS-systole, mm	1.32 ± 0.06	0.91 ± 0.14*	0.76 ± 0.07*	1.31 ± 0.04	0.91 ± 0.07*	0.98 ± 0.10*	1.13 ± 0.07	1.11 ± 0.16	0.97 ± 0.13	1.18 ± 0.07	1.42 ± 0.20	0.78 ± 0.21
LVPW-diastole, mm	0.93 ± 0.03	0.94 ± 0.07	0.82 ± 0.06	0.86 ± 0.02	0.78 ± 0.06	0.81 ± 0.05	0.82 ± 0.03	0.87 ± 0.11	0.78 ± 0.09	0.81 ± 0.04	0.90 ± 0.08	0.84 ± 0.05
LVPW-systole, mm	1.32 ± 0.04	1.01 ± 0.09*	0.99 ± 0.10*	1.27 ± 0.04	0.97 ± 0.08*	1.04 ± 0.07	1.15 ± 0.03	1.06 ± 0.18	0.94 ± 0.13	1.25 ± 0.07	1.20 ± 0.11	1.14 ± 0.13
LVID-diastole, mm	3.98 ± 0.13	5.10 ± 0.17*	5.69 ± 0.16*	3.78 ± 0.09	4.77 ± 0.21*	5.12 ± 0.14*	3.92 ± 0.11	4.91 ± 0.36*	5.59 ± 0.31*	4.04 ± 0.10	4.78 ± 0.24*	4.87 ± 0.22
LVID-systole, mm	2.67 ± 0.14	4.43 ± 0.28*	5.04 ± 0.21*	2.40 ± 0.11	3.97 ± 0.26*	4.34 ± 0.20*	2.64 ± 0.11	4.13 ± 0.58*	5.01 ± 0.43*	2.65 ± 0.11	3.76 ± 0.36*	3.92 ± 0.29*
Cardiac Function, Simpsons												
EF, %	59.17 ± 1.58	27.29 ± 1.38*	23.13 ± 3.76*	65.54 ± 1.60	37.32 ± 2.61*#	29.86 ± 3.25*	61.14 ± 2.04	31.60 ± 7.55*	26.42 ± 5.37*	61.00 ± 2.99	41.91 ± 5.00*#	33.53 ± 5.15*
FAC, %	48.86 ± 2.38	17.96 ± 2.87*	16.63 ± 3.04*	56.17 ± 2.56	29.22 ± 3.34*#	22.47 ± 2.17*	53.19 ± 2.86	17.96 ± 5.79*	20.30 ± 4.44*	53.63 ± 3.27	31.75 ± 5.61*#	29.55 ± 2.61*
LVEDV, µl	75.76 ± 4.20	140.86 ± 16.13*	179.78 ± 19.63*	65.24 ± 2.57	117.95 ± 11.09*	141.86 ± 11.46*#	67.15 ± 5.86	168.10 ± 31.40*	170.04 ± 17.36*	64.65 ± 6.15	108.39 ± 17.54*	114.53 ± 9.42*
LVESV, µl	31.37 ± 2.56	103.20 ± 12.78*	143.07 ± 20.50*	22.68 ± 1.64	76.84 ± 9.87*	102.88 ± 11.72*#	26.34 ± 3.21	121.41 ± 30.05*	133.01 ± 19.43*	25.50 ± 4.08	71.47 ± 16.23*	69.10 ± 10.20*
CO, ml/min	21.31 ± 1.00	17.51 ± 1.89	16.86 ± 1.64	21.71 ± 0.85	20.51 ± 1.25	19.72 ± 1.52	18.54 ± 1.44	22.38 ± 2.80	18.83 ± 1.65	18.18 ± 1.14	17.91 ± 2.25	22.82 ± 3.01
SV, µl	44.39 ± 2.09	37.66 ± 3.67	35.97 ± 3.41	42.91 ± 1.65	41.10 ± 1.98	38.98 ± 3.16	40.81 ± 3.14	46.68 ± 9.21	37.02 ± 3.60	39.15 ± 2.71	36.92 ± 3.87	45.44 ± 5.02
Doppler Imaging												
IVRT, ms	16.52 ± 0.81	18.74 ± 2.07	19.95 ± 1.94	15.25 ± 1.00	16.77 ± 0.91	25.67 ± 4.57*‡	15.84 ± 1.37	16.17 ± 2.96	23.13 ± 6.79	16.27 ± 0.79	19.91 ± 1.09	21.87 ± 2.81
IVCT, ms	14.95 ± 1.21	19.64 ± 2.75	31.28 ± 7.58*‡	11.22 ± 0.67	20.99 ± 3.04*	18.99 ± 3.50#	17.56 ± 2.80	29.72 ± 10.63	17.42 ± 3.45	15.22 ± 0.96	23.17 ± 2.73	26.31 ± 0.78
ET, ms	41.02 ± 1.58	36.51 ± 2.35	39.22 ± 2.37	39.89 ± 0.92	38.47 ± 1.57	35.60 ± 2.08	44.34 ± 1.97	40.47 ± 2.24	39.72 ± 4.36	46.55 ± 1.14#	42.79 ± 0.96#	51.96 ± 6.38#
Tei index	0.77 ± 0.04	1.09 ± 0.08*	1.25 ± 0.11*	0.67 ± 0.04	1.00 ± 0.13*	1.24 ± 0.20*	0.76 ± 0.08	1.24 ± 0.47	1.12 ± 0.52*#‡	0.68 ± 0.01	1.01 ± 0.08*	0.94 ± 0.04
E'	23.71 ± 1.48	22.24 ± 4.50	13.61 ± 3.01*	25.73 ± 1.59	18.51 ± 1.74*	16.54 ± 2.47*	21.03 ± 1.83	22.34 ± 6.82	18.76 ± 2.76	27.72 ± 1.96	19.32 ± 1.26*	25.38 ± 10.87
E'/A'	1.14 ± 0.06	1.28 ± 0.25	1.22 ± 0.32	1.31 ± 0.14	1.25 ± 0.11	0.98 ± 0.10	1.19 ± 0.05	1.18 ± 0.06	1.15 ± 0.12	1.35 ± 0.08	1.68 ± 0.32	0.96 ± 0.14
E/E'	22.22 ± 1.42	32.16 ± 6.37	45.23 ± 7.72*	23.20 ± 1.44	34.47 ± 4.93*	41.50 ± 4.69*	25.99 ± 2.29	20.31 ± 3.49	29.15 ± 3.41	21.26 ± 1.84	29.83 ± 4.61	33.64 ± 12.42

TABLE 3.2.4. Cardiac functional parameters in male mice at baseline, 7 and 28 days post-MI measured by 2D echocardiography. Data are shown as mean \pm SEM, n=5-17, p < 0.05, *vs baseline; # vs WT counterpart; ‡ vs 7 days post-MI.

ECHOCARDIOGRAPHY	WT			sEH null			WT+ <i>t</i> AUCB:0d Tx		
	Baseline	7d	28d	Baseline	7d	28d	Baseline	7d	28d
HR, beats/min	467 \pm 8	471 \pm 10	497 \pm 8	462 \pm 14	470 \pm 16	480 \pm 16	445 \pm 15	466 \pm 11	470 \pm 9
Wall measurements									
Corrected LV mass, mg	147.25 \pm 6.48	164.0 \pm 8.9	209.3 \pm 28.4*	113.2 \pm 5.7	145.3 \pm 11.6	127.4 \pm 25.5#	127.0 \pm 1.2	172.5 \pm 16.4*	173.4 \pm 34.1
IVS-diastole, mm	0.93 \pm 0.03	0.74 \pm 0.06*	0.71 \pm 0.10*	0.85 \pm 0.03	0.65 \pm 0.07*	0.46 \pm 0.07#	0.84 \pm 0.04	0.66 \pm 0.04	0.70 \pm 0.24
IVS-systole, mm	1.41 \pm 0.03	0.96 \pm 0.09*	0.89 \pm 0.12*	1.21 \pm 0.04	0.87 \pm 0.10*	0.66 \pm 0.08*	1.25 \pm 0.07	0.82 \pm 0.06*	0.77 \pm 0.18*
LVPW-diastole, mm	0.98 \pm 0.04	0.96 \pm 0.06	0.90 \pm 0.08	0.87 \pm 0.03	0.85 \pm 0.06	0.72 \pm 0.11	0.92 \pm 0.04	0.86 \pm 0.06	0.74 \pm 0.11
LVPW-systole, mm	1.36 \pm 0.04	1.18 \pm 0.09	1.01 \pm 0.12*	1.17 \pm 0.02	1.09 \pm 0.09	0.82 \pm 0.13*‡	1.33 \pm 0.04	0.96 \pm 0.08*	1.24 \pm 0.23
LVID-diastole, mm	4.46 \pm 0.08	5.32 \pm 0.14*	6.34 \pm 0.22*‡	4.20 \pm 0.10	5.36 \pm 0.18*	6.06 \pm 0.31*‡	4.46 \pm 0.12	5.90 \pm 0.21*#	5.76 \pm 0.03*
LVID-systole, mm	3.08 \pm 0.08	4.55 \pm 0.21*	5.76 \pm 0.27*‡	2.95 \pm 0.10	4.60 \pm 0.23*	5.49 \pm 0.38*‡	3.08 \pm 0.11	5.27 \pm 0.26*#	5.17 \pm 0.003*
Cardiac Function, Simpsons									
EF, %	58.51 \pm 1.18	32.11 \pm 2.28*	20.83 \pm 2.74*‡	56.34 \pm 1.48	29.58 \pm 2.43*	21.77 \pm 3.08*‡	57.45 \pm 1.58	23.57 \pm 2.31*#	24.88 \pm 3.69*
FAC, %	49.56 \pm 1.21	26.91 \pm 2.89*	16.37 \pm 2.77*‡	48.05 \pm 1.71	22.21 \pm 2.51*	12.44 \pm 3.21*‡	48.52 \pm 1.79	16.08 \pm 3.46*#	21.29 \pm 4.49*
LVEDV, μ l	95.84 \pm 4.85	170.70 \pm 15.71*	215.50 \pm 18.56*	92.83 \pm 4.95	146.46 \pm 12.04*	220.50 \pm 28.08*‡	96.37 \pm 3.89	204.65 \pm 13.18*	211.93 \pm 24.77*
LVESV, μ l	39.39 \pm 1.82	117.03 \pm 12.04*	172.41 \pm 17.79*‡	41.06 \pm 3.16	105.91 \pm 11.24*	177.75 \pm 26.75*‡	41.43 \pm 2.89	156.69 \pm 11.45*	161.93 \pm 26.07*
CO, ml/min	25.85 \pm 1.63	25.09 \pm 2.35	21.47 \pm 2.46	23.53 \pm 0.82	19.78 \pm 1.67	21.77 \pm 3.08	25.14 \pm 0.72	22.96 \pm 2.77	27.24 \pm 2.08
SV, μ l	56.45 \pm 3.53	53.27 \pm 5.37	43.09 \pm 4.84*	51.77 \pm 2.17	40.55 \pm 2.62	42.75 \pm 4.47	54.93 \pm 1.60	47.96 \pm 5.21	50.00 \pm 6.77
Doppler Imaging									
IVRT, ms	15.84 \pm 0.45	18.73 \pm 2.18	17.24 \pm 1.48	14.77 \pm 0.51	18.78 \pm 0.93	21.49 \pm 2.71*	15.22 \pm 0.97	18.17 \pm 0.85	24.45 \pm 3.19*#
IVCT, ms	16.99 \pm 1.28	24.19 \pm 5.41	27.99 \pm 2.13	15.54 \pm 0.67	29.94 \pm 2.81*	34.82 \pm 8.28*	16.02 \pm 1.70	32.32 \pm 3.89*	20.78 \pm 3.59
ET, ms	42.93 \pm 0.74	33.43 \pm 2.35	34.48 \pm 1.65*‡	42.55 \pm 0.98	34.79 \pm 1.20*#	34.43 \pm 2.05*	43.41 \pm 2.05	35.54 \pm 1.52*#	38.46 \pm 3.69
Tei index	0.76 \pm 0.03	1.35 \pm 0.22*	1.36 \pm 0.09*	0.71 \pm 0.01	1.47 \pm 0.14*	1.57 \pm 0.22*	0.73 \pm 0.05	1.46 \pm 0.14*	0.94 \pm 0.08
E'	21.72 \pm 0.76	17.95 \pm 2.94	17.58 \pm 1.22	21.79 \pm 1.15	21.22 \pm 1.46	16.41 \pm 3.99	23.78 \pm 1.78	21.90 \pm 2.82	21.52 \pm 3.32
E'/A'	1.13 \pm 0.04	1.53 \pm 0.20	1.29 \pm 0.14	1.12 \pm 0.06	1.37 \pm 0.14	1.26 \pm 0.16	1.36 \pm 0.11	1.42 \pm 0.07	01.07 \pm 0.11
E/E'	25.38 \pm 0.57	26.34 \pm 4.15	32.96 \pm 3.00	32.47 \pm 1.82	28.70 \pm 2.05	44.10 \pm 7.51‡	27.04 \pm 2.37	28.69 \pm 4.23	24.42 \pm 4.72

ECG was used to assess changes in cardiac electrical signalling in control and post-MI mice, specifically QRS duration (ms) to assess ventricular action potential duration and PR interval for atrioventricular conduction time [592]. WT females exhibited increased QRS duration and PR interval, indicating an inability of the signals to propagate effectively to stimulate left ventricular contraction, effects attenuated in sEH null females (Table 3.2.5). While *tAUCB* same-day treatment preserved QRS duration in females, their PR interval was similar to WT (Table 3.2.5). QT prolongation, a hallmark of heart failure in both mice and humans [592], significantly increased in all groups at 7-days post-MI, but were better recovered in sEH null and *tAUCB* same-day treated female mice at 28-days. The pattern of the QT prolongation confirmed the ubiquitous presence of HF and matched the extent of systolic dysfunction observed in all groups (Table 3.2.5). In contrast, while *tAUCB* same-day female mice exhibited a similar preservation in QRS duration, this did not translate into preserved cardiac systolic function at any time point. No preservation was observed in male mice (Table 3.2.6). Together, these data suggest genetic deletion and pharmacological inhibition of sEH preserve post-MI systolic function and electrical conduction in female mice compared to WT counterparts. The effect of the pharmacological inhibitor on cardioprotection in females post-MI appears to be dependent on treatment timing. Crucially, these data highlight the existence of potential sexual dimorphic responses against MI in aged mice.

TABLE 3.2.5. Cardiac functional parameters in female mice at baseline, 7 and 28 days post-MI measured by electrocardiogram. Data are shown as mean \pm SEM, n=5-18, p < 0.05, *vs baseline; # vs WT counterpart; ‡ vs 7 days post-MI.

Females	WT			sEH null			WT+tAUCB:0d Tx		
	Baseline	7d	28d	Baseline	7d	28d	Baseline	7d	28d
ECG									
HR, beats/min	471 \pm 14	488 \pm 11	523 \pm 5	505 \pm 21	475 \pm 31	529 \pm 14	489 \pm 20	467 \pm 17	494 \pm 23
RR, ms	128.1 \pm 3.8	123.3 \pm 2.9	114.8 \pm 1.0	121.6 \pm 4.3	129.4 \pm 8.2	112.7 \pm 4.0	123.8 \pm 4.8	129.1 \pm 5.8	118.9 \pm 6.5
QRS, ms	12.0 \pm 0.3	10.7 \pm 0.2	15.1 \pm 1.7*‡	11.7 \pm 0.2	10.3 \pm 0.4	10.9 \pm 1.6#	11.4 \pm 0.3	11.3 \pm 0.7	10.5 \pm 1.8#
PR, ms	43.3 \pm 1.5	40.8 \pm 1.6	51.8 \pm 3.2*‡	42.1 \pm 1.0	42.0 \pm 0.3	44.6 \pm 1.4#	41.7 \pm 0.7	42.0 \pm 1.1	47.4 \pm 1.3*
QTcF, ms	45.7 \pm 0.8	74.0 \pm 2.2*	65.8 \pm 7.6*	45.1 \pm 1.0	70.2 \pm 5.1*	58.5 \pm 1.1	49.8 \pm 3.4	71.5 \pm 2.1*	55.2 \pm 2.9‡

TABLE 3.2.6. Cardiac functional parameters in male mice at baseline, 7 and 28 days post-MI measured by electrocardiogram. Data are shown as mean \pm SEM, n=5-17, p < 0.05, *vs baseline; # vs WT counterpart; ‡ vs 7 days post-MI.

Males	WT			sEH null			WT+tAUCB:0d Tx		
	Baseline	7d	28d	Baseline	7d	28d	Baseline	7d	28d
ECG									
HR, beats/min	476 \pm 18	473 \pm 20	531 \pm 12	521 \pm 17	444 \pm 24*	552 \pm 35	462 \pm 19	454 \pm 26	488 \pm 21
RR, ms	127.1 \pm 4.7	128.1 \pm 4.8	113.3 \pm 2.6	116.3 \pm 3.7	138.3 \pm 7.3*	110.4 \pm 6.6‡	131.1 \pm 5.5	134.7 \pm 8.9	122.6 \pm 5.6
QRS, ms	11.7 \pm 0.4	11.3 \pm 0.3	16.5 \pm 1.6*‡	12.4 \pm 0.3	13.8 \pm 1.9	16.5 \pm 2.6	12.4 \pm 0.7	9.9 \pm 1.2	11.9 \pm 0.8
PR, ms	42.6 \pm 1.7	44.8 \pm 1.7	46.3 \pm 8.0	42.5 \pm 1.3	42.0 \pm 2.4	44.6 \pm 2.5	45.3 \pm 1.8	46.3 \pm 1.9	46.6 \pm 2.4
QTcF, ms	48.2 \pm 1.4	74.0 \pm 2.2*	65.8 \pm 7.6*	49.3 \pm 0.6	79.4 \pm 3.9*	75.7 \pm 7.9*	47.8 \pm 1.9	71.8 \pm 3.0*	63.4 \pm 1.1

3.2.3 *Murine left ventricle demonstrates marked changes in oxylipid metabolism*

Female mouse hearts demonstrated increased production of prostanoids in non-infarct regions, suggesting a pro-inflammatory response (Table 3.2.7). In contrast, the ω -hydroxylase metabolites 19-HETE or 20-HETE were not detected in human LV, while the non-infarct regions from of sEH null and *tAUCB* same-day treated mice demonstrated lower levels compared to controls (Table 3.2.7).

TABLE 3.2.7. Oxylipid metabolite profile (ng/g tissue) in mouse left ventricular tissue measured by LC-MS/MS. Data are shown as mean \pm SEM, n=3-6. p < 0.05, *vs control; # vs WT group; ‡ vs non-infarct.

Mouse						
	WT		Females sEH null		WT+ <i>t</i> AUCB:0d	
	Control	Non-Infarct	Control	Non-Infarct	Control	Non-Infarct
Arachidonic Acid	1326.89 \pm 305.87	859.63 \pm 221.34	1402.92 \pm 379.11	1286.38 \pm 279.61	1078.45 \pm 234.14	1465.75 \pm 139.42
Epoxygenase-dependent metabolism						
12,13-EpOME	5.09 \pm 0.79	3.53 \pm 0.60	12.64 \pm 2.54#	15.50 \pm 3.95#	8.75 \pm 2.01	8.27 \pm 2.43
9,10-EpOME	14.38 \pm 2.70	9.18 \pm 1.76	30.04 \pm 7.38	25.94 \pm 8.75	25.38 \pm 7.63	18.14 \pm 6.14
14,15-EET	1.64 \pm 0.05	1.33 \pm 0.10	3.65 \pm 0.45#	2.53 \pm 0.67	3.01 \pm 0.57	2.22 \pm 0.56
11,12-EET	1.34 \pm 0.19	0.94 \pm 0.15	2.60 \pm 0.40#	2.04 \pm 0.58	2.23 \pm 0.49	1.79 \pm 0.51
8,9-EET	1.45 \pm 0.28	2.04 \pm 0.71	3.69 \pm 0.94	3.63 \pm 1.06	4.47 \pm 0.68#	3.04 \pm 0.61
5,6-EET	ND	ND	ND	ND	ND	ND
17,18-EpETE	0.65 \pm 0.11	0.54 \pm 0.19	2.60 \pm 0.47#	2.98 \pm 0.75#	1.30 \pm 0.26	1.56 \pm 0.72
19,20-EpDPE	47.66 \pm 6.25	39.40 \pm 9.46	69.20 \pm 8.48	44.89 \pm 12.10	61.36 \pm 12.02	50.70 \pm 14.23
Soluble epoxide hydrolase-dependent metabolism						
12,13-diHOME	2.08 \pm 0.18	2.22 \pm 0.49	1.37 \pm 0.05	1.51 \pm 0.40	3.67 \pm 1.30	2.54 \pm 0.77
9,10-diHOME	2.44 \pm 0.41	2.50 \pm 0.68	3.62 \pm 0.70	4.95 \pm 2.07	3.30 \pm 0.98	6.27 \pm 3.64
14,15-DHET	0.17 \pm 0.01	0.27 \pm 0.08	0.20 \pm 0.02	0.16 \pm 0.04	0.29 \pm 0.04	0.20 \pm 0.03
11,12-DHET	0.35 \pm 0.05	0.40 \pm 0.12	0.38 \pm 0.04	0.42 \pm 0.07	0.40 \pm 0.07	0.38 \pm 0.07
8,9-DHET	0.36 \pm 0.04	0.53 \pm 0.15	0.53 \pm 0.15	0.57 \pm 0.12	0.57 \pm 0.16	0.51 \pm 0.22
5,6-DHET	0.26 \pm 0.02	0.39 \pm 0.10	0.37 \pm 0.03	0.32 \pm 0.10	0.39 \pm 0.07	0.40 \pm 0.11
Epoxygenase:Diol Metabolite Ratios						
12,13-EpOME:DiHome	2.43 \pm 0.22	2.68 \pm 0.68	7.52 \pm 0.53#	10.21 \pm 0.58#	2.62 \pm 0.34	1.89 \pm 0.80
9,10-EpOME:DiHome	6.04 \pm 0.77	6.32 \pm 1.38	8.50 \pm 1.35	5.61 \pm 0.56	7.65 \pm 0.06	4.79 \pm 1.27
14,15-EET:DHET	9.68 \pm 0.70	9.25 \pm 2.18	18.70 \pm 2.64#	16.18 \pm 3.20	10.42 \pm 0.96	7.28 \pm 1.63
11,12-EET:DHET	3.85 \pm 0.23	4.23 \pm 0.92	5.92 \pm 1.11	4.67 \pm 0.61	5.52 \pm 0.89	3.36 \pm 0.34
8,9-EET:DHET	4.85 \pm 0.20	6.55 \pm 1.79	6.74 \pm 1.33	6.12 \pm 0.74	8.86 \pm 2.17	7.49 \pm 1.88
ω -Hydrolase-dependent metabolism						
19-HETE	0.79 \pm 0.08	1.18 \pm 0.17	0.89 \pm 0.18	0.37 \pm 0.09	0.84 \pm 0.28	0.81 \pm 0.35
20-HETE	0.51 \pm 0.07	0.66 \pm 0.06	1.27 \pm 0.30#	0.65 \pm 0.03	0.74 \pm 0.11	0.55 \pm 0.13
Lipoxygenase-dependent metabolism						
13-HODE	54.52 \pm 11.64	40.46 \pm 14.01	55.94 \pm 4.41	58.38 \pm 19.74	74.69 \pm 23.76	67.97 \pm 28.58
9-HODE	31.39 \pm 3.76	29.88 \pm 11.34	40.91 \pm 3.94	43.56 \pm 15.81	58.93 \pm 20.07	49.38 \pm 21.11
15-HETE	6.83 \pm 0.64	9.67 \pm 3.88	11.78 \pm 1.10	11.76 \pm 3.25	16.12 \pm 4.36	14.81 \pm 4.97
11-HETE	2.54 \pm 0.22	2.94 \pm 0.84	3.71 \pm 0.05	4.15 \pm 0.87	3.25 \pm 0.80	556.81 \pm 236.36
12-HETE	7.91 \pm 1.45	7.84 \pm 3.10	5.95 \pm 1.04	7.35 \pm 1.98	5.88 \pm 1.69	4.42 \pm 2.14
8-HETE	ND	ND	ND	ND	ND	ND
5-HETE	1.60 \pm 0.28	1.51 \pm 0.51	1.28 \pm 0.22	1.54 \pm 0.41	1.27 \pm 0.42	0.95 \pm 0.49
Cyclooxygenase-dependent metabolism						
6ketoPGF _{1α}	3.41 \pm 0.25	7.28 \pm 2.34	4.86 \pm 0.72	9.08 \pm 1.84	3.57 \pm 0.39	14.15 \pm 6.30*
TXB ₂	0.48 \pm 0.07	1.06 \pm 0.31	0.66 \pm 0.08	1.03 \pm 0.19	0.60 \pm 0.07	1.57 \pm 0.61
PGF _{2α}	ND	ND	ND	ND	ND	ND
PGE ₂	ND	ND	ND	ND	ND	ND
8isoPGF _{2α}	0.15 \pm 0.02	0.50 \pm 0.26	0.55 \pm 0.11	0.45 \pm 0.15	0.57 \pm 0.19#	0.47 \pm 0.07
PGB ₂	ND	ND	ND	ND	ND	ND
PGD ₂	0.47 \pm 0.05	0.53 \pm 0.22	0.62 \pm 0.13	1.05 \pm 0.32	0.76 \pm 0.41	1.17 \pm 0.39

Female sEH null mice also demonstrated a significantly increased 12,13-EpOME:DiHOME ratio, indicative of lower DiHOME formation in these hearts (Fig. 3.2.11A). No such changes were observed in 9,10-EpOME:DiHOME ratios (Fig. 3.2.11B).

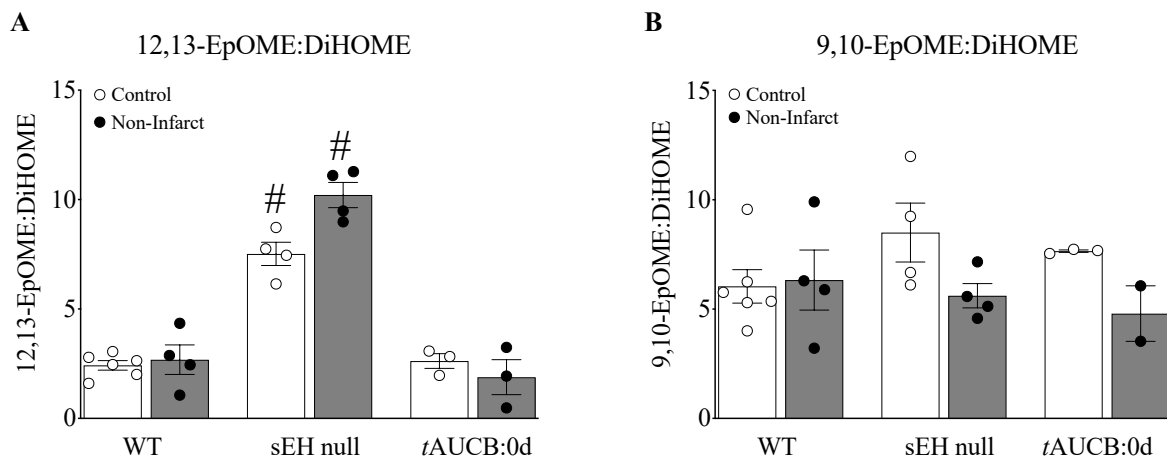


FIGURE 3.2.11. Linoleic acid epoxygenase oxylipid metabolites (ng/g tissue) in female mouse left ventricular tissue measured by LC-MS/MS. (A) 12,13-EpOME:DiHOME ratio, (B) 9,10-EpOME:DiHOME ratios. Data are shown as mean \pm SEM, $n=3-6$. $p < 0.05$, *vs control group; # vs WT group.

Similarly, 14,15-EET:DHET ratios also increased in sEH null female hearts (Fig. 3.2.12A) with no changes were observed in other EET:DHET ratios (Fig. 3.2.12B, C). While 19,20-EpDPE levels were not significantly altered (Fig. 3.2.13A), the epoxygenase metabolite of eicosapentaenoic acid, 17,18-EpETE, was increased in control and non-infarct region of sEH null females (Fig. 3.2.13B). Interestingly 17,18-EpETE has been demonstrated to hold anti-arrhythmic properties[593]. Together, the shifts in oxylipid metabolism observed in sEH null females correlate with preservations in survival and cardiac function observed in these mice. Interestingly, females with same-day treatment of *t*AUCB did not demonstrate the same significant shifts in oxylipid metabolism (Fig. 3.2.12; Fig. 3.2.13), correlating with increased expression levels of epoxide hydrolases (Fig. 3.2.7) and limited cardioprotection (Table 3.2.3, Table 3.2.4).

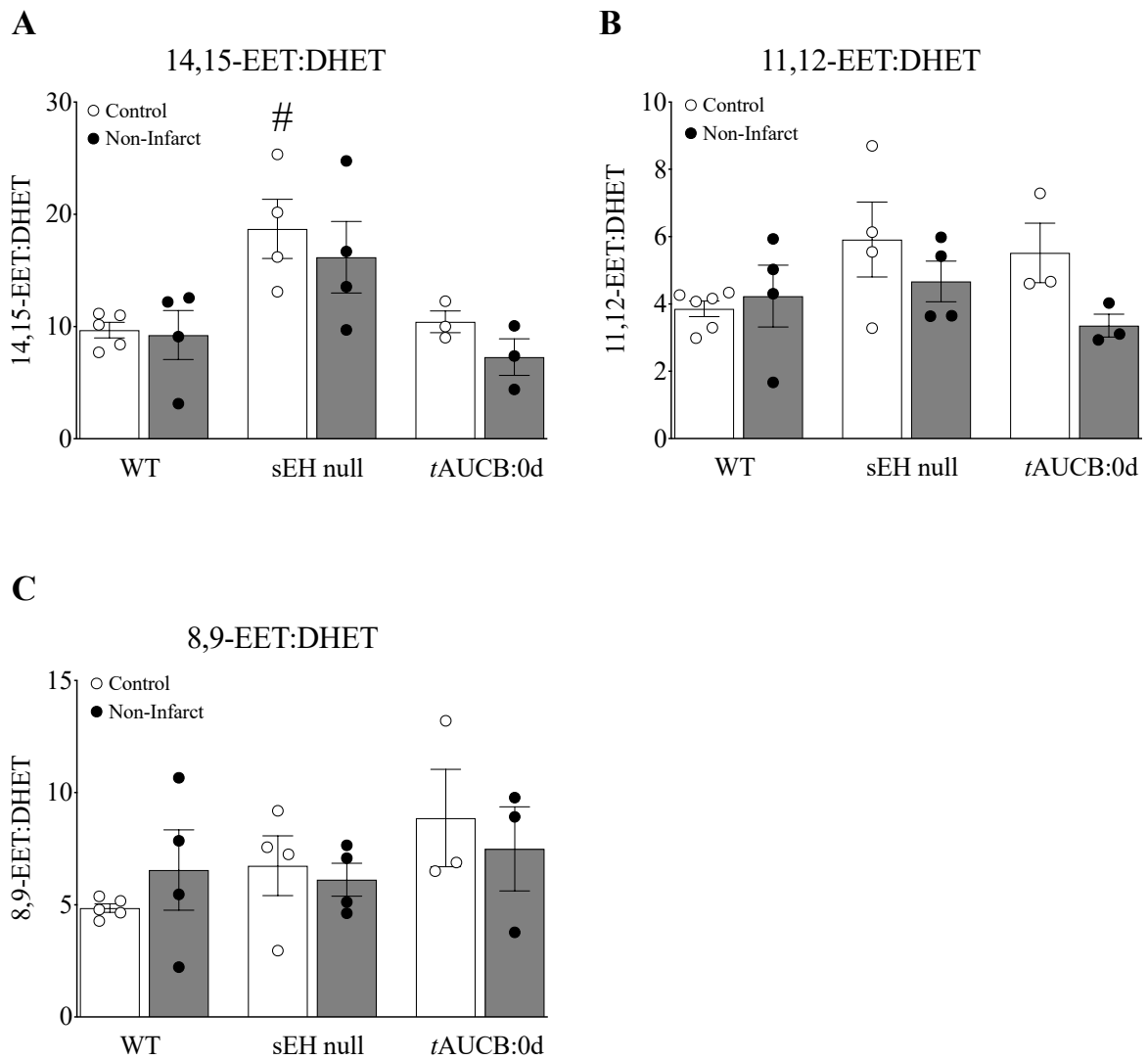


FIGURE 3.2.12. Epoxygenase oxylipid metabolites (ng/g tissue) of arachidonic acid in female mouse left ventricular tissue measured by LC-MS/MS. A) 14,15-EET:DHET ratios, B) 11,12-EET:DHET ratios, C) 8,9-EET:DHET ratios. Data are shown as mean \pm SEM, n=3-6. $p < 0.05$. # vs WT group.

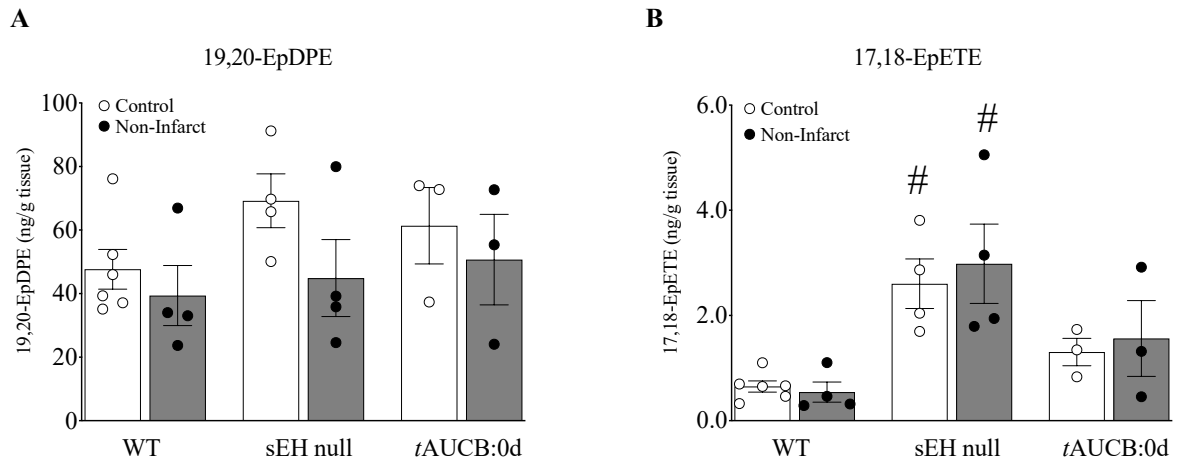


FIGURE 3.2.13. DHA and EPA epoxygenase oxylipid metabolites (ng/g tissue) in mouse left ventricular tissue measured by LC-MS/MS. A) 19,20-EpDPE levels, and B) 17,18-EpETE levels (mouse only). Data are shown as mean \pm SEM, $n=3-6$. $p < 0.05$, # vs WT group.

3.2.4 *Female mice with genetic deletion of sEH demonstrate improved protein expression and mitochondrial function post-MI*

In the previous section, we demonstrated a decline in mitochondrial function without changes to mitochondrial protein expression of ETC enzymes in aged mouse hearts, suggesting an impact of overall quality[594]. Consistently, we observed no significant alterations in the expression of key proteins in mitochondrial oxidative metabolism such as citrate synthase, complex I and II in hearts from WT, sEH null or *tAUCB* treated female (Fig. 3.2.14) or male (Fig. 3.2.15) mice.

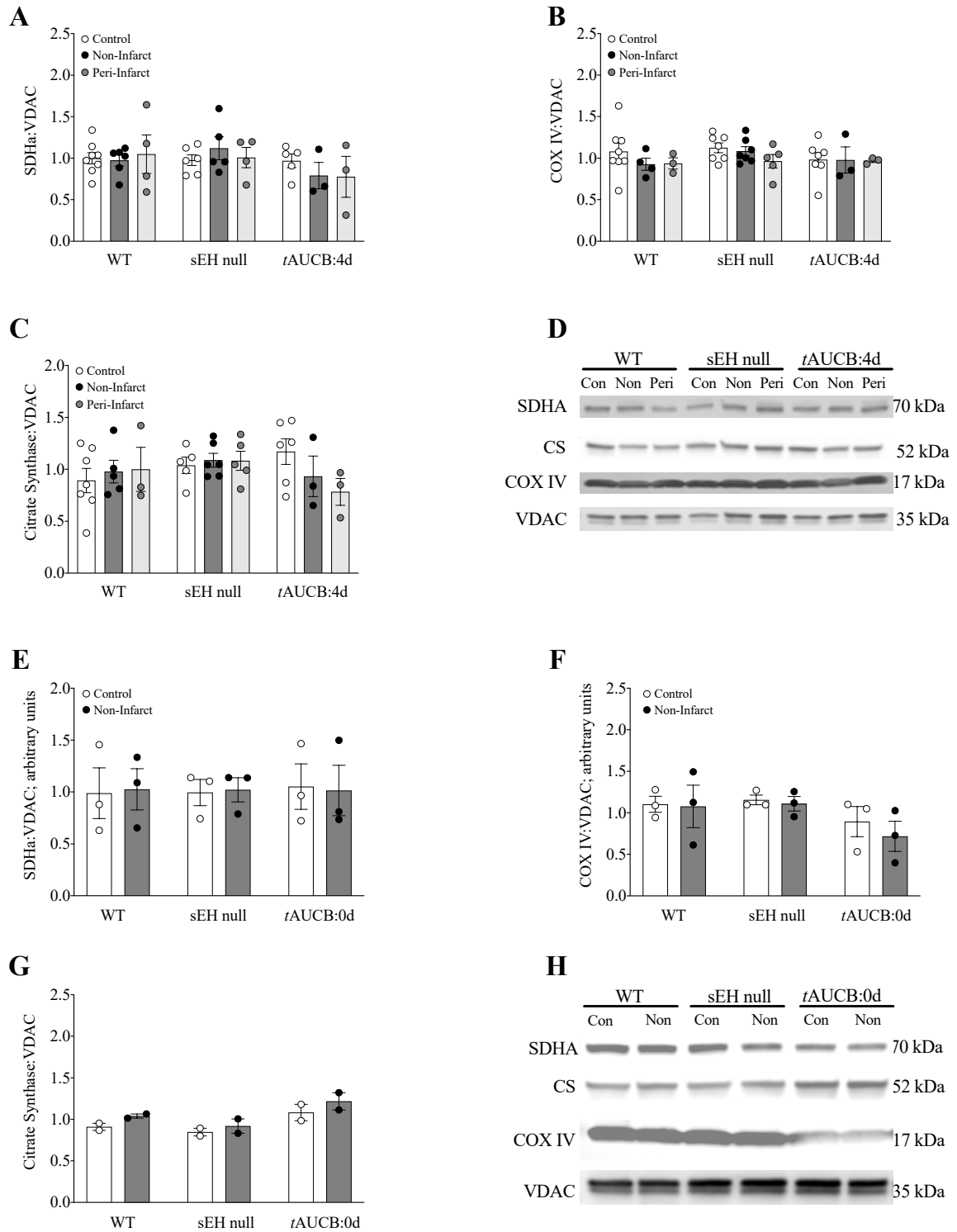


FIGURE 3.2.14. Key mitochondrial protein expression in female WT, sEH null and *tAUCB* treated hearts. (A/E) Succinate dehydrogenase a (SDHa), (B/F) COX IV, (C/G) Citrate synthase (CS) and (D/H) representative blots normalized to VDAC. N = 3-10. $p < 0.05$.

Male

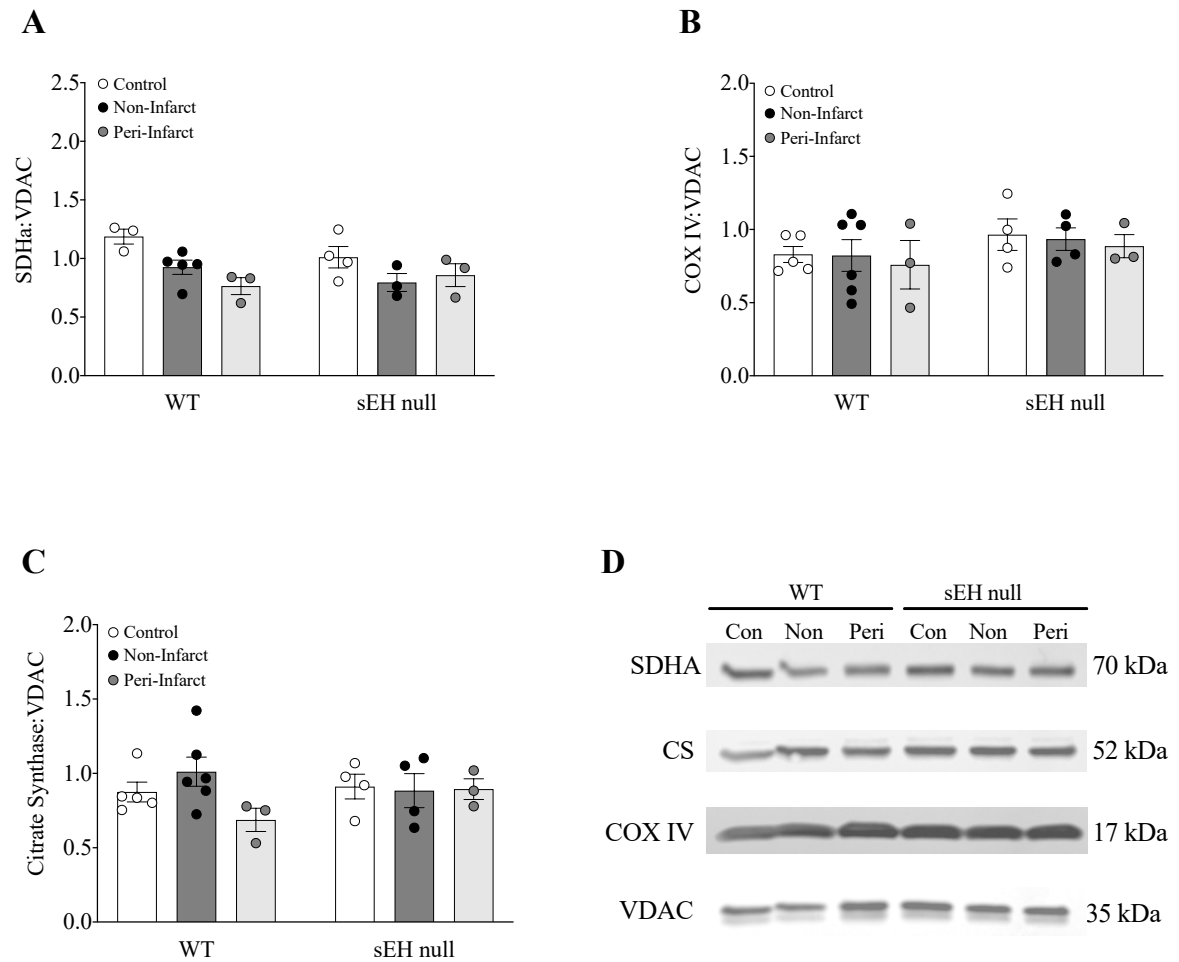


FIGURE 3.2.15. Key mitochondrial protein expression in male WT, sEH null and *tAUCB* treated. (A) Succinate dehydrogenase a (SDHa), (B) COX IV, (C) Citrate synthase (CS) and (D) representative blots normalized to VDAC. N = 3-10. $p < 0.05$.

Defects in mitochondrial respiration are widely accepted as the driving force behind the cardiac dysfunction observed post-MI and throughout the progression to HF [595, 596]. In contrast to protein expression, citrate synthase activity was decreased in non- and peri-infarct regions of post-MI WT hearts but not in sEH null or *tAUCB* same-day treated mice (Fig. 3.2.16). Interestingly, significant increases in complex I activity was observed in post-MI hearts from female sEH null and *tAUCB* same-day treated mice (Fig. 3.2.16). No significant differences in complex II or IV were observed in female mouse hearts and no changes in any ETC enzymes were observed in male hearts (Fig. 3.2.16, Fig. 3.2.17).

Female

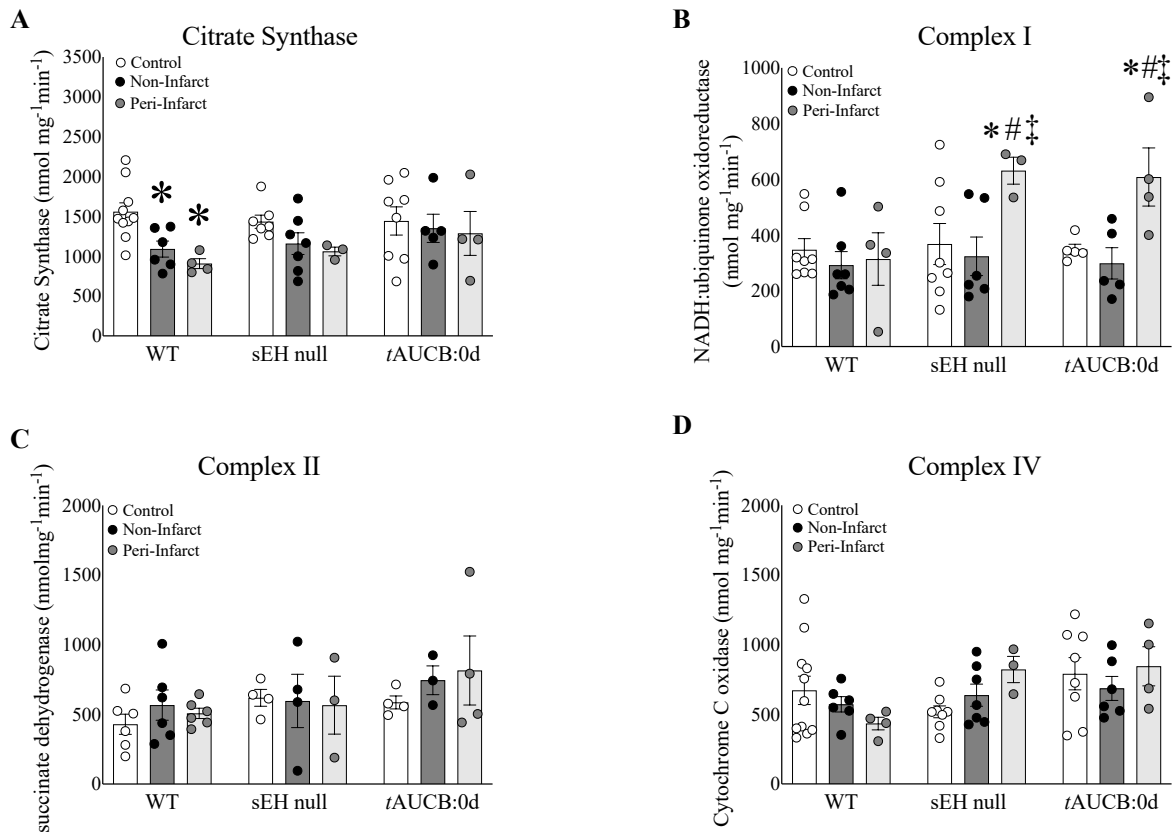


FIGURE 3.2.16. Enzymatic activities in female control, non-infarct and peri-infarct LV tissue from WT, sEH null and *tAUCB* treated mice. (A) Citrate Synthase (CS), (B) NADH:ubiquinone oxidoreductase, Complex I, (C) Succinate dehydrogenase (Complex II) and (D) Cytochrome C oxidase (Complex IV) activities. N = 3-10. $p < 0.05$, *vs baseline; # vs WT counterpart; ‡ vs non-infarct.

Male

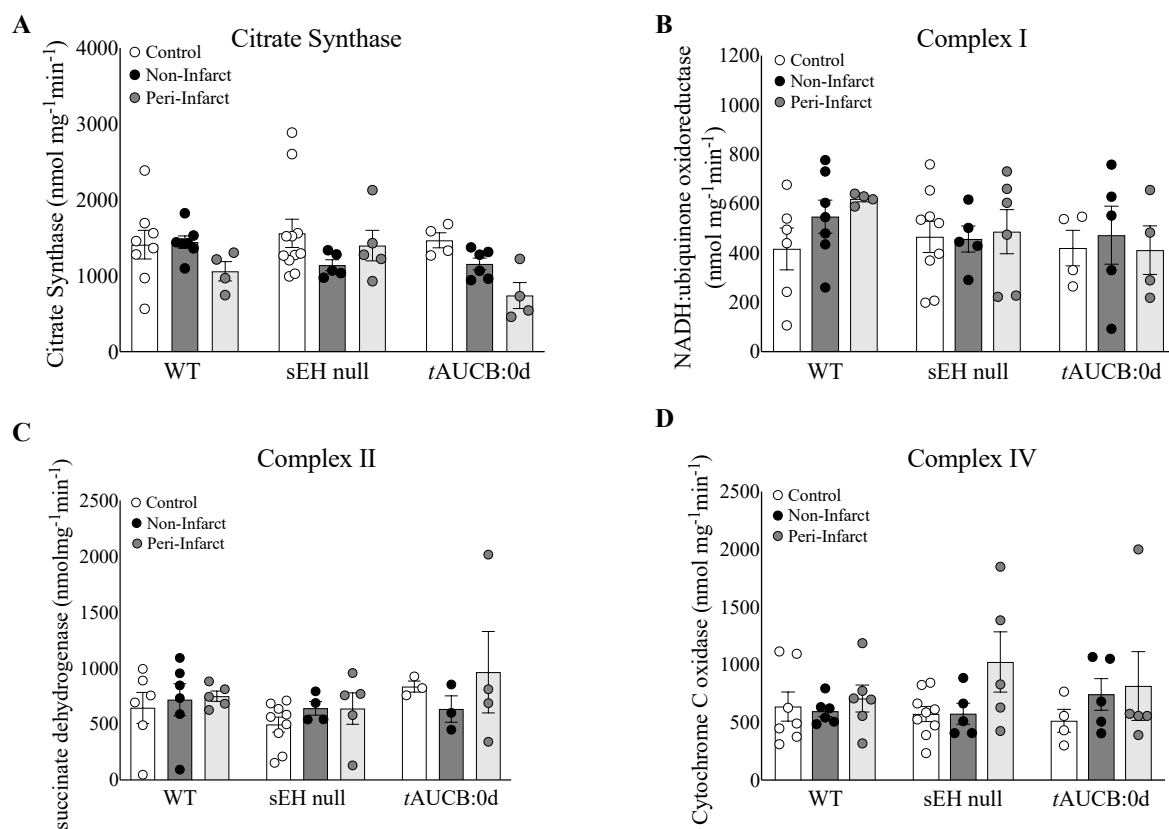


FIGURE 3.2.17. Enzymatic activities in male control, non-infarct and peri-infarct LV tissue from WT, sEH null and *tAUCB* treated mice. (A) Citrate Synthase (CS), (B) NADH:ubiquinone oxidoreductase, Complex I, (C) Succinate dehydrogenase (Complex II) and (D) Cytochrome C oxidase (Complex IV) activities. N = 3-10. $p < 0.05$.

Mitochondria undergo excess fission following ischemic injury, suggesting preserving or promoting fusion processes may be beneficial[597]. Yet, there remain discrepancies in the literature regarding changes in fusion proteins in chronic post-ischemic cardiac remodelling. The process of mitochondrial fusion is driven by GTPases, MFN-1 and MFN-2, which mediate outer mitochondrial membrane fusion and optic atrophy 1 (OPA1), which mediates inner mitochondrial membrane fusion and preserves cristae structure[598]. Conversely, dynamin-related protein 1 (DRP1) translocates to the mitochondria from the cytosol initiating mitochondrial fission [599]. Assessment of LV mitochondria from female mice demonstrated increased OPA1 expression in non- and peri-infarct regions obtained from sEH null hearts compared to WT mice. Interestingly, in mice pre-treated with *t*AUCB for 4 days all groups demonstrated increased OPA1 expression, including control (Fig. 3.2.18A). MFN-1 and MFN-2 expression significantly increased in the non-infarct region of sEH null females compared to controls (Fig. 3.2.18B/C). Similarly, mitochondrial MFN-2 expression significantly increased in the peri-infarct regions of sEH null and *t*AUCB pre-treated females compared to WT (Fig. 3.2.18C). Mitochondrial DRP1 expression significantly decreased in the non-infarct region of sEH null females compared to controls, suggesting less mitochondrial translocation (Fig. 3.2.18D).

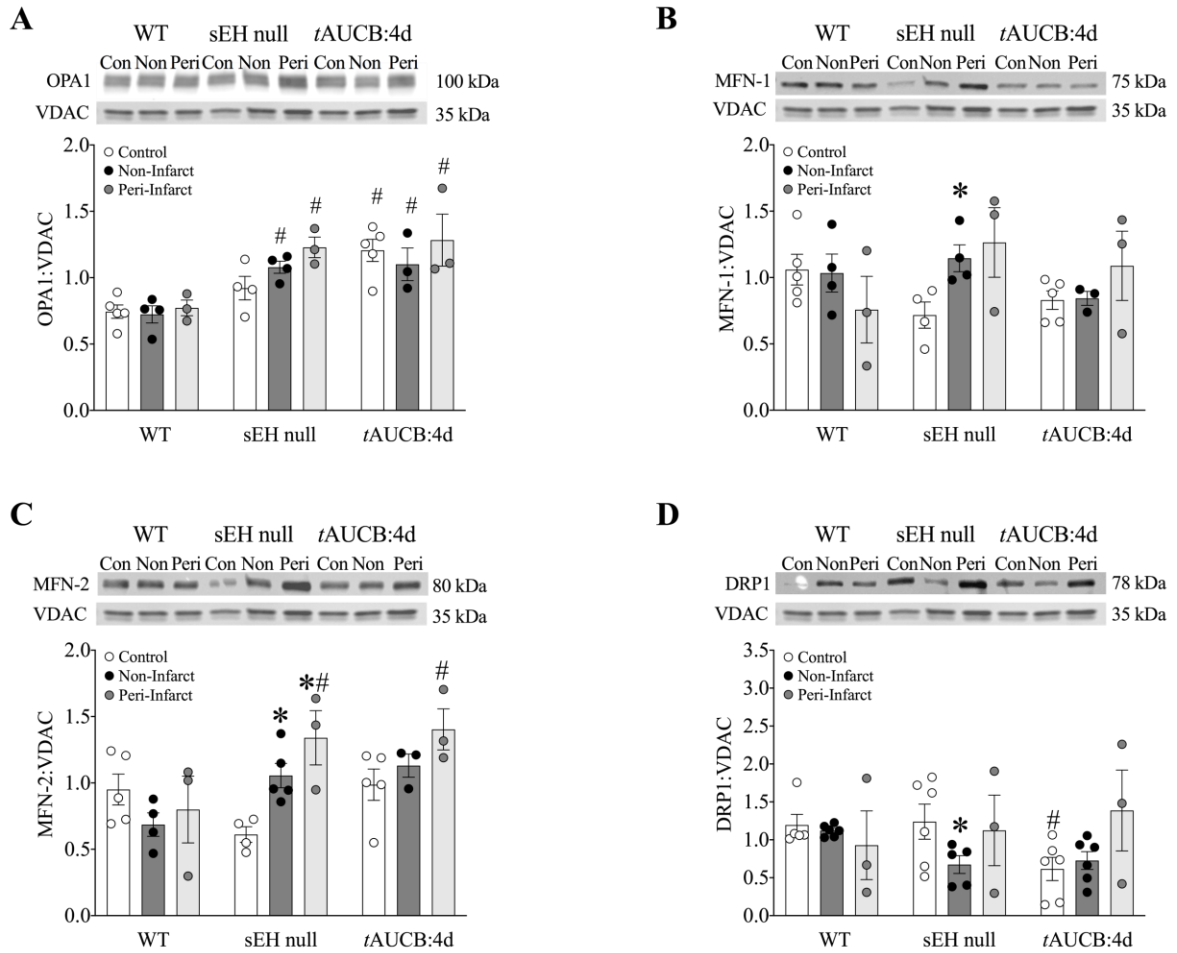


FIGURE 3.2.18. Protein expression in mitochondrial fractionates from female mouse hearts at 28 days post-MI. (A) OPA1, (B) MFN-1, (C) MFN-2 and (D) DRP-1 normalized to VDAC in isolated mitochondria in female WT, sEH null and *tAUCB:4d* control, non-infarct and peri-infarct regions. Data are means \pm SEM, N = 3-6. $p < 0.05$; * vs Control; # vs WT group; ‡ vs non-infarct.

In contrast to the mitochondrial fractions, microsomal MFN-2 expression significantly increased in the non-infarct region of WT females, an effect attenuated in sEH null and *t*AUCB pre-treated mice (Fig. 3.2.19A). Cytosolic DRP-1 expression significantly declined in the non-infarct region of WT female mice, with no such change observed in sEH null or *t*AUCB pre-treated females (Fig. 3.2.19B). The effects observed in females were not observed in males (Fig. 3.2.20).

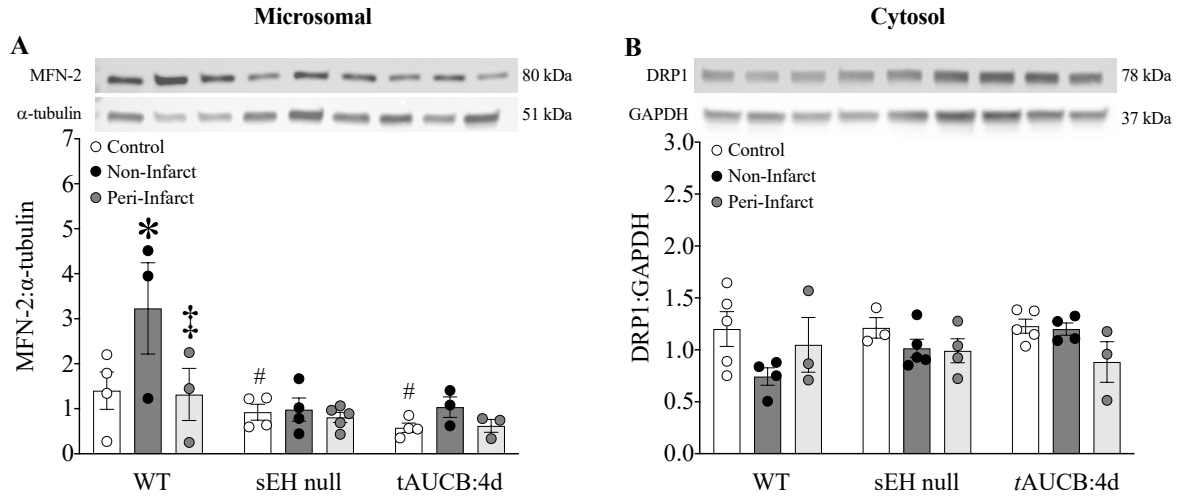
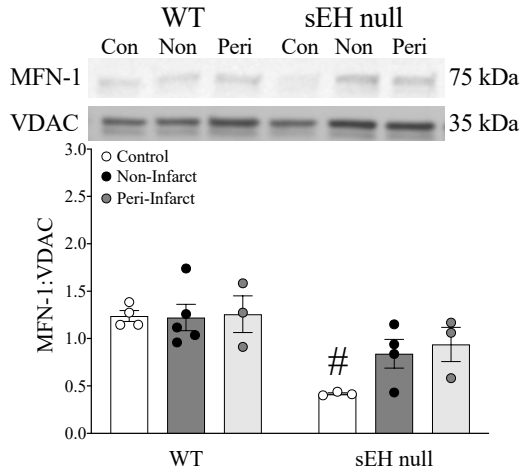


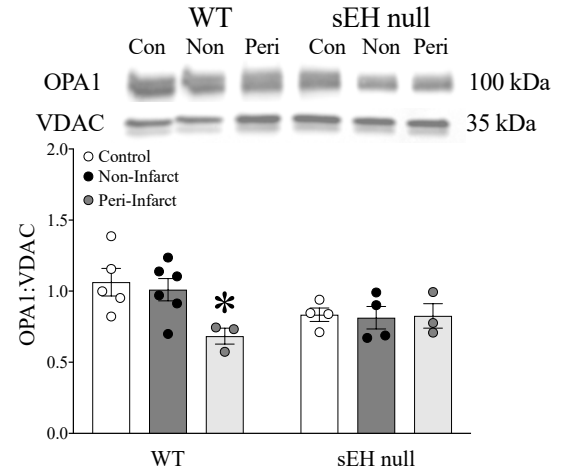
FIGURE 3.2.19. Protein expression in microsomal (A) and cytosolic (B) fractionates from female mouse hearts at 28 days post-MI. (A) MFN-2 protein expression normalized to α -tubulin and (B) cytosolic DRP1 normalized to GAPDH in female WT, sEH null and tAUCB:4d control, non-infarct and peri-infarct hearts at 28 days post-MI. Data are means \pm SEM, N = 3-6. $p < 0.05$; * vs Control; # vs WT group; ‡ vs non-infarct.

Mitochondria

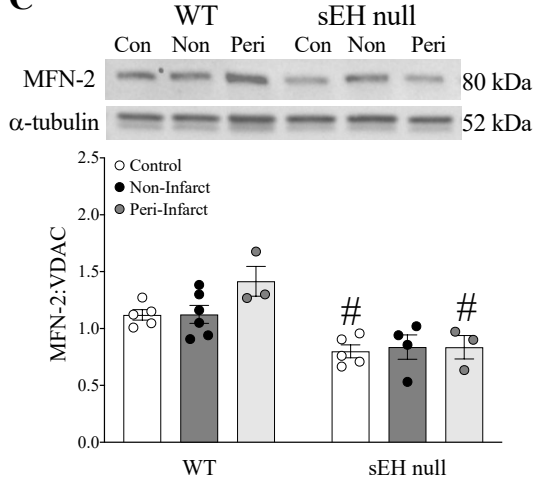
A



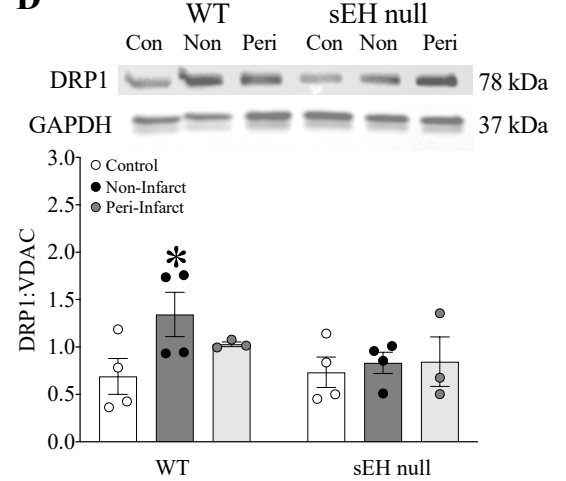
B



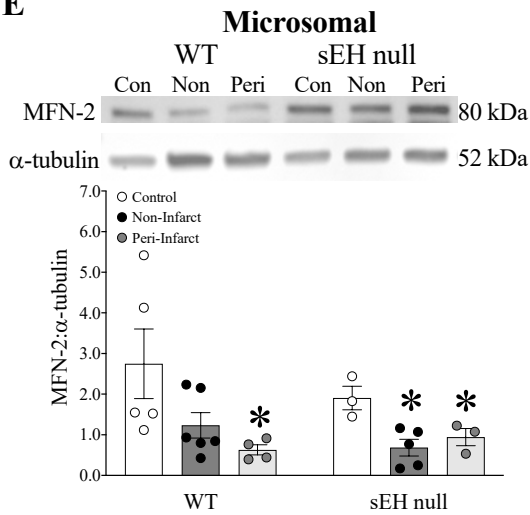
C



D



E



F

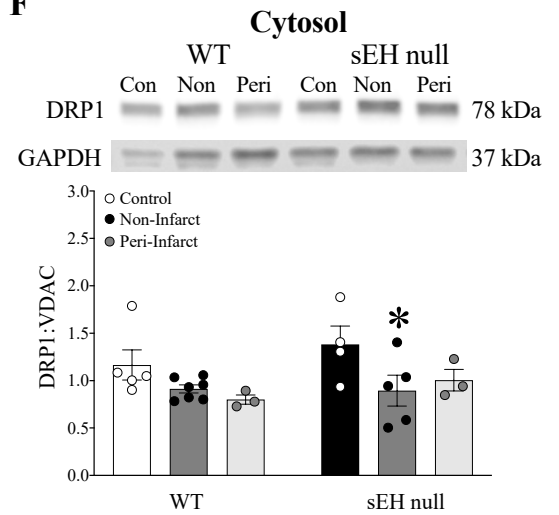


FIGURE 3.2.20. Protein expression in mitochondrial (A-D), microsomal (E) and cytosolic (F) fractionates from male mouse hearts at 28 days post-MI. (A) OPA1, (B) MFN-1, (C) MFN-2 and (D) DRP1 normalized to VDAC in isolated mitochondria in male WT and sEH null control, non-infarct and peri-infarct regions. (E) Microsomal MFN-2 protein expression normalized to α -tubulin and (F) cytosolic DRP1 normalized to GAPDH in male WT and sEH null control, non-infarct and peri-infarct hearts at 28 days post-MI. Data are means \pm SEM, N = 3-6. $p < 0.05$; * vs Control; # vs WT group; ‡ vs non-infarct.

Analysis of mitochondrial O₂ consumption was used to characterize mitochondrial function by determining respiratory rates such as basal state (resting or controlled respiration) and an ADP-stimulated state (active respiration and ATP synthesis), where the ratio represents a level of physiological efficiency expressed as RCR. Interestingly, we observed a significant increase in RCR in the non-infarct region of WT females, while no change was observed in either sEH null or *tAUCB* pre-treated mice (Fig. 3.2.21A). However, there was a marked decline in corresponding ATP production from mitochondria in the post-MI WT hearts, which was increased in sEH null females and maintained in *tAUCB* treated mice (Fig. 3.2.21B). Considering malate and glutamate were used as respiratory substrates, which are controlled exclusively by complex I, our observations of better complex I activity in post-MI hearts from female sEH null and *tAUCB* treated mice suggest that these hearts have preserved mitochondrial efficiency compared to WT female mice. These changes were not observed in male hearts (Fig. 3.2.22A, B). Taken together, these data suggest overall mitochondrial preservation is associated with conserved mitochondrial dynamic proteins and improved overall survival in aged female mice with deletion of sEH or pre-treatment with *tAUCB* (Fig. 3.2.23).

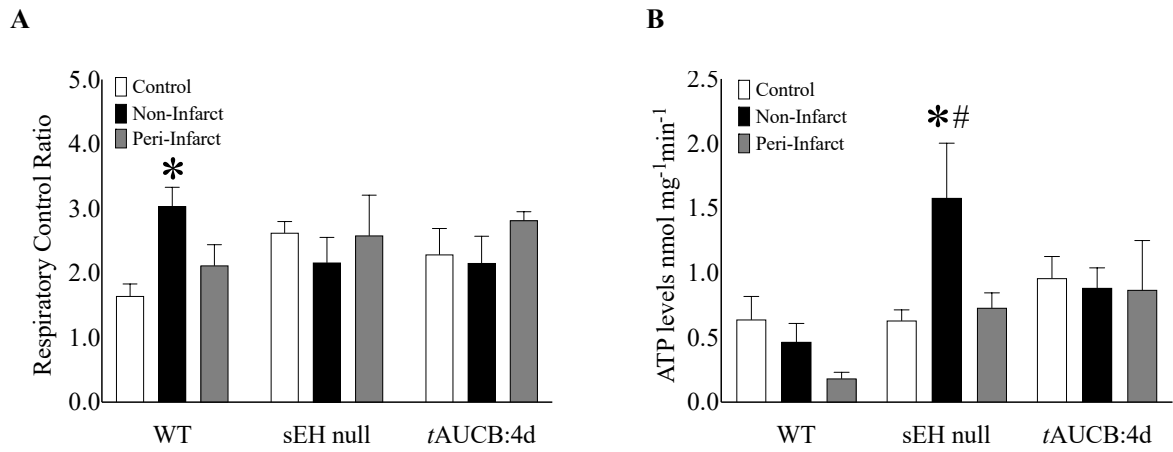


FIGURE 3.2.21. (A) Respiratory control ratio (RCR) in whole cardiac fibres taken from WT, sEH null and *tAUCB:4d* pre-treatment female mice. (B) ATP levels in nmol mg⁻¹ from WT, sEH null and *tAUCB:4d* pre-treatment female mice in control and post-MI hearts. Data are means \pm SEM, N = 3-6. $p < 0.05$; * vs Control; # vs WT group.

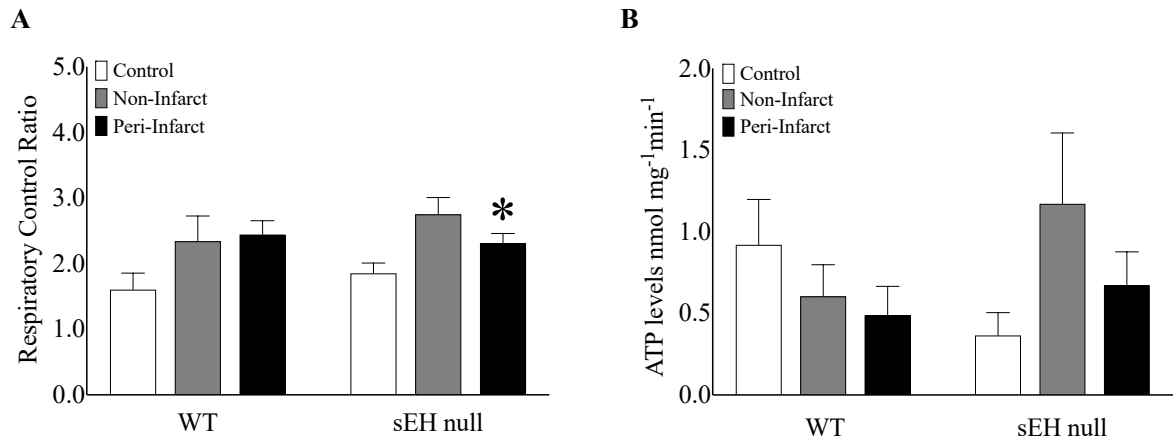


FIGURE 3.2.22. (A) Respiratory control ratio (RCR) in whole cardiac fibres taken from WT and sEH null male mice. (B) ATP levels in nmol mg^{-1} from WT and sEH null male mice in control and post-MI hearts. Data are means \pm SEM, $N = 3-6$. $p < 0.05$; * vs Control.

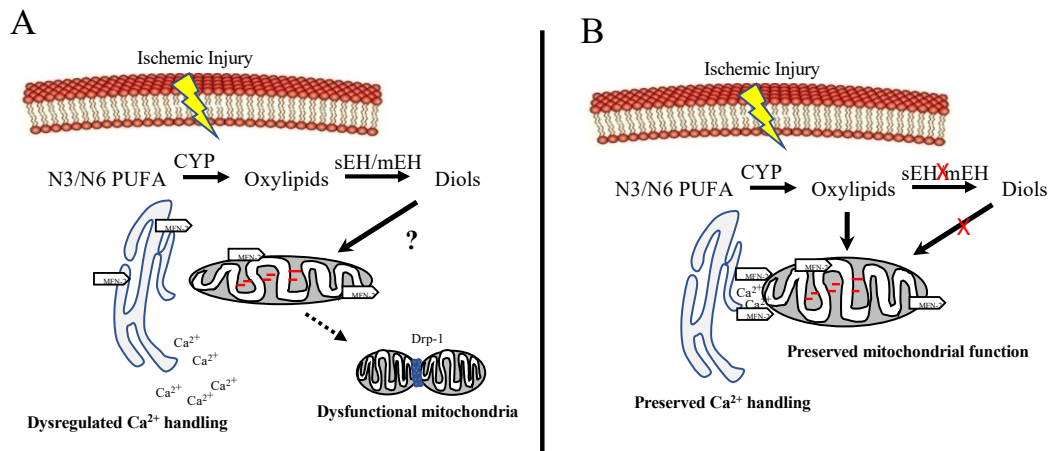


FIGURE 3.2.23. A proposed mechanism of protection arising from sEH inhibition or deletion in female hearts. A) Hearts where sEH activity is not inhibited are marked by increased mitochondrial dysfunction manifesting with disrupted dynamics, impaired electrical signalling and mechanical function at 28-days post-ischemia. This was associated with increased diol metabolite formation. B) In contrast, female hearts where sEH is genetically deleted or pharmacologically inhibited are marked by reduced mitochondrial dysfunction, culminating in preserved ATP production and slowing the progression of cardiac dysfunction. Interestingly, pre-treatment with sEHi demonstrates a higher degree of cardioprotection, suggesting sEHi protection is time-dependent.

3.2.5 *Conclusions*

In summary, in this section we utilize an aged mouse model to demonstrate sEH genetic deletion or pharmacological inhibition improves survival and conserves cardiac and mitochondrial function in aged mice 28 days post-MI. Unexpectedly, in contrast to our original hypothesis and with our results in young mouse models, cardiac responses in sEH null and *tAUCB* treated mice demonstrated significant sexual dimorphism. Namely, aged females exhibited a more robust cardioprotection following sEH deletion/inhibition than males. Moreover, the protection arising from sEH inhibition with *tAUCB* appears to be time dependent.

3.3 OXYLIPID METABOLISM IN HUMAN LEFT VENTRICULAR TISSUE

3.3.1 Clinical parameters from human explanted hearts

There were no significant differences in demographic or clinical parameters in male or female NFC human transplanted hearts (Table 3.3.1). In the ICM group, a higher proportion of females met NYHA class IV standards when referred to transplant as compared to males (Table 3.3.1). No other relevant differences in anthropometric factors or medical history was noted between male and female patients.

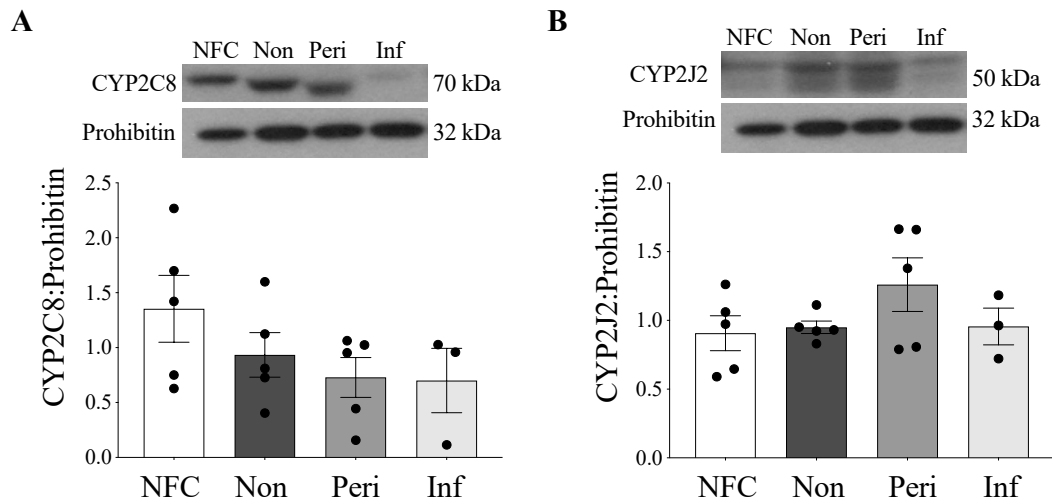
TABLE 3.3.1. Clinical parameters for non-failing control (NFC) and ischemic cardiomyopathy (ICM) human transplant hearts.

NFC					
Variable	Male (n=5)	IQR; %	Female (n=5)	IQR; %	p -Value
Demographic					
Age at transplant	38.0	25.0-42.5	48.0	31.5-59.5	0.21
Anthropometric					
Weight (kg)	66.0	61.0-69.0	67.2	64.0-69.5	0.70
Height (m)	1.73	1.56-1.79	1.62	1.59-1.71	0.70
BMI (kg/m ²)	22.1	21.5-25.1	24.4	23.8-26.6	0.40
ICM					
Variable	Males (n=12)	IQR; %	Females (n=5)	IQR; %	p -Value
Demographic					
Age at transplant	56.5	47.3-62.8	58.0	54.0-61.0	0.62
Anthropometric					
Weight (kg)	85.0	74.0-95.5	73.9	53.5-78.5	0.051
Height (m)	171.0	168.0-179.5	162.0	160.0-164.5	0.0005
BMI (kg/m ²)	28.5	24.6-32.0	26.5	20.6-30.3	0.33
Physical assessment					
HR (bpm)	88.0	74.0-91.0	90.0	79.5-110.5	0.42
BP (syst)	120.0	90.0-124.0	127.5	110.8-148.0	0.17
BP (diast)	60.0	54.0-82.0	62.5	48.3-79.5	0.64
NYHA class III (%)	8	67	1	20	0.079
NYHA class IV (%)	3	25	4	80	0.036
Comorbidities (%)					
COPD/Asthma	5	42	0	0	na
DM	5	42	1	20	0.39
Dyslipidemia	8	67	2	40	0.31
Kidney disease	5	42	3	60	0.49
HTN	6	50	0	0	na
Liver Disease	1	8	1	20	0.50
Echocardiography					
EF (%)	17.5	10.0-28.3	24.4	15.0-42.0	0.29
LVID;d (mm)	50.0	47.0-58.0	51.0	42.0-52.0	0.58
LVID;s (mm)	48.0	32.0-50.0	39.0	32.0-46.0	0.60
Devices (%)					
Pacemaker/ICD	7	58	2	40	0.49
ICD	3	25	1	20	0.82
BiV-ICD	4	33	0	0	na
Medications					
ACEI/ARB (%)	9	75	2	40	0.17
Beta Blocker (%)	9	75	4	80	0.82
eGFR (ml/min)	48.5	37.0-72.3	41.0	36.0-64.0	0.59
Creatinine (μmol/L)	134.0	97.0-175.5	121.0	88.5-138.0	0.34

3.3.2 *Epoxide hydrolases are upregulated in ischemic human LV*

Expression of key epoxygenases and epoxide hydrolases were assessed by protein immunoblotting. CYP P450 isozymes, CYP2C8 and CYP2J2, are primarily responsible for cardiac LA and AA metabolism to the EpOMEs and EETs [600]. There were no significant changes in either CYP2J2 or CYP2C8 expression levels in human hearts between NFC and ICM tissues (Fig.3.3.1).

Female



Male

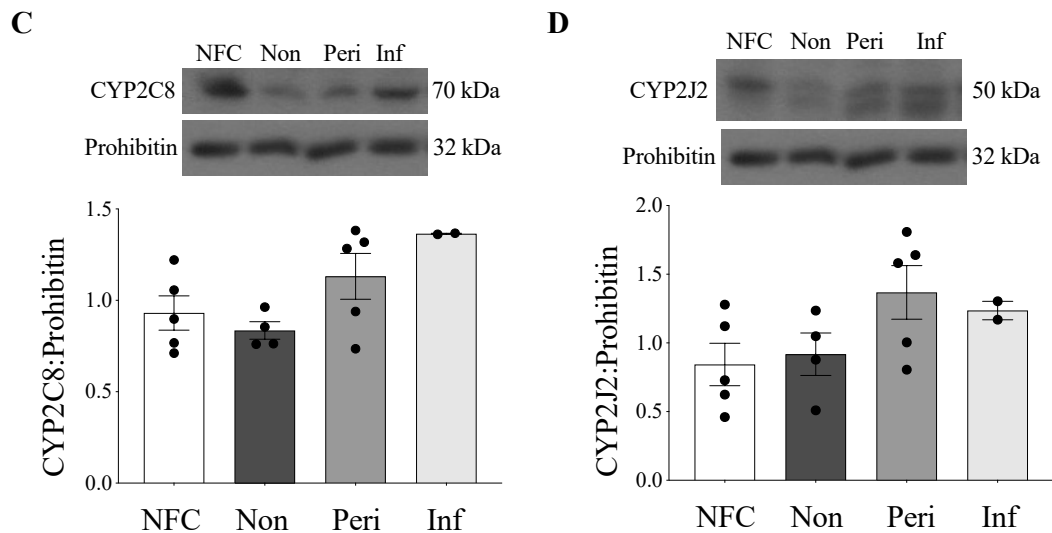
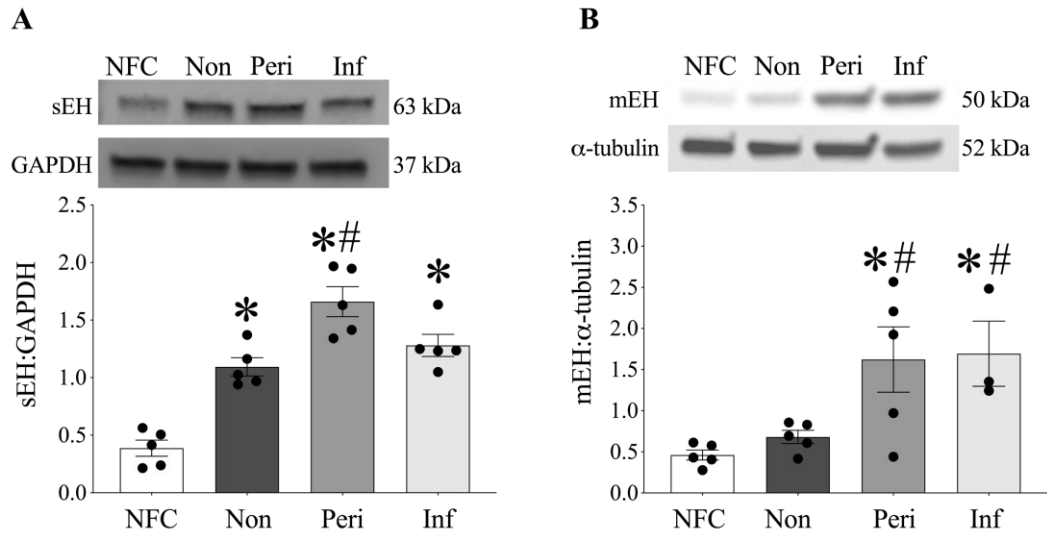


FIGURE 3.3.1. CYP epoxygenase protein expression in microsomal fractions from human NFC and ICM hearts. (A) CYP2C8 expression and (B) CYP2J2 expression in non-failing control and ICM female hearts. (C) CYP2C8 expression and (D) CYP2J2 expression in non-failing control and ICM male hearts. Proteins were normalized to prohibitin. Data are represented as mean \pm SEM, N = 3-5, $p < 0.05$.

In contrast with the CYP450 epoxygenases, sEH expression significantly increased in the non-infarct, peri-infarct and infarct regions of female ICM patients, with the peri-infarct region demonstrating the highest increase in expression (Fig. 3.3.2A). Due to its location tethered in the ER, microsomal epoxide hydrolase (mEH) plays a role in basal epoxide hydrolysis and can be upregulated following ischemic injury[601]. mEH expression in female hearts significantly increased in the peri-infarct and infarct regions (Fig. 3.3.2B). sEH expression also significantly increased in non, peri and infarct regions in male hearts (Fig. 3.3.2C), while mEH expression increased only in the peri-infarct and infarct regions post-MI in males (Fig. 3.3.2D).

Female



Male

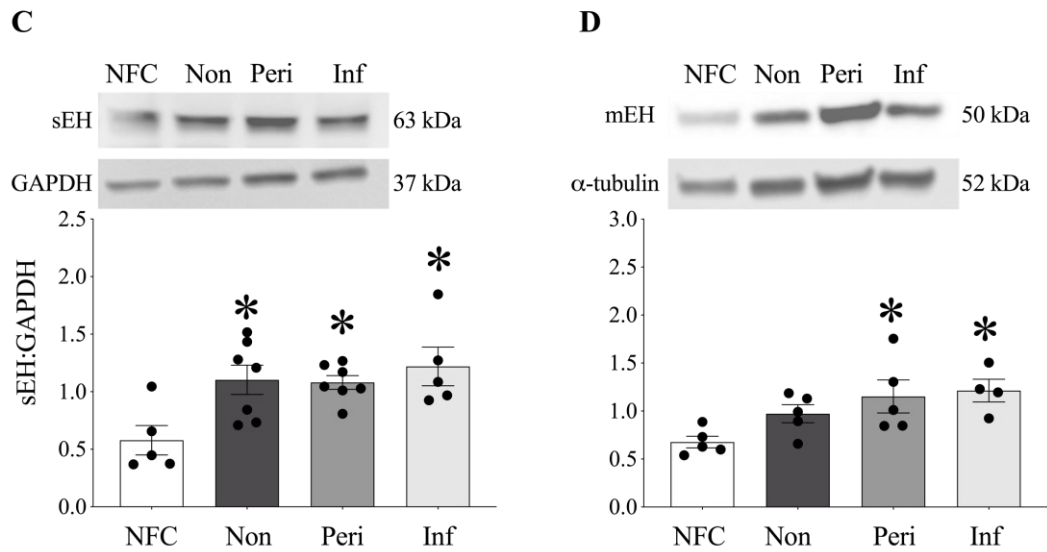


FIGURE 3.3.2. Epoxide hydrolase protein expression in cytosolic and mitochondrial fractions in female and male human hearts. (A) sEH expression and (B) mEH expression in non-failing control and MI female hearts. (C) sEH expression and (D) mEH expression in non-failing control and MI male hearts. sEH was normalized to GAPDH with mEH normalized to α -tubulin. Data are represented as mean \pm SEM, $n = 3-7$, $p < 0.05$; *vs NFC; # vs non-infarct.

3.3.3 *Decreased mitochondrial function in LV myocardium from ICM hearts*

In order to assess function of the mitochondrial electron transport chain (ETC) we determined the enzymatic catalytic activity of ETC subunits: NADH:ubiquinone oxidoreductase (complex I), succinate dehydrogenase (SDH, complex II) and cytochrome c oxidase (COX IV, complex IV). Significant decreases in complex I and II activities were observed in peri-infarct and infarct regions of ICM female hearts (Fig. 3.3.3). Complex IV activity was significantly reduced in the non, peri and infarct regions (Figure 1G). Citrate synthase (CS) activity, a marker of cellular aerobic metabolism due to its role as the rate-limiting factor for entry into the Krebs' cycle[602], was significantly decreased in peri and infarct regions from female hearts (Figure 3.3.3). In contrast, no change in complex I activity was observed in tissue from male LV, while complex II activity significantly decreased in peri- and infarct regions, and complex IV and CS activity significantly declined in all regions assessed in LV tissue from male ICM hearts (Figure 3.3.4A-D). Importantly, no changes in ETC protein expression were detected in any region assessed in ICM hearts from either male or female patients (Fig. 3.3.5). This suggests the presence of decreased mitochondrial quality rather than mitochondrial loss.

Female

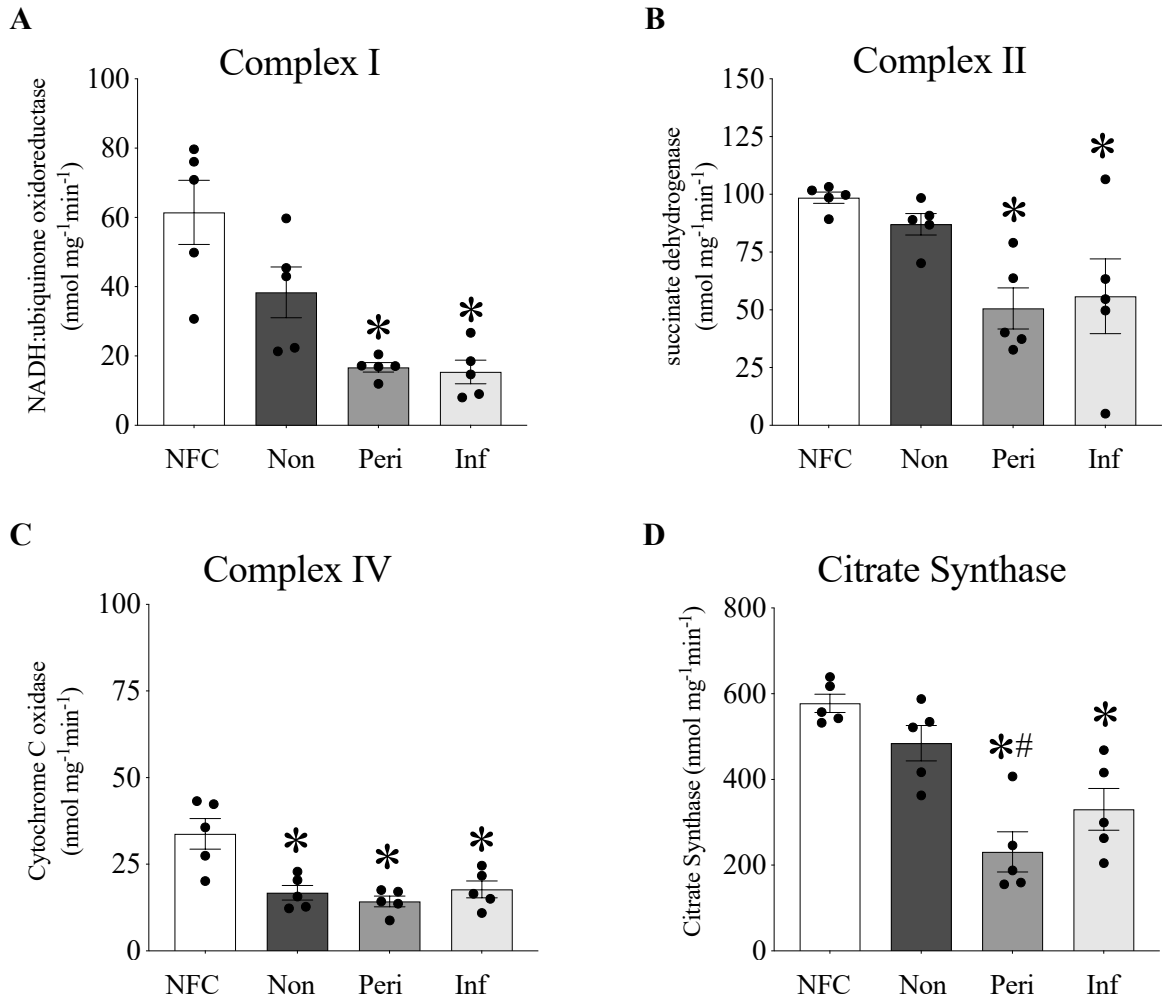


FIGURE 3.3.3. ETC complex activity (nmol mg⁻¹min⁻¹) in non-failing control and ICM female hearts. (A) Complex I (NADH:ubiquinone oxidoreductase) activity, (B) Complex II (succinate dehydrogenase, SDH), (C) Complex IV (cytochrome C oxidase, COX IV) and (D) citrate synthase (CS) activity. Data are represented as mean \pm SEM, n = 3-7, p < 0.05; *vs NFC; # vs non-infarct.

Male

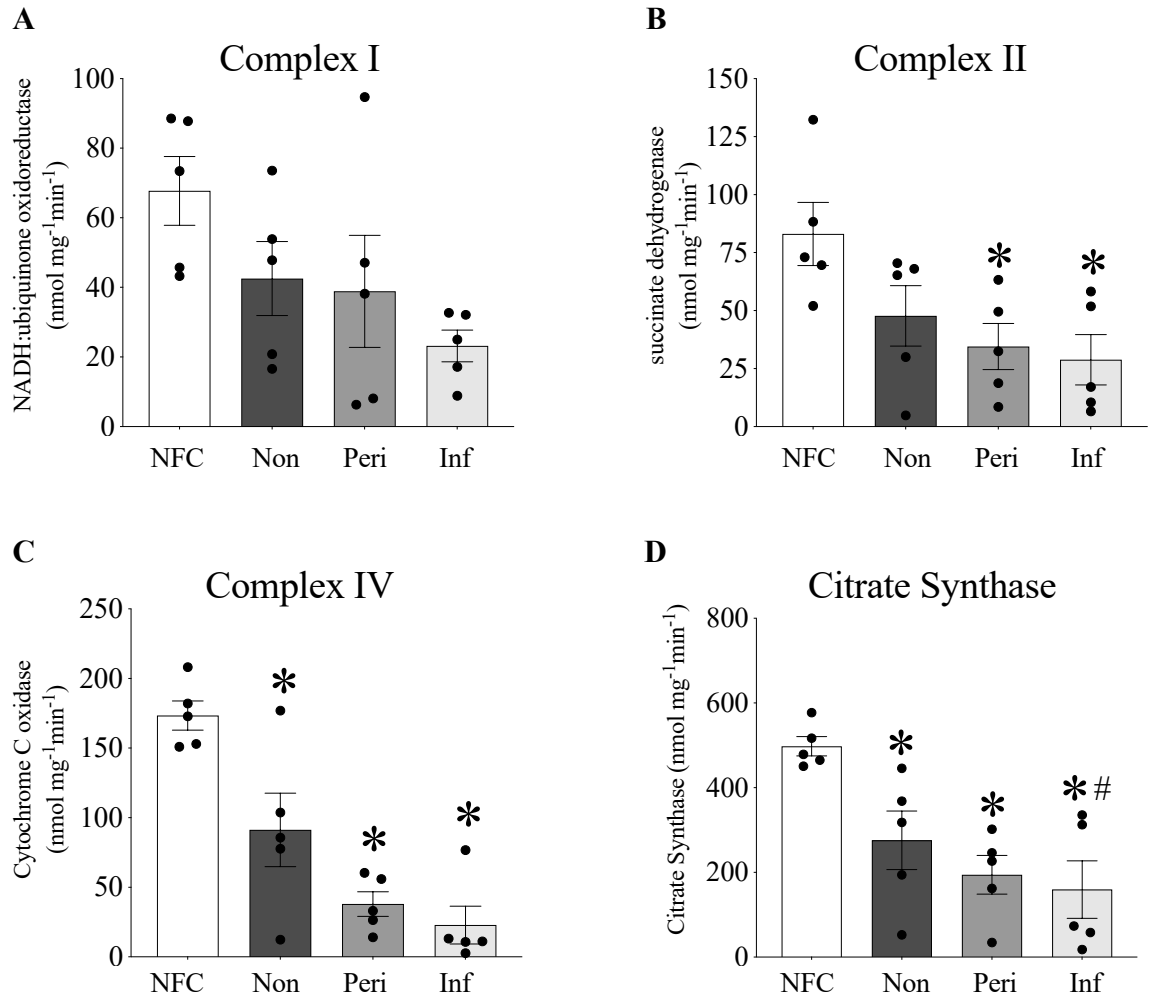
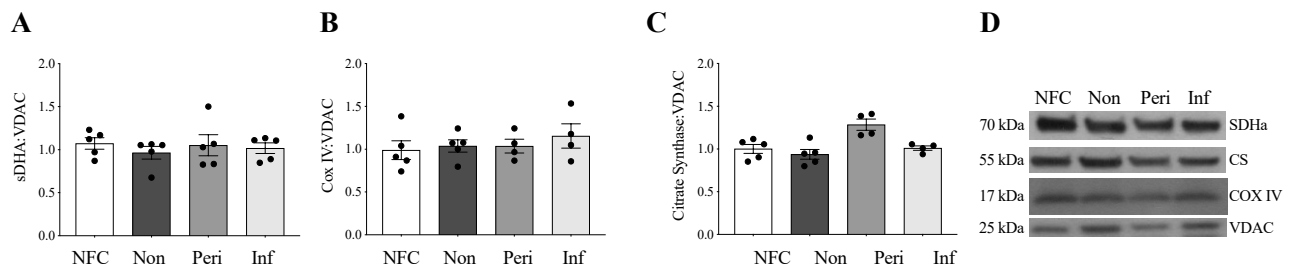


FIGURE 3.3.4. ETC complex activity (nmol mg⁻¹min⁻¹) in non-failing control and ICM male hearts. (A) Complex I (NADH:ubiquinone oxidoreductase) activity, (B) Complex II (succinate dehydrogenase, SDH), (C) Complex IV (cytochrome C oxidase, COX IV) and (D) citrate synthase (CS) activity. Data are represented as mean \pm SEM, n = 3-7, p < 0.05; *vs NFC; # vs non-infarct.

Female



Male

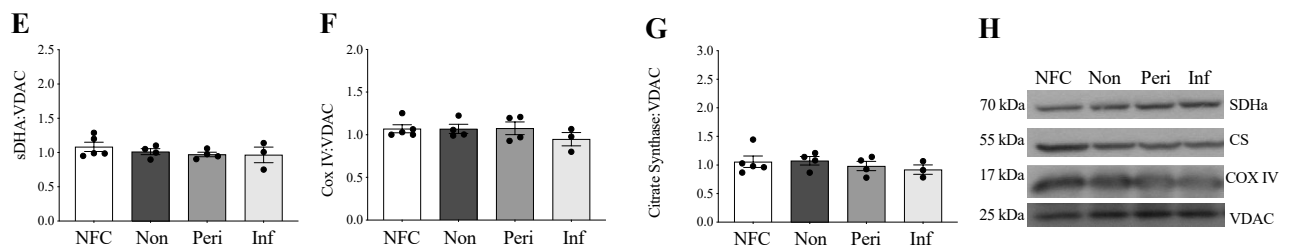


FIGURE 3.3.5. Protein expression of key mitochondrial ETC enzymes in mitochondrial fractions from human female (A/D) and male (E-H) NFC and ICM hearts. (A/E) Succinate dehydrogenase A (SDHA) expression, (B/F) Cytochrome C oxidase (COX IV) expression, (C/G) Citrate synthase (CS) expression, (D/H) representative blots. All proteins were normalized to VDAC. Data are represented as mean \pm SEM, $n = 3-5$, $p < 0.05$.

3.3.4 *Human ischemic left ventricle demonstrates marked changes in oxylipid metabolism*

Oxylipid levels quantified in human LV tissue using LC-MS/MS are summarized in Table 3.3.2. Assessment of human LV demonstrated significantly decreased amounts of AA throughout ICM hearts (Table 3.3.2). Increased production of COX metabolites of AA (prostanoids), such as PGE₂ and PGD₂, were detected in non-infarct regions from human tissues reflecting a pro-inflammatory response. CYP-derived epoxygenase metabolites of LA (12,13-EpOME and 9,10-EpOME) were increased in the non-infarct LV compared to NFC and metabolites of AA (8,9-EET and 11,12-EET) were increased in the non-infarct region in females but not males (Table 3.3.2). The epoxide hydrolase metabolites of the EpOMEs, 12,13-DiHOME and 19,20-DiHOME, significantly increased in the non-infarct LV of both sexes (Table 3.3.2). The ratio of 12,13-EpOME:DiHOME was significantly increased in the non-infarct region of female LV, an effect significantly attenuated in the peri and infarct regions (Figure 3.3.6A). The infarct region of female hearts also demonstrated significantly decreased a 9,10-EpOME:DiHOME ratio (Fig. 3.3.6B). No changes in EET:DHET ratios was noted in female ICM hearts (Fig. 3.3.7). In contrast to females, male ICM hearts demonstrated no significant alterations in the overall epoxygenase:diol metabolite ratios, with the exception of 8,9-EET:DHET, which was significantly decreased in the non-infarct, peri-infarct and infarct regions (Fig. 3.3.6, Fig. 3.3.7). The epoxygenase derivative of docosahexaenoic acid, 19,20-EpDPE, was significantly reduced in the peri and infarct regions of both sexes (Fig. 3.3.8). 19,20- EpDPE is a metabolite of DHA associated with cardioprotection following MI[603]. The epoxygenase metabolite of eicosapentaenoic acid, 17,18-EpETE, was not detected in human tissues (Table 3.3.2). No levels of the ω-

hydroxylase metabolites 19-HETE or 20-HETE were detected in the human LV of either sex. Hydroxyoctadecadienoic acids (HODEs) are lipoxygenase metabolites associated with oxidative stress. 13-HODE and 9-HODE, significantly increased in both male and female ICM hearts (Table 3.3.2).

TABLE 3.3.2. Oxylipid metabolite profile (ng/g tissue) in human left ventricular tissue measured by LC-MS/MS. Data are shown as mean \pm SEM, n=3-6. p < 0.05, *vs control; # vs WT group; ‡ vs non-infarct; † vs peri-infarct group.

Human								
	Females				Males			
	NFC	Non-Infarct	Peri-Infarct	Infarct	NFC	Non-Infarct	Peri-Infarct	Infarct
Arachidonic Acid	2.66 $\times 10^6 \pm 0.38 \times 10^6$	1.07 $\times 10^6 \pm 0.24 \times 10^6$ *	1.45 $\times 10^6 \pm 0.44 \times 10^6$	0.65 $\times 10^6 \pm 0.16 \times 10^6$ *	3.10 $\times 10^6 \pm 0.76 \times 10^6$	0.86 $\times 10^6 \pm 0.20 \times 10^6$ *	0.61 $\times 10^6 \pm 0.11 \times 10^6$ *	0.52 $\times 10^6 \pm 0.16 \times 10^6$ *
Epoxygenase-dependent metabolism								
12,13-EpOME	19.12 \pm 3.15	142.70 \pm 30.11*	68.43 \pm 42.08	54.61 \pm 15.01	17.51 \pm 3.88	145.30 \pm 40.27*	89.34 \pm 21.49	59.63 \pm 11.81
9,10-EpOME	57.35 \pm 10.34	470.00 \pm 119.10*	105.13 \pm 32.13‡	181.15 \pm 46.75‡	63.68 \pm 22.08	564.20 \pm 163.20*	233.8 \pm 65.65	191.50 \pm 35.07
14,15-EET	10.88 \pm 1.24	16.19 \pm 2.91	9.59 \pm 2.68	13.09 \pm 4.18	8.77 \pm 1.01	11.84 \pm 1.36	10.97 \pm 1.78	11.10 \pm 2.24
11,12-EET	6.74 \pm 0.86	16.88 \pm 2.94*	6.02 \pm 1.56‡	8.38 \pm 2.77	5.57 \pm 0.89	14.55 \pm 3.40	9.55 \pm 1.76	10.55 \pm 2.84
8,9-EET	12.63 \pm 1.88	31.93 \pm 5.77*	12.25 \pm 2.45‡	18.02 \pm 3.54	11.63 \pm 1.43	19.95 \pm 2.97	16.50 \pm 2.60	13.88 \pm 1.97
5,6-EET	ND	ND	ND	ND	ND	ND	ND	ND
17,18-EpETE	ND	ND	ND	ND	ND	ND	ND	ND
19,20-EpDPE	35.63 \pm 2.32	22.54 \pm 4.93	15.24 \pm 2.54*	14.78 \pm 4.98*	35.17 \pm 8.25	29.23 \pm 2.53	7.19 \pm 1.46*‡	12.79 \pm 2.78*
Soluble epoxide hydrolase-dependent metabolism								
12,13-diHOME	6.09 \pm 1.60	14.00 \pm 2.32*	7.25 \pm 1.81	10.93 \pm 1.64	4.87 \pm 0.66	16.41 \pm 2.24*	9.70 \pm 2.44	11.03 \pm 1.77
9,10-diHOME	11.98 \pm 3.79	76.27 \pm 25.19*	20.15 \pm 5.02‡	32.88 \pm 6.40	8.71 \pm 2.29	76.48 \pm 12.11*	50.13 \pm 10.85	40.73 \pm 11.90
14,15-DHET	0.48 \pm 0.07	0.62 \pm 0.06	0.47 \pm 0.07	0.62 \pm 0.07	0.64 \pm 0.08	0.73 \pm 0.07	0.56 \pm 0.11‡	0.87 \pm 0.10‡
11,12-DHET	0.85 \pm 0.12	0.96 \pm 0.19	0.54 \pm 0.09	0.70 \pm 0.11	0.75 \pm 0.08	0.71 \pm 0.07	0.73 \pm 0.13	0.83 \pm 0.11
8,9-DHET	0.68 \pm 0.12	2.02 \pm 0.17*	0.88 \pm 0.18‡	1.72 \pm 0.69	0.75 \pm 0.10	2.79 \pm 0.52	3.70 \pm 0.83	2.54 \pm 0.80
5,6-DHET	0.45 \pm 0.15	0.92 \pm 0.16	0.53 \pm 0.10	0.41 \pm 0.09	0.29 \pm 0.02	1.03 \pm 0.11*	0.87 \pm 0.17	0.76 \pm 0.17
Epoxygenase:Diol Metabolite Ratios								
12,13-EpOME:DiHOME	5.10 \pm 1.42	10.27 \pm 1.21*	3.22 \pm 0.29#	4.53 \pm 1.05#	3.55 \pm 0.48	8.13 \pm 1.39*	8.11 \pm 1.15	4.98 \pm 1.34
9,10-EpOME:DiHOME	7.40 \pm 0.70	6.64 \pm 0.57	5.23 \pm 0.96	3.82 \pm 0.70*	7.03 \pm 0.77	5.48 \pm 0.64*	4.14 \pm 0.73	6.12 \pm 1.12
14,15-EET:DHET	23.54 \pm 3.13	25.57 \pm 3.7	19.72 \pm 5.49	23.43 \pm 7.43	15.21 \pm 3.36	18.17 \pm 2.55	19.79 \pm 2.90	12.50 \pm 1.50
11,12-EET:DHET	8.26 \pm 1.03	19.93 \pm 4.51	11.34 \pm 2.89	11.65 \pm 3.26	7.92 \pm 1.74	15.54 \pm 2.13	16.17 \pm 1.63*	12.02 \pm 2.35
8,9-EET:DHET	20.43 \pm 3.61	15.63 \pm 2.11*	14.58 \pm 3.21	16.84 \pm 11.22	15.72 \pm 3.75	7.34 \pm 1.24*	6.10 \pm 1.22*	5.30 \pm 1.74*
ω -Hydrolase-dependent metabolism								
19-HETE	ND	ND	ND	ND	ND	ND	ND	ND
20-HETE	ND	ND	ND	ND	ND	ND	ND	ND
Lipoxygenase-dependent metabolism								
13-HODE	542.15 \pm 204.56	1468.50 \pm 308.42*	297.93 \pm 97.06‡	413.72 \pm 166.53‡	282.50 \pm 37.58	1387.00 \pm 299.40*	859.00 \pm 219.60	300.70 \pm 82.75‡
9-HODE	359.43 \pm 154.53	1014.17 \pm 204.83*	217.27 \pm 64.37‡	283.35 \pm 116.04‡	159.50 \pm 25.04	926.80 \pm 197.30*	600.30 \pm 143.10	211.30 \pm 59.76‡
15-HETE	48.83 \pm 7.97	30.37 \pm 4.22	25.67 \pm 6.85	20.32 \pm 7.94*	39.88 \pm 9.94	33.60 \pm 6.15	24.63 \pm 4.08	26.12 \pm 9.16
11-HETE	33.79 \pm 5.77	28.03 \pm 5.73	17.29 \pm 3.40	13.57 \pm 5.09	29.58 \pm 7.62	18.82 \pm 2.72	14.05 \pm 2.42	12.72 \pm 3.97*
12-HETE	45.64 \pm 7.85	23.51 \pm 4.94	19.72 \pm 5.12*	13.47 \pm 5.29*	40.85 \pm 12.38	17.35 \pm 3.17*	13.24 \pm 2.18*	14.07 \pm 4.26*
8-HETE	497.33 \pm 97.29	321.02 \pm 67.93	312.65 \pm 71.92	179.97 \pm 70.71*	409.00 \pm 115.00	214.90 \pm 39.18	175.30 \pm 26.49*	168.90 \pm 47.84*
5-HETE	35.98 \pm 5.83	25.35 \pm 4.94	19.10 \pm 3.24	12.52 \pm 3.85*	26.80 \pm 6.67	20.53 \pm 3.59	16.51 \pm 3.02	14.38 \pm 4.64
Cyclooxygenase-dependent metabolism								
6ketoPGF _{1α}	5.70 \pm 1.07	0.60 \pm 0.09	3.76 \pm 2.50	3.32 \pm 2.29	5.42 \pm 2.12	2.40 \pm 0.58	2.37 \pm 0.89	1.35 \pm 0.40
TXB ₂	0.23 \pm 0.06	0.11 \pm 0.06	0.07 \pm 0.04	0.07 \pm 0.04	0.24 \pm 0.06	0.08 \pm 0.01	0.08 \pm 0.03	0.20 \pm 0.17
PGF _{2α}	1.12 \pm 0.49	1.09 \pm 0.31	3.22 \pm 0.81	1.29 \pm 0.61	2.22 \pm 1.47	2.15 \pm 0.71	2.86 \pm 0.51	4.10 \pm 2.97
PGE ₂	8.99 \pm 2.66	25.99 \pm 3.63*	9.59 \pm 2.93‡	12.73 \pm 2.76‡	5.95 \pm 1.51	27.53 \pm 3.14	21.05 \pm 4.84	13.81 \pm 3.70
8isoPGF _{2α}	1.06 \pm 0.09	1.52 \pm 0.20	0.94 \pm 0.33	0.95 \pm 0.05	1.03 \pm 0.09	1.48 \pm 0.07	1.35 \pm 0.26	0.91 \pm 0.21
PGB ₂	ND	ND	ND	ND	ND	ND	ND	ND
PGD ₂	16.52 \pm 4.38	47.35 \pm 6.82	33.00 \pm 18.19	82.77 \pm 61.36	10.58 \pm 2.92	44.82 \pm 5.49*	33.13 \pm 7.03	18.53 \pm 4.82

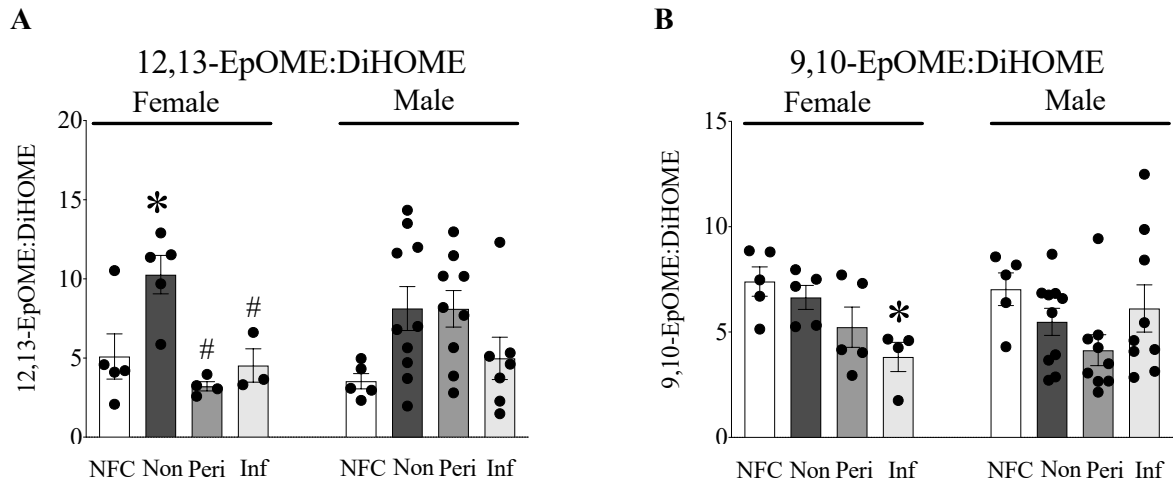


FIGURE 3.3.6. Linoleic acid epoxygenase oxylipid metabolites (ng/g tissue) in human (G-M) left ventricular tissue measured by LC-MS/MS. A) 12,13-EpOME:DiHOME ratio, B) 9,10-EpOME:DiHOME ratios. Data are shown as mean \pm SEM, n=3-5. $p < 0.05$, *vs NFC; # vs non-infarct.

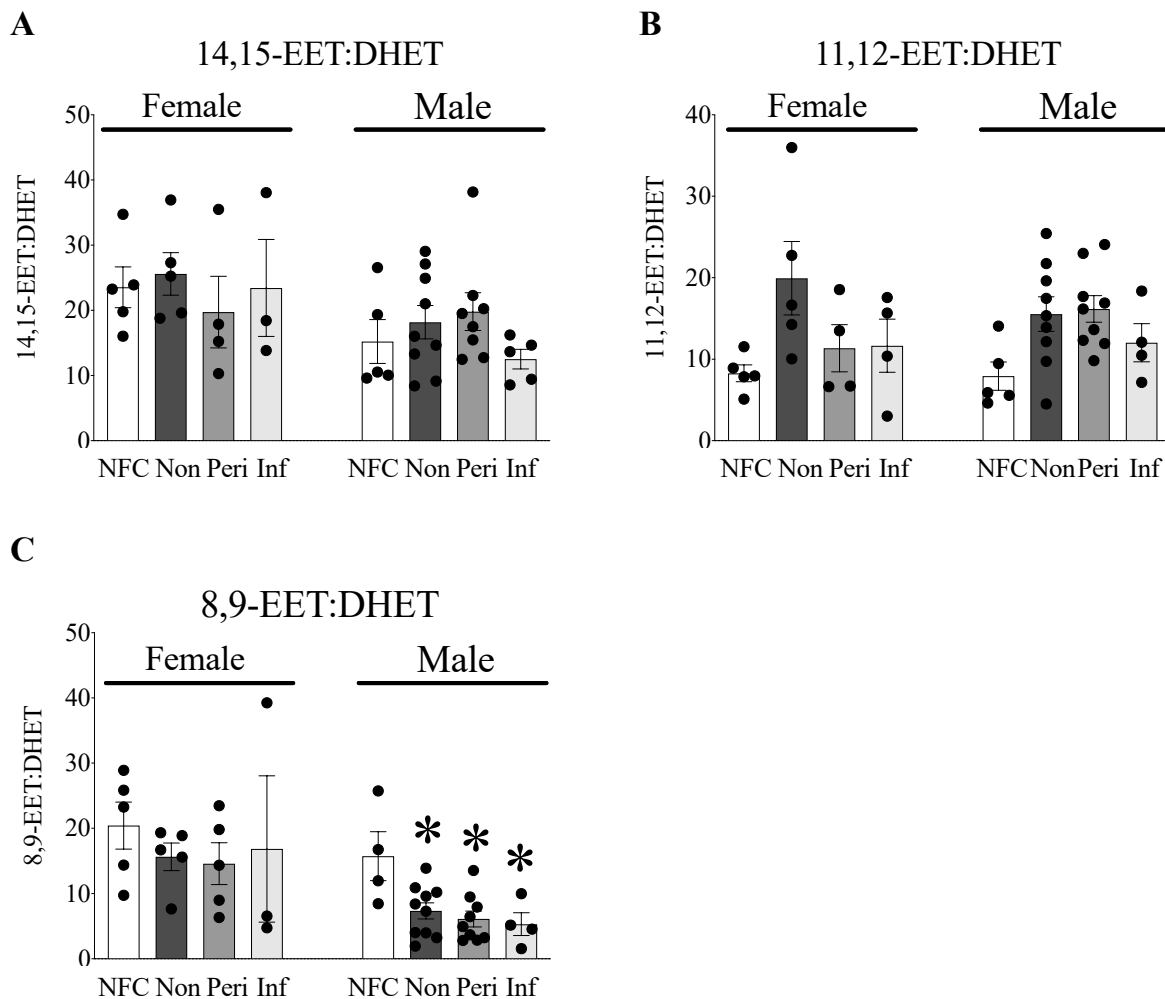


FIGURE 3.3.7. Epoxygenase oxylipid metabolites (ng/g tissue) of arachidonic acid in human left ventricular tissue measured by LC-MS/MS. A) 14,15-EET:DHET ratios, B) 11,12-EET:DHET ratios, C) 8,9-EET:DHET ratios. Data are shown as mean \pm SEM, $n=3-5$. $p < 0.05$. * vs NFC.

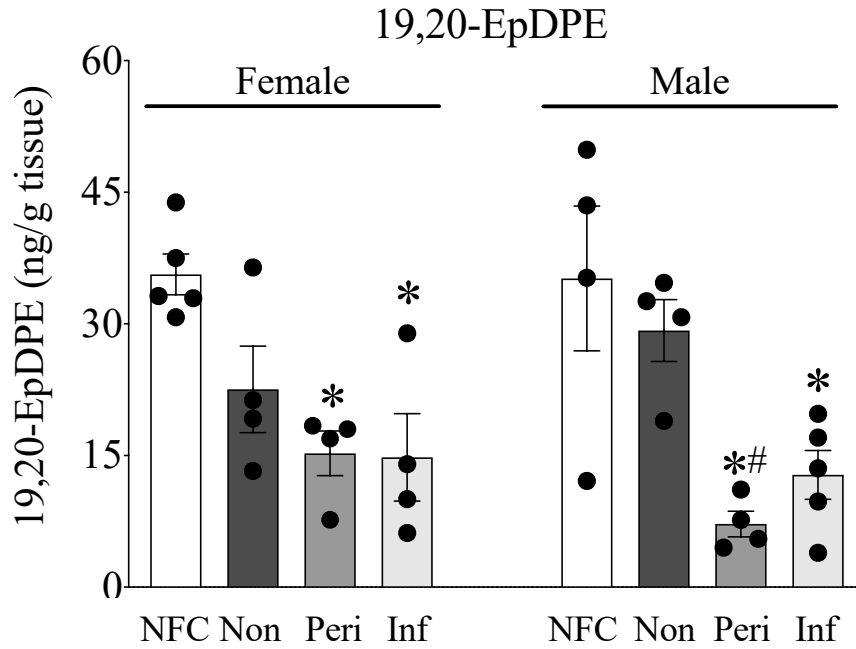


FIGURE 3.3.8. DHA oxylipid metabolite EpDPE (ng/g tissue) in human left ventricular tissue measured by LC-MS/MS. Data are shown as mean \pm SEM, n=3-5. $p < 0.05$, * vs NFC; # vs non-infarct.

3.3.5 *Human LV demonstrates loss of mitochondrial ultrastructure and organization*

There were no significant changes in MFN-1, MFN-2 or OPA1 protein expression in mitochondrial fractions from human female (Fig. 3.3.9) or male (Fig. 3.3.10) explanted hearts. DRP1 expression was decreased in both mitochondrial (Fig. 3.3.9) and cytosolic (Fig. 3.3.9) fractions in LV tissues from females. In contrast, no such changes in mitochondrial DRP1 expression were observed in male tissues and reduction in cytosolic DRP1 expression was observed only in infarct regions (Fig. 3.3.10). Mitochondria and SR networks are essential in mediating Ca^{2+} loading, necessary for muscular contraction, lipid exchange and organelle dynamics[598]. Tethering of the mitochondria and SR is done primarily through MFN-2[597]. Much of the research into the role of MFN-2 has used either knockout models or whole-cell lysates and thus not differentiated between mitochondrial and SR/ER fractions. Here, using differential centrifugation we separated tissue lysates into mitochondrial and microsomal (SR/ER) fractions. In contrast to the results observed in the mitochondria, microsomal fractions from human LV demonstrated a significant increase in MFN-2 expression in female hearts with ICM (Fig. 3.3.9), an effect not observed in male hearts (Fig. 3.3.10). Electron micrographs of LV tissue demonstrate loss of mitochondrial ultrastructure and organization in non-infarct regions from ICM hearts compared to NFC hearts in both females and males (Fig. 3.3.11).

Female

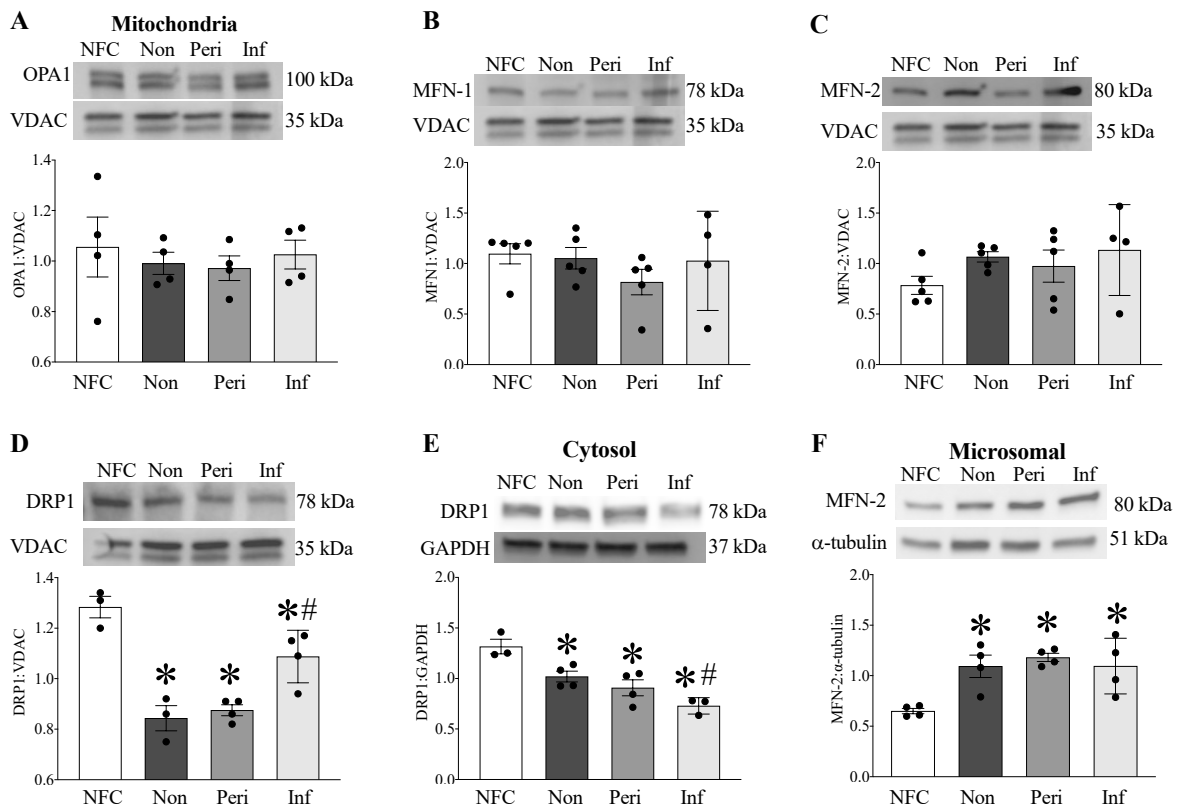


FIGURE 3.3.9. Protein expression in mitochondrial and microsomal fractions in female (A-F) NFC and ICM human hearts. Mitochondrial (A) MFN-1, (B) MFN-2, (C) OPA1, and (D) DRP-1 expression and representative blots normalized to VDAC. Cytosolic DRP-1 (E) normalized to GAPDH. Microsomal (F) MFN-2 normalized to α -tubulin. Data are represented as mean \pm SEM, n = 3-5, p < 0.05; * vs NFC.

Male

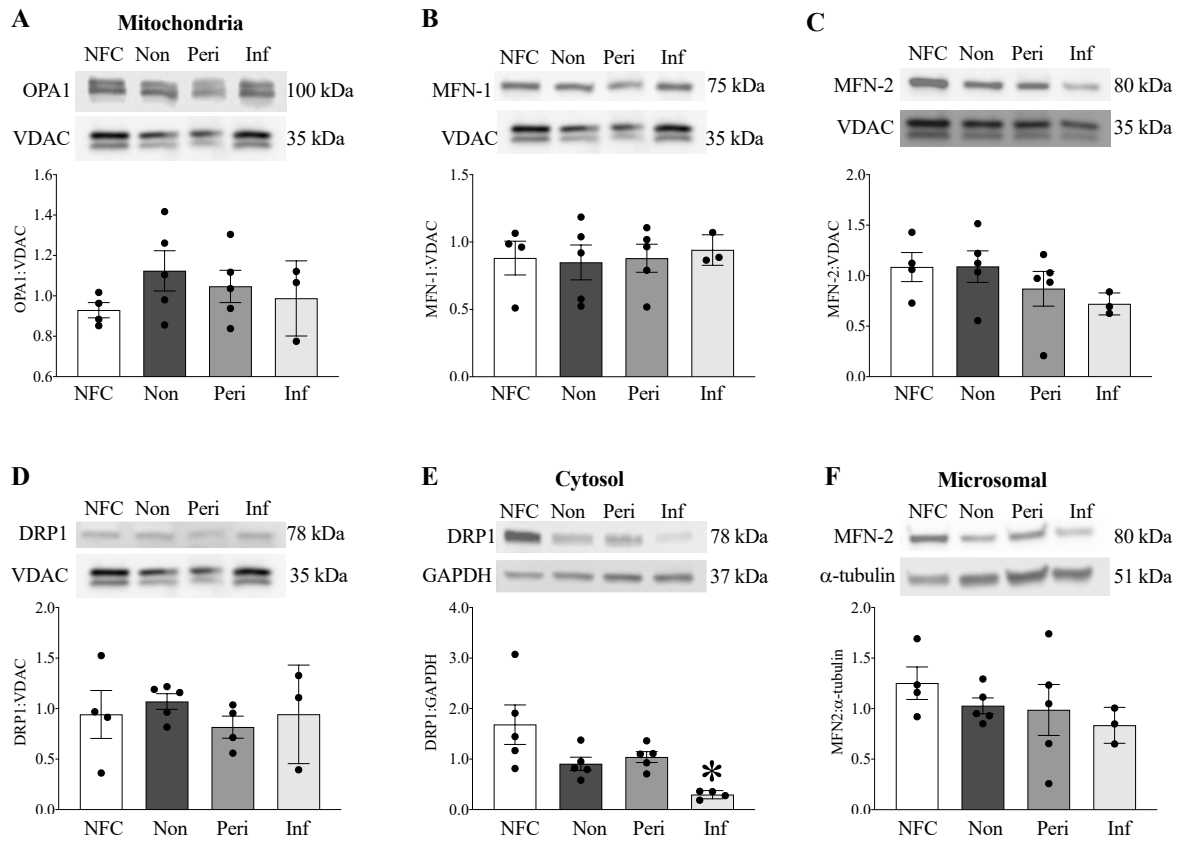


FIGURE 3.3.10. Protein expression in mitochondrial and microsomal fractions in male (A-F) NFC and ICM human hearts. Mitochondrial (A) MFN-1, (B) MFN-2, (C) OPA1, and (D) DRP-1 expression and representative blots normalized to VDAC. Cytosolic DRP-1 (E) normalized to GAPDH. Microsomal (F) MFN-2 normalized to α -tubulin. Data are represented as mean \pm SEM, n = 3-5, p < 0.05; * vs NFC.

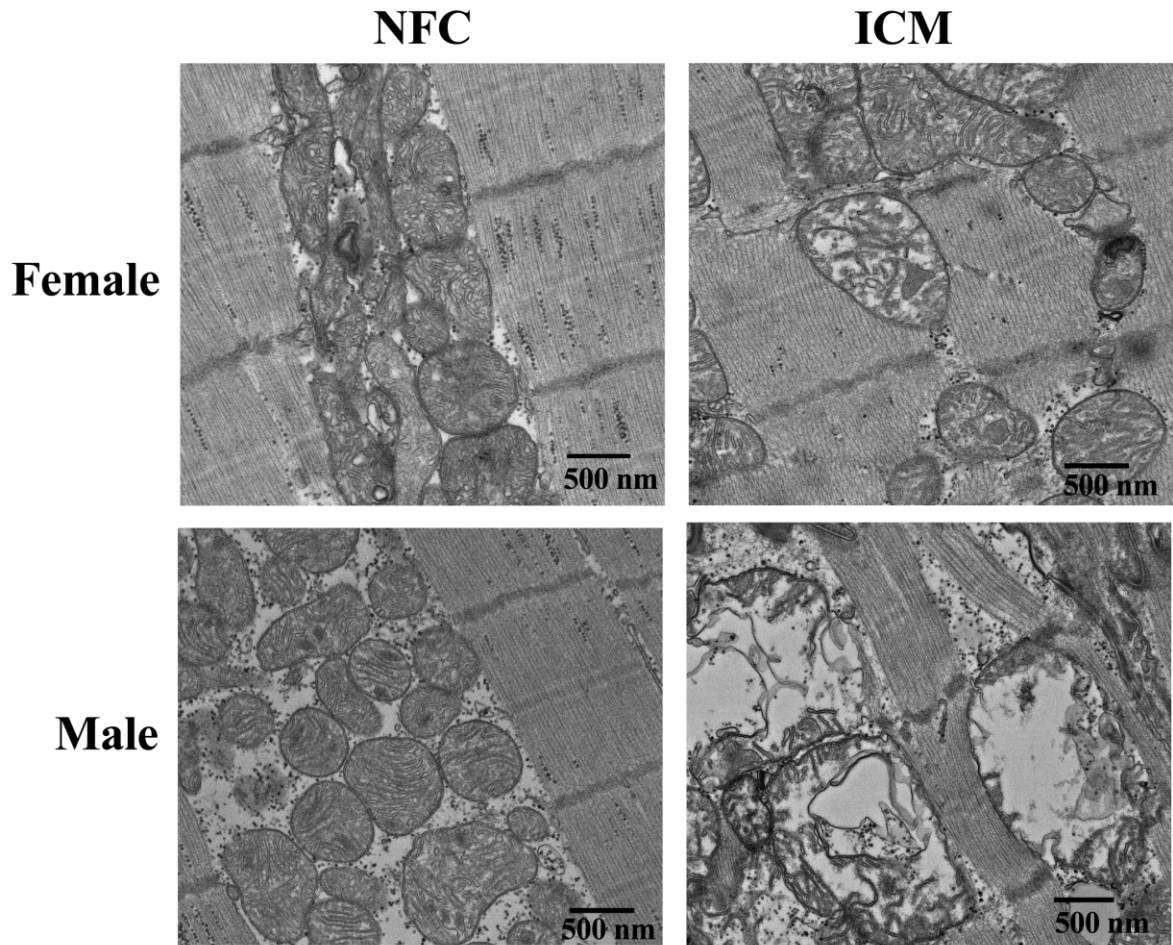


FIGURE 3.3.11. Representative transmission electron micrograph images taken from female and male NFC and ICM human hearts. Magnification set at 10000X.

3.3.6 *Conclusions*

The aim of the present section was to characterize oxylipid metabolism in human hearts from NFC or ICM males and females. We demonstrate significant increases in epoxide hydrolase expression in both sexes, with a more robust response observed in the peri-infarct region of females. These changes in expression correlate with fundamental shifts in oxylipid metabolism, notably increased DiHOME metabolite accumulation in the myocardium. Finally, these changes are associated with disrupted mitochondrial ultrastructure in ICM patients, accompanied by decreased mitochondrial function through the ETC.

Chapter 4

DISCUSSION AND CONCLUSIONS

⁴The discussion below is expanded and adapted from:

Jamieson KL, Samokhvalov V, Akhnokh M, Lee K, Cho WJ, Takawale A, et al. Genetic Deletion of Soluble Epoxide Hydrolase Provides Cardioprotective Responses Following Myocardial Infarction in Aged Mice. *Prostaglandins Other Lipid Mediat.* 2017;132(47-58)

And: Jamieson KL, Darwesh AM, Sosnowski DK, Zhang H, Shah S, Wang W, Zhabyeyev P, Yang J, Hammock B, Edin ML, et al. Sexual Dimorphic Responses to Myocardial Infarction Following Inhibition of Soluble Epoxide Hydrolase in Aged Mice and Human Explanted Hearts. Submitted to JMCC, April 2020

CVD is the second-leading cause of death for Canadians, for which IHD accounts for a significant portion of morbidity and mortality observed in these individuals. While mortality from both MI and subsequent HF has declined, the clinical and financial burden remains significant [604]. Numerous risk factors such as smoking, obesity and genetics contribute to adverse outcomes; however, the importance of age-related contributions to IHD are often overlooked [605, 606]. The natural decline in cardiac function occurs progressively in the absence of comorbid medical conditions as individuals age. At the cellular level, aged hearts demonstrate decreased myocyte cell counts, impaired endothelial function, enhanced fibroblast proliferation and increased collagen matrix [606]. At the macroscopic level, aged individuals exhibit increased epicardial fat [607], increased coronary artery calcification [608], and increased left ventricular thickness [605]. Together these changes contribute to a generalized decrease in systolic and diastolic cardiac function that reduces the myocardial capability to respond to stress. The rate and progression of cellular aging can vary between individuals and species but ultimately affects every cell in the organism. Accumulation of damaged mitochondria is an overarching mechanism associated with mammalian aging, which can increase an organ's susceptibility to injury [609]. Importantly, sexual dimorphism in mitochondrial function occurs in healthy myocardium, yet data suggest it is more apparent following injury wherein females exhibit greater CV protection [471, 474, 475, 610].

It is well-characterized males and females demonstrate fundamental sex differences in cardiovascular aging that alter the lifetime risk for MI [611]. Females demonstrate differential age-related cardiovascular remodelling compared to males, resulting in a greater propensity for the development of age-related diastolic dysfunction [611]. Conversely, males show a steeper decline in systolic function over aging [612]. Females also have unique risk

factors for IHD that require consideration. Menopause occurs on average around age 51 in the western world and increases the risk of IHD to that of males or even exceeding it [613, 614]. Pre-menopausal women are at lower risk for MI in part due to improved vascular perfusion, which is at least partially mediated through the levels of estrogens that flux throughout the normal estrus cycle [439]. Other unique factors include pregnancy-related conditions such as eclampsia[615] and the development of gestational diabetes[616]. However, the higher risk profile for males has led to an underestimation of the number of women at risk for MI, and contributed to poor physician recognition of their symptoms [617]. While females are less likely to experience MI than males, middle-aged women experience worse prognosis compared to their male peers, include a higher rate of mortality within the first year [438, 446, 448, 617]. Comorbidities or physician bias are unable to fully account for this difference, indicating an underlying risk for middle-aged women that remains to be solved. However, mortality rates are not due to the effects of gender and sex alone. For instance, race/ethnicity/nationality, lower socioeconomic status and lower education levels also affect risk for MI-related mortality amongst women [438]. Nonetheless, effectively targeting and treating this population requires a fundamental understanding of the differences in principal cardiac biology. The research described in this dissertation add to the understanding of how age-related changes contribute to decreased cardiac function and reduced capacity to respond to stress observed in aged individuals. Of key consideration has been targeting metabolism of essential fatty acids, LA and AA, through inhibition of the enzyme sEH. Finally, we assess potential sex differences using a murine model of chronic LAD ligation.

In Chapter 3.1 we report that sEH deletion preserves cardiac function and mitochondrial bioenergetics in young and aged mice following MI. Post-MI aged sEH null mice demonstrated sustained systolic and diastolic function, maintained mitochondrial bioenergetics and attenuated markers of injury compared to age-matched WT animals. Interestingly, the protection associated with sEH deletion in aged mice was markedly reduced compared to young animals, highlighting detrimental consequences of biological ageing on cardiac function.

The study described in Chapter 3.2 was a continuation of the previous study in aged mice, assessing effects of both sEH deletion and sEH inhibition with sEHi *tAUCB* in a chronic LAD ligation model. We demonstrate a sexual dimorphic response to sEH inhibition whereby cardioprotection was observed in female but not male mice. Interestingly, the cardioprotective effects of our sEHi appears to be dependent on when the drug was administered, with pre-treatment yielding a stronger cardioprotective response. Finally, in Chapter 3.3 we sought to characterize key pathways involved in N-3 and N-6 metabolism in and NFC and ICM human explanted hearts. Human hearts demonstrated significantly altered metabolism coupled with increased expression of sEH and correlating with damaged mitochondria. Together with Chapter 3.2, these data provide strong evidence that inhibiting sEH is a potential viable therapeutic target for middle-aged women.

4.1. Age-related changes in cardioprotective effects arising from sEH genetic deletion

Our study in young and aged mice demonstrated similar systolic and diastolic changes in both WT and sEH null mice 16 months old, an age comparable to approximately 55 human years [574]. Declining cardiac function observed in murine models of ageing is well

documented, characterized by decreased EF and FS, increased left ventricular internal diameters, increased myocardial stiffness and increased wall thickness [618, 619]. In the absence of disease and morbidities, the cardiovascular system has compensatory responses that limit drastic functional changes in the ageing heart; however, as individuals age they become more susceptible to adverse outcomes following injury or disease, in part due to a reduced ability to manage a response [618, 620]. Myocardial infarction is a severe injury, marked by substantial cell death, inflammation and subsequent cardiac remodelling that can eventually progress to heart failure [621]. Consistent with previous studies, the LAD ligation model in this study resulted in a significant infarct in all animals [622]. EM images taken in non-infarct regions showed disorderly, rounded mitochondria with diffuse cristae in aged hearts compared to young counterparts of either genotype, a common hallmark of age [623, 624]. Images taken from the infarct region exhibit damage in both sEH null and WT mitochondria, which was expected using a permanent LAD ligation model. However, sEH null mice at both ages demonstrated some level of maintained mitochondrial ultrastructure, indicating cardiac protection.

In this initial comparison between young and aged mice, there was no significant change in baseline sEH protein expression or activity in aged WT hearts compared to young cohorts [326]. However, this study failed to account for sex differences; recently we demonstrated that sEH expression in fact increases in males, but not females over natural aging [625]. Indeed, increased sEH activity found in various disease models has been thought to contribute to deleterious consequences post-injury, such as increased inflammation and cell death [626, 627]. The significant increase in 14,15-DHET levels observed in young post-MI WT mice suggests a similar post-injury increase in sEH activity, which conceivably

contributes to extensive damage seen in young WT mice [25]. However, post-MI 14,15-DHET levels did not increase in the aged WT hearts. Both aged WT and sEH null sham mice demonstrated an increase in mEH expression compared to young, which may account for the higher than expected 14,15-DHET expression seen in sEH null mice at either age, since mEH does metabolize EETs [588]. mEH is known to effect oxylipid metabolism post-MI, and recent studies suggest inhibiting both mEH and sEH may be more successful in mediating ischemic injury than sEH alone [601].

Prolonged ischemia results in both necrotic and apoptotic cell death throughout the myocardium. Myocardial apoptosis has been shown to increase shortly after MI in both the infarcted and non-infarcted regions of the heart [628]. 20S proteasome activity is involved in regulating the cell death cascades through the cleavage of pro-death proteins and removal of proteins damaged by oxidative stress, mutation or misfolding [629]. However, excessive activation of 20S proteasome is detrimental to survival, as evidence demonstrates proteasome inhibitors have cardioprotective properties in murine models of acute myocardial ischemic injury [630]. We observed increases in both caspase-3 and the 20S proteasome post-MI in both young and aged WT mice, suggesting increased injury and activation of cell death pathways. Importantly, the sEH deletion significantly attenuated the increases in both age groups, supporting the cardioprotective effect toward MI injury throughout aging.

Cardiac function relies heavily on mitochondrial oxidative phosphorylation and the ETC to meet the ATP supply of the demanding myocardium. Aconitase, a key enzyme in the citric acid cycle, has an important role in mitochondrial function and serves as a biomarker for mitochondrial oxidative stress and function. Age-related decreases in aconitase activity and increased oxidative stress have been shown in murine models [631]. We also observed

decreased aconitase activity in WT hearts attenuated in sEH null mice, suggesting preserved mitochondrial function, and supported by the marked decrease in mitochondrial respiration in WT compared to sEH null animals. Efficient respiration relies on efficient enzymatic activity of the ETC complexes; decreased respiratory efficiency contributes to an overall age-related decline in cardiac function [632]. Our results are consistent with previous work demonstrating little change in cardiac mitochondrial protein expression with increased age but a decline in mitochondrial enzyme activity [633]. Several studies have documented age-dependent impairment of mitochondrial function, mainly in the decline in mitochondrial respiratory capacity (state 3) due to diminished activity of complexes I and IV, but relatively unaltered complexes II and III [634]. The slower rate of mitochondrial electron transfer with age favors mitochondrial superoxide production, leading to a negative feedback between complex I inhibition and accumulation of cellular injury. Complex I directly regulates the production of ATP via the ETC and a reductive capacity by the oxidation of NADH [635]. An appropriate equilibrium between the oxidized and reduced forms of NADH is required to sustain glycolysis [636]. This is due to the fact that NAD⁺ is needed to oxidize glyceraldehyde-3-phosphate to 1,3-biphosphoglycerate, an essential step in the oxidation of glucose to obtain energy. When NAD⁺ is not available, glycolysis is blocked and both glyceraldehyde-3-phosphate and dihydroxyacetone accumulate, which can further exacerbate mitochondrial dysfunction [637, 638]. Mitochondrial dysfunction is considered a primary contributing factor to ageing and associated morbidities, including cardiovascular pathology [634]. Despite an age-related decrease in mitochondrial enzymatic activity, aged sEH null animals had preserved mitochondrial respiration. This suggests sEH deletion

maintains mitochondrial bioenergetics through a protective mechanism not wholly dependent on the regulation of mitochondrial enzymatic activity.

The high energy demand required to maintain cardiac function dictates the cell to utilize a variety of substrates, including free fatty acids, glucose and amino acids, for the production of ATP [635]. Cardiac function is also highly dependent on the constant delivery of oxygen; disruption of these processes by ischemic injury causes profound disturbances in myocardial metabolism. During ischemia, the lack of blood flow and decreased oxygen levels results in the loss of ATP production and the accumulation of toxic metabolites such as lactate [639]. Comparative metabolomics has demonstrated the accumulation of adverse metabolites during myocardial injury. Products from the purine degradation pathway, as well as the TCA intermediate and complex II substrate succinate were commonly identified [640]. Hochachka et al first demonstrated elevations in succinate occurred during anaerobiosis in diving mammals [636]. The build-up of succinate from ischemic injury has been observed in experiments using rabbit papillary muscles, cardiomyocytes and in the isolated mouse heart [641-643]. Succinate accumulation is considered an important marker of myocardial damage, but the exact role of succinate and the physiological basis behind the accumulation remain unknown [639, 642]. Here we report robust activation of succinate oxidation in post-MI aged WT mice that is not accompanied by an increase in ATP production. Evidence suggests succinate served as an extra-glycolytic source for energy in situations of low nutrient and oxygen availability, therefore increasing tolerance to long-term anaerobiosis [636]. The mechanism underlying the increase might include decreased mitochondrial function or direct injury of mitochondrial structures that are vulnerable to stress factors [644]. For instance, accumulation of succinate occurs in damaged myocardium as a result of I/R

injury. Intensive oxidation of accumulated succinate has been well documented to produce multiple deleterious consequences in the exposed myocardium [642]. An increase in succinate oxidation post-MI in aged WT mice thus provides strong evidence of overall compromised mitochondrial function. Remarkably, this deleterious effect of succinate oxidation was blunted in sEH null mice suggesting a crucial role of sEH in negative regulation of mitochondrial function. Previously we demonstrated that genetic and pharmacological suppression of sEH limits mitochondrial damage, which appears to be an inherent part of the cardioprotective mechanism(s). Interestingly, this change was only observed in the aged mice following ischemic injury.

Our clinically-relevant murine ageing model demonstrated multiple differences compared to younger counterparts. Even in the absence of injury, aged mice demonstrated significant changes to function and energetics of both the heart and mitochondria. The overall decline in baseline cardiac function determined in this study is well-documented in other aged murine models [618, 619]. Furthermore, cardiac aging resulted in overall increased levels of cellular stress biomarkers, as well as lower mitochondrial enzymatic activity, RCR, ATP levels, and changes in mitochondrial ultrastructure. These changes are recapitulated throughout the literature [623, 630, 631, 632]. Interestingly, in some cases aged mice post-MI did not show the same deleterious effects compared to their respective shams as did their young counterparts. For instance, young WT post-MI mice demonstrated a marked decrease in complex II enzymatic activity, however aged WT post-MI mice demonstrated no significant change. These unexpected discrepancies are likely because of general cardiac compensation over age that limits the amount of damage the heart can sustain without perishing completely [620]. Remarkably, we observed an increase in succinate oxidation in

aged WT mice post-MI not associated with improved ATP production. This seems to suggest a compensatory injurious respiratory pathway unique to aging mice; the fact that sEH null animals did not demonstrate this shift may be a protective mechanism heretofore not recognized. This is supported by the fact that while sEH null animals exhibited age-related changes similar to WT, mitochondrial bioenergetic efficiency as measured by RCR remained relatively unchanged. Our data indicate sEH deletion provides protection in both young and aged hearts; however, the consequences from natural aging hinder robust protective effects visualized in young sEH null animals post-MI.

The factors triggering and causing the decline in function during cardiovascular ageing remains unresolved. Optimally functioning mitochondria can contribute to reduced cardiac damage in different ways, including reduced oxidative damage, decreased glycolysis and normalization of oxidative metabolism, as well limiting pro-cell death pathways. We hypothesize that preserving mitochondrial function will limit the susceptibility of an aged heart to further injury [645]. We found that aged mice with the whole-body deletion of sEH had preserved primary mitochondrial function with increased efficiency of oxidative phosphorylation, which was associated with better recovery following post-MI injury. We have previously demonstrated that deletion or pharmacological inhibition of sEH protects against myocardial ischemic injury through improved mitochondrial form and function [25, 175, 192, 326]. In this continuing study, we demonstrated the protective effects are significantly reduced but still conserved in aged sEH null mice. Interestingly, the beneficial effects on cardiac function arising from sEH deletion impact baseline function and are more robust in young animals.

The initial study described here had several important limitations and considerations. In previous studies in young animals, there were no differences between males and females post-LAD ligation [175]. Therefore, the young and aged cohorts utilized in this study contained combined males and females. However, the data described in Chapter 3.2 demonstrate clear and previously uncharacterized sex differences in cardiac responses. This is supported by a recent study where we demonstrated significant changes over generalized aging in sEH null females and males compared to their WT counterparts [625]. That study demonstrated female nulls are protected from decreases in systolic function observed in males [625]. Thus, some of the age-related differences observed in this preliminary *in vivo* LAD ligation study may be attributed to heretofore unrecognized sex differences. Moreover, this study assessed injury 7 days post-MI and no differences in survival were noted, as all animals survived to this endpoint. Effects on survival and long-term cardiac remodelling were assessed by holding the animals for 28 days post-LAD ligation.

4.2. *Sexual dimorphism in cardiac responses to sEH genetic deletion or pharmacologic inhibition in a chronic LAD ligation model*

This chapter utilized a clinically relevant animal model to identify fundamental sex differences in cardioprotective ischemic responses following sEH inhibition; notably, aged female mice benefit more than aged males. The protective advantage includes preservation of both mitochondrial quality and cardiac function. We noted a compensatory increase in sEH expression in females but not males treated with sEHi *tAUCB*. This is interesting, considering we have recently demonstrated female WT mice do not demonstrate increased sEH expression over aging, unlike males [625]. While sEH inhibition is cardioprotective in

injury models, the importance of epoxide hydrolysis in removing endogenous and exogenous toxic metabolites highlights sEH as a mammalian clearance pathway [646]. mEH, present in the microsomes, also plays an important role in epoxide metabolism [601]. We demonstrated a significant increase in mEH expression in both sEH null and *tAUCB* 4-day pre-treatment peri-infarct regions, suggesting compensation to loss of sEH activity. Interestingly, inhibiting both sEH and mEH through genetic knock-out has been shown to be more effective than either alone in combating ischemic injury [601]. Future studies will need to confirm this in aged animal models.

Early research into cardioprotective effects of sEH inhibition focused on production of the CYP-derived AA metabolites, EETs [25]. However, accumulating evidence suggests LA metabolites also contribute to adverse outcomes in IHD. Previously, we demonstrated a cardioprotective response observed in young mice with cardiomyocyte overexpression of CYP2J2 is lost in aged mice, attributed to increased DiHOME levels [326]. Recently, Bannehr et al. demonstrated perfusion with 12,13-EpOME and 12,13-DiHOME reduced post-ischemic cardiac recovery in young C57Bl/6 mice but co-perfusion of 12,13-EpOME with an sEH inhibitor protected the effect, suggesting the diol is toxic [647]. Interestingly, only female CYP2J2-Tr mice treated with *tAUCB* following LAD ligation exhibited improved survival, suggesting a sexual dimorphic response and supporting the notion that targeting sEH metabolism of may be more beneficial than increasing epoxygenase activity alone.

The increased 12,13-EpOME:DiHOME and 14,15-EET:DHET ratios observed in sEH null female mice correlated with improved survival and cardioprotection, suggesting a metabolite profile including reduced DiHOMEs and increased EETs is important.

Interestingly, treatment with an sEH_i appeared to be highly dependent on when the sEH_i was administered in our aged cohorts, as the females pre-treated with *t*AUCB exhibited more substantial cardioprotection compared to the same-day sEH_i treatment. These data suggest the implementation of pharmacological inhibition has an effect on lipid availability and subsequent cardioprotection in this model of ischemic injury. These data suggest the use of *t*AUCB would be more effective as a prophylactic, however more research must be done to ensure the safety profiles of these agents if they are to be consumed over long time periods, as they may have significant off-target effects. This is crucial considering the effect of *t*AUCB treatment in males appears to be significantly worse than in females in an unknown mechanism. Ultimately, whether sEH_i's would be more effective as prophylactics for women hinges on a comprehensive risk-benefit analysis for this cohort. The dose of *t*AUCB given in the drinking water (10mg/L) was decided based on previous pharmacokinetic data from the agent's developer, Dr. Bruce Hammock [590]. This level in the drinking water ultimately results in a dose of about 0.1 mg/kg for an aged mouse that is drinking normally. The IC₅₀ for *t*AUCB is 0.5 nM; blood concentrations as measured in plasma exceeded this range. However, it is well-established sEH levels are higher in males [625] and it may be that effective inhibition in aged male mice requires either a higher dose of sEH_i or perhaps a dose administered earlier than four days prior to the injury. However, considering the fact that the mortality in the treatment group was worse than the WT group alone, increasing the dose may increase the mortality in males, which would be counterproductive. Ultimately, more research into a mechanism behind these effects is necessary before any firm conclusions can be determined. While data regarding the co-regulatory effects of mEH and sEH over metabolite profiles involved in cardioprotective responses is limited, the increased

expression of mEH detected in *tAUCB*-treated hearts potentially accounts for the reduced protection observed in these groups. Moreover, these results are consistent with an important metabolic role for epoxide hydrolases [601]. The timing and balance of different lipid mediators such as DiHOMEs and EETs can markedly influence how a heart responds to ischemic injury.

Mitochondria are fundamental facilitators of myocardial energy production and cell death pathways, as such maintaining a healthy pool is essential to ensure proper heart function. Cellular quality control processes will adjust over a lifespan to accommodate cardiac growth and meet energetic needs [599]. Importantly, dysfunctional processes leading to decreased removal of damaged mitochondria or limited biogenesis of mitochondria are associated with adverse cardiac outcomes [648]. No differences were observed in the expression of proteins involved in regulating mitochondrial dynamics in age-matched WT mice despite these mice having significantly reduced cardiac function. Due to their critical role in inner mitochondrial membrane and cristae structure [648], the increased expression of mitochondrial dynamic proteins MFN-1/2 and OPA1 observed in sEH null or *tAUCB* treated female mice suggests better mitochondrial quality in these groups. These results are consistent with published data demonstrating sEH inhibition is associated with preserved mitochondrial quality in models of IR injury and that oxylipids can regulate OPA1-dependent responses [174, 182]. In contrast, diols like 12,13-DiHOME have been shown to decrease mitochondrial function in cardiomyocytes, potentially causing decreased cardiac function [649]. Improved mitochondrial integrity can promote better cellular function including tethering of mitochondria with ER, which can facilitate inter-organelle communication, leading to better calcium handling [650]. Interestingly, differences in ECG

parameters, QRS duration and PR interval, observed in sEH null or *tAUCB* treated female mice support the notion of better calcium handling following LAD injury. Additionally, the increased levels of anti-arrhythmic 17,18-EEQ observed in female mice may contribute to these protective effects [593]. Importantly, mitochondrial preservation in sEH null or *tAUCB* treated female mice paralleled the improved survival rates, shifts in oxylipid metabolism and attenuation of cardiac dysfunction, which were consistent with other studies of ischemic injury [170, 174, 649, 651]. Taken together, these data support the hypothesis that alterations in the oxylipid profile, notably an increased availability of beneficial oxylipids and decreased level of detrimental diols, favours improved mitochondrial quality leading to better post-ischemic cardiac function.

While sex differences in sEH expression and activity have been reported in various tissues, including the heart, few studies have assessed these differences in aged models. We have recently demonstrated fundamental differences between sEH null males and females over natural aging that are associated with alterations in mitochondrial oxidative stress responses [625]. Moreover, evidence demonstrates sEH gene deletion provides protection in aged female mice following cerebral ischemia [452]. While no mechanisms have been identified, differences potentially involve epigenetic methylation of *Ephx2* by estrogen signalling mediated through the estrogen receptors [457]. Our data report robust sex differences in response to cardiac ischemia in aged mice with sEH genetic deletion or pharmacologic inhibition. Intriguingly, the cardioprotective response observed in aged sEH null or *tAUCB* treated female mice in this study was largely absent in males. There is limited evidence in the literature of reported sex differences for cardiovascular outcomes, however, Hutchens et. al. demonstrated young sEH null male mice had worse recovery compared to

WT in a model of cardio-resuscitation [652]. Differences in EET-mediated effects on the vasculature were also reported although the molecular mechanism remains unknown [652]. The effects observed in our current study suggest sexually dimorphic changes that occur during aging have a critical role. Ultimately, further studies are needed to fully address the mechanisms observed in this study. The data presented in this chapter corroborate a growing body of work supporting the need for sex-specific research.

4.3. *Characterization of human explanted myocardium*

In Chapter 3.3 we characterized N-3 and N-6 PUFA metabolism in human explanted hearts obtained from NFC and ICM individuals, demonstrating key differences in sEH expression and metabolite profiles. While animal models demonstrate the role of sEH in mediating development and progression of CVD, data are limited regarding the role of altered CYP-derived oxylipid metabolism in humans [180, 646]. Population analyses suggest genetic variation in the *EPHX2* gene is associated with the development of IHD [412, 653], but sEH expression is tissue-dependent and assessment in myocardial biopsies is relatively rare [646]. Theken et al. demonstrated increased epoxygenase metabolites in human plasma in patients with stable coronary artery disease [281]. Interestingly, they noted increased ratio of epoxide:diol metabolite ratios, however plasma levels are not necessary indicative of tissue levels available to work directly within the myocyte [281]. Here, we characterized myocardial specimens from patients with ischemic heart failure, which demonstrated increased sEH and mEH expression in myocardium compared to NFCs. Importantly, we noted limited shifts in epoxide:diol ratios. However, we demonstrate DiHOME levels

markedly increased in human myocardium obtained from ICM tissues. This novel finding supports animal data suggesting a maladaptive role for DiHOME accumulation in IHD.

Consistent with literature, we demonstrate significantly reduced activity of key enzymes in the ETC in humans with ICM, not associated with changes in protein expression [654, 655]. There are discrepancies in the literature regarding which ETC enzyme contributes the most to the reduction in OXPHOS observed; most studies indicate a role for complexes I, III and IV [655]. However, many of these studies relied on one ventricular sample to represent the entirety of the infarcted heart. We used three samples across the infarcted myocardium, providing a greater understanding of how energy production through ETC changes according to the proximity to the infarct region. The data from human patients outlined in Chapter 3.3 adds to a growing body of work acknowledging sex-specific tissue characterization is clinically relevant. The lack of data regarding age and particularly sex interactions in ischemic injury leaves a “knowledge-gap” that needs to be addressed in pharmaceutical research.

There are several important challenges to consider when extrapolating the animal studies to the human data described in this thesis. For example, in contrast to the animal data, no changes were observed in the expression of proteins involved in regulating mitochondrial dynamics from either male or female human ICM hearts [656]. The discrepancy we observed between human and mouse could be a result of species differences. Humans with MI often present with CAD or other morbidities that are not represented in the mouse model. While mice exhibit similar cardiac aging patterns to man, unlike humans mice do not spontaneously develop hypertension or unfavourable lipid profiles over normal aging [657]. Other lifestyle factors that contribute to MI risk in humans, such as smoking and physical inactivity, are

understandably not easily replicable in mice. Furthermore, the permanent LAD model is an extreme injury that results in complete and severe coronary occlusion. For humans, this level of occlusion often results in death before intervention can be achieved (the so-called “widow-maker”). Importantly, while mice can survive this injury, they do not experience the treatment interventions that individuals who survive the initial ischemic event will undergo. Thus, care must be taken when comparing mouse models using permanent LAD occlusion to humans with life-long development of CAD that ultimately drives MI.

4.4. *Final Conclusions*

Fatty acids are essential components of the body that help maintain normal physiological function and facilitate protective responses to pathological stimuli. Our understanding of the diverse physiological and pathophysiological roles that CYP-dependent metabolites of n-3 and n-6 PUFA have in the cardiovascular system continues to expand. Many genetic and environmental factors alter CYP expression resulting in significant changes in the production or removal of bioactive products. Together with small changes in the dietary intake of fatty acids, significant changes in biological activities can have a significant impact on cardiac function as well cardiac dysfunction. Further confounding factors include aging, sex and the prevalence of co-morbidities.

The studies described in this dissertation demonstrate that targeting sEH through genetic deletion or through pharmacologic inhibition with *t*AUCB preserves cardiac function in aged mice. This effect was more robust in females, associated with improvements in mitochondrial function. Additionally, we used human NFC and ICM explanted hearts to

characterize oxylipid metabolite levels and epoxide hydrolase expression in human ischemic myocardia.

1. Initially, we demonstrated genetic deletion of sEH preserves systolic cardiac function in both young and aged mice. Both sEH null and WT mice demonstrated a generalized age-related decline in cardiac function over aging, associated with decreased overall in mitochondrial enzymatic activity. However, in each case sEH null mice exhibited improved mitochondrial respiration post-MI, suggesting a blunted, but not eliminated, level of cardiac protection. However, this model used middle-aged mice with combined sexes.
2. Subsequently, using a chronic model of myocardial infarction we demonstrated there is apparent sexual dimorphism in cardiac responses to sEH deletion or inhibition post-MO, a heretofore unrecognized finding. Genetic deletion or pharmacologic inhibition of sEH preserves cardiac function over 28 days post-MI in aged female, but not male mice. This protection was associated with improved mitochondrial dynamic protein expression in females. Importantly, the functional data suggest a differential effect between timing of *tAUCB* treatments, with pre-treatment improving functional parameters more than same-day treatment. These data suggest both sEH and mEH may play a role in mediating injury in this model.
3. Human explanted hearts from ICM patients demonstrate significant changes in oxylipid metabolite formation compared to controls. These changes, particularly a significant increase in DiHOMEs, are associated with decreased mitochondrial function and loss of mitochondrial ultrastructure in these hearts. Together, these data

suggest sEH is a viable target for treatment of ischemia in aged hearts. Moreover, our data suggest it may be more effective in aged females rather than males.

Chapter 5

FUTURE DIRECTIONS

5.1. *Mechanisms of sexual dimorphism following myocardial infarction in mice with genetic deletion or pharmacologic inhibition of sEH*

Robust sex differences in response to sEH genetic deletion or pharmacologic inhibition were an unexpected result reported in this dissertation. Female mice demonstrated differentially affected survival rates, cardiac function and cardiac mitochondrial function post-MI. We recently demonstrated changes over natural aging are associated with improvements in mitochondrial oxidative stress responses in sEH null females but not males or WT animals [625]. These data suggest female sEH null mice may have an existing advantage over natural aging, potentially affecting longer term cardiac outcomes following ischemic injury. However, mechanism(s) behind the effects observed in these studies has remained elusive and is an essential focus for future research.

We have thoroughly discussed potential mechanisms of oxylipid-mediated cardioprotection in the introduction to this dissertation, as such this section will focus on potential mechanisms that exhibit some degree of sex-specific regulation. Investigation into sexual dimorphic responses in any system generally involves assessing the role of sex steroid signalling; indeed, sex steroids have well-established regulatory effects over cardiovascular pathophysiology [658]. The main sex steroid assessed in female systems is undoubtedly 17 β -estradiol (estrogen, E2), and E2 signalling interplays with oxylipid metabolic pathways [458]. For example, in the presence of endothelial dysfunction, E2 potentiates EET vascular release through upregulating CYP450 epoxygenases via PI3K/AKT pathways [659]. PI3K signalling was identified as a potential target of oxylipids and is upregulated post-ischemia in sEH null mice [25], while *in vitro* its upregulation is associated with preventing cardiomyocyte apoptosis following hypoxia/reoxygenation [208]. Moreover, PI3K α

signalling has been linked to activation of K_{ATP} channels and subsequent cardioprotection from ischemia [23]. It is still unknown whether oxylipids affect K_{ATP} channels directly or indirectly through downstream PI3K signalling. These pathways have also been linked to E2 signalling. ER β can activate cardioprotective PI3K/AKT signalling [660], while disrupting the K_{ATP} subunit in female mice reduces the female advantage following IRI [661]. It is feasible that sEH deletion/inhibition alters the oxylipid metabolite profile in a manner that acts synergistically with E2 signalling, ultimately promoting the cardioprotective effects observed in females. Future studies in both aged and young animal models are required for validation.

A fundamental consideration of this dissertation has been the effect of oxylipid metabolism on mitochondrial form and function. Due their role in energy production and cell life/death pathways, mitochondria are often key effectors of sex steroids [662-664]. PGC-1 α acts through multiple signalling pathways to regulate mitochondrial biogenesis and oxidative stress [665]. Importantly, it appears to have a role in reducing oxidative stress through upregulating key antioxidant gene expression and activity, including superoxide dismutase 2 (SOD2) and Sirtuin-3 (SIRT3) [665]. In our previous aging study, we demonstrated aged sEH null females exhibit preserved cardiac function and mitochondrial form associated with conserved levels of SOD2 and Sirt3 [625]. Moreover, in their obese mouse model Liu et. al. demonstrated treatment with sEHi AUDA correlated with increased PGC-1 α activation and cardioprotection [666]. They additionally demonstrated increased mitofusin expression in sEHi-treated mice, a similar effect to what we observed with our chronic LAD [666]. While evidence in ischemic models is limited, E2 appears to stimulate mitochondrial biogenesis through PGC-1 α in models of non-ischemic cardiomyopathy, resulting in cardiac

preservation [667]. Thus, the cardioprotection observed in our female mice with sEH deletion or sEHi treatment may involve augmented oxylipid signalling which, coupled with preserved E2 in aged female mice, works to synergistically promote PGC-1 α signalling and subsequently conserve downstream mitochondrial function.

However, neither of these mechanisms would explain why young females, with normal E2 levels and no age-related cardiac dysfunction, exhibit no differences upon sEH inhibition or deletion with ischemia or IR compared to young males. This suggests these sexual dimorphic effects are age-dependent. It may be more relevant to decipher why males lose cardioprotection arising from sEH deletion or inhibition over aging. Aged CYP2J2-Tr mice exhibit significant alterations in DiHOME levels correlating to worse recovery upon IR, suggesting aging significantly affects the accumulation or release of these metabolites [326]. Moreover, male sEH null mice do not demonstrate preserved oxidative stress responses over aging as females do [625]. Ultimately, clarifying how oxylipid release, storage and metabolism changes over aging and how these alterations interact or interfere with other signalling pathways including sex steroid signalling is key to deciphering the sexual dimorphism observed in this study. However, the intersectional nature of age, sex and genotype makes it unlikely that the observed outcomes are mediated through one single pathway. Oxylipid metabolism involves many metabolites which have multitudinous, conflicting and compensatory effects. Regardless, understanding why aged females are more receptive to sEH deletion or inhibition following ischemia is important for translating research into humans and for creating more targeted pharmaceuticals.

5.2. Use of alternative transgenic lines to assess oxylipid metabolism in ischemia

The data outlined in Chapter 3.2 describes the use of sEH genetic knock-out mice. However, emerging data supports the role of mEH, previously investigated for its role in xenobiotic metabolism, as an important metaboliser of fatty acids [588, 601]. Our data show mEH is upregulated sEH inhibition in females at 28 days post-MI, perhaps as compensation. Interestingly, Edin et al. demonstrated that sEH and mEH double-knockout is more effective at combatting IRI than sEH knock-out alone [601]. This effect, similar to what we have observed in young sEH null mice [459], was sex-independent [601]. However, we observed sexual dimorphism in *in vivo* ischemic response only upon aging, and age-related changes in mEH null mice have not been investigated. Considering that we also observed increased mEH in human myocardium from ICM patients (Chapter 3.3) and that human mEH inhibitors are currently being developed [668], assessing age-related changes in both a single mEH knock-out and double sEH/mEH knock-out may give important information about the co-regulatory roles of these enzymes in oxylipid metabolism following ischemic injury throughout aging.

One of the most interesting findings was the total mortality observed in the CYP2J2-Tr line in response to ischemia. In the CYP2J2-Tr line, only aged females demonstrated improved survival post-MI with treatment of sEHi, however this experimental line had to be discontinued before robust analysis could be performed. We have previously demonstrated adverse responses upon IRI in aged mice correlate with increased DiHOME levels [326]. DiHOMEs have been suggested as a treatment for metabolic disorders [669, 670], however our cardiac data suggest accumulation of DiHOMEs is cardiotoxic [649]. Further use of this

transgenic line, particularly in aged males and females, may help resolve these conflicting data.

This thesis describes mitochondrial differences observed with whole-body deletion of sEH as well as treatment with the sEHi tAUCB. These mitochondrial effects may not be limited to the heart; as such, assessment of extra-cardiac organs for mitochondrial or functional changes is an important consideration. For example, sEH is a well-established target in the context of renal disease [671]. As renal function and cardiac function are interlinked, particularly following MI, assessing mitochondrial function in other organs may yield important data regarding potential off-target effects, as well as give a better picture of the whole-body changes that occur in response to this disease model.

Another investigation that would help elucidate the effects of oxylipids in myocardial infarction would be a dietary model, e.g. a linoleic acid-enriched diet, either used throughout the lifespan or starting from a set date prior to ischemic injury. Combining this dietary change with any of the genetic models discussed in this thesis or combined with the sEHi would help elucidate whether synergistic dietary changes could affect the protection observed in our mouse models, and help elucidate the effects of N6 and N3 metabolites [672].

5.3. In vivo ischemia/reperfusion injury in aged mice with deletion or inhibition of sEH and effects of inflammation

The murine injury model in this dissertation utilized a permanent model of LAD ligation. However, most humans that experience MI undergo reperfusion as a gold-standard treatment. Reperfusion injury is a significant clinical consideration that results in its own pathology, separate from the initial ischemic event [673]. sEH genetic deletion or inhibition with sEHi

AUDA is protective *in vivo* in young males following IRI [674] and we have recently used the Langendorff method to demonstrate that inhibiting sEH with *t*AUCB or through genetic deletion attenuates IRI in young mice, in a sex-independent fashion [459]. The effects of age on these observations have not been assessed *in vivo*. While stimulating IRI in mice *in vivo* can be challenging, it is a necessary step to evaluate how these effects observed in young mice change upon natural aging.

One of the hallmarks of IRI is inflammation. Targeting cardiac inflammation post-MI has shown promise in animal studies, yet clinical translation has proven challenging [675]. sEH inhibitors have known anti-inflammatory effects; interestingly, in our previous study in young mice we demonstrated sEH deletion/inhibition in young animals correlated with attenuation of a specific innate immune response, the NLRP3 inflammasome [459]. Studies have suggested NLRP3 inflammasome response contributes to ischemic myocardial damage [676, 677], however much remains unknown. As we demonstrate sexual dimorphism only upon aging, analysing changes in NLRP3 inflammasome activation post-IRI in aged male and female mice, whether *ex vivo* or *in vivo*, would be novel and clinically-relevant. Inflammation constitutes a key cardiac response to MI and, importantly, interacts with the proliferative phase following the necrotic cell death of myocytes that ultimately leads to scar formation i.e. cardiac fibrosis [678]. Fibrosis is a well-established result of myocardial ischemic injury and is a better marker of scar formation than TTC infarct assessment alone. Assessing the development and progression of cardiac fibrosis, through histological or immunostaining analyses, is thus a key concern for future research in this area.

5.4. *Assessing earlier endpoints is essential in myocardial response to ischemia*

The research presented in this dissertation utilized two times post-MI as endpoints to assess cardiac post-ischemic responses, 7 and 28-days post-MI. However, while these endpoints are useful for assessing cardiac adaptation to MI, it is difficult to assess whether responses observed are due to the injury, compensation or cardioprotection. For example, in this chapter we discussed AKT activation as a potential mediator of the cardioprotective effects observed upon sEH inhibition/deletion. Yet, AKT activation can have both protective and maladaptive effects in cardiac remodelling depending on whether the activation is acute or chronic [679]. The time following injury also effects inflammatory responses. By the 28 days used as the endpoint in Chapter 3.2, the inflammatory cascade has mostly subsided. Much of the initial inflammatory cascade, and in particular NLRP3 inflammasome activation, occurs anywhere from 1-72 hours following injury [676]. Any form of future research proposed in this chapter would require earlier assessment than utilized in this dissertation.

Additionally, a key finding with our use of sEH inhibitor *t*AUCB was that pre-treatment with *t*AUCB demonstrated more robust cardioprotection than same-day treatment. As it is not always possible to predict when an individual will experience MI, understanding effects of different treatment administration is fundamental for translational research of these pharmacologic sEH inhibitors. Assessing different applications of the sEHi would allow for further elucidation of potential prophylactic properties of this drug.

REFERENCES

1. Erkkila, A., et al., *Dietary fatty acids and cardiovascular disease: an epidemiological approach*. Prog Lipid Res, 2008. **47**(3): p. 172-87.
2. Kritchevsky, D., *History of recommendations to the public about dietary fat*. J Nutr, 1998. **128**(2 Suppl): p. 449S-452S.
3. Keys, A., J.T. Anderson, and F. Grande, *Prediction of serum-cholesterol responses of man to changes in fats in the diet*. Lancet, 1957. **273**(7003): p. 959-66.
4. Mensink, R.P. and M.B. Katan, *Effect of dietary fatty acids on serum lipids and lipoproteins. A meta-analysis of 27 trials*. Arterioscler Thromb, 1992. **12**(8): p. 911-9.
5. Mensink, R.P., et al., *Effects of dietary fatty acids and carbohydrates on the ratio of serum total to HDL cholesterol and on serum lipids and apolipoproteins: a meta-analysis of 60 controlled trials*. Am J Clin Nutr, 2003. **77**(5): p. 1146-55.
6. von Schacky, C., *A review of omega-3 ethyl esters for cardiovascular prevention and treatment of increased blood triglyceride levels*. Vasc Health Risk Manag, 2006. **2**(3): p. 251-62.
7. von Schacky, C., *Omega-3 fatty acids and cardiovascular disease*. Curr Opin Clin Nutr Metab Care, 2007. **10**(2): p. 129-35.
8. Willett, W.C., *The role of dietary n-6 fatty acids in the prevention of cardiovascular disease*. J Cardiovasc Med (Hagerstown), 2007. **8 Suppl 1**: p. S42-5.
9. Harris, W.S., *Omega-3 fatty acids and cardiovascular disease: a case for omega-3 index as a new risk factor*. Pharmacol Res, 2007. **55**(3): p. 217-23.
10. Simopoulos, A.P., *The omega-6/omega-3 fatty acid ratio, genetic variation, and cardiovascular disease*. Asia Pac J Clin Nutr, 2008. **17 Suppl 1**: p. 131-4.
11. Scott, J., *Pathophysiology and biochemistry of cardiovascular disease*. Curr Opin Genet Dev, 2004. **14**(3): p. 271-9.
12. Fletcher, L. and D. Thomas, *Congestive heart failure: understanding the pathophysiology and management*. J Am Acad Nurse Pract, 2001. **13**(6): p. 249-57.
13. Reed, G.W., J.E. Rossi, and C.P. Cannon, *Acute myocardial infarction*. Lancet, 2017. **389**(10065): p. 197-210.
14. Frangogiannis, N.G., *Pathophysiology of Myocardial Infarction*. Compr Physiol, 2015. **5**(4): p. 1841-75.
15. Rogers, C. and N. Bush, *Heart Failure: Pathophysiology, Diagnosis, Medical Treatment Guidelines, and Nursing Management*. Nurs Clin North Am, 2015. **50**(4): p. 787-99.
16. Bui, A.L., T.B. Horwich, and G.C. Fonarow, *Epidemiology and risk profile of heart failure*. Nat Rev Cardiol, 2011. **8**(1): p. 30-41.
17. Kim, S.A., J.B. Park, and M.F. O'Rourke, *Vasculopathy of Aging and the Revised Cardiovascular Continuum*. Pulse (Basel), 2015. **3**(2): p. 141-7.
18. Sprecher, H., *Biochemistry of essential fatty acids*. Prog Lipid Res, 1981. **20**: p. 13-22.
19. Haag, M., *Essential fatty acids and the brain*. Can J Psychiatry, 2003. **48**(3): p. 195-203.
20. Roels, O.A., *Linolenic acid and coronary heart disease*. Nutr Rev, 1967. **25**(2): p. 37-9.

21. Stephen, A.M. and N.J. Wald, *Trends in individual consumption of dietary fat in the United States, 1920-1984*. Am J Clin Nutr, 1990. **52**(3): p. 457-69.
22. Burgess, A., et al., *Epoxyeicosatrienoic acids and heme oxygenase-1 interaction attenuates diabetes and metabolic syndrome complications*. Prostaglandins Other Lipid Mediat, 2012. **97**(1-2): p. 1-16.
23. Bodiga, S., et al., *Protective actions of epoxyeicosatrienoic acid: dual targeting of cardiovascular PI3K and KATP channels*. J Mol Cell Cardiol, 2009. **46**(6): p. 978-88.
24. Gauthier, K.M., et al., *Roles of epoxyeicosatrienoic acids in vascular regulation and cardiac preconditioning*. J Cardiovasc Pharmacol, 2007. **50**(6): p. 601-8.
25. Seubert, J.M., et al., *Role of soluble epoxide hydrolase in postischemic recovery of heart contractile function*. Circ Res, 2006. **99**(4): p. 442-50.
26. Spector, A.A. and A.W. Norris, *Action of epoxyeicosatrienoic acids on cellular function*. Am J Physiol Cell Physiol, 2007. **292**(3): p. C996-1012.
27. Seubert, J.M., et al., *Role of epoxyeicosatrienoic acids in protecting the myocardium following ischemia/reperfusion injury*. Prostaglandins Other Lipid Mediat, 2007. **82**(1-4): p. 50-9.
28. Fleming, I., *The pharmacology of the cytochrome P450 epoxygenase/soluble epoxide hydrolase axis in the vasculature and cardiovascular disease*. Pharmacol Rev, 2014. **66**(4): p. 1106-40.
29. Imig, J.D., *Epoxides and soluble epoxide hydrolase in cardiovascular physiology*. Physiol Rev, 2012. **92**(1): p. 101-30.
30. Larsen, B.T., D.D. Gutterman, and O.A. Hatoum, *Emerging role of epoxyeicosatrienoic acids in coronary vascular function*. Eur J Clin Invest, 2006. **36**(5): p. 293-300.
31. Imig, J.D. and B.D. Hammock, *Soluble epoxide hydrolase as a therapeutic target for cardiovascular diseases*. Nat Rev Drug Discov, 2009. **8**(10): p. 794-805.
32. Fan, F., et al., *Molecular mechanisms and cell signaling of 20-hydroxyeicosatetraenoic acid in vascular pathophysiology*. Front Biosci (Landmark Ed), 2016. **21**: p. 1427-63.
33. Sinal, C.J., et al., *Targeted disruption of soluble epoxide hydrolase reveals a role in blood pressure regulation*. J Biol Chem, 2000. **275**(51): p. 40504-10.
34. Rodriguez-Leyva, D., et al., *The cardiovascular effects of flaxseed and its omega-3 fatty acid, alpha-linolenic acid*. Can J Cardiol, 2010. **26**(9): p. 489-96.
35. Dyerberg, J. and H.O. Bang, *Lipid metabolism, atherogenesis, and haemostasis in Eskimos: the role of the prostaglandin-3 family*. Haemostasis, 1979. **8**(3-5): p. 227-33.
36. Yokoyama, M., et al., *Effects of eicosapentaenoic acid on major coronary events in hypercholesterolaemic patients (JELIS): a randomised open-label, blinded endpoint analysis*. Lancet, 2007. **369**(9567): p. 1090-8.
37. Tavazzi, L., et al., *Effect of n-3 polyunsaturated fatty acids in patients with chronic heart failure (the GISSI-HF trial): a randomised, double-blind, placebo-controlled trial*. Lancet, 2008. **372**(9645): p. 1223-30.
38. Ascherio, A., et al., *Dietary intake of marine n-3 fatty acids, fish intake, and the risk of coronary disease among men*. N Engl J Med, 1995. **332**(15): p. 977-82.

39. Kromhout, D., et al., *n-3 fatty acids and cardiovascular events after myocardial infarction*. *N Engl J Med*, 2010. **363**(21): p. 2015-26.
40. Marchioli, R., et al., *Early protection against sudden death by n-3 polyunsaturated fatty acids after myocardial infarction: time-course analysis of the results of the Gruppo Italiano per lo Studio della Sopravvivenza nell'Infarto Miocardico (GISSI)-Prevenzione*. *Circulation*, 2002. **105**(16): p. 1897-903.
41. Fumagalli, M., et al., *Greenlandic Inuit show genetic signatures of diet and climate adaptation*. *Science*, 2015. **349**(6254): p. 1343-7.
42. Hu, X.F., et al., *Prevalence of heart attack and stroke and associated risk factors among Inuit in Canada: A comparison with the general Canadian population*. *Int J Hyg Environ Health*, 2019. **222**(2): p. 319-326.
43. Egert, S. and P. Stehle, *Impact of n-3 fatty acids on endothelial function: results from human interventions studies*. *Curr Opin Clin Nutr Metab Care*, 2011. **14**(2): p. 121-31.
44. Shukla, S.K., et al., *Cardiovascular friendly natural products: a promising approach in the management of CVD*. *Nat Prod Res*, 2010. **24**(9): p. 873-98.
45. Bieche, I., et al., *Reverse transcriptase-PCR quantification of mRNA levels from cytochrome (CYP)1, CYP2 and CYP3 families in 22 different human tissues*. *Pharmacogenet Genomics*, 2007. **17**(9): p. 731-42.
46. Pavek, P. and Z. Dvorak, *Xenobiotic-induced transcriptional regulation of xenobiotic metabolizing enzymes of the cytochrome P450 superfamily in human extrahepatic tissues*. *Curr Drug Metab*, 2008. **9**(2): p. 129-43.
47. Stegeman, J.J., et al., *Cytochrome P-450 and monooxygenase activity in cardiac microsomes from the fish *Stenotomus chrysops**. *Mol Pharmacol*, 1982. **21**(2): p. 517-26.
48. Myasoedova, K.N., *New findings in studies of cytochromes P450*. *Biochemistry (Mosc)*, 2008. **73**(9): p. 965-9.
49. Wu, S., et al., *Molecular cloning, expression, and functional significance of a cytochrome P450 highly expressed in rat heart myocytes*. *J Biol Chem*, 1997. **272**(19): p. 12551-9.
50. Gervasini, G., J.A. Carrillo, and J. Benitez, *Potential role of cerebral cytochrome P450 in clinical pharmacokinetics: modulation by endogenous compounds*. *Clin Pharmacokinet*, 2004. **43**(11): p. 693-706.
51. El-Sherbeni, A.A. and A.O. El-Kadi, *Alterations in cytochrome P450-derived arachidonic acid metabolism during pressure overload-induced cardiac hypertrophy*. *Biochem Pharmacol*, 2014. **87**(3): p. 456-66.
52. Michaud, V., et al., *Metabolic activity and mRNA levels of human cardiac CYP450s involved in drug metabolism*. *PLoS One*, 2010. **5**(12): p. e15666.
53. Zordoky, B.N., M.E. Aboutabl, and A.O. El-Kadi, *Modulation of cytochrome P450 gene expression and arachidonic acid metabolism during isoproterenol-induced cardiac hypertrophy in rats*. *Drug Metab Dispos*, 2008. **36**(11): p. 2277-86.
54. Thum, T. and J. Borlak, *Testosterone, cytochrome P450, and cardiac hypertrophy*. *FASEB J*, 2002. **16**(12): p. 1537-49.
55. Thum, T. and J. Borlak, *Gene expression in distinct regions of the heart*. *Lancet*, 2000. **355**(9208): p. 979-83.

56. Minamiyama, Y., et al., *Isoforms of cytochrome P450 on organic nitrate-derived nitric oxide release in human heart vessels*. FEBS Lett, 1999. **452**(3): p. 165-9.
57. Chehal, M.K. and D.J. Granville, *Cytochrome p450 2C (CYP2C) in ischemic heart injury and vascular dysfunction*. Can J Physiol Pharmacol, 2006. **84**(1): p. 15-20.
58. Choudhary, D., et al., *Comparative expression profiling of 40 mouse cytochrome P450 genes in embryonic and adult tissues*. Arch Biochem Biophys, 2003. **414**(1): p. 91-100.
59. Imaoka, S., T. Hashizume, and Y. Funae, *Localization of rat cytochrome P450 in various tissues and comparison of arachidonic acid metabolism by rat P450 with that by human P450 orthologs*. Drug Metab Pharmacokinet, 2005. **20**(6): p. 478-84.
60. Delozier, T.C., et al., *Detection of human CYP2C8, CYP2C9, and CYP2J2 in cardiovascular tissues*. Drug Metab Dispos, 2007. **35**(4): p. 682-8.
61. Fleming, I., et al., *Endothelium-derived hyperpolarizing factor synthase (Cytochrome P450 2C9) is a functionally significant source of reactive oxygen species in coronary arteries*. Circ Res, 2001. **88**(1): p. 44-51.
62. El-Sherbeni, A.A., et al., *Determination of the dominant arachidonic acid cytochrome p450 monooxygenases in rat heart, lung, kidney, and liver: protein expression and metabolite kinetics*. AAPS J, 2013. **15**(1): p. 112-22.
63. Batty, J.A., et al., *An investigation of CYP2D6 genotype and response to metoprolol CR/XL during dose titration in patients with heart failure: a MERIT-HF substudy*. Clin Pharmacol Ther, 2014. **95**(3): p. 321-30.
64. Thum, T. and J. Borlak, *Cytochrome P450 mono-oxygenase gene expression and protein activity in cultures of adult cardiomyocytes of the rat*. Br J Pharmacol, 2000. **130**(8): p. 1745-52.
65. Wu, S., et al., *Molecular cloning and expression of CYP2J2, a human cytochrome P450 arachidonic acid epoxygenase highly expressed in heart*. J Biol Chem, 1996. **271**(7): p. 3460-8.
66. Zhang, Q.Y., X. Ding, and L.S. Kaminsky, *CDNA cloning, heterologous expression, and characterization of rat intestinal CYP2J4*. Arch Biochem Biophys, 1997. **340**(2): p. 270-8.
67. Renaud, H.J., et al., *Tissue distribution and gender-divergent expression of 78 cytochrome P450 mRNAs in mice*. Toxicol Sci, 2011. **124**(2): p. 261-77.
68. Nithipatikom, K., et al., *Determination of cytochrome P450 metabolites of arachidonic acid in coronary venous plasma during ischemia and reperfusion in dogs*. Anal Biochem, 2001. **292**(1): p. 115-24.
69. Nithipatikom, K., et al., *Inhibition of cytochrome P450omega-hydroxylase: a novel endogenous cardioprotective pathway*. Circ Res, 2004. **95**(8): p. e65-71.
70. Perez-Chacon, G., et al., *Control of free arachidonic acid levels by phospholipases A2 and lysophospholipid acyltransferases*. Biochim Biophys Acta, 2009. **1791**(12): p. 1103-13.
71. Jenkins, C.M., A. Cedars, and R.W. Gross, *Eicosanoid signalling pathways in the heart*. Cardiovasc Res, 2009. **82**(2): p. 240-9.
72. Mancuso, D.J., et al., *Cardiac ischemia activates calcium-independent phospholipase A2beta, precipitating ventricular tachyarrhythmias in transgenic mice: rescue of the lethal electrophysiologic phenotype by mechanism-based inhibition*. J Biol Chem, 2003. **278**(25): p. 22231-6.

73. Roman, R.J., *P-450 metabolites of arachidonic acid in the control of cardiovascular function*. *Physiol Rev*, 2002. **82**(1): p. 131-85.
74. Konkel, A. and W.H. Schunck, *Role of cytochrome P450 enzymes in the bioactivation of polyunsaturated fatty acids*. *Biochim Biophys Acta*, 2011. **1814**(1): p. 210-22.
75. Spector, A.A., et al., *Epoxyeicosatrienoic acids (EETs): metabolism and biochemical function*. *Prog Lipid Res*, 2004. **43**(1): p. 55-90.
76. Fang, X., et al., *Effect of soluble epoxide hydrolase inhibition on epoxyeicosatrienoic acid metabolism in human blood vessels*. *Am J Physiol Heart Circ Physiol*, 2004. **287**(6): p. H2412-20.
77. Laethem, R.M., et al., *Formation of 19(S)-, 19(R)-, and 18(R)-hydroxyeicosatetraenoic acids by alcohol-inducible cytochrome P450 2E1*. *J Biol Chem*, 1993. **268**(17): p. 12912-8.
78. Rifkind, A.B., et al., *Arachidonic acid metabolism by human cytochrome P450s 2C8, 2C9, 2E1, and 1A2: regioselective oxygenation and evidence for a role for CYP2C enzymes in arachidonic acid epoxyoxygenation in human liver microsomes*. *Arch Biochem Biophys*, 1995. **320**(2): p. 380-9.
79. Oliw, E.H., J. Bylund, and C. Herman, *Bisallylic hydroxylation and epoxidation of polyunsaturated fatty acids by cytochrome P450*. *Lipids*, 1996. **31**(10): p. 1003-21.
80. Gainer, J.V., et al., *Functional variant of CYP4A11 20-hydroxyeicosatetraenoic acid synthase is associated with essential hypertension*. *Circulation*, 2005. **111**(1): p. 63-9.
81. Cheng, J., et al., *Vascular characterization of mice with endothelial expression of cytochrome P450 4F2*. *FASEB J*, 2014. **28**(7): p. 2915-31.
82. VanRollins, M., et al., *Arachidonic acid diols produced by cytochrome P-450 monooxygenases are incorporated into phospholipids of vascular endothelial cells*. *J Biol Chem*, 1996. **271**(24): p. 14001-9.
83. Zhao, G., et al., *Epoxyeicosatrienoic acids protect rat hearts against tumor necrosis factor-alpha-induced injury*. *J Lipid Res*, 2012. **53**(3): p. 456-66.
84. Westphal, C., A. Konkel, and W.H. Schunck, *Cytochrome p450 enzymes in the bioactivation of polyunsaturated Fatty acids and their role in cardiovascular disease*. *Adv Exp Med Biol*, 2015. **851**: p. 151-87.
85. Van Rollins, M., P.D. Frade, and O.A. Carretero, *Oxidation of 5,8,11,14,17-eicosapentaenoic acid by hepatic and renal microsomes*. *Biochim Biophys Acta*, 1988. **966**(1): p. 133-49.
86. VanRollins, M., et al., *Oxidation of docosahexaenoic acid by rat liver microsomes*. *J Biol Chem*, 1984. **259**(9): p. 5776-83.
87. Barbosa-Sicard, E., et al., *Eicosapentaenoic acid metabolism by cytochrome P450 enzymes of the CYP2C subfamily*. *Biochem Biophys Res Commun*, 2005. **329**(4): p. 1275-81.
88. Lucas, D., et al., *Stereoselective epoxidation of the last double bond of polyunsaturated fatty acids by human cytochromes P450*. *J Lipid Res*, 2010. **51**(5): p. 1125-33.
89. Arnold, C., et al., *Arachidonic acid-metabolizing cytochrome P450 enzymes are targets of {omega}-3 fatty acids*. *J Biol Chem*, 2010. **285**(43): p. 32720-33.
90. Alonso-Galicia, M., et al., *20-HETE agonists and antagonists in the renal circulation*. *Am J Physiol*, 1999. **277**(5 Pt 2): p. F790-6.

91. Kayama, Y., et al., *Cardiac 12/15 lipoxygenase-induced inflammation is involved in heart failure*. J Exp Med, 2009. **206**(7): p. 1565-74.
92. Waldman, M., et al., *The role of 20-HETE in cardiovascular diseases and its risk factors*. Prostaglandins Other Lipid Mediat, 2016. **125**: p. 108-17.
93. Gebremedhin, D., et al., *Production of 20-HETE and its role in autoregulation of cerebral blood flow*. Circ Res, 2000. **87**(1): p. 60-5.
94. Miyata, N. and R.J. Roman, *Role of 20-hydroxyeicosatetraenoic acid (20-HETE) in vascular system*. J Smooth Muscle Res, 2005. **41**(4): p. 175-93.
95. Wu, C.C., et al., *20-HETE and blood pressure regulation: clinical implications*. Cardiol Rev, 2014. **22**(1): p. 1-12.
96. Williams, J.M., et al., *20-hydroxyeicosatetraenoic acid: a new target for the treatment of hypertension*. J Cardiovasc Pharmacol, 2010. **56**(4): p. 336-44.
97. Hoopes, S.L., et al., *Vascular actions of 20-HETE*. Prostaglandins Other Lipid Mediat, 2015. **120**: p. 9-16.
98. Roman, R.J., et al., *Renal and cardiovascular actions of 20-hydroxyeicosatetraenoic acid and epoxyeicosatrienoic acids*. Clin Exp Pharmacol Physiol, 2000. **27**(11): p. 855-65.
99. Alonso-Galicia, M., et al., *Role of 20-hydroxyeicosatetraenoic acid in the renal and vasoconstrictor actions of angiotensin II*. Am J Physiol Regul Integr Comp Physiol, 2002. **283**(1): p. R60-8.
100. Garcia, V. and M.L. Schwartzman, *Recent developments on the vascular effects of 20-hydroxyeicosatetraenoic acid*. Curr Opin Nephrol Hypertens, 2016.
101. Sarkis, A. and R.J. Roman, *Role of cytochrome P450 metabolites of arachidonic acid in hypertension*. Curr Drug Metab, 2004. **5**(3): p. 245-56.
102. Hill, E. and R.C. Murphy, *Quantitation of 20-hydroxy-5,8,11,14-eicosatetraenoic acid (20-HETE) produced by human polymorphonuclear leukocytes using electron capture ionization gas chromatography/mass spectrometry*. Biol Mass Spectrom, 1992. **21**(5): p. 249-53.
103. Tsai, I.J., et al., *20-Hydroxyeicosatetraenoic acid synthesis is increased in human neutrophils and platelets by angiotensin II and endothelin-1*. Am J Physiol Heart Circ Physiol, 2011. **300**(4): p. H1194-200.
104. Cheng, J., et al., *20-hydroxy-5,8,11,14-eicosatetraenoic acid mediates endothelial dysfunction via I κ B kinase-dependent endothelial nitric-oxide synthase uncoupling*. J Pharmacol Exp Ther, 2010. **332**(1): p. 57-65.
105. Cheng, J., et al., *20-hydroxyeicosatetraenoic acid causes endothelial dysfunction via eNOS uncoupling*. Am J Physiol Heart Circ Physiol, 2008. **294**(2): p. H1018-26.
106. Ishizuka, T., et al., *20-Hydroxyeicosatetraenoic acid stimulates nuclear factor- κ B activation and the production of inflammatory cytokines in human endothelial cells*. J Pharmacol Exp Ther, 2008. **324**(1): p. 103-10.
107. Wang, J.S., et al., *Endothelial dysfunction and hypertension in rats transduced with CYP4A2 adenovirus*. Circ Res, 2006. **98**(7): p. 962-9.
108. Schwartzman, M., et al., *Renal cytochrome P450-related arachidonate metabolite inhibits (Na⁺ + K⁺)ATPase*. Nature, 1985. **314**(6012): p. 620-2.
109. Escalante, B., et al., *Effect of cytochrome P450 arachidonate metabolites on ion transport in rabbit kidney loop of Henle*. Science, 1991. **251**(4995): p. 799-802.

110. Escalante, B., et al., *Vasoactivity of 20-hydroxyeicosatetraenoic acid is dependent on metabolism by cyclooxygenase*. J Pharmacol Exp Ther, 1989. **248**(1): p. 229-32.
111. Ito, O., et al., *Expression of cytochrome P-450 4 enzymes in the kidney and liver: regulation by PPAR and species-difference between rat and human*. Mol Cell Biochem, 2006. **284**(1-2): p. 141-8.
112. Zou, A.P., et al., *20-HETE is an endogenous inhibitor of the large-conductance Ca(2+)-activated K⁺ channel in renal arterioles*. Am J Physiol, 1996. **270**(1 Pt 2): p. R228-37.
113. Randriamboavonjy, V., R. Busse, and I. Fleming, *20-HETE-induced contraction of small coronary arteries depends on the activation of Rho-kinase*. Hypertension, 2003. **41**(3 Pt 2): p. 801-6.
114. McGiff, J.C. and J. Quilley, *20-hydroxyeicosatetraenoic acid and epoxyeicosatrienoic acids and blood pressure*. Curr Opin Nephrol Hypertens, 2001. **10**(2): p. 231-7.
115. Hercule, H.C. and A.O. Oyekan, *Cytochrome P450 omega/omega-1 hydroxylase-derived eicosanoids contribute to endothelin(A) and endothelin(B) receptor-mediated vasoconstriction to endothelin-1 in the rat preglomerular arteriole*. J Pharmacol Exp Ther, 2000. **292**(3): p. 1153-60.
116. Lee, S.J., et al., *Cytochrome P-450 metabolites in endothelin-stimulated cardiac hormone secretion*. Am J Physiol Regul Integr Comp Physiol, 2004. **286**(5): p. R888-93.
117. Palmer, R.M., A.G. Ferrige, and S. Moncada, *Nitric oxide release accounts for the biological activity of endothelium-derived relaxing factor*. Nature, 1987. **327**(6122): p. 524-6.
118. Rees, D.D., R.M. Palmer, and S. Moncada, *Role of endothelium-derived nitric oxide in the regulation of blood pressure*. Proc Natl Acad Sci U S A, 1989. **86**(9): p. 3375-8.
119. Moore, P.K., et al., *L-NG-nitro arginine (L-NOARG), a novel, L-arginine-reversible inhibitor of endothelium-dependent vasodilatation in vitro*. Br J Pharmacol, 1990. **99**(2): p. 408-12.
120. Oyekan, A.O. and J.C. McGiff, *Functional response of the rat kidney to inhibition of nitric oxide synthesis: role of cytochrome p450-derived arachidonate metabolites*. Br J Pharmacol, 1998. **125**(5): p. 1065-73.
121. Archer, S.L., et al., *Nitric oxide and cGMP cause vasorelaxation by activation of a charybdotoxin-sensitive K channel by cGMP-dependent protein kinase*. Proc Natl Acad Sci U S A, 1994. **91**(16): p. 7583-7.
122. Bolotina, V.M., et al., *Nitric oxide directly activates calcium-dependent potassium channels in vascular smooth muscle*. Nature, 1994. **368**(6474): p. 850-3.
123. Fujino, K., et al., *Effects of nitroglycerin on ATP-induced Ca(++)-mobilization, Ca(++)-activated K channels and contraction of cultured smooth muscle cells of porcine coronary artery*. J Pharmacol Exp Ther, 1991. **256**(1): p. 371-7.
124. Li, P.L., A.P. Zou, and W.B. Campbell, *Regulation of potassium channels in coronary arterial smooth muscle by endothelium-derived vasodilators*. Hypertension, 1997. **29**(1 Pt 2): p. 262-7.

125. Carrier, G.O., et al., *Nitrovasodilators relax mesenteric microvessels by cGMP-induced stimulation of Ca-activated K channels*. Am J Physiol, 1997. **273**(1 Pt 2): p. H76-84.
126. Robertson, B.E., et al., *cGMP-dependent protein kinase activates Ca-activated K channels in cerebral artery smooth muscle cells*. Am J Physiol, 1993. **265**(1 Pt 1): p. C299-303.
127. Sun, C.W., et al., *Nitric oxide-20-hydroxyeicosatetraenoic acid interaction in the regulation of K⁺ channel activity and vascular tone in renal arterioles*. Circ Res, 1998. **83**(11): p. 1069-79.
128. Sun, C.W., et al., *Role of cGMP versus 20-HETE in the vasodilator response to nitric oxide in rat cerebral arteries*. Am J Physiol Heart Circ Physiol, 2000. **279**(1): p. H339-50.
129. Alonso-Galicia, M., et al., *Inhibition of 20-HETE production contributes to the vascular responses to nitric oxide*. Hypertension, 1997. **29**(1 Pt 2): p. 320-5.
130. Harder, D.R., et al., *Formation and action of a P-450 4A metabolite of arachidonic acid in cat cerebral microvessels*. Am J Physiol, 1994. **266**(5 Pt 2): p. H2098-107.
131. Hall, C.N., et al., *Capillary pericytes regulate cerebral blood flow in health and disease*. Nature, 2014. **508**(7494): p. 55-60.
132. Singh, H., et al., *Vascular cytochrome P450 4A expression and 20-hydroxyeicosatetraenoic acid synthesis contribute to endothelial dysfunction in androgen-induced hypertension*. Hypertension, 2007. **50**(1): p. 123-9.
133. Sacerdoti, D., et al., *Renal cytochrome P-450-dependent metabolism of arachidonic acid in spontaneously hypertensive rats*. Biochem Pharmacol, 1988. **37**(3): p. 521-7.
134. Sacerdoti, D., et al., *Treatment with tin prevents the development of hypertension in spontaneously hypertensive rats*. Science, 1989. **243**(4889): p. 388-90.
135. Garcia, V., et al., *Angiotensin II receptor blockade or deletion of vascular endothelial ACE does not prevent vascular dysfunction and remodeling in 20-HETE-dependent hypertension*. Am J Physiol Regul Integr Comp Physiol, 2015. **309**(1): p. R71-8.
136. Cheng, J., et al., *Induction of angiotensin-converting enzyme and activation of the renin-angiotensin system contribute to 20-hydroxyeicosatetraenoic acid-mediated endothelial dysfunction*. Arterioscler Thromb Vasc Biol, 2012. **32**(8): p. 1917-24.
137. Sodhi, K., et al., *CYP4A2-induced hypertension is 20-hydroxyeicosatetraenoic acid- and angiotensin II-dependent*. Hypertension, 2010. **56**(5): p. 871-8.
138. Carroll, M.A., et al., *Cytochrome P-450-dependent HETEs: profile of biological activity and stimulation by vasoactive peptides*. Am J Physiol, 1996. **271**(4 Pt 2): p. R863-9.
139. Carroll, M.A., et al., *Cytochrome P450-derived renal HETEs: storage and release*. Kidney Int, 1997. **51**(6): p. 1696-702.
140. Alsaad, A.M., et al., *Chronic doxorubicin cardiotoxicity modulates cardiac cytochrome P450-mediated arachidonic acid metabolism in rats*. Drug Metab Dispos, 2012. **40**(11): p. 2126-35.
141. Levick, S.P., et al., *Arachidonic acid metabolism as a potential mediator of cardiac fibrosis associated with inflammation*. J Immunol, 2007. **178**(2): p. 641-6.
142. Hinglais, N., et al., *Colocalization of myocardial fibrosis and inflammatory cells in rats*. Lab Invest, 1994. **70**(2): p. 286-94.

143. Kanzaki, Y., et al., *Myocardial inflammatory cell infiltrates in cases of dilated cardiomyopathy as a determinant of outcome following partial left ventriculectomy*. Jpn Circ J, 2001. **65**(9): p. 797-802.
144. Lv, X., et al., *Cytochrome P450 omega-hydroxylase inhibition reduces cardiomyocyte apoptosis via activation of ERK1/2 signaling in rat myocardial ischemia-reperfusion*. Eur J Pharmacol, 2008. **596**(1-3): p. 118-26.
145. Gross, E.R., et al., *Cytochrome P450 omega-hydroxylase inhibition reduces infarct size during reperfusion via the sarcolemmal KATP channel*. J Mol Cell Cardiol, 2004. **37**(6): p. 1245-9.
146. Wei, Y., et al., *The cardioprotection of dihydrotanshinone I against myocardial ischemia-reperfusion injury via inhibition of arachidonic acid omega-hydroxylase*. Can J Physiol Pharmacol, 2016. **94**(12): p. 1267-1275.
147. Bao, Y., et al., *20-Hydroxyeicosatetraenoic acid induces apoptosis in neonatal rat cardiomyocytes through mitochondrial-dependent pathways*. J Cardiovasc Pharmacol, 2011. **57**(3): p. 294-301.
148. Zhao, H., et al., *20-Hydroxyeicosatetraenoic Acid Is a Key Mediator of Angiotensin II-induced Apoptosis in Cardiac Myocytes*. J Cardiovasc Pharmacol, 2015. **66**(1): p. 86-95.
149. Kaduce, T.L., et al., *20-hydroxyeicosatetraenoic acid (20-HETE) metabolism in coronary endothelial cells*. J Biol Chem, 2004. **279**(4): p. 2648-56.
150. Yousif, M.H., I.F. Benter, and R.J. Roman, *Cytochrome P450 metabolites of arachidonic acid play a role in the enhanced cardiac dysfunction in diabetic rats following ischaemic reperfusion injury*. Auton Autacoid Pharmacol, 2009. **29**(1-2): p. 33-41.
151. Joseph, G., et al., *Elevated 20-HETE Impairs Coronary Collateral Growth in Metabolic Syndrome Via Endothelial Dysfunction*. Am J Physiol Heart Circ Physiol, 2016: p. ajpheart 00561 2016.
152. Nguyen, X., et al., *Kinetic profile of the rat CYP4A isoforms: arachidonic acid metabolism and isoform-specific inhibitors*. Am J Physiol, 1999. **276**(6 Pt 2): p. R1691-700.
153. Luo, G., et al., *Cloning and expression of murine CYP2Cs and their ability to metabolize arachidonic acid*. Arch Biochem Biophys, 1998. **357**(1): p. 45-57.
154. Qu, W., et al., *Cytochrome P450 CYP2J9, a new mouse arachidonic acid omega-1 hydroxylase predominantly expressed in brain*. J Biol Chem, 2001. **276**(27): p. 25467-79.
155. Poloyac, S.M., et al., *The effect of isoniazid on CYP2E1- and CYP4A-mediated hydroxylation of arachidonic acid in the rat liver and kidney*. Drug Metab Dispos, 2004. **32**(7): p. 727-33.
156. Escalante, B., et al., *Cytochrome P450-dependent arachidonic acid metabolites, 19- and 20-hydroxyeicosatetraenoic acids, enhance sodium-potassium ATPase activity in vascular smooth muscle*. J Cardiovasc Pharmacol, 1990. **16**(3): p. 438-43.
157. Ma, Y.H., et al., *20-Hydroxyeicosatetraenoic acid is an endogenous vasoconstrictor of canine renal arcuate arteries*. Circ Res, 1993. **72**(1): p. 126-36.
158. Quigley, R., et al., *Effects of 20-HETE and 19(S)-HETE on rabbit proximal straight tubule volume transport*. Am J Physiol Renal Physiol, 2000. **278**(6): p. F949-53.

159. Zhang, F., et al., *Decreased levels of cytochrome P450 2E1-derived eicosanoids sensitize renal arteries to constrictor agonists in spontaneously hypertensive rats*. Hypertension, 2005. **45**(1): p. 103-8.
160. Elkhatali, S., et al., *19-Hydroxyeicosatetraenoic acid and isoniazid protect against angiotensin II-induced cardiac hypertrophy*. Toxicol Appl Pharmacol, 2015. **289**(3): p. 550-9.
161. Zu, L., et al., *Relationship between metabolites of arachidonic acid and prognosis in patients with acute coronary syndrome*. Thromb Res, 2016. **144**: p. 192-201.
162. Oni-Orisan, A., et al., *Epoxyeicosatrienoic acids and cardioprotection: the road to translation*. J Mol Cell Cardiol, 2014. **74**: p. 199-208.
163. Yang, L., et al., *The role of epoxyeicosatrienoic acids in the cardiovascular system*. Br J Clin Pharmacol, 2015. **80**(1): p. 28-44.
164. Mercer, J.R., *Mitochondrial bioenergetics and therapeutic intervention in cardiovascular disease*. Pharmacol Ther, 2014. **141**(1): p. 13-20.
165. Halestrap, A.P., *A pore way to die: the role of mitochondria in reperfusion injury and cardioprotection*. Biochem Soc Trans, 2010. **38**(4): p. 841-60.
166. Halestrap, A.P. and A.P. Richardson, *The mitochondrial permeability transition: a current perspective on its identity and role in ischaemia/reperfusion injury*. J Mol Cell Cardiol, 2015. **78**: p. 129-41.
167. Levraut, J., et al., *Cell death during ischemia: relationship to mitochondrial depolarization and ROS generation*. Am J Physiol Heart Circ Physiol, 2003. **284**(2): p. H549-58.
168. Ong, S.B., et al., *The mitochondrial permeability transition pore and its role in myocardial ischemia reperfusion injury*. J Mol Cell Cardiol, 2015. **78**: p. 23-34.
169. Seubert, J., et al., *Enhanced postischemic functional recovery in CYP2J2 transgenic hearts involves mitochondrial ATP-sensitive K⁺ channels and p42/p44 MAPK pathway*. Circ Res, 2004. **95**(5): p. 506-14.
170. Katragadda, D., et al., *Epoxyeicosatrienoic acids limit damage to mitochondrial function following stress in cardiac cells*. J Mol Cell Cardiol, 2009. **46**(6): p. 867-75.
171. Batchu, S.N., et al., *Novel soluble epoxide hydrolase inhibitor protects mitochondrial function following stress*. Can J Physiol Pharmacol, 2012. **90**(6): p. 811-23.
172. Sarkar, P., et al., *Epoxyeicosatrienoic acids pretreatment improves amyloid beta-induced mitochondrial dysfunction in cultured rat hippocampal astrocytes*. Am J Physiol Heart Circ Physiol, 2014. **306**(4): p. H475-84.
173. El-Sikhry, H.E., et al., *Sonodynamic and photodynamic mechanisms of action of the novel hypocrellin sonosensitizer, SL017: mitochondrial cell death is attenuated by 11, 12-epoxyeicosatrienoic acid*. Invest New Drugs, 2011. **29**(6): p. 1328-36.
174. El-Sikhry, H.E., et al., *Novel Roles of Epoxyeicosanoids in Regulating Cardiac Mitochondria*. PLoS One, 2016. **11**(8): p. e0160380.
175. Akhnokh, M.K., et al., *Inhibition of Soluble Epoxide Hydrolase Limits Mitochondrial Damage and Preserves Function Following Ischemic Injury*. Front Pharmacol, 2016. **7**: p. 133.
176. Xu, Z., et al., *A murine model of myocardial ischemia-reperfusion injury through ligation of the left anterior descending artery*. J Vis Exp, 2014(86).

177. Dhanasekaran, A., et al., *Multiple antiapoptotic targets of the PI3K/Akt survival pathway are activated by epoxyeicosatrienoic acids to protect cardiomyocytes from hypoxia/anoxia*. *Am J Physiol Heart Circ Physiol*, 2008. **294**(2): p. H724-35.
178. Gross, G.J., et al., *Effects of the selective EET antagonist, 14,15-EEZE, on cardioprotection produced by exogenous or endogenous EETs in the canine heart*. *Am J Physiol Heart Circ Physiol*, 2008. **294**(6): p. H2838-44.
179. Xu, D., et al., *Prevention and reversal of cardiac hypertrophy by soluble epoxide hydrolase inhibitors*. *Proc Natl Acad Sci U S A*, 2006. **103**(49): p. 18733-8.
180. Monti, J., et al., *Soluble epoxide hydrolase is a susceptibility factor for heart failure in a rat model of human disease*. *Nat Genet*, 2008. **40**(5): p. 529-37.
181. Chaudhary, K.R., et al., *Role of B-type natriuretic peptide in epoxyeicosatrienoic acid-mediated improved post-ischaeamic recovery of heart contractile function*. *Cardiovasc Res*, 2009. **83**(2): p. 362-70.
182. Batchu, S.N., et al., *Cardioprotective effect of a dual acting epoxyeicosatrienoic acid analogue towards ischaemia reperfusion injury*. *Br J Pharmacol*, 2011. **162**(4): p. 897-907.
183. Gross, G.J., et al., *Mechanisms by which epoxyeicosatrienoic acids (EETs) elicit cardioprotection in rat hearts*. *J Mol Cell Cardiol*, 2007. **42**(3): p. 687-91.
184. Gumina, R.J., et al., *Knockout of Kir6.2 negates ischemic preconditioning-induced protection of myocardial energetics*. *Am J Physiol Heart Circ Physiol*, 2003. **284**(6): p. H2106-13.
185. Suzuki, M., et al., *Role of sarcolemmal K(ATP) channels in cardioprotection against ischemia/reperfusion injury in mice*. *J Clin Invest*, 2002. **109**(4): p. 509-16.
186. Baczko, I., W.R. Giles, and P.E. Light, *Pharmacological activation of plasma-membrane KATP channels reduces reoxygenation-induced Ca(2+) overload in cardiac myocytes via modulation of the diastolic membrane potential*. *Br J Pharmacol*, 2004. **141**(6): p. 1059-67.
187. Yao, Z., I. Cavero, and G.J. Gross, *Activation of cardiac KATP channels: an endogenous protective mechanism during repetitive ischemia*. *Am J Physiol*, 1993. **264**(2 Pt 2): p. H495-504.
188. Oudit, G.Y. and J.M. Penninger, *Cardiac regulation by phosphoinositide 3-kinases and PTEN*. *Cardiovasc Res*, 2009. **82**(2): p. 250-60.
189. Lu, T., et al., *Activation of ATP-sensitive K(+) channels by epoxyeicosatrienoic acids in rat cardiac ventricular myocytes*. *J Physiol*, 2001. **537**(Pt 3): p. 811-27.
190. Cukras, C.A., I. Jeliaskova, and C.G. Nichols, *Structural and functional determinants of conserved lipid interaction domains of inward rectifying Kir6.2 channels*. *J Gen Physiol*, 2002. **119**(6): p. 581-91.
191. Lu, T., M. VanRollins, and H.C. Lee, *Stereospecific activation of cardiac ATP-sensitive K(+) channels by epoxyeicosatrienoic acids: a structural determinant study*. *Mol Pharmacol*, 2002. **62**(5): p. 1076-83.
192. Batchu, S.N., et al., *Role of PI3Kalpha and sarcolemmal ATP-sensitive potassium channels in epoxyeicosatrienoic acid mediated cardioprotection*. *J Mol Cell Cardiol*, 2012. **53**(1): p. 43-52.
193. Gross, G.J., et al., *Roles of endothelial nitric oxide synthase (eNOS) and mitochondrial permeability transition pore (MPTP) in epoxyeicosatrienoic acid*

- (EET)-induced cardioprotection against infarction in intact rat hearts. *J Mol Cell Cardiol*, 2013. **59**: p. 20-9.
194. Merkel, M.J., et al., *Inhibition of soluble epoxide hydrolase preserves cardiomyocytes: role of STAT3 signaling*. *Am J Physiol Heart Circ Physiol*, 2010. **298**(2): p. H679-87.
195. Terashvili, M., et al., *Antinociception produced by 14,15-epoxyeicosatrienoic acid is mediated by the activation of beta-endorphin and met-enkephalin in the rat ventrolateral periaqueductal gray*. *J Pharmacol Exp Ther*, 2008. **326**(2): p. 614-22.
196. Gross, G.J., et al., *Evidence for a role of opioids in epoxyeicosatrienoic acid-induced cardioprotection in rat hearts*. *Am J Physiol Heart Circ Physiol*, 2010. **298**(6): p. H2201-7.
197. Cao, J., et al., *Agonists of epoxyeicosatrienoic acids reduce infarct size and ameliorate cardiac dysfunction via activation of HO-1 and Wnt1 canonical pathway*. *Prostaglandins Other Lipid Mediat*, 2015. **116-117**: p. 76-86.
198. Sacerdoti, D., et al., *EETs and HO-1 cross-talk*. *Prostaglandins Other Lipid Mediat*, 2016. **125**: p. 65-79.
199. Sacerdoti, D., et al., *Rat mesenteric arterial dilator response to 11,12-epoxyeicosatrienoic acid is mediated by activating heme oxygenase*. *Am J Physiol Heart Circ Physiol*, 2006. **291**(4): p. H1999-2002.
200. Sacerdoti, D., et al., *11,12-epoxyeicosatrienoic acid stimulates heme-oxygenase-1 in endothelial cells*. *Prostaglandins Other Lipid Mediat*, 2007. **82**(1-4): p. 155-61.
201. Lakkisto, P., et al., *Heme oxygenase-1 induction protects the heart and modulates cellular and extracellular remodelling after myocardial infarction in rats*. *Exp Biol Med (Maywood)*, 2011. **236**(12): p. 1437-48.
202. Bastakoty, D., et al., *Temporary, Systemic Inhibition of the WNT/beta-Catenin Pathway promotes Regenerative Cardiac Repair following Myocardial Infarct*. *Cell Stem Cells Regen Med*, 2016. **2**(2).
203. Nakagawa, A., et al., *Activation of endothelial beta-catenin signaling induces heart failure*. *Sci Rep*, 2016. **6**: p. 25009.
204. Dawson, K., M. Aflaki, and S. Nattel, *Role of the Wnt-Frizzled system in cardiac pathophysiology: a rapidly developing, poorly understood area with enormous potential*. *J Physiol*, 2013. **591**(6): p. 1409-32.
205. Chen, J.K., J. Capdevila, and R.C. Harris, *Cytochrome p450 epoxygenase metabolism of arachidonic acid inhibits apoptosis*. *Mol Cell Biol*, 2001. **21**(18): p. 6322-31.
206. Spector, A.A. and H.Y. Kim, *Cytochrome P450 epoxygenase pathway of polyunsaturated fatty acid metabolism*. *Biochim Biophys Acta*, 2015. **1851**(4): p. 356-65.
207. Yin, H., et al., *Role of mitochondria in programmed cell death mediated by arachidonic acid-derived eicosanoids*. *Mitochondrion*, 2013. **13**(3): p. 209-24.
208. Dhanasekaran, A., et al., *Protective effects of epoxyeicosatrienoic acids on human endothelial cells from the pulmonary and coronary vasculature*. *Am J Physiol Heart Circ Physiol*, 2006. **291**(2): p. H517-31.
209. Li, R., et al., *Cytochrome P450 2J2 is protective against global cerebral ischemia in transgenic mice*. *Prostaglandins Other Lipid Mediat*, 2012. **99**(3-4): p. 68-78.

210. Chen, W., et al., *CYP2J2 and EETs Protect against Oxidative Stress and Apoptosis in Vivo and in Vitro Following Lung Ischemia/Reperfusion*. Cell Physiol Biochem, 2014. **33**(6): p. 1663-80.
211. Yang, S., et al., *Cytochrome P-450 epoxygenases protect endothelial cells from apoptosis induced by tumor necrosis factor-alpha via MAPK and PI3K/Akt signaling pathways*. Am J Physiol Heart Circ Physiol, 2007. **293**(1): p. H142-51.
212. Liu, Y., et al., *Attenuation of cisplatin-induced renal injury by inhibition of soluble epoxide hydrolase involves nuclear factor kappaB signaling*. J Pharmacol Exp Ther, 2012. **341**(3): p. 725-34.
213. Liu, Y., et al., *Epoxyeicosatrienoic acids prevent cisplatin-induced renal apoptosis through a p38 mitogen-activated protein kinase-regulated mitochondrial pathway*. Mol Pharmacol, 2013. **84**(6): p. 925-34.
214. Krijnen, P.A., et al., *Apoptosis in myocardial ischaemia and infarction*. J Clin Pathol, 2002. **55**(11): p. 801-11.
215. Samokhvalov, V., et al., *Epoxyeicosatrienoic acids protect cardiac cells during starvation by modulating an autophagic response*. Cell Death Dis, 2013. **4**: p. e885.
216. Terman, A. and U.T. Brunk, *Autophagy in cardiac myocyte homeostasis, aging, and pathology*. Cardiovasc Res, 2005. **68**(3): p. 355-65.
217. Lopez-Vicario, C., et al., *Inhibition of soluble epoxide hydrolase modulates inflammation and autophagy in obese adipose tissue and liver: role for omega-3 epoxides*. Proc Natl Acad Sci U S A, 2015. **112**(2): p. 536-41.
218. Moreo, A., et al., *Influence of myocardial fibrosis on left ventricular diastolic function: noninvasive assessment by cardiac magnetic resonance and echo*. Circ Cardiovasc Imaging, 2009. **2**(6): p. 437-43.
219. Park, J.Y., et al., *Association of inflammation, myocardial fibrosis and cardiac remodelling in patients with mild aortic stenosis as assessed by biomarkers and echocardiography*. Clin Exp Pharmacol Physiol, 2014. **41**(3): p. 185-91.
220. Kania, G., P. Blyszczuk, and U. Eriksson, *Mechanisms of cardiac fibrosis in inflammatory heart disease*. Trends Cardiovasc Med, 2009. **19**(8): p. 247-52.
221. Souders, C.A., S.L. Bowers, and T.A. Baudino, *Cardiac fibroblast: the renaissance cell*. Circ Res, 2009. **105**(12): p. 1164-76.
222. Deng, Y., et al., *Endothelial CYP epoxygenase overexpression and soluble epoxide hydrolase disruption attenuate acute vascular inflammatory responses in mice*. FASEB J, 2011. **25**(2): p. 703-13.
223. Deng, Y., K.N. Theken, and C.R. Lee, *Cytochrome P450 epoxygenases, soluble epoxide hydrolase, and the regulation of cardiovascular inflammation*. J Mol Cell Cardiol, 2010. **48**(2): p. 331-41.
224. Node, K., et al., *Anti-inflammatory properties of cytochrome P450 epoxygenase-derived eicosanoids*. Science, 1999. **285**(5431): p. 1276-9.
225. Kompa, A.R., et al., *Soluble epoxide hydrolase inhibition exerts beneficial anti-remodeling actions post-myocardial infarction*. Int J Cardiol, 2013. **167**(1): p. 210-9.
226. Sirish, P., et al., *Unique mechanistic insights into the beneficial effects of soluble epoxide hydrolase inhibitors in the prevention of cardiac fibrosis*. Proc Natl Acad Sci U S A, 2013. **110**(14): p. 5618-23.

227. Samokhvalov, V., et al., *PPARgamma signaling is required for mediating EETs protective effects in neonatal cardiomyocytes exposed to LPS*. *Front Pharmacol*, 2014. **5**: p. 242.
228. Dai, M., et al., *Epoxyeicosatrienoic acids regulate macrophage polarization and prevent LPS-induced cardiac dysfunction*. *J Cell Physiol*, 2015. **230**(9): p. 2108-19.
229. Yang, L., et al., *CYP epoxygenase 2J2 prevents cardiac fibrosis by suppression of transmission of pro-inflammation from cardiomyocytes to macrophages*. *Prostaglandins Other Lipid Mediat*, 2015. **116-117**: p. 64-75.
230. Harder, D.R., W.B. Campbell, and R.J. Roman, *Role of cytochrome P-450 enzymes and metabolites of arachidonic acid in the control of vascular tone*. *J Vasc Res*, 1995. **32**(2): p. 79-92.
231. Fang, X., et al., *Pathways of epoxyeicosatrienoic acid metabolism in endothelial cells. Implications for the vascular effects of soluble epoxide hydrolase inhibition*. *J Biol Chem*, 2001. **276**(18): p. 14867-74.
232. Xin, M., E.N. Olson, and R. Bassel-Duby, *Mending broken hearts: cardiac development as a basis for adult heart regeneration and repair*. *Nat Rev Mol Cell Biol*, 2013. **14**(8): p. 529-41.
233. Fleming, I., *The factor in EDHF: Cytochrome P450 derived lipid mediators and vascular signaling*. *Vascul Pharmacol*, 2016. **86**: p. 31-40.
234. Fromel, T. and I. Fleming, *Whatever happened to the epoxyeicosatrienoic Acid-like endothelium-derived hyperpolarizing factor? The identification of novel classes of lipid mediators and their role in vascular homeostasis*. *Antioxid Redox Signal*, 2015. **22**(14): p. 1273-92.
235. Imig, J.D., *Epoxyeicosatrienoic Acids and 20-Hydroxyeicosatetraenoic Acid on Endothelial and Vascular Function*. *Adv Pharmacol*, 2016. **77**: p. 105-41.
236. Schinzari, F., M. Tesouro, and C. Cardillo, *Vascular hyperpolarization in human physiology and cardiovascular risk conditions and disease*. *Acta Physiol (Oxf)*, 2017. **219**(1): p. 124-137.
237. Ellinsworth, D.C., et al., *Endothelial control of vasodilation: integration of myoendothelial microdomain signalling and modulation by epoxyeicosatrienoic acids*. *Pflugers Arch*, 2014. **466**(3): p. 389-405.
238. Li, P.L. and W.B. Campbell, *Epoxyeicosatrienoic acids activate K⁺ channels in coronary smooth muscle through a guanine nucleotide binding protein*. *Circ Res*, 1997. **80**(6): p. 877-84.
239. Miura, H., et al., *Role for hydrogen peroxide in flow-induced dilation of human coronary arterioles*. *Circ Res*, 2003. **92**(2): p. e31-40.
240. Miura, H. and D.D. Gutterman, *Human coronary arteriolar dilation to arachidonic acid depends on cytochrome P-450 monooxygenase and Ca²⁺-activated K⁺ channels*. *Circ Res*, 1998. **83**(5): p. 501-7.
241. Miura, H., et al., *Flow-induced dilation of human coronary arterioles: important role of Ca(2+)-activated K(+) channels*. *Circulation*, 2001. **103**(15): p. 1992-8.
242. Campbell, W.B., et al., *Identification of epoxyeicosatrienoic acids as endothelium-derived hyperpolarizing factors*. *Circ Res*, 1996. **78**(3): p. 415-23.
243. Fisslthaler, B., et al., *Cytochrome P450 2C is an EDHF synthase in coronary arteries*. *Nature*, 1999. **401**(6752): p. 493-7.

244. Oltman, C.L., et al., *Epoxyeicosatrienoic acids and dihydroxyeicosatrienoic acids are potent vasodilators in the canine coronary microcirculation*. *Circ Res*, 1998. **83**(9): p. 932-9.
245. Coffman, J.D. and D.E. Gregg, *Reactive hyperemia characteristics of the myocardium*. *Am J Physiol*, 1960. **199**: p. 1143-9.
246. Hanif, A., et al., *Vascular Endothelial Over-Expression of Human Soluble Epoxide Hydrolase (Tie2-sEH Tr) Attenuates Coronary Reactive Hyperemia in Mice: Role of Oxylipins and omega-Hydroxylases*. *PLoS One*, 2017. **12**(1): p. e0169584.
247. Hanif, A., et al., *Effect of Soluble Epoxide Hydrolase on the Modulation of Coronary Reactive Hyperemia: Role of Oxylipins and PPARgamma*. *PLoS One*, 2016. **11**(9): p. e0162147.
248. Chung, N.A., et al., *Angiogenesis in myocardial infarction. An acute or chronic process?* *Eur Heart J*, 2002. **23**(20): p. 1604-8.
249. Pozzi, A. and R. Zent, *Regulation of endothelial cell functions by basement membrane- and arachidonic acid-derived products*. *Wiley Interdiscip Rev Syst Biol Med*, 2009. **1**(2): p. 254-72.
250. Fleming, I., et al., *The coronary endothelium-derived hyperpolarizing factor (EDHF) stimulates multiple signalling pathways and proliferation in vascular cells*. *Pflugers Arch*, 2001. **442**(4): p. 511-8.
251. Michaelis, U.R., et al., *Cytochrome P450 2C9-derived epoxyeicosatrienoic acids induce angiogenesis via cross-talk with the epidermal growth factor receptor (EGFR)*. *FASEB J*, 2003. **17**(6): p. 770-2.
252. Pozzi, A., et al., *Characterization of 5,6- and 8,9-epoxyeicosatrienoic acids (5,6- and 8,9-EET) as potent in vivo angiogenic lipids*. *J Biol Chem*, 2005. **280**(29): p. 27138-46.
253. Potente, M., et al., *Cytochrome P450 2C9-induced endothelial cell proliferation involves induction of mitogen-activated protein (MAP) kinase phosphatase-1, inhibition of the c-Jun N-terminal kinase, and up-regulation of cyclin D1*. *J Biol Chem*, 2002. **277**(18): p. 15671-6.
254. Wang, Y., et al., *Arachidonic acid epoxygenase metabolites stimulate endothelial cell growth and angiogenesis via mitogen-activated protein kinase and phosphatidylinositol 3-kinase/Akt signaling pathways*. *J Pharmacol Exp Ther*, 2005. **314**(2): p. 522-32.
255. Potente, M., et al., *11,12-Epoxyeicosatrienoic acid-induced inhibition of FOXO factors promotes endothelial proliferation by down-regulating p27Kip1*. *J Biol Chem*, 2003. **278**(32): p. 29619-25.
256. Xu, D.Y., et al., *A potent soluble epoxide hydrolase inhibitor, t-AUCB, acts through PPARgamma to modulate the function of endothelial progenitor cells from patients with acute myocardial infarction*. *Int J Cardiol*, 2013. **167**(4): p. 1298-304.
257. Edin, M.L., et al., *Endothelial expression of human cytochrome P450 epoxygenase CYP2C8 increases susceptibility to ischemia-reperfusion injury in isolated mouse heart*. *Faseb j*, 2011. **25**(10): p. 3436-47.
258. Talman, V. and H. Ruskoaho, *Cardiac fibrosis in myocardial infarction-from repair and remodeling to regeneration*. *Cell Tissue Res*, 2016. **365**(3): p. 563-81.

259. Li, N., et al., *Beneficial effects of soluble epoxide hydrolase inhibitors in myocardial infarction model: Insight gained using metabolomic approaches*. J Mol Cell Cardiol, 2009. **47**(6): p. 835-45.
260. Merabet, N., et al., *Soluble epoxide hydrolase inhibition improves myocardial perfusion and function in experimental heart failure*. J Mol Cell Cardiol, 2012. **52**(3): p. 660-6.
261. Wu, A.H., *Management of patients with non-ischaemic cardiomyopathy*. Heart, 2007. **93**(3): p. 403-8.
262. Ai, D., et al., *Soluble epoxide hydrolase plays an essential role in angiotensin II-induced cardiac hypertrophy*. Proc Natl Acad Sci U S A, 2009. **106**(2): p. 564-9.
263. Westphal, C., et al., *CYP2J2 overexpression protects against arrhythmia susceptibility in cardiac hypertrophy*. PLoS One, 2013. **8**(8): p. e73490.
264. Wang, B., et al., *CYP2J2 and its metabolites (epoxyeicosatrienoic acids) attenuate cardiac hypertrophy by activating AMPKalpha2 and enhancing nuclear translocation of Akt1*. Aging Cell, 2016. **15**(5): p. 940-52.
265. Nishikimi, T., N. Maeda, and H. Matsuoka, *The role of natriuretic peptides in cardioprotection*. Cardiovasc Res, 2006. **69**(2): p. 318-28.
266. Rompe, F., et al., *Direct angiotensin II type 2 receptor stimulation acts anti-inflammatory through epoxyeicosatrienoic acid and inhibition of nuclear factor kappaB*. Hypertension, 2010. **55**(4): p. 924-31.
267. Wang, X., et al., *CYP2J2-derived epoxyeicosatrienoic acids suppress endoplasmic reticulum stress in heart failure*. Mol Pharmacol, 2014. **85**(1): p. 105-15.
268. Qiu, H., et al., *Soluble epoxide hydrolase inhibitors and heart failure*. Cardiovasc Ther, 2011. **29**(2): p. 99-111.
269. Lind, M., et al., *Glycemic control and excess mortality in type 1 diabetes*. N Engl J Med, 2014. **371**(21): p. 1972-82.
270. Miller, R.G., et al., *A Contemporary Estimate of Total Mortality and Cardiovascular Disease Risk in Young Adults With Type 1 Diabetes: The Pittsburgh Epidemiology of Diabetes Complications Study*. Diabetes Care, 2016. **39**(12): p. 2296-2303.
271. American Diabetes, A., *Standards of medical care in diabetes--2011*. Diabetes Care, 2011. **34 Suppl 1**: p. S11-61.
272. Boudina, S. and E.D. Abel, *Diabetic cardiomyopathy, causes and effects*. Rev Endocr Metab Disord, 2010. **11**(1): p. 31-9.
273. Luo, P., et al., *Inhibition or deletion of soluble epoxide hydrolase prevents hyperglycemia, promotes insulin secretion, and reduces islet apoptosis*. J Pharmacol Exp Ther, 2010. **334**(2): p. 430-8.
274. Chen, L., et al., *Beneficial effects of inhibition of soluble epoxide hydrolase on glucose homeostasis and islet damage in a streptozotocin-induced diabetic mouse model*. Prostaglandins Other Lipid Mediat, 2013. **104-105**: p. 42-8.
275. Xu, X., et al., *Increased CYP2J3 expression reduces insulin resistance in fructose-treated rats and db/db mice*. Diabetes, 2010. **59**(4): p. 997-1005.
276. Luria, A., et al., *Soluble epoxide hydrolase deficiency alters pancreatic islet size and improves glucose homeostasis in a model of insulin resistance*. Proc Natl Acad Sci U S A, 2011. **108**(22): p. 9038-43.
277. Huang, H., J. Weng, and M.H. Wang, *EETs/sEH in diabetes and obesity-induced cardiovascular diseases*. Prostaglandins Other Lipid Mediat, 2016. **125**: p. 80-9.

278. Dewey, S., et al., *Proteomic analysis of hearts from Akita mice suggests that increases in soluble epoxide hydrolase and antioxidative programming are key changes in early stages of diabetic cardiomyopathy*. J Proteome Res, 2013. **12**(9): p. 3920-33.
279. Roche, C., et al., *Soluble epoxide hydrolase inhibition improves coronary endothelial function and prevents the development of cardiac alterations in obese insulin-resistant mice*. Am J Physiol Heart Circ Physiol, 2015. **308**(9): p. H1020-9.
280. Ma, B., et al., *Cardiac-specific overexpression of CYP2J2 attenuates diabetic cardiomyopathy in male streptozotocin-induced diabetic mice*. Endocrinology, 2013. **154**(8): p. 2843-56.
281. Theken, K.N., et al., *Evaluation of cytochrome P450-derived eicosanoids in humans with stable atherosclerotic cardiovascular disease*. Atherosclerosis, 2012. **222**(2): p. 530-6.
282. Mozaffarian, D., *JELIS, fish oil, and cardiac events*. Lancet, 2007. **369**(9567): p. 1062-3.
283. Swedberg, K., *n-3 Fatty acids in cardiovascular disease*. N Engl J Med, 2011. **365**(12): p. 1159; author reply 1159.
284. Mozaffarian, D. and J.H. Wu, *Omega-3 fatty acids and cardiovascular disease: effects on risk factors, molecular pathways, and clinical events*. J Am Coll Cardiol, 2011. **58**(20): p. 2047-67.
285. Khawaja, O.A., J.M. Gaziano, and L. Djousse, *N-3 fatty acids for prevention of cardiovascular disease*. Curr Atheroscler Rep, 2014. **16**(11): p. 450.
286. Mozaffarian, D., et al., *Circulating long-chain omega-3 fatty acids and incidence of congestive heart failure in older adults: the cardiovascular health study: a cohort study*. Ann Intern Med, 2011. **155**(3): p. 160-70.
287. Grimsgaard, S., et al., *Effects of highly purified eicosapentaenoic acid and docosahexaenoic acid on hemodynamics in humans*. Am J Clin Nutr, 1998. **68**(1): p. 52-9.
288. Kelley, D.S., et al., *Docosahexaenoic acid supplementation improves fasting and postprandial lipid profiles in hypertriglyceridemic men*. Am J Clin Nutr, 2007. **86**(2): p. 324-33.
289. Mori, T.A., et al., *Docosahexaenoic acid but not eicosapentaenoic acid lowers ambulatory blood pressure and heart rate in humans*. Hypertension, 1999. **34**(2): p. 253-60.
290. Mori, T.A., et al., *Differential effects of eicosapentaenoic acid and docosahexaenoic acid on vascular reactivity of the forearm microcirculation in hyperlipidemic, overweight men*. Circulation, 2000. **102**(11): p. 1264-9.
291. Theobald, H.E., et al., *Low-dose docosahexaenoic acid lowers diastolic blood pressure in middle-aged men and women*. J Nutr, 2007. **137**(4): p. 973-8.
292. Woodman, R.J., et al., *Effects of purified eicosapentaenoic and docosahexaenoic acids on glycemic control, blood pressure, and serum lipids in type 2 diabetic patients with treated hypertension*. Am J Clin Nutr, 2002. **76**(5): p. 1007-15.
293. Nestel, P., et al., *The n-3 fatty acids eicosapentaenoic acid and docosahexaenoic acid increase systemic arterial compliance in humans*. Am J Clin Nutr, 2002. **76**(2): p. 326-30.

294. Leifert, W.R., E.J. McMurchie, and D.A. Saint, *Inhibition of cardiac sodium currents in adult rat myocytes by n-3 polyunsaturated fatty acids*. J Physiol, 1999. **520 Pt 3**: p. 671-9.
295. Hallaq, H., T.W. Smith, and A. Leaf, *Modulation of dihydropyridine-sensitive calcium channels in heart cells by fish oil fatty acids*. Proc Natl Acad Sci U S A, 1992. **89**(5): p. 1760-4.
296. Xiao, Y.F., et al., *Single point mutations affect fatty acid block of human myocardial sodium channel alpha subunit Na⁺ channels*. Proc Natl Acad Sci U S A, 2001. **98**(6): p. 3606-11.
297. Kang, J.X. and A. Leaf, *Effects of long-chain polyunsaturated fatty acids on the contraction of neonatal rat cardiac myocytes*. Proc Natl Acad Sci U S A, 1994. **91**(21): p. 9886-90.
298. Kang, J.X. and A. Leaf, *Prevention and termination of beta-adrenergic agonist-induced arrhythmias by free polyunsaturated fatty acids in neonatal rat cardiac myocytes*. Biochem Biophys Res Commun, 1995. **208**(2): p. 629-36.
299. Kang, J.X., Y.F. Xiao, and A. Leaf, *Free, long-chain, polyunsaturated fatty acids reduce membrane electrical excitability in neonatal rat cardiac myocytes*. Proc Natl Acad Sci U S A, 1995. **92**(9): p. 3997-4001.
300. Falck, J.R., et al., *17(R),18(S)-epoxyeicosatetraenoic acid, a potent eicosapentaenoic acid (EPA) derived regulator of cardiomyocyte contraction: structure-activity relationships and stable analogues*. J Med Chem, 2011. **54**(12): p. 4109-18.
301. Liu, Y., et al., *Stable EET urea agonist and soluble epoxide hydrolase inhibitor regulate rat pulmonary arteries through TRPCs*. Hypertens Res, 2011. **34**(5): p. 630-9.
302. Ovide-Bordeaux, S. and A. Grynberg, *Docosahexaenoic acid affects insulin deficiency- and insulin resistance-induced alterations in cardiac mitochondria*. Am J Physiol Regul Integr Comp Physiol, 2004. **286**(3): p. R519-27.
303. Hsu, H.C., C.Y. Chen, and M.F. Chen, *N-3 polyunsaturated fatty acids decrease levels of doxorubicin-induced reactive oxygen species in cardiomyocytes -- involvement of uncoupling protein UCP2*. J Biomed Sci, 2014. **21**: p. 101.
304. Hsu, H.C., et al., *Eicosapentaenoic acid attenuated oxidative stress-induced cardiomyoblast apoptosis by activating adaptive autophagy*. Eur J Nutr, 2014. **53**(2): p. 541-7.
305. Samokhvalov, V., et al., *CYP-epoxygenase metabolites of docosahexaenoic acid protect HL-1 cardiac cells against LPS-induced cytotoxicity Through SIRT1*. Cell Death Discov, 2015. **1**.
306. Engelbrecht, A.M., et al., *Long-chain polyunsaturated fatty acids protect the heart against ischemia/reperfusion-induced injury via a MAPK dependent pathway*. J Mol Cell Cardiol, 2005. **39**(6): p. 940-54.
307. Castillo, R.L., C. Arias, and J.G. Farias, *Omega 3 chronic supplementation attenuates myocardial ischaemia-reperfusion injury through reinforcement of antioxidant defense system in rats*. Cell Biochem Funct, 2014. **32**(3): p. 274-81.
308. Zeghichi-Hamri, S., et al., *Protective effect of dietary n-3 polyunsaturated fatty acids on myocardial resistance to ischemia-reperfusion injury in rats*. Nutr Res, 2010. **30**(12): p. 849-57.

309. Richard, D., et al., *Infusion of docosahexaenoic acid protects against myocardial infarction*. Prostaglandins Leukot Essent Fatty Acids, 2014. **90**(4): p. 139-43.
310. Burban, M., et al., *An Intravenous Bolus of Epa: Dha 6: 1 Protects Against Myocardial Ischemia-Reperfusion-Induced Shock*. Shock, 2016. **46**(5): p. 549-556.
311. Samokhvalov, V., et al., *SIRT Is Required for EDP-Mediated Protective Responses toward Hypoxia-Reoxygenation Injury in Cardiac Cells*. Front Pharmacol, 2016. **7**: p. 124.
312. Yamanushi, T.T., et al., *Oral administration of eicosapentaenoic acid or docosahexaenoic acid modifies cardiac function and ameliorates congestive heart failure in male rats*. J Nutr, 2014. **144**(4): p. 467-74.
313. Sakamoto, A., et al., *Eicosapentaenoic acid ameliorates palmitate-induced lipotoxicity via the AMP kinase/dynamin-related protein-1 signaling pathway in differentiated H9c2 myocytes*. Exp Cell Res, 2017. **351**(1): p. 109-120.
314. Tavazzi, L., et al., *Effect of n-3 polyunsaturated fatty acids in patients with chronic heart failure (the GISSI-HF trial): a randomised, double-blind, placebo-controlled trial*. Lancet, 2008. **372**(9645): p. 1223-30.
315. Nodari, S., et al., *Effects of n-3 polyunsaturated fatty acids on left ventricular function and functional capacity in patients with dilated cardiomyopathy*. J Am Coll Cardiol, 2011. **57**(7): p. 870-9.
316. Chrysohoou, C., et al., *Short term omega-3 polyunsaturated fatty acid supplementation induces favorable changes in right ventricle function and diastolic filling pressure in patients with chronic heart failure; A randomized clinical trial*. Vascul Pharmacol, 2016. **79**: p. 43-50.
317. Kohashi, K., et al., *Effects of eicosapentaenoic acid on the levels of inflammatory markers, cardiac function and long-term prognosis in chronic heart failure patients with dyslipidemia*. J Atheroscler Thromb, 2014. **21**(7): p. 712-29.
318. Chen, J., et al., *Omega-3 fatty acids prevent pressure overload-induced cardiac fibrosis through activation of cyclic GMP/protein kinase G signaling in cardiac fibroblasts*. Circulation, 2011. **123**(6): p. 584-93.
319. Eclov, J.A., et al., *EPA, not DHA, prevents fibrosis in pressure overload-induced heart failure: potential role of free fatty acid receptor 4*. J Lipid Res, 2015. **56**(12): p. 2297-308.
320. Takamura, M., et al., *Long-Term Administration of Eicosapentaenoic Acid Improves Post-Myocardial Infarction Cardiac Remodeling in Mice by Regulating Macrophage Polarization*. J Am Heart Assoc, 2017. **6**(2).
321. Ito, S., et al., *Highly purified eicosapentaenoic acid ameliorates cardiac injury and adipose tissue inflammation in a rat model of metabolic syndrome*. Obes Sci Pract, 2016. **2**(3): p. 318-329.
322. Greene, J.F., et al., *Toxicity of epoxy fatty acids and related compounds to cells expressing human soluble epoxide hydrolase*. Chem Res Toxicol, 2000. **13**(4): p. 217-26.
323. Moghaddam, M.F., et al., *Bioactivation of leukotoxins to their toxic diols by epoxide hydrolase*. Nat Med, 1997. **3**(5): p. 562-6.
324. Greene, J.F., et al., *Metabolism of monoepoxides of methyl linoleate: bioactivation and detoxification*. Arch Biochem Biophys, 2000. **376**(2): p. 420-32.

325. Zeldin, D.C., *Epoxygenase pathways of arachidonic acid metabolism*. J Biol Chem, 2001. **276**(39): p. 36059-62.
326. Chaudhary, K.R., et al., *Differential effects of soluble epoxide hydrolase inhibition and CYP2J2 overexpression on postischemic cardiac function in aged mice*. Prostaglandins Other Lipid Mediat, 2013. **104-105**: p. 8-17.
327. Thompson, D.A. and B.D. Hammock, *Dihydroxyoctadecamonoenoate esters inhibit the neutrophil respiratory burst*. J Biosci, 2007. **32**(2): p. 279-91.
328. Fromel, T., et al., *Soluble epoxide hydrolase regulates hematopoietic progenitor cell function via generation of fatty acid diols*. Proc Natl Acad Sci U S A, 2012. **109**(25): p. 9995-10000.
329. Yang, W., et al., *Characterization of epoxyeicosatrienoic acid binding site in U937 membranes using a novel radiolabeled agonist, 20-125i-14,15-epoxyeicosa-8(Z)-enoic acid*. J Pharmacol Exp Ther, 2008. **324**(3): p. 1019-27.
330. Chen, Y., et al., *20-125Iodo-14,15-epoxyeicosa-5(Z)-enoic acid: a high-affinity radioligand used to characterize the epoxyeicosatrienoic acid antagonist binding site*. J Pharmacol Exp Ther, 2009. **331**(3): p. 1137-45.
331. Chen, Y., et al., *20-Iodo-14,15-epoxyeicosa-8(Z)-enoyl-3-azidophenylsulfonamide: photoaffinity labeling of a 14,15-epoxyeicosatrienoic acid receptor*. Biochemistry, 2011. **50**(18): p. 3840-8.
332. Pfister, S.L., K.M. Gauthier, and W.B. Campbell, *Vascular pharmacology of epoxyeicosatrienoic acids*. Adv Pharmacol, 2010. **60**: p. 27-59.
333. Ding, Y., et al., *The biological actions of 11,12-epoxyeicosatrienoic acid in endothelial cells are specific to the R/S-enantiomer and require the G(s) protein*. J Pharmacol Exp Ther, 2014. **350**(1): p. 14-21.
334. Liu, X., et al., *Functional screening for G protein-coupled receptor targets of 14,15-epoxyeicosatrienoic acid*. Prostaglandins Other Lipid Mediat, 2016.
335. Ye, D., et al., *Mechanism of rat mesenteric arterial KATP channel activation by 14,15-epoxyeicosatrienoic acid*. Am J Physiol Heart Circ Physiol, 2006. **290**(4): p. H1326-36.
336. Ye, D., W. Zhou, and H.C. Lee, *Activation of rat mesenteric arterial KATP channels by 11,12-epoxyeicosatrienoic acid*. Am J Physiol Heart Circ Physiol, 2005. **288**(1): p. H358-64.
337. Node, K., et al., *Activation of Galpha s mediates induction of tissue-type plasminogen activator gene transcription by epoxyeicosatrienoic acids*. J Biol Chem, 2001. **276**(19): p. 15983-9.
338. Inceoglu, B., et al., *Soluble epoxide hydrolase inhibition reveals novel biological functions of epoxyeicosatrienoic acids (EETs)*. Prostaglandins Other Lipid Mediat, 2007. **82**(1-4): p. 42-9.
339. Behm, D.J., et al., *Epoxyeicosatrienoic acids function as selective, endogenous antagonists of native thromboxane receptors: identification of a novel mechanism of vasodilation*. J Pharmacol Exp Ther, 2009. **328**(1): p. 231-9.
340. Ellinsworth, D.C., et al., *Interactions between thromboxane A(2), thromboxane/prostaglandin (TP) receptors, and endothelium-derived hyperpolarization*. Cardiovasc Res, 2014. **102**(1): p. 9-16.
341. Hara, T., et al., *Free fatty acid receptors FFAR1 and GPR120 as novel therapeutic targets for metabolic disorders*. J Pharm Sci, 2011. **100**(9): p. 3594-601.

342. Oh, D.Y. and W.S. Lagakos, *The role of G-protein-coupled receptors in mediating the effect of fatty acids on inflammation and insulin sensitivity*. *Curr Opin Clin Nutr Metab Care*, 2011. **14**(4): p. 322-7.
343. Oh, D.Y. and J.M. Olefsky, *Omega 3 fatty acids and GPR120*. *Cell Metab*, 2012. **15**(5): p. 564-5.
344. Hirasawa, A., et al., *Free fatty acids regulate gut incretin glucagon-like peptide-1 secretion through GPR120*. *Nat Med*, 2005. **11**(1): p. 90-4.
345. Mobraten, K., et al., *Omega-3 and omega-6 PUFAs induce the same GPR120-mediated signalling events, but with different kinetics and intensity in Caco-2 cells*. *Lipids Health Dis*, 2013. **12**: p. 101.
346. Oh, D.Y., et al., *GPR120 is an omega-3 fatty acid receptor mediating potent anti-inflammatory and insulin-sensitizing effects*. *Cell*, 2010. **142**(5): p. 687-98.
347. Wang, Y. and F. Huang, *N-3 Polyunsaturated Fatty Acids and Inflammation in Obesity: Local Effect and Systemic Benefit*. *Biomed Res Int*, 2015. **2015**: p. 581469.
348. Gotoh, C., et al., *The regulation of adipogenesis through GPR120*. *Biochem Biophys Res Commun*, 2007. **354**(2): p. 591-7.
349. Tanaka, T., et al., *Free fatty acids induce cholecystokinin secretion through GPR120*. *Naunyn Schmiedebergs Arch Pharmacol*, 2008. **377**(4-6): p. 523-7.
350. Wu, Q., et al., *Identification of G-protein-coupled receptor 120 as a tumor-promoting receptor that induces angiogenesis and migration in human colorectal carcinoma*. *Oncogene*, 2013. **32**(49): p. 5541-50.
351. Ichimura, A., et al., *Dysfunction of lipid sensor GPR120 leads to obesity in both mouse and human*. *Nature*, 2012. **483**(7389): p. 350-4.
352. Raptis, D.A., et al., *GPR120 on Kupffer cells mediates hepatoprotective effects of omega3-fatty acids*. *J Hepatol*, 2014. **60**(3): p. 625-32.
353. Cintra, D.E., et al., *Unsaturated fatty acids revert diet-induced hypothalamic inflammation in obesity*. *PLoS One*, 2012. **7**(1): p. e30571.
354. Grill, V. and E. Qvigstad, *Fatty acids and insulin secretion*. *Br J Nutr*, 2000. **83 Suppl 1**: p. S79-84.
355. Yonezawa, T., et al., *Free fatty acids-sensing G protein-coupled receptors in drug targeting and therapeutics*. *Curr Med Chem*, 2013. **20**(31): p. 3855-71.
356. Mancini, A.D. and V. Poitout, *The fatty acid receptor FFA1/GPR40 a decade later: how much do we know?* *Trends Endocrinol Metab*, 2013. **24**(8): p. 398-407.
357. Ehse, J.A., et al., *Increased number of islet-associated macrophages in type 2 diabetes*. *Diabetes*, 2007. **56**(9): p. 2356-70.
358. Heilbronn, L.K. and L.V. Campbell, *Adipose tissue macrophages, low grade inflammation and insulin resistance in human obesity*. *Curr Pharm Des*, 2008. **14**(12): p. 1225-30.
359. Briscoe, C.P., et al., *The orphan G protein-coupled receptor GPR40 is activated by medium and long chain fatty acids*. *J Biol Chem*, 2003. **278**(13): p. 11303-11.
360. Salehi, A., et al., *Free fatty acid receptor 1 (FFA(1)R/GPR40) and its involvement in fatty-acid-stimulated insulin secretion*. *Cell Tissue Res*, 2005. **322**(2): p. 207-15.
361. Itoh, Y., et al., *Free fatty acids regulate insulin secretion from pancreatic beta cells through GPR40*. *Nature*, 2003. **422**(6928): p. 173-6.
362. Wang, X. and C.B. Chan, *n-3 polyunsaturated fatty acids and insulin secretion*. *J Endocrinol*, 2015. **224**(3): p. R97-106.

363. Ma, S.K., et al., *Overexpression of G-protein-coupled receptor 40 enhances the mitogenic response to epoxyeicosatrienoic acids*. PLoS One, 2015. **10**(2): p. e0113130.
364. Fang, I.M., C.H. Yang, and C.M. Yang, *Docosahexaenoic acid reduces linoleic acid induced monocyte chemoattractant protein-1 expression via PPARgamma and nuclear factor-kappaB pathway in retinal pigment epithelial cells*. Mol Nutr Food Res, 2014. **58**(10): p. 2053-65.
365. Huang, C.H., et al., *A soybean and fish oil mixture with different n-6/n-3 PUFA ratios modulates the inflammatory reaction in mice with dextran sulfate sodium-induced acute colitis*. Clin Nutr, 2015. **34**(5): p. 1018-24.
366. Allred, C.D., et al., *PPARgamma1 as a molecular target of eicosapentaenoic acid in human colon cancer (HT-29) cells*. J Nutr, 2008. **138**(2): p. 250-6.
367. Zuniga, J., et al., *N-3 PUFA supplementation triggers PPAR-alpha activation and PPAR-alpha/NF-kappaB interaction: anti-inflammatory implications in liver ischemia-reperfusion injury*. PLoS One, 2011. **6**(12): p. e28502.
368. Peters, J.M., Y.M. Shah, and F.J. Gonzalez, *The role of peroxisome proliferator-activated receptors in carcinogenesis and chemoprevention*. Nat Rev Cancer, 2012. **12**(3): p. 181-95.
369. Kim, H.S., et al., *PPAR-gamma activation increases insulin secretion through the up-regulation of the free fatty acid receptor GPR40 in pancreatic beta-cells*. PLoS One, 2013. **8**(1): p. e50128.
370. Cohen, G., et al., *Role of lipid peroxidation and PPAR-delta in amplifying glucose-stimulated insulin secretion*. Diabetes, 2011. **60**(11): p. 2830-42.
371. Iglesias, J., et al., *PPARbeta/delta affects pancreatic beta cell mass and insulin secretion in mice*. J Clin Invest, 2012. **122**(11): p. 4105-17.
372. Clark, R.B., *The role of PPARs in inflammation and immunity*. J Leukoc Biol, 2002. **71**(3): p. 388-400.
373. Wray, J.A., et al., *The epoxygenases CYP2J2 activates the nuclear receptor PPARalpha in vitro and in vivo*. PLoS One, 2009. **4**(10): p. e7421.
374. Fang, X., et al., *Activation of peroxisome proliferator-activated receptor alpha by substituted urea-derived soluble epoxide hydrolase inhibitors*. J Pharmacol Exp Ther, 2005. **314**(1): p. 260-70.
375. Ng, V.Y., et al., *Cytochrome P450 eicosanoids are activators of peroxisome proliferator-activated receptor alpha*. Drug Metab Dispos, 2007. **35**(7): p. 1126-34.
376. Liu, Y., et al., *The antiinflammatory effect of laminar flow: the role of PPARgamma, epoxyeicosatrienoic acids, and soluble epoxide hydrolase*. Proc Natl Acad Sci U S A, 2005. **102**(46): p. 16747-52.
377. Huang, Y.S., et al., *Eicosadienoic acid differentially modulates production of pro-inflammatory modulators in murine macrophages*. Mol Cell Biochem, 2011. **358**(1-2): p. 85-94.
378. Holness, M.J., et al., *Evaluation of the role of peroxisome-proliferator-activated receptor alpha in the regulation of cardiac pyruvate dehydrogenase kinase 4 protein expression in response to starvation, high-fat feeding and hyperthyroidism*. Biochem J, 2002. **364**(Pt 3): p. 687-94.
379. Samokhvalov, V., et al., *PPARdelta signaling mediates the cytotoxicity of DHA in H9c2 cells*. Toxicol Lett, 2015. **232**(1): p. 10-20.

380. Harris, W.S., et al., *Omega-3 fatty acids in cardiac biopsies from heart transplantation patients: correlation with erythrocytes and response to supplementation*. *Circulation*, 2004. **110**(12): p. 1645-9.
381. Pawar, A. and D.B. Jump, *Unsaturated fatty acid regulation of peroxisome proliferator-activated receptor alpha activity in rat primary hepatocytes*. *J Biol Chem*, 2003. **278**(38): p. 35931-9.
382. Stulnig, T.M., et al., *Polyunsaturated eicosapentaenoic acid displaces proteins from membrane rafts by altering raft lipid composition*. *J Biol Chem*, 2001. **276**(40): p. 37335-40.
383. Wassall, S.R. and W. Stillwell, *Docosahexaenoic acid domains: the ultimate non-raft membrane domain*. *Chem Phys Lipids*, 2008. **153**(1): p. 57-63.
384. Hashimoto, M., et al., *Effects of eicosapentaenoic acid and docosahexaenoic acid on plasma membrane fluidity of aortic endothelial cells*. *Lipids*, 1999. **34**(12): p. 1297-304.
385. Grossfield, A., S.E. Feller, and M.C. Pitman, *A role for direct interactions in the modulation of rhodopsin by omega-3 polyunsaturated lipids*. *Proc Natl Acad Sci U S A*, 2006. **103**(13): p. 4888-93.
386. Wen, H., et al., *20-Hydroxyeicosatetraenoic acid (20-HETE) is a novel activator of transient receptor potential vanilloid 1 (TRPV1) channel*. *J Biol Chem*, 2012. **287**(17): p. 13868-76.
387. Pedersen, S.F., G. Owsianik, and B. Nilius, *TRP channels: an overview*. *Cell Calcium*, 2005. **38**(3-4): p. 233-52.
388. Thilo, F., et al., *Increased transient receptor potential vanilloid type 1 (TRPV1) channel expression in hypertrophic heart*. *Biochem Biophys Res Commun*, 2010. **401**(1): p. 98-103.
389. Earley, S., *Vanilloid and melastatin transient receptor potential channels in vascular smooth muscle*. *Microcirculation*, 2010. **17**(4): p. 237-49.
390. Yang, D., et al., *Activation of TRPV1 by dietary capsaicin improves endothelium-dependent vasorelaxation and prevents hypertension*. *Cell Metab*, 2010. **12**(2): p. 130-41.
391. Zahner, M.R., et al., *Cardiac vanilloid receptor 1-expressing afferent nerves and their role in the cardiogenic sympathetic reflex in rats*. *J Physiol*, 2003. **551**(Pt 2): p. 515-23.
392. Wang, L. and D.H. Wang, *TRPV1 gene knockout impairs postischemic recovery in isolated perfused heart in mice*. *Circulation*, 2005. **112**(23): p. 3617-23.
393. Zhong, B. and D.H. Wang, *TRPV1 gene knockout impairs preconditioning protection against myocardial injury in isolated perfused hearts in mice*. *Am J Physiol Heart Circ Physiol*, 2007. **293**(3): p. H1791-8.
394. Buckley, C.L. and A.J. Stokes, *Mice lacking functional TRPV1 are protected from pressure overload cardiac hypertrophy*. *Channels (Austin)*, 2011. **5**(4): p. 367-74.
395. Horton, J.S., C.L. Buckley, and A.J. Stokes, *Successful TRPV1 antagonist treatment for cardiac hypertrophy and heart failure in mice*. *Channels (Austin)*, 2013. **7**(1): p. 17-22.
396. Nithipatikom, K., et al., *Effects of selective inhibition of cytochrome P-450 omega-hydroxylases and ischemic preconditioning in myocardial protection*. *Am J Physiol Heart Circ Physiol*, 2006. **290**(2): p. H500-5.

397. Garcia, V., et al., *20-HETE Signals Through G Protein-Coupled Receptor GPR75 (Gq) to Affect Vascular Function and Trigger Hypertension*. *Circ Res*, 2017.
398. Khan, M.Z. and L. He, *Neuro-psychopharmacological perspective of Orphan receptors of Rhodopsin (class A) family of G protein-coupled receptors*. *Psychopharmacology (Berl)*, 2017. **234**(8): p. 1181-1207.
399. Liu, B., et al., *The novel chemokine receptor, G-protein-coupled receptor 75, is expressed by islets and is coupled to stimulation of insulin secretion and improved glucose homeostasis*. *Diabetologia*, 2013. **56**(11): p. 2467-76.
400. Garcia, V., et al., *20-HETE Activates the Transcription of Angiotensin-Converting Enzyme via Nuclear Factor-kappaB Translocation and Promoter Binding*. *J Pharmacol Exp Ther*, 2016. **356**(3): p. 525-33.
401. Zhu, Q., et al., *A novel polymorphism of the CYP2J2 gene is associated with coronary artery disease in Uygur population in China*. *Clin Biochem*, 2013. **46**(12): p. 1047-54.
402. Arun Kumar, A.S., et al., *Association of CYP2C8, CYP2C9 and CYP2J2 gene polymorphisms with myocardial infarction in South Indian population*. *Pharmacol Rep*, 2015. **67**(1): p. 97-101.
403. Fu, Z., et al., *Diploypes of CYP2C9 gene is associated with coronary artery disease in the Xinjiang Han population for women in China*. *Lipids Health Dis*, 2014. **13**: p. 143.
404. Tagetti, A., et al., *Intakes of omega-3 polyunsaturated fatty acids and blood pressure change over time: Possible interaction with genes involved in 20-HETE and EETs metabolism*. *Prostaglandins Other Lipid Mediat*, 2015. **120**: p. 126-33.
405. Tzveova, R., et al., *Gender-Specific Effect of CYP2C8*3 on the Risk of Essential Hypertension in Bulgarian Patients*. *Biochem Genet*, 2015. **53**(11-12): p. 319-33.
406. Duflot, T., et al., *Design and discovery of soluble epoxide hydrolase inhibitors for the treatment of cardiovascular diseases*. *Expert Opin Drug Discov*, 2014. **9**(3): p. 229-43.
407. Zhu, X.L., et al., *Relationship between EPHX2 gene polymorphisms and essential hypertension in Uygur, Kazakh, and Han*. *Genet Mol Res*, 2015. **14**(2): p. 3474-80.
408. Spiecker, M., et al., *Risk of coronary artery disease associated with polymorphism of the cytochrome P450 epoxygenase CYP2J2*. *Circulation*, 2004. **110**(15): p. 2132-6.
409. Liu, P.Y., et al., *Synergistic effect of cytochrome P450 epoxygenase CYP2J2*7 polymorphism with smoking on the onset of premature myocardial infarction*. *Atherosclerosis*, 2007. **195**(1): p. 199-206.
410. Fornage, M., et al., *Polymorphism of the soluble epoxide hydrolase is associated with coronary artery calcification in African-American subjects: The Coronary Artery Risk Development in Young Adults (CARDIA) study*. *Circulation*, 2004. **109**(3): p. 335-9.
411. Lee, C.R., et al., *Genetic variation in soluble epoxide hydrolase (EPHX2) and risk of coronary heart disease: The Atherosclerosis Risk in Communities (ARIC) study*. *Hum Mol Genet*, 2006. **15**(10): p. 1640-9.
412. Lee, C.R., et al., *CYP2J2 and CYP2C8 polymorphisms and coronary heart disease risk: the Atherosclerosis Risk in Communities (ARIC) study*. *Pharmacogenet Genomics*, 2007. **17**(5): p. 349-58.

413. Wei, Q., et al., *Sequence variation in the soluble epoxide hydrolase gene and subclinical coronary atherosclerosis: interaction with cigarette smoking*. *Atherosclerosis*, 2007. **190**(1): p. 26-34.
414. Yasar, U., et al., *Allelic variants of cytochromes P450 2C modify the risk for acute myocardial infarction*. *Pharmacogenetics*, 2003. **13**(12): p. 715-20.
415. Polonikov, A.V., et al., *A common polymorphism G-50T in cytochrome P450 2J2 gene is associated with increased risk of essential hypertension in a Russian population*. *Dis Markers*, 2008. **24**(2): p. 119-26.
416. Mayer, B., et al., *Association of the T8590C polymorphism of CYP4A11 with hypertension in the MONICA Augsburg echocardiographic substudy*. *Hypertension*, 2005. **46**(4): p. 766-71.
417. Mayer, B., et al., *Association of a functional polymorphism in the CYP4A11 gene with systolic blood pressure in survivors of myocardial infarction*. *J Hypertens*, 2006. **24**(10): p. 1965-70.
418. Yang, H., et al., *CYP4A11 gene T8590C polymorphism is associated with essential hypertension in the male western Chinese Han population*. *Clin Exp Hypertens*, 2014. **36**(6): p. 398-403.
419. Fu, Z., et al., *Haplotype-based case-control study of the human CYP4F2 gene and essential hypertension in Japanese subjects*. *Hypertens Res*, 2008. **31**(9): p. 1719-26.
420. Fu, Z., et al., *A haplotype of the CYP4A11 gene associated with essential hypertension in Japanese men*. *J Hypertens*, 2008. **26**(3): p. 453-61.
421. Sugimoto, K., et al., *A polymorphism regulates CYP4A11 transcriptional activity and is associated with hypertension in a Japanese population*. *Hypertension*, 2008. **52**(6): p. 1142-8.
422. Fu, Z., et al., *Haplotype study of the CYP4A11 gene and coronary artery disease in Han and Uyur populations in China*. *Gene*, 2013. **512**(2): p. 510-6.
423. Zhang, R., et al., *A common polymorphism of CYP4A11 is associated with blood pressure in a Chinese population*. *Hypertens Res*, 2011. **34**(5): p. 645-8.
424. Fu, Z., et al., *A novel polymorphism of the CYP4A11 gene is associated with coronary artery disease*. *Clin Appl Thromb Hemost*, 2013. **19**(1): p. 60-5.
425. Liang, J.Q., et al., *Association of a CYP4A11 polymorphism and hypertension in the Mongolian and Han populations of China*. *Genet Mol Res*, 2014. **13**(1): p. 508-17.
426. Zhang, B., et al., *Cytochrome 4A11 Genetic Polymorphisms Increase Susceptibility to Ischemic Stroke and Associate with Atherothrombotic Events After Stroke in Chinese*. *Genet Test Mol Biomarkers*, 2015. **19**(5): p. 235-41.
427. Fu, Z., et al., *Haplotype-based case-control study of CYP4A11 gene and myocardial infarction*. *Hereditas*, 2012. **149**(3): p. 91-8.
428. Ward, N.C., et al., *A single nucleotide polymorphism in the CYP4F2 but not CYP4A11 gene is associated with increased 20-HETE excretion and blood pressure*. *Hypertension*, 2008. **51**(5): p. 1393-8.
429. Fava, C., et al., *The V433M variant of the CYP4F2 is associated with ischemic stroke in male Swedes beyond its effect on blood pressure*. *Hypertension*, 2008. **52**(2): p. 373-80.
430. Fu, Z., et al., *A haplotype of the CYP4F2 gene associated with myocardial infarction in Japanese men*. *Mol Genet Metab*, 2009. **96**(3): p. 145-7.

431. Meng, C., et al., *Correlation between CYP4F2 gene rs2108622 polymorphism and susceptibility to ischemic stroke*. Int J Clin Exp Med, 2015. **8**(9): p. 16122-6.
432. Luo, X.H., G.R. Li, and H.Y. Li, *Association of the CYP4F2 rs2108622 genetic polymorphism with hypertension: a meta-analysis*. Genet Mol Res, 2015. **14**(4): p. 15133-9.
433. Gainer, J.V., et al., *Association of a CYP4A11 variant and blood pressure in black men*. J Am Soc Nephrol, 2008. **19**(8): p. 1606-12.
434. Legato, M.J., P.A. Johnson, and J.E. Manson, *Consideration of Sex Differences in Medicine to Improve Health Care and Patient Outcomes*. JAMA, 2016. **316**(18): p. 1865-1866.
435. Group, E.U.C.C.S., et al., *Gender in cardiovascular diseases: impact on clinical manifestations, management, and outcomes*. Eur Heart J, 2016. **37**(1): p. 24-34.
436. University of Ottawa Heart Institute. *Non-modifiable risk factors: Causes of cardiovascular disease*. 2020; Available from: <http://pwc.ottawaheart.ca/awareness/heart-health-portal/risk-factors/non-modifiable-risk-factors>.
437. Heart and Stroke Foundation, C., *Women's unique risk factors*. 2018.
438. Benjamin, E.J., et al., *Heart Disease and Stroke Statistics-2019 Update: A Report From the American Heart Association*. Circulation, 2019. **139**(10): p. e56-e528.
439. Huang, A. and G. Kaley, *Gender-specific regulation of cardiovascular function: estrogen as key player*. Microcirculation, 2004. **11**(1): p. 9-38.
440. Barrett-Connor, E., *Menopause, atherosclerosis, and coronary artery disease*. Curr Opin Pharmacol, 2013. **13**(2): p. 186-91.
441. Vaccarino, V., et al., *Sex-based differences in early mortality after myocardial infarction. National Registry of Myocardial Infarction 2 Participants*. N Engl J Med, 1999. **341**(4): p. 217-25.
442. Andrikopoulos, G.K., et al., *Younger age potentiates post myocardial infarction survival disadvantage of women*. Int J Cardiol, 2006. **108**(3): p. 320-5.
443. Rosengren, A., et al., *Sex differences in survival after myocardial infarction in Sweden; data from the Swedish National Acute Myocardial Infarction Register*. Eur Heart J, 2001. **22**(4): p. 314-22.
444. Koek, H.L., et al., *Short- and long-term prognosis after acute myocardial infarction in men versus women*. Am J Cardiol, 2006. **98**(8): p. 993-9.
445. MacIntyre, K., et al., *Gender and survival: a population-based study of 201,114 men and women following a first acute myocardial infarction*. J Am Coll Cardiol, 2001. **38**(3): p. 729-35.
446. Public Health Agency of Canada. *Report from the Canadian chronic disease surveillance system: Heart disease in Canada, 2018*. 2019; Available from: <https://www.canada.ca/en/public-health/services/publications/diseases-conditions/report-heart-disease-Canada-2018.html#f10b>.
447. Arora, S., W.D. Rosamond, and M.C. Caughey, *Response by Arora et al to Letter Regarding Article, "Twenty Year Trends and Sex Differences in Young Adults Hospitalized With Acute Myocardial Infarction: The ARIC Community Surveillance Study"*. Circulation, 2019. **140**(8): p. e331-e332.
448. Vaccarino, V., *Myocardial Infarction in Young Women*. Circulation, 2019. **139**(8): p. 1057-1059.

449. Zhang, W., et al., *Role of soluble epoxide hydrolase in the sex-specific vascular response to cerebral ischemia*. J Cereb Blood Flow Metab, 2009. **29**(8): p. 1475-81.
450. Vanella, L., et al., *Soluble epoxide hydrolase null mice exhibit female and male differences in regulation of vascular homeostasis*. Prostaglandins Other Lipid Mediat, 2015. **120**: p. 139-47.
451. Qin, J., et al., *Sexually dimorphic adaptation of cardiac function: roles of epoxyeicosatrienoic acid and peroxisome proliferator-activated receptors*. Physiol Rep, 2016. **4**(12).
452. Zuloaga, K.L., et al., *Soluble epoxide hydrolase gene deletion improves blood flow and reduces infarct size after cerebral ischemia in reproductively senescent female mice*. Front Pharmacol, 2014. **5**: p. 290.
453. Davis, C.M., S.L. Fairbanks, and N.J. Alkayed, *Mechanism of the sex difference in endothelial dysfunction after stroke*. Transl Stroke Res, 2013. **4**(4): p. 381-9.
454. Luria, A., et al., *Compensatory mechanism for homeostatic blood pressure regulation in Ephx2 gene-disrupted mice*. J Biol Chem, 2007. **282**(5): p. 2891-8.
455. Qin, J., et al., *Sexually dimorphic phenotype of arteriolar responsiveness to shear stress in soluble epoxide hydrolase-knockout mice*. Am J Physiol Heart Circ Physiol, 2015. **309**(11): p. H1860-6.
456. Froogh, G., et al., *Female-favorable attenuation of coronary myogenic constriction via reciprocal activations of epoxyeicosatrienoic acids and nitric oxide*. Am J Physiol Heart Circ Physiol, 2016. **310**(11): p. H1448-54.
457. Yang, Y.M., et al., *Estrogen-dependent epigenetic regulation of soluble epoxide hydrolase via DNA methylation*. Proc Natl Acad Sci U S A, 2018. **115**(3): p. 613-618.
458. Huang, A. and D. Sun, *Sexually Dimorphic Regulation of EET Synthesis and Metabolism: Roles of Estrogen*. Front Pharmacol, 2018. **9**: p. 1222.
459. Darwesh, A.M., et al., *Genetic Deletion or Pharmacological Inhibition of Soluble Epoxide Hydrolase Ameliorates Cardiac Ischemia/Reperfusion Injury by Attenuating NLRP3 Inflammasome Activation*. Int J Mol Sci, 2019. **20**(14).
460. Diaz Brinton, R., *Minireview: translational animal models of human menopause: challenges and emerging opportunities*. Endocrinology, 2012. **153**(8): p. 3571-8.
461. Writing Group, M., et al., *Heart Disease and Stroke Statistics-2016 Update: A Report From the American Heart Association*. Circulation, 2016. **133**(4): p. e38-360.
462. Callender, T., et al., *Heart failure care in low- and middle-income countries: a systematic review and meta-analysis*. PLoS Med, 2014. **11**(8): p. e1001699.
463. Ibanez, B., et al., *Evolving therapies for myocardial ischemia/reperfusion injury*. J Am Coll Cardiol, 2015. **65**(14): p. 1454-71.
464. Weir, R.A., J.J. McMurray, and E.J. Velazquez, *Epidemiology of heart failure and left ventricular systolic dysfunction after acute myocardial infarction: prevalence, clinical characteristics, and prognostic importance*. Am J Cardiol, 2006. **97**(10A): p. 13F-25F.
465. Jugdutt, B.I., *Aging and heart failure: changing demographics and implications for therapy in the elderly*. Heart Fail Rev, 2010. **15**(5): p. 401-5.
466. Lesnefsky, E.J., Q. Chen, and C.L. Hoppel, *Mitochondrial Metabolism in Aging Heart*. Circ Res, 2016. **118**(10): p. 1593-611.

467. Lesnefsky, E.J., P. Minkler, and C.L. Hoppel, *Enhanced modification of cardiolipin during ischemia in the aged heart*. *J Mol Cell Cardiol*, 2009. **46**(6): p. 1008-15.
468. Navarro, A. and A. Boveris, *The mitochondrial energy transduction system and the aging process*. *Am J Physiol Cell Physiol*, 2007. **292**(2): p. C670-86.
469. Hoppel, C.L., et al., *Mitochondrial Dysfunction in Cardiovascular Aging*. *Adv Exp Med Biol*, 2017. **982**: p. 451-464.
470. Kauppila, T.E.S., J.H.K. Kauppila, and N.G. Larsson, *Mammalian Mitochondria and Aging: An Update*. *Cell Metab*, 2017. **25**(1): p. 57-71.
471. Ostadal, B., et al., *Developmental and sex differences in cardiac tolerance to ischemia-reperfusion injury: the role of mitochondria (1)*. *Can J Physiol Pharmacol*, 2019. **97**(9): p. 808-814.
472. Besik, J., et al., *Tolerance to acute ischemia in adult male and female spontaneously hypertensive rats*. *Physiol Res*, 2007. **56**(3): p. 267-74.
473. Colom, B., et al., *Caloric restriction and gender modulate cardiac muscle mitochondrial H₂O₂ production and oxidative damage*. *Cardiovasc Res*, 2007. **74**(3): p. 456-65.
474. Lagranha, C.J., et al., *Sex differences in the phosphorylation of mitochondrial proteins result in reduced production of reactive oxygen species and cardioprotection in females*. *Circ Res*, 2010. **106**(11): p. 1681-91.
475. Ventura-Clapier, R., et al., *Mitochondria: a central target for sex differences in pathologies*. *Clin Sci (Lond)*, 2017. **131**(9): p. 803-822.
476. Yanes, L.L., et al., *Postmenopausal hypertension: role of 20-HETE*. *Am J Physiol Regul Integr Comp Physiol*, 2011. **300**(6): p. R1543-8.
477. Berezan, D.J., et al., *Aging increases cytochrome P450 4A modulation of alpha1-adrenergic vasoconstriction in mesenteric arteries*. *J Cardiovasc Pharmacol*, 2008. **51**(3): p. 327-30.
478. Berezan, D.J., et al., *Ovariectomy, but not estrogen deficiency, increases CYP4A modulation of alpha(1)-adrenergic vasoconstriction in aging female rats*. *Am J Hypertens*, 2008. **21**(6): p. 685-90.
479. Lopez, E.F., et al., *Obesity superimposed on aging magnifies inflammation and delays the resolving response after myocardial infarction*. *Am J Physiol Heart Circ Physiol*, 2015. **308**(4): p. H269-80.
480. Toth, P., et al., *Role of 20-HETE, TRPC channels, and BKCa in dysregulation of pressure-induced Ca²⁺ signaling and myogenic constriction of cerebral arteries in aged hypertensive mice*. *Am J Physiol Heart Circ Physiol*, 2013. **305**(12): p. H1698-708.
481. Toth, P., et al., *Age-related autoregulatory dysfunction and cerebrovascular injury in mice with angiotensin II-induced hypertension*. *J Cereb Blood Flow Metab*, 2013. **33**(11): p. 1732-42.
482. Yousif, M.H. and I.F. Benter, *Role of cytochrome P450 metabolites of arachidonic acid in regulation of corporal smooth muscle tone in diabetic and older rats*. *Vascul Pharmacol*, 2007. **47**(5-6): p. 281-7.
483. Lima, R., et al., *Roles played by 20-HETE, angiotensin II and endothelin in mediating the hypertension in aging female spontaneously hypertensive rats*. *Am J Physiol Regul Integr Comp Physiol*, 2013. **304**(3): p. R248-51.

484. Al-Naamani, N., et al., *Plasma 12- and 15-hydroxyeicosanoids are predictors of survival in pulmonary arterial hypertension*. *Pulm Circ*, 2016. **6**(2): p. 224-33.
485. Martin, D.S., O. Klinkova, and K.M. Eyster, *Regional differences in sexually dimorphic protein expression in the spontaneously hypertensive rat (SHR)*. *Mol Cell Biochem*, 2012. **362**(1-2): p. 103-14.
486. Lee, A.R., et al., *Aging, estrogen loss and epoxyeicosatrienoic acids (EETs)*. *PLoS One*, 2013. **8**(8): p. e70719.
487. Dolezelova, S., et al., *Progression of hypertension and kidney disease in aging fawn-hooded rats is mediated by enhanced influence of renin-angiotensin system and suppression of nitric oxide system and epoxyeicosanoids*. *Clin Exp Hypertens*, 2016. **38**(7): p. 644-651.
488. Jamieson, K.L., et al., *Genetic Deletion of Soluble Epoxide Hydrolase Provides Cardioprotective Responses Following Myocardial Infarction in Aged Mice*. *Prostaglandins Other Lipid Mediat*, 2017.
489. Chabova, V.C., et al., *Effects of chronic cytochrome P-450 inhibition on the course of hypertension and end-organ damage in Ren-2 transgenic rats*. *Vascul Pharmacol*, 2007. **47**(2-3): p. 145-59.
490. Hoagland, K.M., A.K. Flasch, and R.J. Roman, *Inhibitors of 20-HETE formation promote salt-sensitive hypertension in rats*. *Hypertension*, 2003. **42**(4): p. 669-73.
491. Su, P., K.M. Kaushal, and D.L. Kroetz, *Inhibition of renal arachidonic acid omega-hydroxylase activity with ABT reduces blood pressure in the SHR*. *Am J Physiol*, 1998. **275**(2 Pt 2): p. R426-38.
492. Certikova Chabova, V., et al., *Combined inhibition of 20-hydroxyeicosatetraenoic acid formation and of epoxyeicosatrienoic acids degradation attenuates hypertension and hypertension-induced end-organ damage in Ren-2 transgenic rats*. *Clin Sci (Lond)*, 2010. **118**(10): p. 617-32.
493. Aboutabl, M.E., B.N. Zordoky, and A.O. El-Kadi, *3-methylcholanthrene and benzo(a)pyrene modulate cardiac cytochrome P450 gene expression and arachidonic acid metabolism in male Sprague Dawley rats*. *Br J Pharmacol*, 2009. **158**(7): p. 1808-19.
494. Gross, G.J., et al., *Factors mediating remote preconditioning of trauma in the rat heart: central role of the cytochrome p450 epoxygenase pathway in mediating infarct size reduction*. *J Cardiovasc Pharmacol Ther*, 2013. **18**(1): p. 38-45.
495. Gross, G.J., et al., *Abdominal surgical incision induces remote preconditioning of trauma (RPCT) via activation of bradykinin receptors (BK2R) and the cytochrome P450 epoxygenase pathway in canine hearts*. *Cardiovasc Drugs Ther*, 2011. **25**(6): p. 517-22.
496. Ishihara, Y. and N. Shimamoto, *Sulfaphenazole attenuates myocardial cell apoptosis accompanied with cardiac ischemia-reperfusion by suppressing the expression of BimEL and Noxa*. *J Pharmacol Sci*, 2012. **119**(3): p. 251-9.
497. Huang, C., et al., *Autophagy and protein kinase C are required for cardioprotection by sulfaphenazole*. *Am J Physiol Heart Circ Physiol*, 2010. **298**(2): p. H570-9.
498. Ishihara, Y., et al., *Suppression of myocardial ischemia-reperfusion injury by inhibitors of cytochrome P450 in rats*. *Eur J Pharmacol*, 2009. **611**(1-3): p. 64-71.

499. Taddei, S., et al., *Identification of a cytochrome P450 2C9-derived endothelium-derived hyperpolarizing factor in essential hypertensive patients*. J Am Coll Cardiol, 2006. **48**(3): p. 508-15.
500. Hunter, A.L., et al., *Cytochrome p450 2C inhibition reduces post-ischemic vascular dysfunction*. Vascul Pharmacol, 2005. **43**(4): p. 213-9.
501. Hillig, T., et al., *Cytochrome P450 2C9 plays an important role in the regulation of exercise-induced skeletal muscle blood flow and oxygen uptake in humans*. J Physiol, 2003. **546**(Pt 1): p. 307-14.
502. Xu, F., et al., *Antihypertensive effect of mechanism-based inhibition of renal arachidonic acid omega-hydroxylase activity*. Am J Physiol Regul Integr Comp Physiol, 2002. **283**(3): p. R710-20.
503. Kroetz, D.L. and F. Xu, *Regulation and inhibition of arachidonic acid omega-hydroxylases and 20-HETE formation*. Annu Rev Pharmacol Toxicol, 2005. **45**: p. 413-38.
504. Miyata, N., et al., *Beneficial effects of a new 20-hydroxyecosatetraenoic acid synthesis inhibitor, TS-011 [N-(3-chloro-4-morpholin-4-yl) phenyl-N'-hydroxyimidoformamide], on hemorrhagic and ischemic stroke*. J Pharmacol Exp Ther, 2005. **314**(1): p. 77-85.
505. Ulu, A., et al., *Soluble epoxide hydrolase inhibitors reduce the development of atherosclerosis in apolipoprotein e-knockout mouse model*. J Cardiovasc Pharmacol, 2008. **52**(4): p. 314-23.
506. Anandan, S.K., et al., *1-(1-acetyl-piperidin-4-yl)-3-adamantan-1-yl-urea (AR9281) as a potent, selective, and orally available soluble epoxide hydrolase inhibitor with efficacy in rodent models of hypertension and dysglycemia*. Bioorg Med Chem Lett, 2011. **21**(3): p. 983-8.
507. Imig, J.D., et al., *An orally active epoxide hydrolase inhibitor lowers blood pressure and provides renal protection in salt-sensitive hypertension*. Hypertension, 2005. **46**(4): p. 975-81.
508. Huang, H., et al., *Increasing or stabilizing renal epoxyecosatrienoic acid production attenuates abnormal renal function and hypertension in obese rats*. Am J Physiol Renal Physiol, 2007. **293**(1): p. F342-9.
509. Imig, J.D., et al., *Soluble epoxide hydrolase inhibition lowers arterial blood pressure in angiotensin II hypertension*. Hypertension, 2002. **39**(2 Pt 2): p. 690-4.
510. Yu, Z., et al., *Soluble epoxide hydrolase regulates hydrolysis of vasoactive epoxyecosatrienoic acids*. Circ Res, 2000. **87**(11): p. 992-8.
511. Yang, L., et al., *Mechanisms of vascular dysfunction in COPD and effects of a novel soluble epoxide hydrolase inhibitor in smokers*. Chest, 2016.
512. Meirer, K., et al., *Design, Synthesis and Cellular Characterization of a Dual Inhibitor of 5-Lipoxygenase and Soluble Epoxide Hydrolase*. Molecules, 2016. **22**(1).
513. Hye Khan, M.A., et al., *A dual COX-2/sEH inhibitor improves the metabolic profile and reduces kidney injury in Zucker diabetic fatty rat*. Prostaglandins Other Lipid Mediat, 2016. **125**: p. 40-7.
514. Liao, J., et al., *Inhibition of Chronic Pancreatitis and Murine Pancreatic Intraepithelial Neoplasia by a Dual Inhibitor of c-RAF and Soluble Epoxide Hydrolase in LSL-KrasG(1)(2)D/Pdx-1-Cre Mice*. Anticancer Res, 2016. **36**(1): p. 27-37.

515. Inceoglu, A.B., et al., *Inhibition of soluble epoxide hydrolase limits niacin-induced vasodilation in mice*. J Cardiovasc Pharmacol, 2012. **60**(1): p. 70-5.
516. Wang, Q., et al., *Soluble epoxide hydrolase is involved in the development of atherosclerosis and arterial neointima formation by regulating smooth muscle cell migration*. Am J Physiol Heart Circ Physiol, 2015. **309**(11): p. H1894-903.
517. Althurwi, H.N., et al., *Soluble epoxide hydrolase inhibitor, TUPS, protects against isoprenaline-induced cardiac hypertrophy*. Br J Pharmacol, 2013. **168**(8): p. 1794-807.
518. Aboutabl, M.E., et al., *Inhibition of soluble epoxide hydrolase confers cardioprotection and prevents cardiac cytochrome P450 induction by benzo(a)pyrene*. J Cardiovasc Pharmacol, 2011. **57**(3): p. 273-81.
519. Granville, D.J., et al., *Reduction of ischemia and reperfusion-induced myocardial damage by cytochrome P450 inhibitors*. Proc Natl Acad Sci U S A, 2004. **101**(5): p. 1321-6.
520. Ishihara, Y., et al., *Effects of sulfaphenazole derivatives on cardiac ischemia-reperfusion injury: association of cytochrome P450 activity and infarct size*. J Pharmacol Sci, 2010. **113**(4): p. 335-42.
521. Khan, M., et al., *Sulfaphenazole protects heart against ischemia-reperfusion injury and cardiac dysfunction by overexpression of iNOS, leading to enhancement of nitric oxide bioavailability and tissue oxygenation*. Antioxid Redox Signal, 2009. **11**(4): p. 725-38.
522. Ishihara, Y., et al., *Accumulation of cytochrome P450 induced by proteasome inhibition during cardiac ischemia*. Arch Biochem Biophys, 2012. **527**(1): p. 16-22.
523. Fan, F., Y. Muroya, and R.J. Roman, *Cytochrome P450 eicosanoids in hypertension and renal disease*. Curr Opin Nephrol Hypertens, 2015. **24**(1): p. 37-46.
524. Miyata, N., et al., *HET0016, a potent and selective inhibitor of 20-HETE synthesizing enzyme*. Br J Pharmacol, 2001. **133**(3): p. 325-9.
525. Kehl, F., et al., *20-HETE contributes to the acute fall in cerebral blood flow after subarachnoid hemorrhage in the rat*. Am J Physiol Heart Circ Physiol, 2002. **282**(4): p. H1556-65.
526. Nakamura, T., et al., *Imidazole derivatives as new potent and selective 20-HETE synthase inhibitors*. Bioorg Med Chem Lett, 2004. **14**(2): p. 333-6.
527. Chen, H.J., et al., *[PPAR alpha activator fenofibrate regressed left ventricular hypertrophy and increased myocardium PPAR alpha expression in spontaneously hypertensive rats]*. Zhejiang Da Xue Xue Bao Yi Xue Ban, 2007. **36**(5): p. 470-6.
528. Althurwi, H.N., O.H. Elshenawy, and A.O. El-Kadi, *Fenofibrate modulates cytochrome P450 and arachidonic acid metabolism in the heart and protects against isoproterenol-induced cardiac hypertrophy*. J Cardiovasc Pharmacol, 2014. **63**(2): p. 167-77.
529. Evangelista, E.A., et al., *Activity, inhibition, and induction of cytochrome P450 2J2 in adult human primary cardiomyocytes*. Drug Metab Dispos, 2013. **41**(12): p. 2087-94.
530. Tremblay, H., et al., *One-pot synthesis of polyunsaturated fatty acid amides with anti-proliferative properties*. Bioorg Med Chem Lett, 2014. **24**(24): p. 5635-8.

531. Proudman, S.M., et al., *Fish oil in recent onset rheumatoid arthritis: a randomised, double-blind controlled trial within algorithm-based drug use*. Ann Rheum Dis, 2015. **74**(1): p. 89-95.
532. Khaddaj-Mallat, R., C. Morin, and E. Rousseau, *Novel n-3 PUFA monoacylglycerides of pharmacological and medicinal interest: Anti-inflammatory and anti-proliferative effects*. Eur J Pharmacol, 2016. **792**: p. 70-77.
533. Morin, C., et al., *MAG-EPA resolves lung inflammation in an allergic model of asthma*. Clin Exp Allergy, 2013. **43**(9): p. 1071-82.
534. Cruz-Hernandez, C., et al., *Benefits of structured and free monoacylglycerols to deliver eicosapentaenoic (EPA) in a model of lipid malabsorption*. Nutrients, 2012. **4**(11): p. 1781-93.
535. Khaddaj-Mallat, R. and E. Rousseau, *MAG-EPA and 17,18-EpETE target cytoplasmic signalling pathways to reduce short-term airway hyperresponsiveness*. Pflugers Arch, 2015. **467**(7): p. 1591-605.
536. Morin, C., P.U. Blier, and S. Fortin, *Eicosapentaenoic acid and docosapentaenoic acid monoglycerides are more potent than docosahexaenoic acid monoglyceride to resolve inflammation in a rheumatoid arthritis model*. Arthritis Res Ther, 2015. **17**: p. 142.
537. Morin, C., P.U. Blier, and S. Fortin, *MAG-EPA reduces severity of DSS-induced colitis in rats*. Am J Physiol Gastrointest Liver Physiol, 2016. **310**(10): p. G808-21.
538. Morin, C., et al., *Effect of docosahexaenoic acid monoacylglyceride on systemic hypertension and cardiovascular dysfunction*. Am J Physiol Heart Circ Physiol, 2015. **309**(1): p. H93-H102.
539. Spector, A.A., *Arachidonic acid cytochrome P450 epoxygenase pathway*. J Lipid Res, 2009. **50 Suppl**: p. S52-6.
540. Imig, J.D., *Epoxide hydrolase and epoxygenase metabolites as therapeutic targets for renal diseases*. Am J Physiol Renal Physiol, 2005. **289**(3): p. F496-503.
541. Dimitropoulou, C., et al., *Protein phosphatase 2A and Ca²⁺-activated K⁺ channels contribute to 11,12-epoxyeicosatrienoic acid analog mediated mesenteric arterial relaxation*. Prostaglandins Other Lipid Mediat, 2007. **83**(1-2): p. 50-61.
542. Falck, J.R., et al., *11,12-epoxyeicosatrienoic acid (11,12-EET): structural determinants for inhibition of TNF-alpha-induced VCAM-1 expression*. Bioorg Med Chem Lett, 2003. **13**(22): p. 4011-4.
543. Gauthier, K.M., et al., *14,15-EET analogs: characterization of structural requirements for agonist and antagonist activity in bovine coronary arteries*. Pharmacol Res, 2004. **49**(6): p. 515-24.
544. Imig, J.D., et al., *Afferent arteriolar dilation to 11, 12-EET analogs involves PP2A activity and Ca²⁺-activated K⁺ Channels*. Microcirculation, 2008. **15**(2): p. 137-50.
545. Imig, J.D., et al., *Development of epoxyeicosatrienoic acid analogs with in vivo anti-hypertensive actions*. Front Physiol, 2010. **1**: p. 157.
546. Hye Khan, M.A., et al., *Epoxyeicosatrienoic acid analogue lowers blood pressure through vasodilation and sodium channel inhibition*. Clin Sci (Lond), 2014. **127**(7): p. 463-74.
547. Sporkova, A., et al., *Vasodilatory responses of renal interlobular arteries to epoxyeicosatrienoic acids analog are not enhanced in Ren-2 transgenic hypertensive*

- rats: evidence against a role of direct vascular effects of epoxyeicosatrienoic acids in progression of experimental heart failure.* *Physiol Res*, 2016.
548. Jichova, S., et al., *Epoxyeicosatrienoic acid analog attenuates the development of malignant hypertension, but does not reverse it once established: a study in Cyp11a1-Ren-2 transgenic rats.* *J Hypertens*, 2016. **34**(10): p. 2008-25.
549. Hye Khan, M.A., et al., *Orally active epoxyeicosatrienoic acid analog attenuates kidney injury in hypertensive Dahl salt-sensitive rat.* *Hypertension*, 2013. **62**(5): p. 905-13.
550. Khan, A.H., et al., *Epoxyeicosatrienoic acid analog attenuates angiotensin II hypertension and kidney injury.* *Front Pharmacol*, 2014. **5**: p. 216.
551. Kodani, S.D. and B.D. Hammock, *The 2014 Bernard B. Brodie award lecture-epoxide hydrolases: drug metabolism to therapeutics for chronic pain.* *Drug Metab Dispos*, 2015. **43**(5): p. 788-802.
552. Morisseau, C. and B.D. Hammock, *Impact of soluble epoxide hydrolase and epoxyeicosanoids on human health.* *Annu Rev Pharmacol Toxicol*, 2013. **53**: p. 37-58.
553. Morisseau, C., et al., *Potent urea and carbamate inhibitors of soluble epoxide hydrolases.* *Proc Natl Acad Sci U S A*, 1999. **96**(16): p. 8849-54.
554. Chiamvimonvat, N., et al., *The soluble epoxide hydrolase as a pharmaceutical target for hypertension.* *J Cardiovasc Pharmacol*, 2007. **50**(3): p. 225-37.
555. Davis, B.B., et al., *Attenuation of vascular smooth muscle cell proliferation by 1-cyclohexyl-3-dodecyl urea is independent of soluble epoxide hydrolase inhibition.* *J Pharmacol Exp Ther*, 2006. **316**(2): p. 815-21.
556. Davis, B.B., et al., *Inhibitors of soluble epoxide hydrolase attenuate vascular smooth muscle cell proliferation.* *Proc Natl Acad Sci U S A*, 2002. **99**(4): p. 2222-7.
557. Smith, K.R., et al., *Attenuation of tobacco smoke-induced lung inflammation by treatment with a soluble epoxide hydrolase inhibitor.* *Proc Natl Acad Sci U S A*, 2005. **102**(6): p. 2186-91.
558. Zhang, L.N., et al., *Inhibition of soluble epoxide hydrolase attenuated atherosclerosis, abdominal aortic aneurysm formation, and dyslipidemia.* *Arterioscler Thromb Vasc Biol*, 2009. **29**(9): p. 1265-70.
559. Pang, W., et al., *Activation of peroxisome proliferator-activated receptor-gamma downregulates soluble epoxide hydrolase in cardiomyocytes.* *Clin Exp Pharmacol Physiol*, 2011. **38**(6): p. 358-64.
560. Harris, T.R., et al., *The potential of soluble epoxide hydrolase inhibition in the treatment of cardiac hypertrophy.* *Congest Heart Fail*, 2008. **14**(4): p. 219-24.
561. Taylor, S.J., et al., *Design and synthesis of substituted nicotinamides as inhibitors of soluble epoxide hydrolase.* *Bioorg Med Chem Lett*, 2009. **19**(20): p. 5864-8.
562. Eldrup, A.B., et al., *Optimization of piperidyl-ureas as inhibitors of soluble epoxide hydrolase.* *Bioorg Med Chem Lett*, 2010. **20**(2): p. 571-5.
563. Lazaar, A.L., et al., *Pharmacokinetics, pharmacodynamics and adverse event profile of GSK2256294, a novel soluble epoxide hydrolase inhibitor.* *Br J Clin Pharmacol*, 2016. **81**(5): p. 971-9.
564. Sin, D.D. and S.F. Man, *Why are patients with chronic obstructive pulmonary disease at increased risk of cardiovascular diseases? The potential role of systemic*

- inflammation in chronic obstructive pulmonary disease*. *Circulation*, 2003. **107**(11): p. 1514-9.
565. Maclay, J.D. and W. MacNee, *Cardiovascular disease in COPD: mechanisms*. *Chest*, 2013. **143**(3): p. 798-807.
566. Maclay, J.D., et al., *Vascular dysfunction in chronic obstructive pulmonary disease*. *Am J Respir Crit Care Med*, 2009. **180**(6): p. 513-20.
567. Morphy, R. and Z. Rankovic, *The physicochemical challenges of designing multiple ligands*. *J Med Chem*, 2006. **49**(16): p. 4961-70.
568. Meirer, K., D. Steinhilber, and E. Proschak, *Inhibitors of the arachidonic acid cascade: interfering with multiple pathways*. *Basic Clin Pharmacol Toxicol*, 2014. **114**(1): p. 83-91.
569. Hwang, S.H., et al., *Rationally designed multitarget agents against inflammation and pain*. *Curr Med Chem*, 2013. **20**(13): p. 1783-99.
570. Wecksler, A.T., et al., *Biological evaluation of a novel sorafenib analogue, t-CUPM*. *Cancer Chemother Pharmacol*, 2015. **75**(1): p. 161-71.
571. Falck, J.R., et al., *14,15-Epoxyeicosa-5,8,11-trienoic acid (14,15-EET) surrogates containing epoxide bioisosteres: influence upon vascular relaxation and soluble epoxide hydrolase inhibition*. *J Med Chem*, 2009. **52**(16): p. 5069-75.
572. Niebauer, J., et al., *Endotoxin and immune activation in chronic heart failure: a prospective cohort study*. *Lancet*, 1999. **353**(9167): p. 1838-42.
573. Oelze, M., et al., *Vasodilator-stimulated phosphoprotein serine 239 phosphorylation as a sensitive monitor of defective nitric oxide/cGMP signaling and endothelial dysfunction*. *Circ Res*, 2000. **87**(11): p. 999-1005.
574. Dutta, S. and P. Sengupta, *Men and mice: Relating their ages*. *Life Sci*, 2016. **152**: p. 244-8.
575. Whitehead, J.C., et al., *A clinical frailty index in aging mice: comparisons with frailty index data in humans*. *J Gerontol A Biol Sci Med Sci*, 2014. **69**(6): p. 621-32.
576. Kassiri, Z., et al., *Loss of angiotensin-converting enzyme 2 accelerates maladaptive left ventricular remodeling in response to myocardial infarction*. *Circ Heart Fail*, 2009. **2**(5): p. 446-55.
577. Kandalam, V., et al., *TIMP2 deficiency accelerates adverse post-myocardial infarction remodeling because of enhanced MT1-MMP activity despite lack of MMP2 activation*. *Circ Res*, 2010. **106**(4): p. 796-808.
578. Zhabyeyev, P., et al., *Inhibition of PI3Kinase-alpha is pro-arrhythmic and associated with enhanced late Na(+) current, contractility, and Ca(2+) release in murine hearts*. *J Mol Cell Cardiol*, 2019. **132**: p. 98-109.
579. Sysa-Shah, P., et al., *Electrocardiographic Characterization of Cardiac Hypertrophy in Mice that Overexpress the ErbB2 Receptor Tyrosine Kinase*. *Comp Med*, 2015. **65**(4): p. 295-307.
580. Spinazzi, M., et al., *Assessment of mitochondrial respiratory chain enzymatic activities on tissues and cultured cells*. *Nat Protoc*, 2012. **7**(6): p. 1235-46.
581. Bradford, M.M., *A rapid and sensitive method for the quantitation of microgram quantities of protein utilizing the principle of protein-dye binding*. *Anal Biochem*, 1976. **72**: p. 248-54.
582. Kuznetsov, A.V., et al., *Analysis of mitochondrial function in situ in permeabilized muscle fibers, tissues and cells*. *Nat Protoc*, 2008. **3**(6): p. 965-76.

583. Walton, J., *Lead aspartate, an en bloc contrast stain particularly useful for ultrastructural enzymology*. J Histochem Cytochem, 1979. **27**(10): p. 1337-42.
584. Newman, J.W., T. Watanabe, and B.D. Hammock, *The simultaneous quantification of cytochrome P450 dependent linoleate and arachidonate metabolites in urine by HPLC-MS/MS*. J Lipid Res, 2002. **43**(9): p. 1563-78.
585. Taylor, R.C. and A. Dillin, *Aging as an event of proteostasis collapse*. Cold Spring Harb Perspect Biol, 2011. **3**(5).
586. Bulteau, A.L., L.I. Szweda, and B. Friguet, *Age-dependent declines in proteasome activity in the heart*. Arch Biochem Biophys, 2002. **397**(2): p. 298-304.
587. Yarian, C.S., D. Toroser, and R.S. Sohal, *Aconitase is the main functional target of aging in the citric acid cycle of kidney mitochondria from mice*. Mech Ageing Dev, 2006. **127**(1): p. 79-84.
588. Vaclavikova, R., D.J. Hughes, and P. Soucek, *Microsomal epoxide hydrolase 1 (EPHX1): Gene, structure, function, and role in human disease*. Gene, 2015. **571**(1): p. 1-8.
589. Chance, B. and B. Hagihara, *Initiation of Succinate Oxidation in Aged Pigeon Heart Mitochondria*. Biochemical and Biophysical Research Communications, 1960. **3**(1): p. 1-5.
590. Liu, J.Y., et al., *Pharmacokinetic optimization of four soluble epoxide hydrolase inhibitors for use in a murine model of inflammation*. Br J Pharmacol, 2009. **156**(2): p. 284-96.
591. Hillis, G.S., et al., *Noninvasive estimation of left ventricular filling pressure by E/e' is a powerful predictor of survival after acute myocardial infarction*. J Am Coll Cardiol, 2004. **43**(3): p. 360-7.
592. Boukens, B.J., et al., *Misinterpretation of the mouse ECG: 'musing the waves of Mus musculus'*. J Physiol, 2014. **592**(21): p. 4613-26.
593. Schunck, W.H., et al., *Therapeutic potential of omega-3 fatty acid-derived epoxyeicosanoids in cardiovascular and inflammatory diseases*. Pharmacol Ther, 2018. **183**: p. 177-204.
594. Jamieson, K.L., et al., *Genetic deletion of soluble epoxide hydrolase provides cardioprotective responses following myocardial infarction in aged mice*. Prostaglandins Other Lipid Mediat, 2017. **132**: p. 47-58.
595. Ide, T., et al., *Mitochondrial DNA damage and dysfunction associated with oxidative stress in failing hearts after myocardial infarction*. Circ Res, 2001. **88**(5): p. 529-35.
596. Rosca, M.G., et al., *Cardiac mitochondria in heart failure: decrease in respirasomes and oxidative phosphorylation*. Cardiovasc Res, 2008. **80**(1): p. 30-9.
597. Ong, S.B., et al., *Mitochondrial-Shaping Proteins in Cardiac Health and Disease - the Long and the Short of It!* Cardiovasc Drugs Ther, 2017. **31**(1): p. 87-107.
598. Lopez-Crisosto, C., et al., *Sarcoplasmic reticulum-mitochondria communication in cardiovascular pathophysiology*. Nat Rev Cardiol, 2017. **14**(6): p. 342-360.
599. Dorn, G.W., 2nd, *Mitochondrial dynamism and heart disease: changing shape and shaping change*. EMBO Mol Med, 2015. **7**(7): p. 865-77.
600. Jamieson, K.L., et al., *Cytochrome P450-derived eicosanoids and heart function*. Pharmacol Ther, 2017. **179**: p. 47-83.
601. Edin, M.L., et al., *Epoxide hydrolase 1 (EPHX1) hydrolyzes epoxyeicosanoids and impairs cardiac recovery after ischemia*. J Biol Chem, 2018. **293**(9): p. 3281-3292.

602. Larsen, S., et al., *Biomarkers of mitochondrial content in skeletal muscle of healthy young human subjects*. J Physiol, 2012. **590**(14): p. 3349-60.
603. Fang, X., et al., *Omega-3 PUFA attenuate mice myocardial infarction injury by emerging a protective eicosanoid pattern*. Prostaglandins Other Lipid Mediat, 2018. **139**: p. 1-9.
604. Lloyd-Jones, D.M., *Slowing Progress in Cardiovascular Mortality Rates: You Reap What You Sow*. JAMA Cardiol, 2016. **1**(5): p. 599-600.
605. Cheng, S., et al., *Age-related left ventricular remodeling and associated risk for cardiovascular outcomes: the Multi-Ethnic Study of Atherosclerosis*. Circ Cardiovasc Imaging, 2009. **2**(3): p. 191-8.
606. North, B.J. and D.A. Sinclair, *The intersection between aging and cardiovascular disease*. Circ Res, 2012. **110**(8): p. 1097-108.
607. Kocher, C., et al., *Sexual dimorphism in obesity-related genes in the epicardial fat during aging*. J Physiol Biochem, 2017. **73**(2): p. 215-224.
608. Kronmal, R.A., et al., *Risk factors for the progression of coronary artery calcification in asymptomatic subjects: results from the Multi-Ethnic Study of Atherosclerosis (MESA)*. Circulation, 2007. **115**(21): p. 2722-30.
609. Dai, D.F. and P.S. Rabinovitch, *Cardiac aging in mice and humans: the role of mitochondrial oxidative stress*. Trends Cardiovasc Med, 2009. **19**(7): p. 213-20.
610. Parks, R.J. and S.E. Howlett, *Sex differences in mechanisms of cardiac excitation-contraction coupling*. Pflugers Arch, 2013. **465**(5): p. 747-63.
611. Merz, A.A. and S. Cheng, *Sex differences in cardiovascular ageing*. Heart, 2016. **102**(11): p. 825-31.
612. Lam, C.S., et al., *Epidemiology and clinical course of heart failure with preserved ejection fraction*. Eur J Heart Fail, 2011. **13**(1): p. 18-28.
613. Palacios, S., et al., *Age of menopause and impact of climacteric symptoms by geographical region*. Climacteric, 2010. **13**(5): p. 419-28.
614. Lubiszewska, B., et al., *The impact of early menopause on risk of coronary artery disease (PREmature Coronary Artery Disease In Women--PRECADIW case-control study)*. Eur J Prev Cardiol, 2012. **19**(1): p. 95-101.
615. Tooher, J., et al., *All Hypertensive Disorders of Pregnancy Increase the Risk of Future Cardiovascular Disease*. Hypertension, 2017. **70**(4): p. 798-803.
616. Tobias, D.K., et al., *Association of History of Gestational Diabetes With Long-term Cardiovascular Disease Risk in a Large Prospective Cohort of US Women*. JAMA Intern Med, 2017. **177**(12): p. 1735-1742.
617. Aggarwal, N.R., et al., *Sex Differences in Ischemic Heart Disease: Advances, Obstacles, and Next Steps*. Circ Cardiovasc Qual Outcomes, 2018. **11**(2): p. e004437.
618. Dutta, D., et al., *Contribution of impaired mitochondrial autophagy to cardiac aging: mechanisms and therapeutic opportunities*. Circ Res, 2012. **110**(8): p. 1125-38.
619. Lin, J., et al., *Age-related cardiac muscle sarcopenia: Combining experimental and mathematical modeling to identify mechanisms*. Exp Gerontol, 2008. **43**(4): p. 296-306.
620. Manning, J.R., et al., *Loss of Rad-GTPase produces a novel adaptive cardiac phenotype resistant to systolic decline with aging*. Am J Physiol Heart Circ Physiol, 2015. **309**(8): p. H1336-45.

621. Ezekowitz, J.A., et al., *Declining in-hospital mortality and increasing heart failure incidence in elderly patients with first myocardial infarction*. J Am Coll Cardiol, 2009. **53**(1): p. 13-20.
622. Virag, J.A. and R.M. Lust, *Coronary artery ligation and intramyocardial injection in a murine model of infarction*. J Vis Exp, 2011(52).
623. Cury, D.P., et al., *Morphometric, quantitative, and three-dimensional analysis of the heart muscle fibers of old rats: transmission electron microscopy and high-resolution scanning electron microscopy methods*. Microsc Res Tech, 2013. **76**(2): p. 184-95.
624. Daum, B., et al., *Age-dependent dissociation of ATP synthase dimers and loss of inner-membrane cristae in mitochondria*. Proc Natl Acad Sci U S A, 2013. **110**(38): p. 15301-6.
625. Jamieson, K.L., et al., *Age and Sex Differences in Hearts of Soluble Epoxide Hydrolase Null Mice*. Front. Physiol, 2020. **11**.
626. Hung, Y.W., et al., *Soluble epoxide hydrolase activity regulates inflammatory responses and seizure generation in two mouse models of temporal lobe epilepsy*. Brain Behav Immun, 2015. **43**: p. 118-29.
627. Koerner, I.P., et al., *Polymorphisms in the human soluble epoxide hydrolase gene EPHX2 linked to neuronal survival after ischemic injury*. J Neurosci, 2007. **27**(17): p. 4642-9.
628. Cheng, W., et al., *Programmed myocyte cell death affects the viable myocardium after infarction in rats*. Exp Cell Res, 1996. **226**(2): p. 316-27.
629. Ben-Nissan, G. and M. Sharon, *Regulating the 20S proteasome ubiquitin-independent degradation pathway*. Biomolecules, 2014. **4**(3): p. 862-84.
630. Yu, X. and D.C. Kem, *Proteasome inhibition during myocardial infarction*. Cardiovasc Res, 2010. **85**(2): p. 312-20.
631. Yarian, C.S., I. Rebrin, and R.S. Sohal, *Aconitase and ATP synthase are targets of malondialdehyde modification and undergo an age-related decrease in activity in mouse heart mitochondria*. Biochem Biophys Res Commun, 2005. **330**(1): p. 151-6.
632. Darnold, J.R., M.L. Vorbeck, and A.P. Martin, *Effect of aging on the oxidative phosphorylation pathway*. Mech Ageing Dev, 1990. **53**(2): p. 157-67.
633. Choksi, K.B., et al., *Mitochondrial electron transport chain functions in long-lived Ames dwarf mice*. Aging (Albany NY), 2011. **3**(8): p. 754-67.
634. Dai, D.F., P.S. Rabinovitch, and Z. Ungvari, *Mitochondria and cardiovascular aging*. Circ Res, 2012. **110**(8): p. 1109-24.
635. Stanley, W.C., F.A. Recchia, and G.D. Lopaschuk, *Myocardial substrate metabolism in the normal and failing heart*. Physiol Rev, 2005. **85**(3): p. 1093-129.
636. Hochachka, P.W. and K.B. Storey, *Metabolic consequences of diving in animals and man*. Science, 1975. **187**(4177): p. 613-21.
637. Hipkiss, A.R., *Energy metabolism, altered proteins, sirtuins and ageing: converging mechanisms?* Biogerontology, 2008. **9**(1): p. 49-55.
638. Hipkiss, A.R., *Error-protein metabolism and ageing*. Biogerontology, 2009. **10**(4): p. 523-9.
639. Di Lisa, F. and P. Bernardi, *Mitochondria and ischemia-reperfusion injury of the heart: fixing a hole*. Cardiovasc Res, 2006. **70**(2): p. 191-9.
640. Chouchani, E.T., et al., *Ischaemic accumulation of succinate controls reperfusion injury through mitochondrial ROS*. Nature, 2014. **515**(7527): p. 431-5.

641. Ashrafian, H., et al., *Fumarate is cardioprotective via activation of the Nrf2 antioxidant pathway*. Cell Metab, 2012. **15**(3): p. 361-71.
642. Hohl, C., et al., *Evidence for succinate production by reduction of fumarate during hypoxia in isolated adult rat heart cells*. Arch Biochem Biophys, 1987. **259**(2): p. 527-35.
643. Taegtmeyer, H., *Metabolic responses to cardiac hypoxia. Increased production of succinate by rabbit papillary muscles*. Circ Res, 1978. **43**(5): p. 808-15.
644. Penney, D.G. and J. Cascarano, *Anaerobic rat heart. Effects of glucose and tricarboxylic acid-cycle metabolites on metabolism and physiological performance*. Biochem J, 1970. **118**(2): p. 221-7.
645. Juhaszova, M., et al., *Protection in the aged heart: preventing the heart-break of old age?* Cardiovasc Res, 2005. **66**(2): p. 233-44.
646. Zhao, T.T., et al., *Soluble epoxide hydrolase and ischemic cardiomyopathy*. Int J Cardiol, 2012. **155**(2): p. 181-7.
647. Bannehr, M., et al., *Linoleic Acid Metabolite DiHOME Decreases Post-ischemic Cardiac Recovery in Murine Hearts*. Cardiovasc Toxicol, 2019. **19**(4): p. 365-371.
648. Thai, P.N., et al., *Mitochondrial Quality Control in Aging and Heart Failure: Influence of Ketone Bodies and Mitofusin-Stabilizing Peptides*. Front Physiol, 2019. **10**: p. 382.
649. Samokhvalov, V., et al., *Deficiency of Soluble Epoxide Hydrolase Protects Cardiac Function Impaired by LPS-Induced Acute Inflammation*. Front Pharmacol, 2018. **9**: p. 1572.
650. Filadi, R., et al., *Mitofusin 2 ablation increases endoplasmic reticulum-mitochondria coupling*. Proc Natl Acad Sci U S A, 2015. **112**(17): p. E2174-81.
651. Batchu, S.N., et al., *Epoxyeicosatrienoic acid prevents postischemic electrocardiogram abnormalities in an isolated heart model*. J Mol Cell Cardiol, 2009. **46**(1): p. 67-74.
652. Hutchens, M.P., et al., *Soluble epoxide hydrolase gene deletion reduces survival after cardiac arrest and cardiopulmonary resuscitation*. Resuscitation, 2008. **76**(1): p. 89-94.
653. Burdon, K.P., et al., *Genetic analysis of the soluble epoxide hydrolase gene, EPHX2, in subclinical cardiovascular disease in the Diabetes Heart Study*. Diab Vasc Dis Res, 2008. **5**(2): p. 128-34.
654. Scheubel, R.J., et al., *Dysfunction of mitochondrial respiratory chain complex I in human failing myocardium is not due to disturbed mitochondrial gene expression*. J Am Coll Cardiol, 2002. **40**(12): p. 2174-81.
655. Sheeran, F.L. and S. Pepe, *Posttranslational modifications and dysfunction of mitochondrial enzymes in human heart failure*. Am J Physiol Endocrinol Metab, 2016. **311**(2): p. E449-60.
656. Chen, L., et al., *Mitochondrial OPA1, apoptosis, and heart failure*. Cardiovasc Res, 2009. **84**(1): p. 91-9.
657. Chiao, Y.A. and P.S. Rabinovitch, *The Aging Heart*. Cold Spring Harb Perspect Med, 2015. **5**(9): p. a025148.
658. Iorga, A., et al., *The protective role of estrogen and estrogen receptors in cardiovascular disease and the controversial use of estrogen therapy*. Biol Sex Differ, 2017. **8**(1): p. 33.

659. Huang, A., et al., *Estrogen elicits cytochrome P450--mediated flow-induced dilation of arterioles in NO deficiency: role of PI3K-Akt phosphorylation in genomic regulation*. *Circ Res*, 2004. **94**(2): p. 245-52.
660. Wang, M., et al., *Estrogen receptor beta mediates increased activation of PI3K/Akt signaling and improved myocardial function in female hearts following acute ischemia*. *Am J Physiol Regul Integr Comp Physiol*, 2009. **296**(4): p. R972-8.
661. Gao, J., et al., *Disrupting KATP channels diminishes the estrogen-mediated protection in female mutant mice during ischemia-reperfusion*. *Clin Proteomics*, 2014. **11**(1): p. 19.
662. Mattingly, K.A., et al., *Estradiol stimulates transcription of nuclear respiratory factor-1 and increases mitochondrial biogenesis*. *Mol Endocrinol*, 2008. **22**(3): p. 609-22.
663. Chen, J.Q., et al., *Regulation of mitochondrial respiratory chain biogenesis by estrogens/estrogen receptors and physiological, pathological and pharmacological implications*. *Biochim Biophys Acta*, 2009. **1793**(10): p. 1540-70.
664. Morkuniene, R., A. Jekabsone, and V. Borutaite, *Estrogens prevent calcium-induced release of cytochrome c from heart mitochondria*. *FEBS Lett*, 2002. **521**(1-3): p. 53-6.
665. Kang, C. and L. Li Ji, *Role of PGC-1alpha signaling in skeletal muscle health and disease*. *Ann N Y Acad Sci*, 2012. **1271**: p. 110-7.
666. Liu, L., et al., *Improved endogenous epoxyeicosatrienoic acid production mends heart function via increased PGC 1alpha-mitochondrial functions in metabolic syndrome*. *J Pharmacol Sci*, 2018. **138**(2): p. 138-145.
667. Chen, Y., et al., *17beta-estradiol prevents cardiac diastolic dysfunction by stimulating mitochondrial function: a preclinical study in a mouse model of a human hypertrophic cardiomyopathy mutation*. *J Steroid Biochem Mol Biol*, 2015. **147**: p. 92-102.
668. Barnych, B., *Development of potent inhibitors of human microsomal epoxide hydrolase*. *European Journal of Medicinal Chemistry*, 2020. **193**.
669. Lynes, M.D., et al., *The cold-induced lipokine 12,13-diHOME promotes fatty acid transport into brown adipose tissue*. *Nat Med*, 2017. **23**(5): p. 631-637.
670. Vasan, S.K., et al., *The proposed systemic thermogenic metabolites succinate and 12,13-diHOME are inversely associated with adiposity and related metabolic traits: evidence from a large human cross-sectional study*. *Diabetologia*, 2019. **62**(11): p. 2079-2087.
671. Liu, J.Y., *Inhibition of Soluble Epoxide Hydrolase for Renal Health*. *Front Pharmacol*, 2018. **9**: p. 1551.
672. Vaughan, R.A., et al., *A High Linoleic Acid Diet does not Induce Inflammation in Mouse Liver or Adipose Tissue*. *Lipids*, 2015. **50**(11): p. 1115-22.
673. Yellon, D.M. and D.J. Hausenloy, *Myocardial reperfusion injury*. *N Engl J Med*, 2007. **357**(11): p. 1121-35.
674. Motoki, A., et al., *Soluble epoxide hydrolase inhibition and gene deletion are protective against myocardial ischemia-reperfusion injury in vivo*. *Am J Physiol Heart Circ Physiol*, 2008. **295**(5): p. H2128-34.
675. Lawler, P.R., et al., *Targeting cardiovascular inflammation: next steps in clinical translation*. *Eur Heart J*, 2020.

676. Takahashi, M., *NLRP3 inflammasome as a novel player in myocardial infarction*. Int Heart J, 2014. **55**(2): p. 101-5.
677. Toldo, S., et al., *Inhibition of the NLRP3 inflammasome limits the inflammatory injury following myocardial ischemia-reperfusion in the mouse*. Int J Cardiol, 2016. **209**: p. 215-20.
678. Liu, Y., et al., *The effector cells and cellular mediators of immune system involved in cardiac inflammation and fibrosis after myocardial infarction*. J Cell Physiol, 2020.
679. Chaanine, A.H. and R.J. Hajjar, *AKT signalling in the failing heart*. Eur J Heart Fail, 2011. **13**(8): p. 825-9.

Appendix 1

The CD31 immunohistochemistry reported in this appendix was performed by Suellen Lamb as part of the University Institute of Virology Histology Core.

A1.1. Male sEH null aged mice demonstrate increased AKT expression

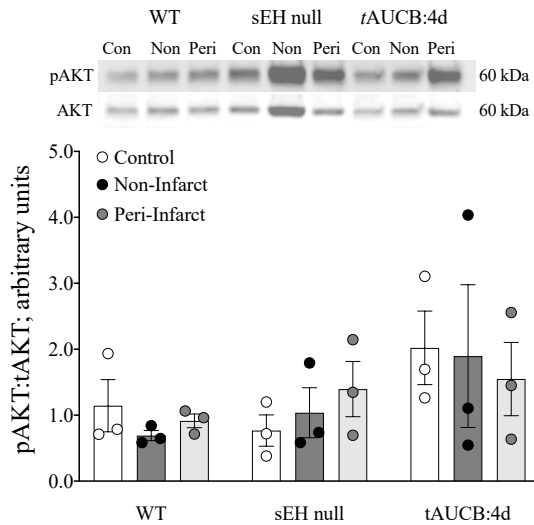
Short-term activation of the PI3K-AKT signalling pathway protects cardiomyocytes from ischemic damage [1, 2]. However, chronic activation of this pathway is maladaptive [3, 4]. Early evidence showed PI3K signalling is activated in sEH null mice following IRI, associated with improved cardiac recovery [5]. EETs can activate PI3K-AKT pro-survival signalling *in vitro* [6, 7] and perfusion with *t*AUCB improved cardiac functional recovery mediated through PI3K-AKT in a Langendorff model of IRI [8]. Based on this previous evidence, AKT signalling was assessed in male and female mouse tissues discussed in Chapter 3.2.

Western blots were run as described in Chapter 2.4. Probing was done with antibodies against phospho-AKT (Ser473) (CS9271S), total-AKT (CS9272S), GAPDH (cs5174), (Cell signaling Technology, Inc., New England Biolabs, Ltd., Whitby, ON, Canada). Quantitation of band strength using densitometry was done using Image J software (NIH, USA) to obtain relative protein expression. All treatment groups were normalized to the appropriate loading control lane. Two-way ANOVA with Tukey's post-hoc test was used to assess differences in western blotting. $P < 0.05$.

We assessed AKT phosphorylated at serine 473 compared to total AKT levels. There were no significant changes in phospho-AKT or total-AKT in female hearts (Fig A1.1.1). However, male sEH null mice demonstrated significant increases in total-AKT in the cytosol compared to WT controls, and these levels were highest in the non- and peri-infarct regions at 28 days post-MI (Fig. A1.1.2). Chronic AKT activation is associated with maladaptive remodelling, [4, 9]. However, the AKT in our data is in the total or non-phosphorylated form.

Ultimately, due to the long timepoint following ischemic injury more studies are needed at earlier time points in order to assess potential modulation of PI3K-AKT signalling pathways.

Females
A



B

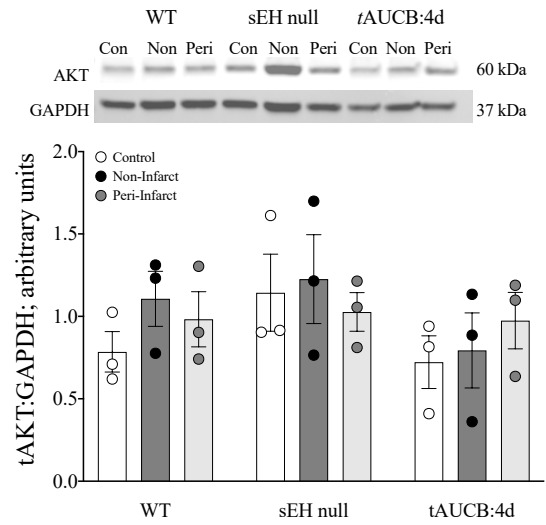
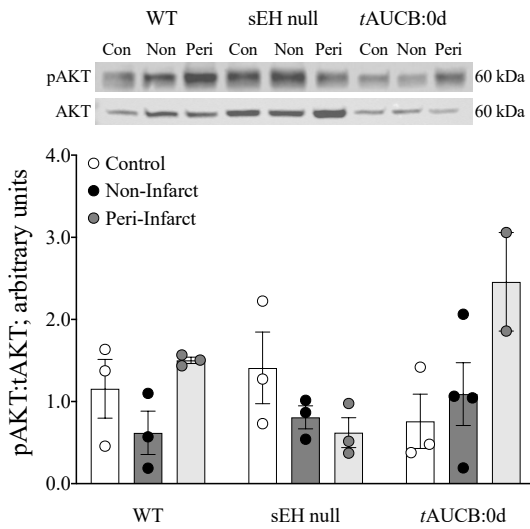


FIGURE A1.1.1. Phospho-AKT and AKT protein expression in cytosolic fractionates from female mouse hearts at 28 days post-MI. (A) pAKT (Ser 473) normalized to total-AKT and (B) AKT normalized to GAPDH in cytosol in female WT, sEH null and *tAUCB:4d* control, non-infarct and peri-infarct regions. Data are means \pm SEM, $N = 3$. $P < 0.05$.

Males

A



B

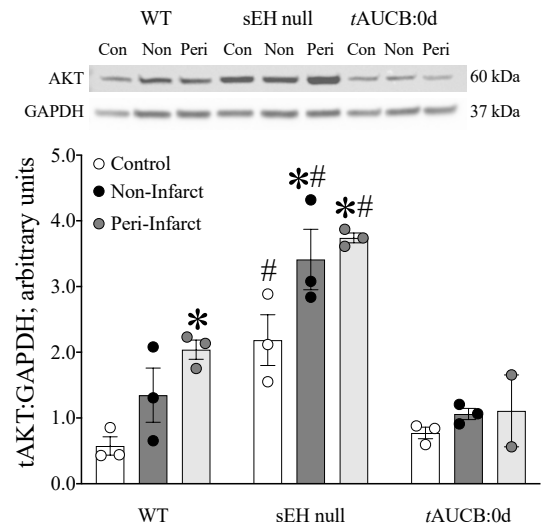


FIGURE A1.3.2. Phospho-AKT and AKT protein expression in cytosolic fractionates from male mouse hearts at 28 days post-MI. (A) pAKT (Ser 473) normalized to total-AKT and (B) AKT normalized to GAPDH in cytosol in in female WT, sEH null and *tAUCB* same-day treated control, non-infarct and peri-infarct regions. Data are means \pm SEM, N = 3. $P < 0.05$. * vs control, # vs WT.

A1.2. Male sEH null aged mice demonstrate decreased caveolin-1 expression post-MI

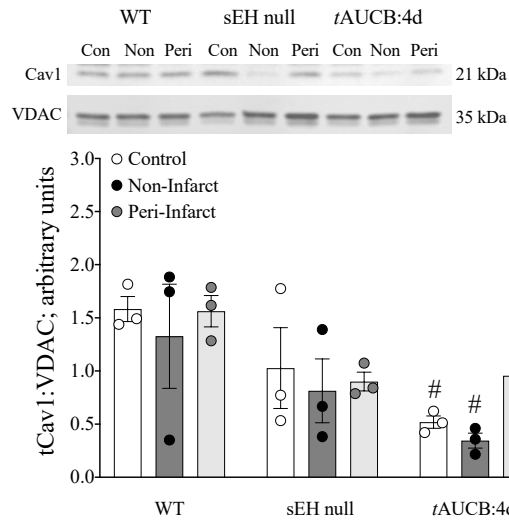
Caveolins are scaffolding and regulatory proteins found in small invaginations of cell membranes, called caveolae [10]. Caveolin-1 (Cav-1) is found in mitochondria and is involved in cardiac homeostasis [10]. Cav-1 deficiency has been linked to increased maladaptive macrophage infiltration and fibrosis [11] and reduced survival post-MI in mice [12]. Previous studies from our lab have shown EETs prevent the loss of Cav-1 in IRI models, resulting in cardioprotection [13]. Based on these previous data, we tested for total Cav-1 expression in mitochondrial fractions taken from the male and female mice used in Chapter 3.2, and in male and female human NFC and ICM myocardial samples described in Chapter 3.3. Westerns were run as described in Chapter 2.4. Membranes were probed against antibodies for total-cav-1 (CS3267S) (Cell signaling Technology, Inc., New England Biolabs, Ltd., Whitby, ON, Canada), and VDAC (ab14734), (Abcam, Toronto, ON, CAN).

Female mice treated with tAUCB demonstrated significantly reduced total Cav-1 expression in control hearts and in the non-infarct region compared to WT (Fig. A1.2.1A). Conversely, male WT mice demonstrated significantly increased Cav-1 expression in non- and peri-infarct regions compared to controls (Fig. A1.2.1B). This effect was attenuated in the peri-infarct region of sEH null males (Fig. A1.2.1B). No changes were observed in human male or female myocardial samples (Fig. A1.2.2).

The increase in Cav-1 observed in WT males 28-days post-MI is consistent with what has been observed in other long-term models of permanent occlusion [14]. Gao et al demonstrated Cav-1 expression in young males was decreased at 7 days post-MI, but had subsequently increased at the 28 day time point [14]. Interestingly, in this study lower levels

of Cav-1 were associated with increased activation of PI3K-AKT signalling and enhanced fibrosis [14]. In our aged male sEH null mice, we observed lower total-Cav-1 at 28 days post-MI correlating with increased total-AKT. However, whether these changes we observed contribute to the worse survival rate in aged male null mice remains the subject of future studies.

Females
A



Males
B

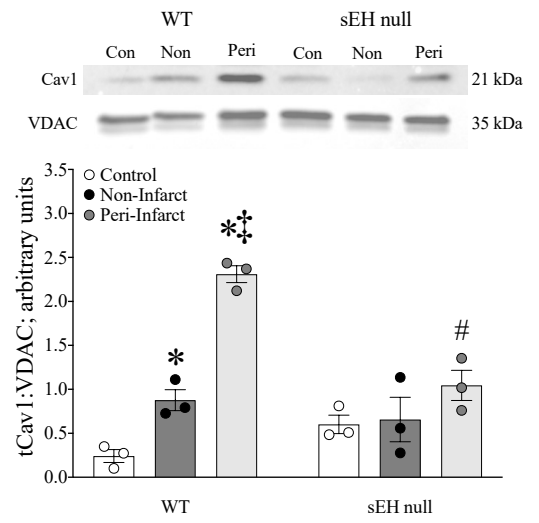


FIGURE A1.2.1. Total-caveolin-1 expression in mitochondrial fractions from female (A) and male (B) mouse hearts at 28 days post-MI. (A) total Cav-1 normalized to VDAC in female mitochondria from WT, sEH null and tAUCB pre-treated mice and (B) total Cav-1 normalized to VDAC in male mitochondria from WT and sEH null control, non-infarct and peri-infarct regions. Data are means \pm SEM, N = 3. $P < 0.05$. * vs control, # vs WT, ‡ vs non-infarct.

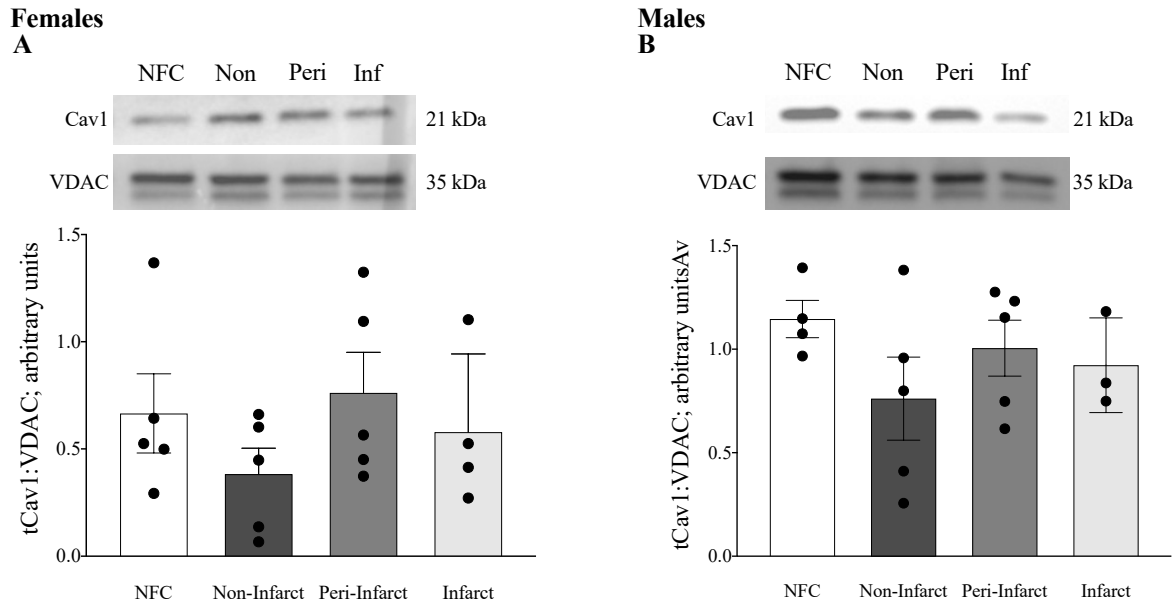


FIGURE A1.2.2. Total-caveolin 1 expression in human mitochondrial fractions from female (A) and male (B) myocardium from NFC and ICM patients. (A) total caveolin 1 normalized to VDAC in females and (B) total caveolin 1 normalized to VDAC in males. Data are means \pm SEM, N = 3-5. $P < 0.05$.

A1.3. sEH null female mice demonstrate increased CD31 expression post-MI

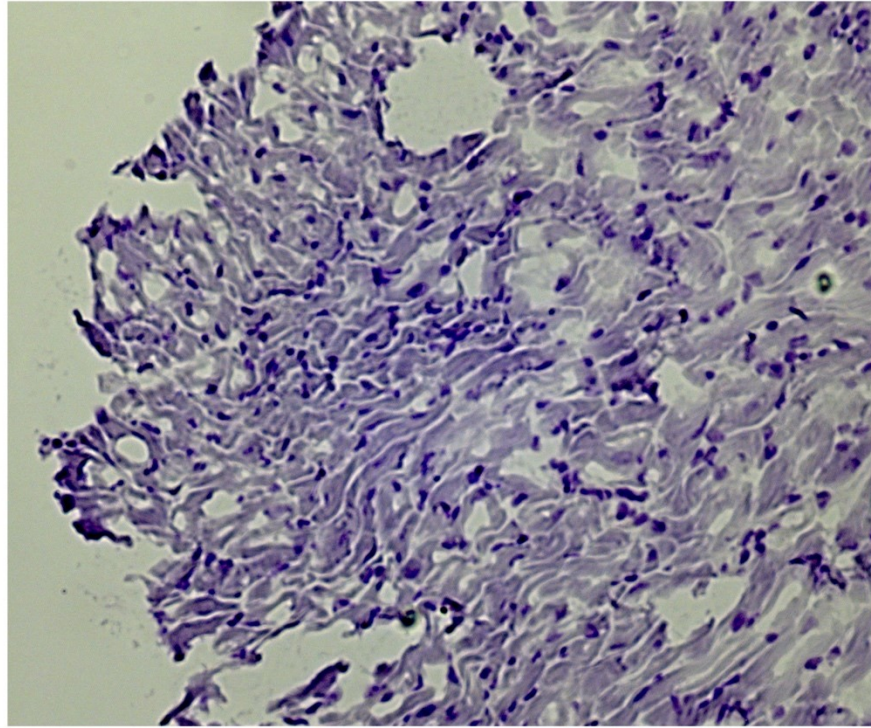
Collateral artery growth involves the formation of new microvessels and has been suggested as a mechanism to treat ischemic disease [15]. CD31, also known as platelet/endothelial cell adhesion molecule-1 (PECAM), is a marker of vascular endothelial cells and is used as an indirect marker of collateral formation [16]. Previous studies show EETs promote angiogenesis [17]. However, while angiogenesis post-MI can be considered cardioprotective, in cancer models both EETs and high-dose *t*AUCB can promote metastasis in a manner linked to triggering endothelial secretion of vascular endothelial growth factor (VEGF) and CD31 [18]. However, later studies demonstrated low-dose *t*AUCB does not demonstrate these significant effects on metastasis [19, 20]. Thus, *t*AUCB treatment may exhibit hormesis [20]. In order to test whether sEH null or *t*AUCB same-day treated mice exhibit collateral formation both post-MI and over general aging, cardiac slices were stained with endothelial marker CD31.

Hearts were excised, rinsed in ice-cold PBS and sliced on the sagittal plane. Hearts were frozen in OCT and stored at -80°C until further processing. All cryoslicing for histological analysis was done by the University of Alberta Histology Core. Hearts were stained for hemoxylin and eosin (H&E) by the HistoCore. No changes were observed in female hearts stained with H&E (Figure A1.3.1). Immunohistochemistry was performed against CD31 using established protocols. Slices were fixed in acetone for 10 minutes, allowed to air dry, then rinsed in 1X TBST and blocked for one hour. Following washing, slices were stained with CD31 (1/50,) (ab28364, ABCAM) overnight. Following peroxidase blocking, hearts were then probed with goat anti rabbit secondary HRP for one hour. Following washing,

slices were counterstained with fresh hematoxylin. Positive staining was confirmed by use of an isotype control (Figure A1.3.2).

Hearts from sEH null and *t*AUCB same-day treated females exhibited increased CD31 at both control and 28 days post-MI (Figure A1.3.3). Interestingly, young and aged sEH null males and females appear to have increased CD31 expression in the myocardium compared to their WT counterparts (Fig A1.3.4, Fig A1.3.5). While these data are preliminary, these results suggest sEH genetic deletion or low-dose sEHi treatment may increase angiogenesis in the heart post-MI in females and over general aging in both sexes.

A isotype



B CD31+

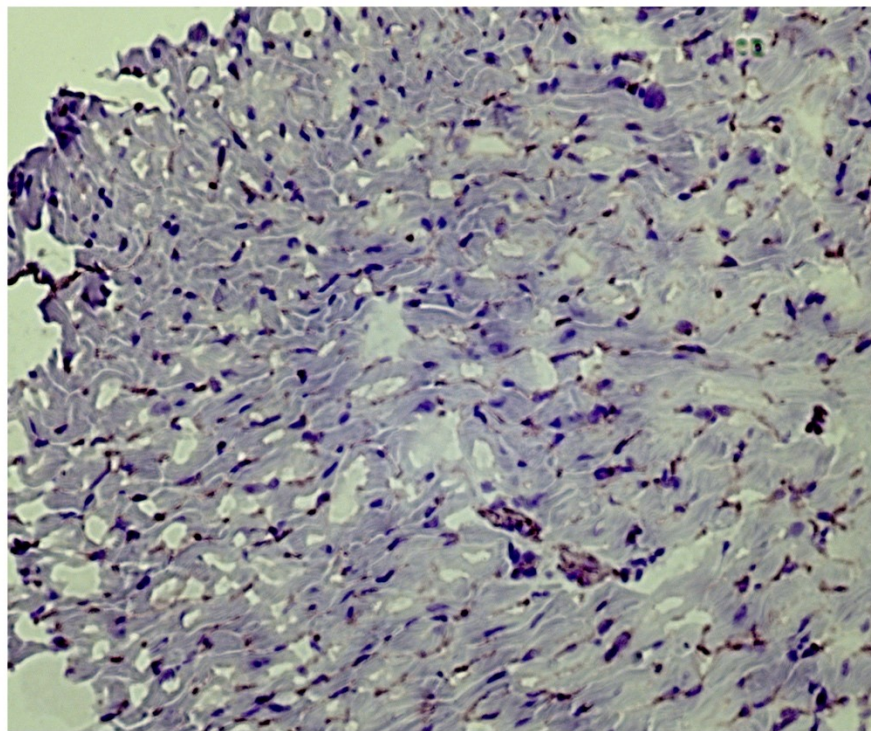


FIGURE A1.3.4. CD31 staining was confirmed by use of an isotype control. (A) Isotype control (B) CD31 staining. Both sections are from the same young WT male mouse.

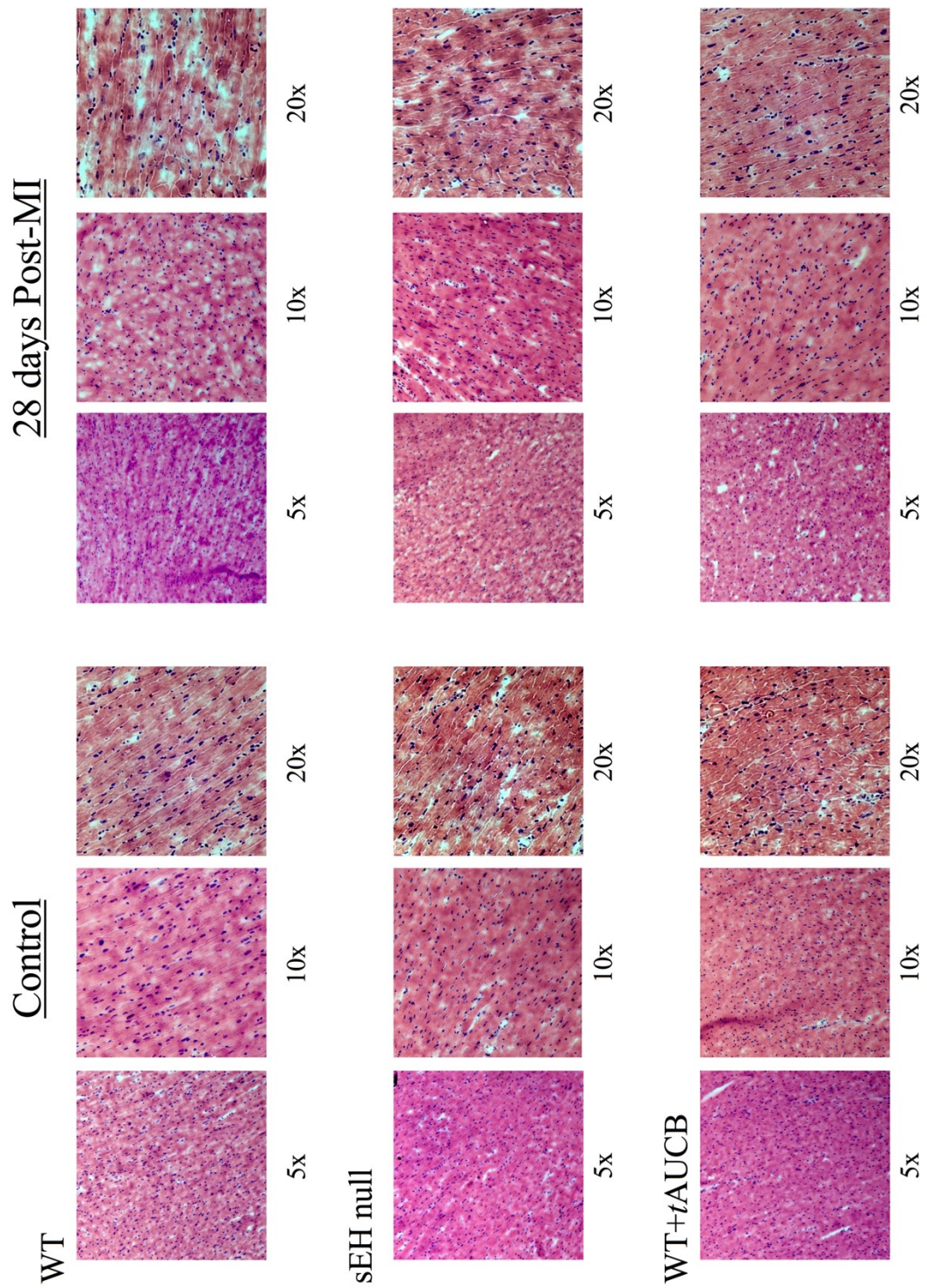


FIGURE A1.3.1. H&E staining in control and at 28 days post-MI for female WT, sEH null and WT+tAUCB same-day treated mice.

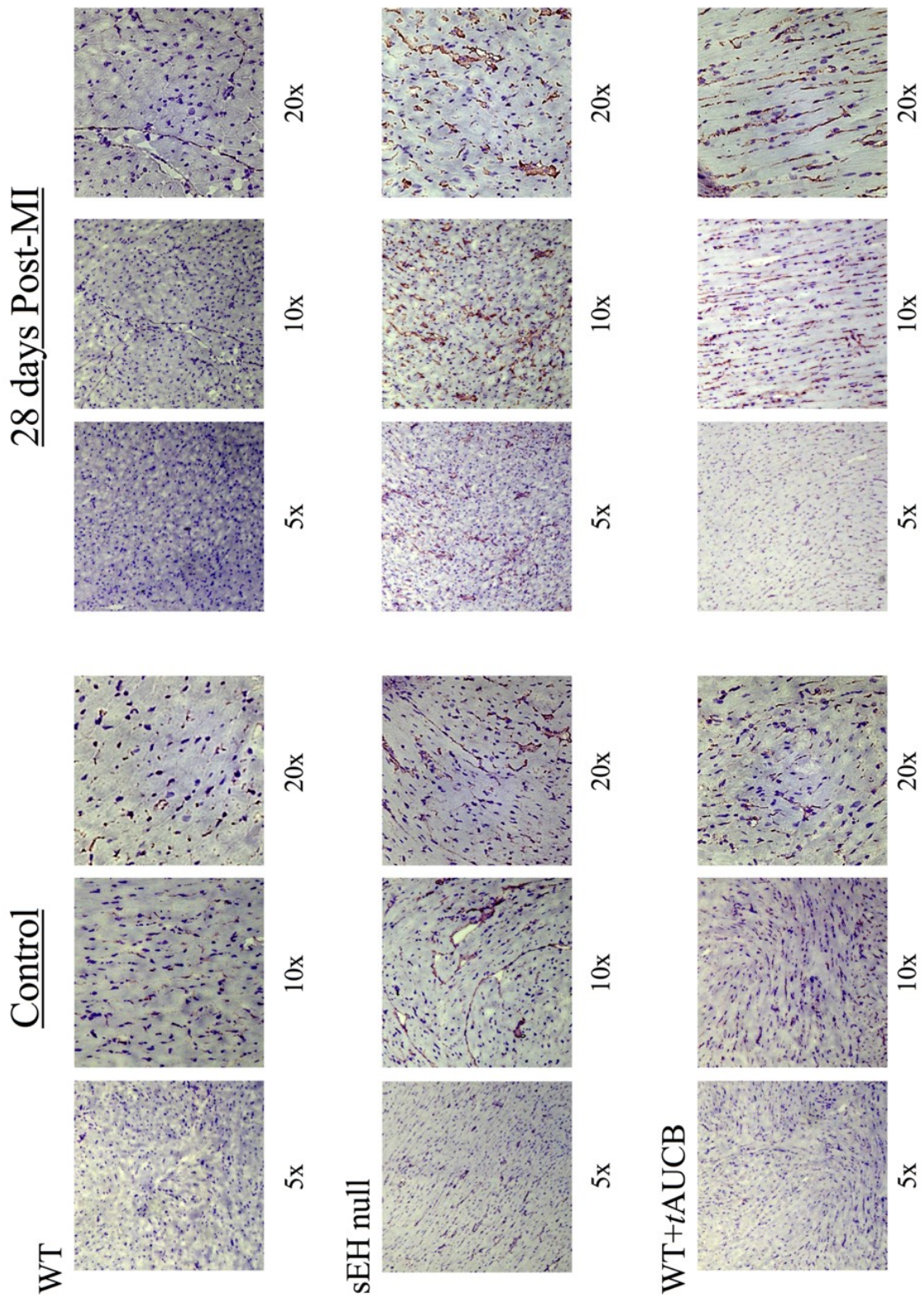


FIGURE A1.3.3 CD31 staining in female WT, sEH null and *tAUCB* same-day treated mice at control and 28 days post-MI.

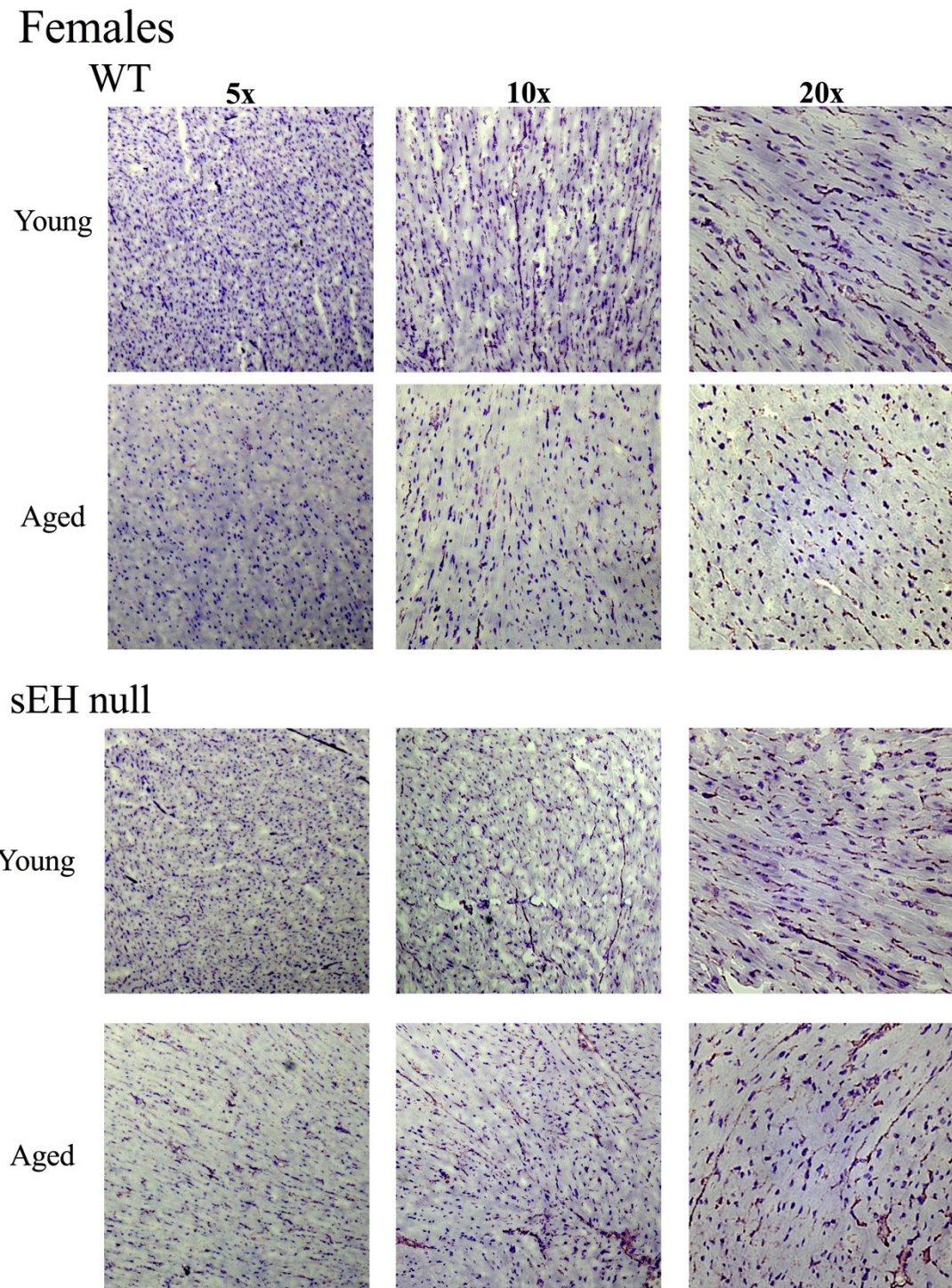


FIGURE A1.3.4. CD31 immunohistochemistry in young and aged WT and sEH null female hearts.

Males

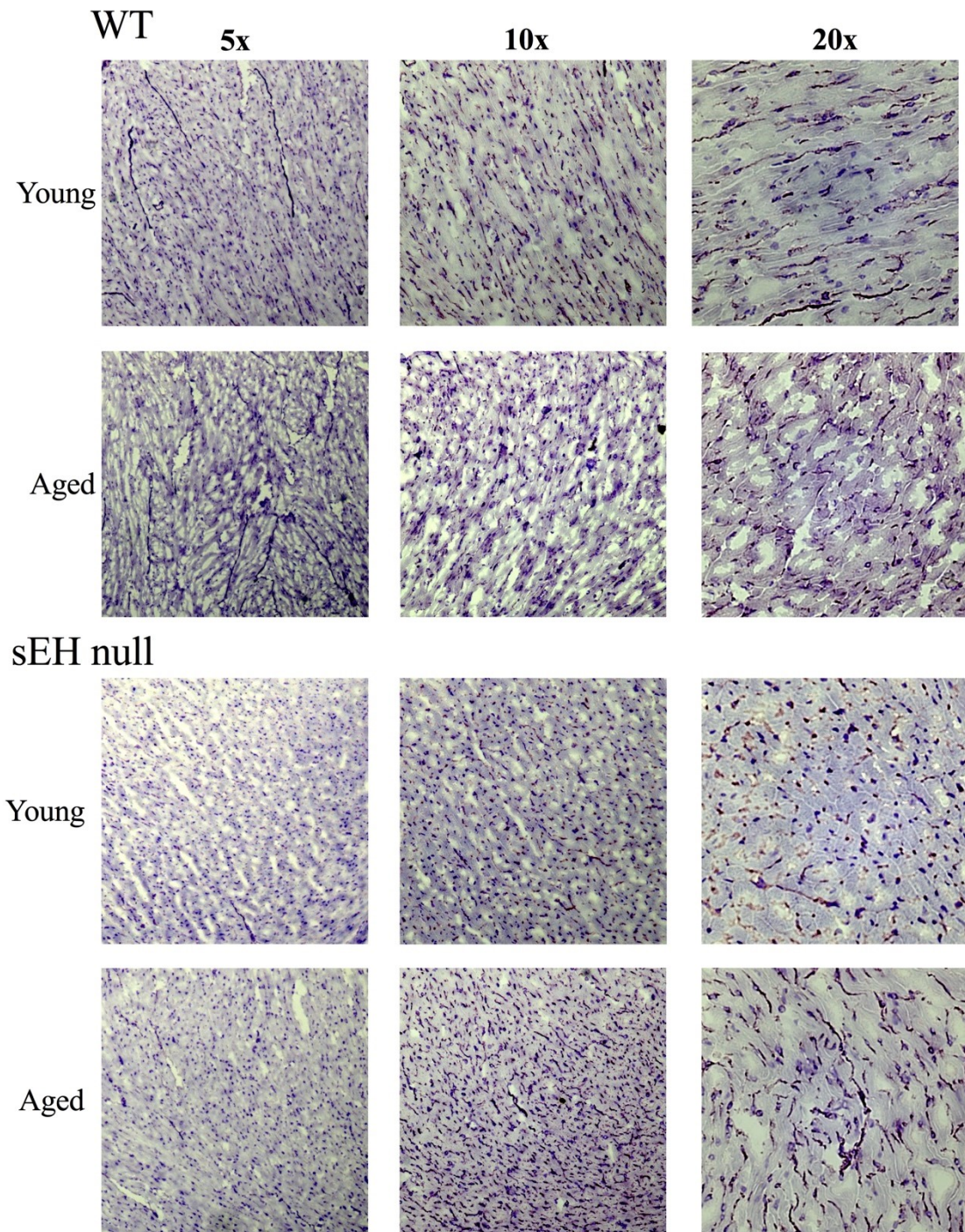


FIGURE A1.3.5. CD31 immunohistochemistry in young and aged WT and sEH null male hearts.

1. Hua, Y., et al., *Chronic Akt activation accentuates aging-induced cardiac hypertrophy and myocardial contractile dysfunction: role of autophagy*. Basic Res Cardiol, 2011. **106**(6): p. 1173-91.
2. Lin, R.C., et al., *PI3K(p110 alpha) protects against myocardial infarction-induced heart failure: identification of PI3K-regulated miRNA and mRNA*. Arterioscler Thromb Vasc Biol, 2010. **30**(4): p. 724-32.
3. Nagoshi, T., et al., *PI3K rescues the detrimental effects of chronic Akt activation in the heart during ischemia/reperfusion injury*. J Clin Invest, 2005. **115**(8): p. 2128-38.
4. Chaanine, A.H. and R.J. Hajjar, *AKT signalling in the failing heart*. Eur J Heart Fail, 2011. **13**(8): p. 825-9.
5. Seubert, J.M., et al., *Role of soluble epoxide hydrolase in postischemic recovery of heart contractile function*. Circ Res, 2006. **99**(4): p. 442-50.
6. Wang, Y., et al., *Arachidonic acid epoxygenase metabolites stimulate endothelial cell growth and angiogenesis via mitogen-activated protein kinase and phosphatidylinositol 3-kinase/Akt signaling pathways*. J Pharmacol Exp Ther, 2005. **314**(2): p. 522-32.
7. Dhanasekaran, A., et al., *Multiple antiapoptotic targets of the PI3K/Akt survival pathway are activated by epoxyeicosatrienoic acids to protect cardiomyocytes from hypoxia/anoxia*. Am J Physiol Heart Circ Physiol, 2008. **294**(2): p. H724-35.
8. Chaudhary, K.R., et al., *Inhibition of soluble epoxide hydrolase by trans-4- [4-(3-adamantan-1-yl-ureido)-cyclohexyloxy]-benzoic acid is protective against ischemia-reperfusion injury*. J Cardiovasc Pharmacol, 2010. **55**(1): p. 67-73.
9. Riad, A., et al., *Toll-like receptor-4 modulates survival by induction of left ventricular remodeling after myocardial infarction in mice*. J Immunol, 2008. **180**(10): p. 6954-61.
10. Patel, H.H., F. Murray, and P.A. Insel, *Caveolae as organizers of pharmacologically relevant signal transduction molecules*. Annu Rev Pharmacol Toxicol, 2008. **48**: p. 359-91.
11. Shivshankar, P., et al., *Caveolin-1 deletion exacerbates cardiac interstitial fibrosis by promoting M2 macrophage activation in mice after myocardial infarction*. J Mol Cell Cardiol, 2014. **76**: p. 84-93.
12. Jasmin, J.F., et al., *Caveolin-1 deficiency exacerbates cardiac dysfunction and reduces survival in mice with myocardial infarction*. Am J Physiol Heart Circ Physiol, 2011. **300**(4): p. H1274-81.
13. Chaudhary, K.R., et al., *Effect of ischemia reperfusion injury and epoxyeicosatrienoic acids on caveolin expression in mouse myocardium*. J Cardiovasc Pharmacol, 2013. **61**(3): p. 258-63.
14. Gao, Y., et al., *Hypoxia induces cardiac fibroblast proliferation and phenotypic switch: a role for caveolae and caveolin-1/PTEN mediated pathway*. J Thorac Dis, 2014. **6**(10): p. 1458-68.
15. Schirmer, S.H., et al., *Stimulation of collateral artery growth: travelling further down the road to clinical application*. Heart, 2009. **95**(3): p. 191-7.

16. Privratsky, J.R. and P.J. Newman, *PECAM-1: regulator of endothelial junctional integrity*. Cell Tissue Res, 2014. **355**(3): p. 607-19.
17. Webler, A.C., et al., *Epoxyeicosatrienoic acids are part of the VEGF-activated signaling cascade leading to angiogenesis*. Am J Physiol Cell Physiol, 2008. **295**(5): p. C1292-301.
18. Panigrahy, D., et al., *Epoxyeicosanoids stimulate multiorgan metastasis and tumor dormancy escape in mice*. J Clin Invest, 2012. **122**(1): p. 178-91.
19. Zhang, G., et al., *Epoxy metabolites of docosahexaenoic acid (DHA) inhibit angiogenesis, tumor growth, and metastasis*. Proc Natl Acad Sci U S A, 2013. **110**(16): p. 6530-5.
20. Zhang, G., et al., *Dual inhibition of cyclooxygenase-2 and soluble epoxide hydrolase synergistically suppresses primary tumor growth and metastasis*. Proc Natl Acad Sci U S A, 2014. **111**(30): p. 11127-32.